THERMAL PERFORMANCE ANALYSIS OF JET IMPINGEMENT HEAT SINK WITH NANOFLUID

Thesis submitted in fulfilment of the
Requirement of the award of the degree of

DOCTOR OF PHILOSOPHY

IN

MECHANICAL ENGINEERING

By

DEEPAK KUMAR

(2K17/PHD/ME/13)

Under the Privileged Guidance of

DR. MOHAMMAD ZUNAID
(Supervisor)

PROF. SAMSHER
(Co - Supervisor)

DEPARTMENT OF MECHANICAL ENGINEERING

DELHI TECHNOLOGICAL UNIVERSITY

(Formerly Delhi College of Engineering)

Bawana Road Delhi -110042, India

June 2022

CANDIDATE'S DECLARATION

I, DEEPAK KUMAR, a student of Ph.D. of Mechanical Engineering Department at Delhi Technological University, Delhi, declare that I own full responsibility for the information, results, conclusions, etc. provided in this thesis "**Thermal Performance Analysis of Jet Impingement Heat Sink with Nanofluid"** submitted to Delhi Technological University, Delhi, for the award of Ph.D. degree. I have completely taken care in acknowledging the contribution of others in this academic work. I further declare that in case of my violation of intellectual property rights or copyrights found at any stage, I, as the candidate will be solely responsible for the same.

DEEPAK KUMAR

CERTIFICATE

This is to certify that the thesis entitled " **Thermal Performance Analysis of Jet Impingement Heat Sink with Nanofluid** " being submitted by **Deepak Kumar** (Roll No. 2K17/PhD/ME/13) **to** the Delhi Technological University, Delhi for the award of the degree of **Doctor of Philosophy** is a bonafide record of original research work carried out by him. He has worked under our guidance and supervision and has fulfilled the requirements for the submission of this thesis, which has reached the requisite standard. The results contained in this thesis have not been submitted, in part or full, to any other University or Institute for the award of any degree or diploma.

DR. MOHAMMAD ZUNAID
Supervisor
(Assistant Professor)
Department of Mechanical Engineering
Delhi Technological University,
Delhi-110042,
INDIA

PROF. SAMSHER
Co - Supervisor
(Professor)
Department of Mechanical Engineering,
Delhi Technological University,
Delhi-110042,
INDIA

ACKNOWLEDGEMENTS

First and foremost, I want to express my gratitude to my supervisors Prof. Samsher Gautam and Dr. Mohammad Zunaid for their valuable guidance, support, and encouragement throughout my Ph.D. program. This thesis could not have attained its present form without their supervision, direction, and interest in the research work. Their painstaking efforts, methodical approach and individual help made it possible for me to complete this work in time.

I express my gratitude to Prof. S.K. Garg, Chairman of DRC, and SRC members, Prof. Avdesh Sharma, Prof. M.M. Hasan, Prof. Raj Kumar Singh and Prof. S. Anbu Kumar for providing valuable comments and suggestions. I am thankful to all faculty and staff members of Mechanical, Production & Industrial and Automobile Engineering Department for their continued valuable support. I appreciate reviewers of research papers, industry people for sparing their valuable time and constructive comments.

I wish to thank my parents, brother, sisters, family members and friends whose blessings made this work reality. I'd like to present my sincere thankfulness to my deceased dear mother, Shakuntla Devi for her great role in my life and their numerous sacrifices for me. I sincerely thank to my wife Neeraj Kumari for their patience, support and loving participation in accomplishing this research work. I would also like to recognize the support and direction of my father Radhe Shyam. At last, but not the least I am thankful to the almighty God for giving me the mental and physical strength to work sincerely, diligently, and honestly and helping and guiding me during my life and throughout my study.

Deepak Kumar

ABSTRACT

Small scale thermal devices are very effective and interesting to use for the applications which involves large amount of heat flux. The current investigation introduces the concept of heat sink with combination of jet impingement, micro – channel and air foil shaped pillars. In the current research three techniques have been operated to enhance the rate of heat transfer in a heat sink. The amalgamation of Impingement of jet, air foil pillars and Nanofluid are used. Nanofluid has a lot of potential to enhance the heat transportation in contrast to the water. The use of Nano particles in the base fluid like water also augment the various properties which helps in the heat dissipation from the components subjected to high temperatures. In the current study, the various combinations of jet-channel and pillars have been investigated comparatively.

A numerical model is designed to explore the thermal performance of jet impingement with constant heat flux. The study has been carried out for a constant value of heat flux at the bottom surface. The investigation has been executed with the help of three dimensional numerical model using Computational fluid Dynamics. In the current work, computational fluid dynamics investigation has been performed in case of air foil shaped pillars in heat sink with impingement of jet. The steady state conditions are assumed for the laminar and incompressible flow. For the purpose of study dimensionless variables are formed. The investigation has been made in terms of thermal and fluid attributes. The performance of jet impingement was predicted in terms of different parameters like temperature rise, drop in pressure and coefficient of heat transfer, Nusselt number, thermal resistance and pumping power.

At the onset the model has been validated with the inspection carried out already in experimental form. The model has been validated with the available experimental and simulation results. The study has been performed using water, CuO – water Nanofluid and

Al_2O_3 – water Nanofluid with different concentrations. CuO is used with 0.5 % and 1% concentration and Al_2O_3 is used with 5% concentration.

Augmentation in pitch ratio, leads to increase in temperature for a particular value of height ratio. Also the heat transfer coefficient gets lowered with the increase in pitch ratio. So proper selection of dimensionless parameters to increase the heat dissipation is of utmost importance. From the results the conclusion is made that the use of airfoil pillars and Nanofluid has increased the thermal characteristics of the three dimensional model in the form of heat exchange coefficient by almost 28.2%. The Nanofluid has been utilized for the 0.5% concentration.

Minimum temperature is found in case of jet-pillar combination. The channel flow diminished the heat exchange coefficient. With pillars, augmentation in height diameter proportion, almost 44 % reduction in the temperature of the base has been noticed. Also 24 % augmentation has been deduced in the convection coefficient, with an increase in the design parameter. Advancement in height ratio leaded to 16 % improvement in the Nusselt number. From the results minimum 14 % reduction in the temperature is detected for height ratio with Nanofluid (CuO -1%). Also in differentiation with water minimum 10 % reduction is noticed.

The model is also analysed for separate combinations of jet-channel and pillars using Al_2O_3 – water Nanofluid with 5% concentration. The relation between thermal resistance and pumping power is predicted.

TABLE OF CONTENTS

LIST OF FIGURE

NOMENCLATURE

Da	Darcy Number
D_j	Diameter of Jet
D_{pl}	Diameter of Pillar
Dr	Darcy Number
Gr	Grashof's Number
h	Coefficient of Heat Transfer
Ha	Hartmann Number
H_{ch}	Height of Channel
Nu	Nusselt Number
p	Pressure
Ph	Pitch of Jet
P_p	Pumping Power
Pr	Prandtl Number
$(\Delta P)_o$	Overall Pressure Drop
q	Discharge
Q	Rate of Heat Transfer
R_e	Reynolds Number
R_T	Thermal Resistance
t_{nz}	Thickness of Nozzle Plate
$(\Delta T)_r$	Rise in Maximum Temperature
W_{ch}	Width of Channel
W_{chw}	Width of wall of channel

$\frac{H_{ch}}{D_j}$	Height Ratio
$\frac{Ph}{D_j}$	Pitch Ratio

Subscripts

f	Fluid
i	Inlet
j	Jet
pl	Pillar
ch	Channel
max	Maximum
p	Pumping
o	Overall
s	substrate
T	Thermal
nz	Nozzle Plate
r	Rise
chw	Wall Of Channel

Greek symbols

C	Specific Heat
K	Thermal Conductivity
μ	Dynamic Viscosity
ρ	Density Of Fluid (kg/m^3)
υ	Kinematic viscosity
τ	Shear stress

Abbreviations

AFPF	Aluminum foam pin fin
CFD	Computational Fluid Dynamics
COBYLA	Constrained Optimization by Linear approximation
DCOJCP	Different Combinations Of Jet-Channel And Pillar
FEM	Finite Element Method
FVM	Finite Volume Method
GNP	Graphene Nano Plates
GWR	Galerkin Weighted Residual
HR	Height Ratio
JIHSWAPNF	Jet Impingement Heat Sink With Airfoil Pillars And Nano Fluid
JIHSWNF	Jet Impingement Heat Sink With Nano Fluid
LMTD	Logarithmic Mean Temperature Difference
MCHSWNF	Microchannel Heat Sink With Nano Fluids
NFL	Nano Fluid
ODE	Ordinary Differential Equation
OPD	Overall Pressure Drop
PCM	Phase Change Material
PDE	Partial Differential Equation
PP	Pumping Power
PPF	Parallel Plain Fin
PR	Pitch Ratio
RIMT	Rise In Maximum Temperature

CHAPTER – 1

INTRODUCTION

1.1 Introduction

There has been a quick growth in the field of electronics in the recent years. The various parameters of electronics components like efficiency and effectiveness are truly dependent on the temperature. In the current scenario disposal of heat has become a typical problem in various components having high temperatures. Heat dissipation in most of the components of our daily life is found to be very challenging. This is because the components are subjected to high temperature conditions. Lifetime as well as effectiveness of a device can be significantly increased by an improvement in the cooling mechanism. So in the today's scenario requirement of an efficient cooling technology is of great importance. And hence thermal management has been a critical issue in the electronics components. High temperature may result in the severe loss of the electronics components.

1.2 Micro-Channel

For the past two decades, thermodynamic systems, thermal converters (cooling system) achieved better performances by imparting the best knowledge pertaining to various processes and permitting their design and optimization in the system. On the other aspect the development is also based on the utilization of the new materials, particularly in the case of newly developed heat exchangers which results in increase in the heat transfer and high heat transfer coefficient. In recent, a very important contribution on increasing the performance of these systems, sometimes to levels once inconceivable, was obtained by using Nano-technologies which have allowed the production of a new generation of compact heat exchangers with micro channels. Micro channel

Heat Exchangers (MCHEX) have [Kandlikar and Grande, 2003], a hydraulic diameter D_h =0.2….0.01 mm involving the advantage of a large heat exchange surface in a very small volume. Also, at very small sizes, the processes of heat and mass transfer occurring in the dynamic and thermal boundary layers are very effective. These new types of heat exchangers provide high heat transfer coefficients and thus they are up to 45% more compact than the classic ones, at the same thermal performances [Richter 1997, Pfalher 1990]. Due to high thermal performance, MCHEX are used increasingly in both single-phase (liquid or gas) and two-phase heat exchange (condensation - evaporation); while the disadvantage of higher pumping power is compensated by the lower scale and cost obtained in the case of improved series production based on Nano-technologies series production improvement [Philips 1987]. Using the MCHEX in vapour compression refrigeration systems, micro channel tubes having a lower internal volume will reduce the amount of refrigerant charged in the plant.

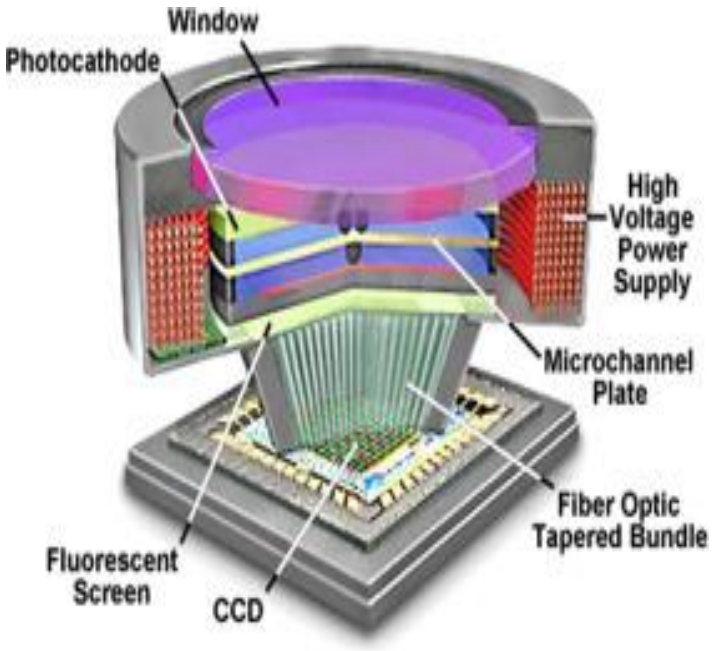

Figure 1.1: Schematic 3D view of a second-generation image intensifier tube equipped with a micro-channel plate [Herwig 2010]

1.3 Classification

Tuckerman and Pease [1981] studied the fluid flow for heat transfer under title "High Performance Heat Sinking in VLSI". This was the first study on micro channel for heat transfer. This work on the micro channel has innovative research to focus in the field of micro channel and fluid flow due to high performance fluid heat transfer through the micro channel.

- Micro channels-1$\mu m < D <$100μm
- Mini channel-100$\mu m <D <$ 1 *mm*
- Compact Passages-1 *mm* $<D <$ 6 *mm*
- Conventional Passages-6 *mm* $<D$

Easiest classification was introduced by [Obot 2003] which was totally based on the hydraulic diameter on behalf of dimension of smallest channel. Obot describe channels of hydraulic diameter range under 1 mm (*Dh < 1mm)* as micro channels, which was also adopted by some other researchers such as [Bahrami and Jovanovich 2006], Bahrami et al. [2006] and Bayraktarand Pidugu [2006]. Higher volumetric rate of heat transfer requires improved manufacturing techniques and requires more complicated manifold designs [Kandlikar et al. 2006]. Many researchers describe the various applications on electronic circuit in field flow heat transfer as compact parameter. Micro channel transfers the heat through the body constraint in two ways. First, the small amount fluid flow in to the refrigerant side of micro channel. Second, the flat tube which is oriented in flat position that reduces flat side, which leads to be either increased airflow or reduced fan power.

- Conventional channel- Dia＞3 mm
- Mini channels -3 mm Dia＞200micro m
- Micro channel – 200micro mm Dia＞10micro m

- Nano channels –Dia<0.1micro m

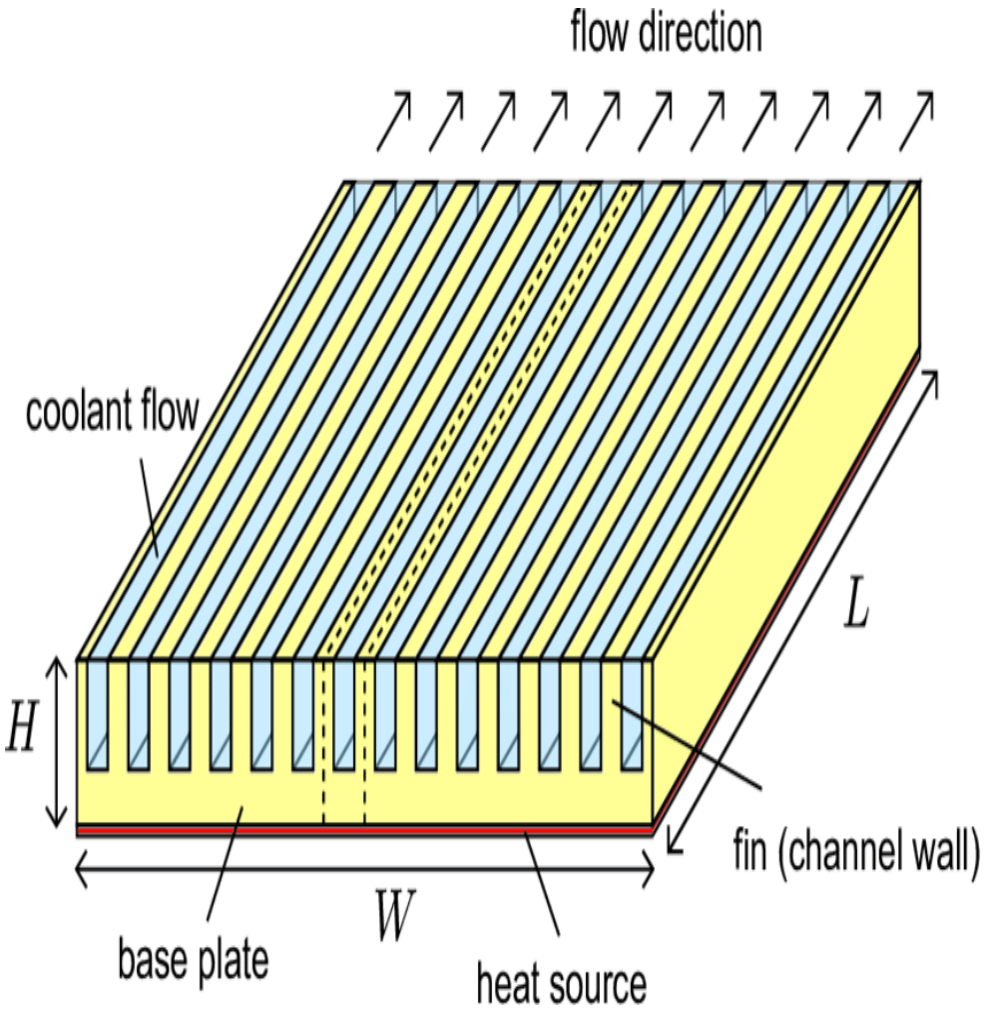

Figure 1.2: Micro-channel heat sink core [Naphon 2010]

Thermal resistance and substrate temperature gradient are widely used to compare the performance of heat sinks. The total thermal resistance is the ratio of the difference between bottom plate temperature and the inlet temperature of the coolant to the heat flux. Substrate temperature gradient is the ratio of difference between maximum substrate temperature and minimum substrate temperature to the heat flux.

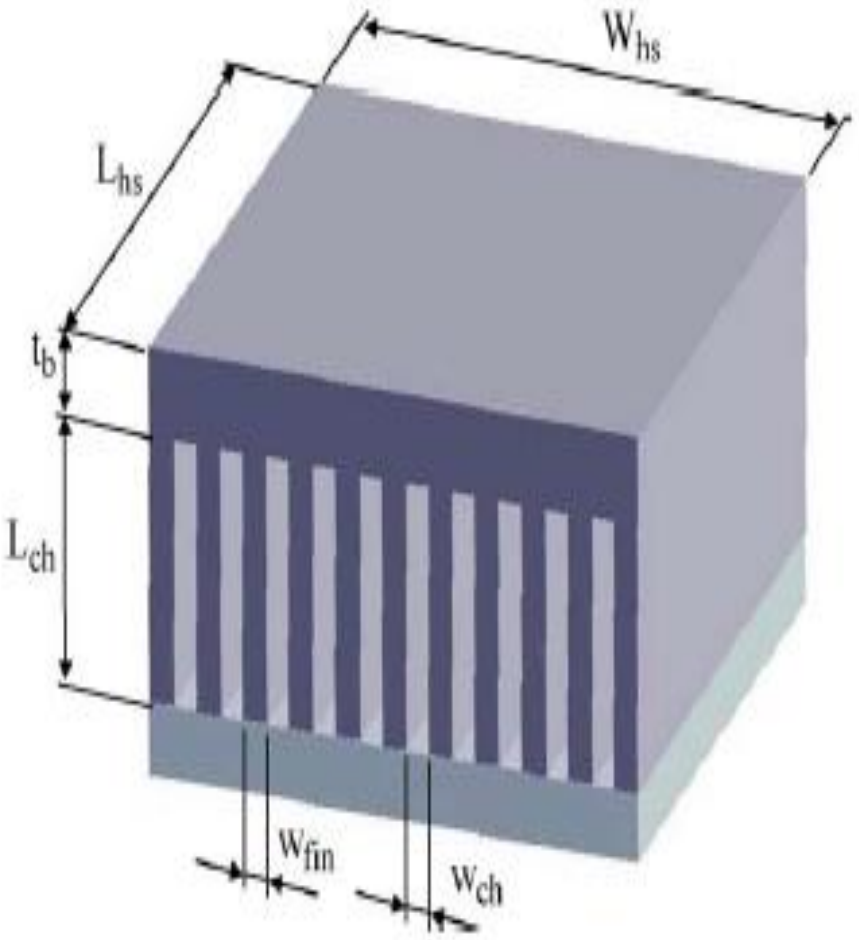

Figure 1.3: Geometric configuration of micro channel heat sink. [Chein 2005]

Where L_{hs} micro channel heat sink length, m

L_{ch} micro channel depth, m

W_{ch} width of micro channel, m

W_{fin} width of fin, m

W_{hs} width of micro channel heat sink, m

1.4 Hydrodynamics of Jet Impingement

The flow field of an impinging jet has been classified into 3 regions

- Free Jet Region,

- Stagnation Region And
- Wall Jet Region (Radial Flow Region)

The free jet region is further classified into three sub regions:

- Potential Core Region,
- Developing Flow Region, And
- Developed Flow Region.

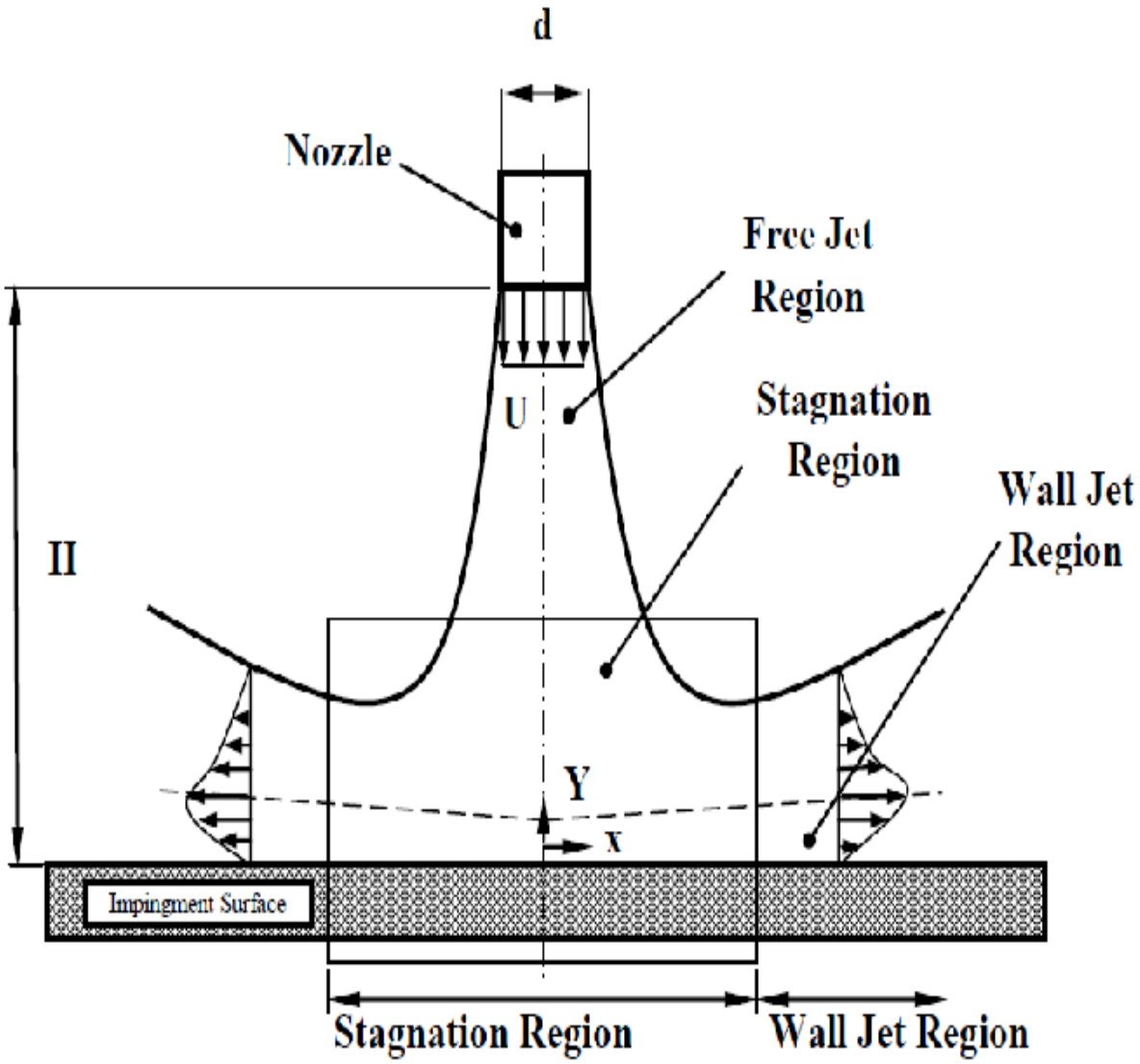

Figure 1.4: Physical Model of Impinging Jet [Shi Yuling, 2004]

1.5 Microchannel Heat Sink Applications

There are a large number of applications of microchannel heat sink. Some of them are shown in the figure 1.5.

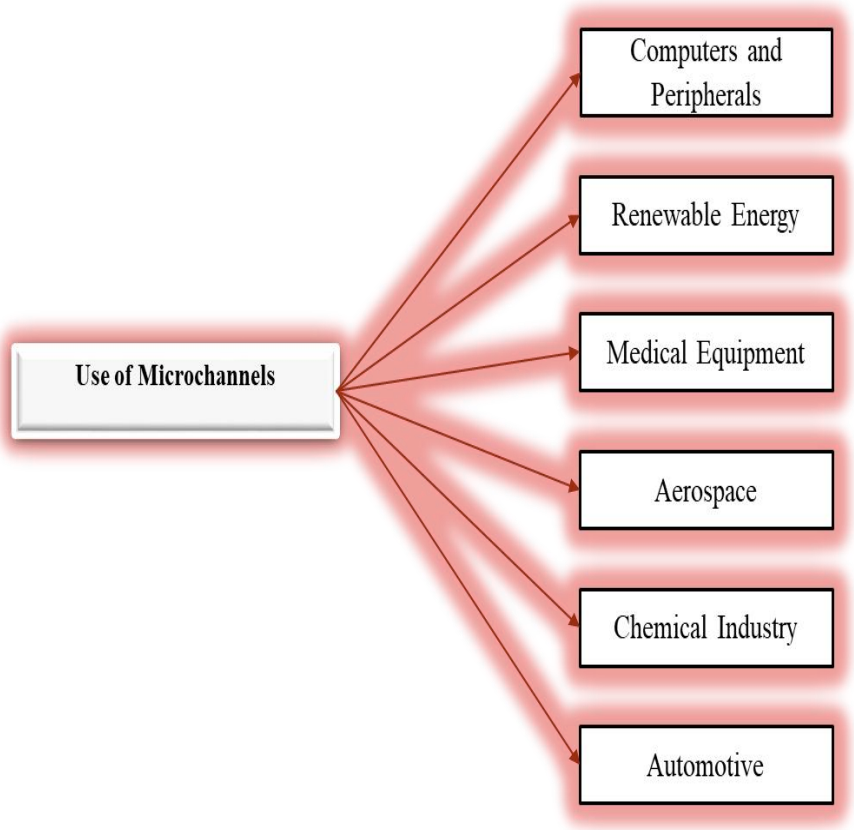

Figure 1.5: Applications

CHAPTER - 2

LITERATURE REVIEW

2.1 Introduction

This chapter describes the general familiar information related to jet impingement heat sink in a microchannel with Nano fluids. In this chapter various papers are reviewed that have information related to microchannel flow.

2.2 Review

2.2.1 Heat Sink

Chapman, C. L et al. [1994] Tested heat sink of aluminum with fin which was extruded and comparative study was made with rectangular pins which were of the cross cut type and pins of elliptical shape. The testing was performed for different factors like drop in pressure, thermal conductivity, surface area and formation of boundary layer. In case of elliptical pin, the vortex was found to be reduced and hence no boundary layer formation. Extruded shape found to be performing better than the other two.

Seo Young Kim et al. [2001] accomplished the numerical study in case of a heat sink with foam of aluminum. The thermal attributes were of the importance for the study. Two factors were found to be most important for the heat transfer change. One was permeability and the other one was effective thermal conductivity.

Kim, SY, & Webb, RL [2003] Studied the phenomenon of convective thermal resistance fie different types of heat sink. Heat sinks taken for study are of plate fin type, heat sink with offset

strip fin and sink of round pin fin type. It was found from the results that higher thermal resistance which was of the convective nature was obtained in thermal sink with pin fin of round shape. Also when compared heat sink of plate fin type shows more thermal convection resistance than offset strip heat sink. There was a decrease in the thermal performance as and when there was a decrease in the offset strip length.

A.Li, H.-Y et al. [2005] explored the performance of heat sink with the help of infrared thermograph. The design variables selected were Reynolds number, fin width, fin height, nozzle and fin tip distance and heat sink type. Thermal resistance was taken as response variable. Results showed that thermal resistance is inversely proportional to Reynolds number. Thermal performance can be increased with an increase in the width of fin but corresponding to a suitable Reynolds number. When comparison was made between fin width and height, it was observed increase in the width of fin is more prominent in decreasing the thermal resistance as compared to increase in the height of the fin. As far as geometric dimensions are concerned, Reynolds number plays an important role. At a lower value of Reynolds number, the effect of geometric dimensions is more on the thermal performance as compared to the higher values of Reynolds number.

Mahalingam, R. & Glezer, A. [2005] found that fabricated fluid jet heat sink in which air is used as a fluid was more effective in terms of dissipation of heat as compared to the thermal sink in which air was forced to flow with the help of a fan. The design of the same was discussed for heat dissipation in case of components having high temperature problems. The value of coefficient of heat transfer was detected higher. The case was analysed both for natural and forced convection conditions. With the help of pressure modifications jets were created. Higher efficiency was found in case of heat sink with synthetic jet.

Li, H.-Y. et al. [2007] identified the performance of heat sink with pin fin and impingement of confined nature. The solution was performed using numerical simulation methods. The effects of various design parameters were studied on the thermal resistance. Reynolds number, fin height, fin width and number of fins were selected as the design parameters. It was found from the results that with the increase in Reynolds number, thermal resistance decreases. But there was a reduction in this trend with further increase in the Reynolds number. Inverse relationship was detected in case of fin height and thermal resistance. Similar trend was observed in case of thermal conductivity and resistance. In case of number of fins, with the addition there was a drop in thermal resistance at first but after that decline was detected.

Li, H.-Y et al. [2007] studied sink attributes using confined impinging numerically. The effect of diverse parameters was explained on R_T. As the value of Re surges, R_T gets decreased. Deduction from end effects was that with the surge in the fin height, thermal accomplishment gets improved. Also the rate of decrease of R_T deteriorate with the increase in height of fin. Also it was observed that the optimal width of the fin is a function of Re. As Re increases it also increases. R_T is inversely proportional to thermal conductivity. The presence of the plate upper side increases R_T.

Chiang, K. [2007] considered the various parameters of PPF used in the heat sink with the application of convection for the heat transfer improvement. The aim was to adopt the criterion of extended surfaces. Design was based on RSM. Performance was studied in terms of resistance of thermal and drop in pressure. Experimental set was used to explore the design variables. Two factors fin height and distance between the fins found to be affecting the effectiveness.

Li, H.-Y. & Chen, K.-Y. [2007] discussed that with the increase in Reynolds number, thermal resistance decreased. But the rate was low. This was the case in thermal sink with plate fin with the scheme of infrared thermography. The result of design parameters like Reynolds number, width

and height of the fin was analyzed on the performance in terms of temperature. Increasing trend was seen in between Reynolds number and optimal distance of impingement. Initially inverse trend was observed in between width of fin and resistance. But after a certain value resistance surges rapidly. As compared to the fin width the influence of fin height seems to be less.

Chandratilleke, T. T. et al. [2009] extended a novel idea in a heat sink which was based on the micro channel to increase the removal of heat. Concept of synthetic jet was introduced for the numerical simulation. This concept of synthetic jet gave enhanced thermal properties. It was observed from the results that this technique gives almost sixty times more rate of heat transfers as compared to simple natural convection base sink. Also in differentiation to channel based flow it gives almost 4 times of Q. So this type of technique is very useful in electronic components which requires high rate of cooling.

Naphon, P. & Wongwises, S. [2010] investigated experimentally thermal properties in CPU of computer. Heat sink with mini rectangular fin was taken for analysis. Real operating conditions were taken. Study was performed under no load and full load conditions. Comparative study was performed for conventional liquid cooling system and liquid jet impingement system. It was found from the results that jet impingement system is more efficient than the conventional system. But there is a disadvantage that it leads to increase in consumption of energy. Also the results are of the real life importance for the design of computers.

Escher, W. et al. [2010] presented combination of heat sink of ultra-thin nature, micro channel, impinging jets. Numerical scheme was proposed for the analysis in three dimensions. A new design was presented in which the inlet was taken tapered and outlet of channel was expanding. Due to these uniformities was as much as 96 %. The impact of different parameters like width of channel, pumping power on the performance in terms of temperature and flow was investigated.

X. Song et al. [2014] Computational fluid dynamics and optimization technique based on surrogate model were implemented in case of a thermal sink with plate fin to study the thermal achievements in the form of thermal resistance as the objective function. The validation of Computational fluid dynamics results was done with the help of experimental values. The interrelation between the design variables and the temperature was pointed out. The gap width was noticed to be the most prominent variable among all the design variables. Also the combination of two techniques is detected to be a promising tool in case of jet impingement heat sink design.

Azizi, Z. et al. [2015] examined the thermal sink with micro channel of cylindrical shape. At 0.3 % of fraction results were noticed higher in terms of h. Maximum twenty-three percent increase in the Nusselt was initiated.

Ariz, M. et al. [2015] Executed numerical analysis in 3 dimensions with low values of Reynolds number. The analysis was performed in case of coupled heat sink of copper based. Diameter of jet, diameter of effusion hole etc. were taken as design variables and the end result of these parameters were studied with the heat transfer rate. It was found from the results that with higher value of the ratio of standoff and diameter of jet provide low value of thermal resistance. Also the interrelation between the power of pumping and overall thermal resistance was established in the study.

Chingulpitak, S. & Wongwises, S [2015] focused on the available literature based on the direction of flow of fluid through the thermal sink. Also the behaviour of the fluid flow which effects the efficiency of heat sink was discussed. The discussion was based on experimental work. It was suggested that more research was needed to understand the drop in pressure and other attributes.

Gong, L. et al. [2015] made comparative study using different types of heat sink. The objective of the study was based on the refinement of the thermal sink structure. The attributes of heat sink

were studied using numerical methods. The concept of field coordination was accepted to analyze the attributes of heat transfer.

Zheng, L. et al [2016] examined the two shapes of the microchannel from the thermal and hydro point of view. In the first case circular microchannel was taken and in the second case annular microchannel thermal sink was analyzed. Reynolds number, size of dimples and arrangement were considered to be design parameters. Outer dimples showed the better heat transfer attributes as compared to the inner attributes in case of annular thermal sink. Negligible effect was detected for the arrangement case. Circular case was noticed to be effective from the point of view of energy savings.

Li, B. et al. [2016] explored numerical as well as experimental study for the differentiating analysis of heat sink of radial shape with and without chimney. The design variables selected were angle of orientation, number of fins and plate and chimney distance. The chimney based sink was predicted to be better as compared to the without chimney. Higher performance was found at angles zero degree and forty-five degrees. At ninety-degree least performance was detected.

Zheng, L. et al. [2016] executed numerical study for the two different micro channels with lumps. The outcome of size of the lump, Re and the lump arrangements was concentrated. In the first case microchannel with circular configuration was taken and in the second case annular configuration was assessed. The first case with lump exhibited deficient capability of heat transfer. With the increase in the lump size in oriented lump, the performance increased. Unacceptable performance was characterized in staggered lump. Outer lump was found to give satisfactory results in differentiation to the inner one. The positioning did not find to affect the performance level. In terms of saving of power lump cases were found superior in comparison to the without lump case.

Tang, Z. et al. [2017] done experimental investigation in heat sink which was of the array cone in shape with impingement of jet. Numerical simulations were also performed to determine the thermal attributes. The reaction of the cone sink parameters was studied on Nusselt number (Nu). Comparative analysis was made for the cone sink and plate heat sink for different cone angles. The former was found to be better one. With surge in Reynolds number this effect was detected more. Direct relationship was observed in between Reynolds number (Re) and Nusselt number (Nu).

Nakharintr, L. & Naphon, P. [2017] proposed a heat sink with one jet for the scrutiny of features in terms of heat dissipation for the magnetic field applications. Brass was used for the modelling of thermal sink which was made using EDM for the specifications. Different concentration of titanium oxide particles was used with water for working fluid. Differentiation was made for the studies with and without magnetic field. Nusselt number escalated in the presence of magnetic field and this value increases with increase in the strength of field. Pressure fall not affected with the concentration of fluid.

A. Kim, T. H et al. [2017] proposed the sink concept using plate fin along jet impingement of uniform air for performance analysis. The proposed relations and the available experimental results were compared. From the previous studies it was found that these studies were based on the non-uniformity. And hence uniformity at the inlet plays an important role on the performance. These correlations can be helpful in determining the performance deviations during actual and ideal conditions. Also using these correlations, the end result of height of fin on the design parameters were studied. Positive relation was seen between the height of fin and the performance of heat sink. As the height is increased from 0.005 m to 0.025 mm, the performance also increased around 60 percent.

Ming, T. et al. [2018] initiated the idea of dimples in connection with the heat sink with micro channel and impingement of jet. This was done to upgrade the heat transfer attributes of the heat sink. The diameter of dimples was differed and the fluid flow attributes as well as thermal attributes were analyzed. Also the distribution of velocity and drop in pressure were studied. From the results it was decided that with the addition of dimples in the heat sink the thermal performance increased. The convex nature of dimples increased the efficiency. In the study diameter of dimple was optimized. There was an inverse relation between the rate of mass flow and cooling surface temperature. Also lower pressure drop was observed with dimples.

Jian Wang et al. [2019] predicted the heat as well as flow properties in thermal sink with finned foam of copper experimentally. The cooling was provided with the help of slot jet impingement as well as with the help of axial fan. Comparative study was made for the heat sink of conventional type and with foam. It was observed that the finned foam type heat sink was having better performance in contrast to the heat sink without foam. The height of the thermal sink also affects the achievements in terms of temperature and heat.

Duan, Z. et al. [2019] performed numerical simulations in a thermal sink of plate fin type which was cooled with the help of an impinging jet of rectangular shape. Numerical simulations were detected in conformity with experimental results. It was simulated that with augmentation in width at inlet of the jet, fall in pressure dwindles for a constant value of flow rate. Also as the height of fin was increased, pressure drop increases. The sink with and without elliptic bottom nature was discussed. Without elliptic profile, drop in pressure was more as compared to the other.

Hempijid, T. & Kittichaikarn, C. [2019] simulated the two types of thermal sink using computational fluid dynamics as a tool. Direction of flow at inlet and outlet of thermal sink was assumed to main parameter to analyze the pressure and thermos characteristics. The V- shaped

thermal sink was noted to be better in terms of thermal performance in differentiation to the other at seventy-five-degree angle. Also the vortices developed at the inlet portion were noted to be affecting the performance of the system. Offsetting the inlet and outlet was found to be affecting the effectiveness of the thermal sink.

Freegah, B. et al. [2019] introduced a new design of thermal sink of plate fin type. Pins of semi round shape are attached to the thermal sink to augment the efficiency.

Ulises Gonzalez-Valle, C. et al. [2019] experimentally explored the performance of the heat sink using water in terms of fluid flow and temperature effects. Three design variables are selected for the study. These were number of nozzles, flood chamber depth and surface features. For sixteen, thirty-two and sixty-four number of jets the variation was observed minimum in case of drop in pressure. Largest temperature of the core was noticed with thirty-two nozzles heat sink. Pumping power and thermal resistance were also discussed to study the attributes. Heat sink was optimized with lowest value of temperature and power.

Yabo, W. et al. [2019] explored the differentiating analysis between conservative heat sink of cross flow nature and the heat sink with jet inlet at the center and numerous outlets. In the conservative model the inlet and outlet were on the opposite sides. It was predicted from the results that in case of conservative sink more energy is required as compared to the other one despite of the higher Nusselt number in conservative sink. Sink having inlet at center vertically is found to be more efficient as compared to the conservative one. Also lower resistance was detected in case of former.

Hussain, A. et al. [2019] compared thermal attributes of proposed and conventional design of heat sink with the help of computational fluid dynamics (CFD). The CFD results were compared with the available experimental data. It was found from the discussion that fillet profile and flow

direction put a great effect on the performance. Similar types of effect were noticed of both the parameters with resistance and temperature of the base of sink.

Hadad, Y. et al. [2020] studied that there was small drop in pressure in thermal sink of water cooled impingement type. Due to this reason these are preferred more as compared to thermal sink of parallel flow type. To study and analyze the performance of heat sink a numerical model was initiated. Both the distributor and collector were also included in the model. This was because of their effect on the performance of heat sink. Design and response parameters were selected. Design parameters were based on the geometry. Hydraulic resistance and thermal resistances were taken as response parameters. It was predicted from the results that geometry of channel has more effect on the drop in pressure in the sink as compared to the geometry of impingement. Sensitivity based investigation was also performed.

Li, Y. et al. [2020] used both numerical and experimental methods in case of AFPF sink. The influence of porosity and density of pore was studied. Square cross section was taken for the channel geometry. The investigation was carried out under steady state conditions. The two sinks AF and AFPF were compared and AFPF was found better as compared to the other one. With increase in the pore density, the heat transfer increases in both the cases. The model was concurred with the experimental values in case of temperature and resistance. AFPF demonstrated better efficiency as compared to AF in terms of convection coefficient. Permeability effects were also taken into account.

2.2.2 JET IMPINGEMENT

Lee, D. & Vafai, K. [1999] presented a relative analysis of cooling in case of impinging jet and micro channel. The study was performed for the target dimension which was taken as prime parameter. It was analyzed from the studies that for smaller target dimensions' micro channel heat

transfer is suitable while in case of larger target dimensions' jet impingement is most suitable. In case of jet impingement technique with a less drop in pressure there is large requirement of rate of coolant flow while in case of micro channel there was a small requirement of rate of coolant flow with a large drop in pressure.

Brignoni, L. A. & Garimella, S. V [1999] executed experimental study in case of air jets used with thermal sink of pin fin nature. The study was carried out at different Reynolds number. The outcome of nozzle size was tested for a given value of Re. Greater value of coefficient of heat transfer was detected in case of less nozzle diameter. Re was taken for the turbulent flow condition. The distance between the nozzle tip and surface targeted was kept constant. Design parameters were reported by considering thermal sink = f (Re). Reynolds number is modified from 5000 to 20000. Also the value of thermal resistance was noticed to be low for less nozzle diameter.

Shah, A. et al. [2004] discussed the abstraction of blower unit with the application of impinging. Numerical study was performed for the characterization. Discussion was made for the distinct configurations of fin. The thickness of the support of the sink was varied. Distinct three values for flow rate of air were selected. Aim was focused on the excellent design of sink so that the probability for the enhancement in the heat transfer can be run. The focus was achieving the same without increasing the pressure drop significantly. The two cases were compared. In the first case material was removed from the fin near the center of the sink. In the other case material was retained. In the material cutting case lower value of fall in pressure was spotted.

Seo Young Kim et al. [2005] performed experimental study in case of multi jet impingement. Investigation was performed by taking heat sink with aluminum foam. The effect of various parameters like pore density, velocity of jet etc. was investigated on the Nusselt number. Comparative study was also made for single and multi-jet impingement. When the thermal

performance was studied for one jet impingement it was found that performance is high in thermal sink with aluminum foam than the heat sink with plate fin. The value observed to be eight to thirty-three percent higher. Also in case of multi jet impingement the value is two to twenty-nine percent more. It was also observed that with the increase in spacing between the jets the performance in terms of cooling decreases with aluminum foam. It was also focused that the single jet impingement shows less performance in comparison to multi jet impingent heat sink.

Kandlikar, S. G. & Bapat, A. V. [2007] reviewed cooling with spray and microchannel with impingement of jet. Comparative study was made for thermal and hydraulic performance of heat sink.

Barrau, J.et al. [2010] utilized the concept of impingement of jet with the micro- channel. The improvement in the temperature stability was also taken care of in this case. The testing of geometry was done experimentally. This lead to the crating a path for the different design parameters optimization.

Naphon, P. & Klangchart, S. [2011] used finite volume method to solve the equations in three dimensions in case of impingement of jet in a heat sink. Fins of rectangular shape were used in the heat sink. Study was focused on the properties of heat and flow of fluid. The results were found in the sincere agreement with the available results. Also the location of port at outlet were discussed in connection with the transfer of heat attributes.

A. Husain et al. [2013] carried out parameter and optimization based studied for cooling of electronic components. Jet impingement heat sink based on silicon was used to analyze the thermal properties for laminar flow conditions in three dimensions. Study was performed using Navier-Stokes equations for steady state incompressible conditions. The optimization was done using two design variables. First variable was taken as the ratio of channel height and diameter of nozzle and

the second variable was the ratio of diameter of the nozzle and spacing in the jets. For a heat flux of 1000 KW/m^2 a temperature rise of 339 K was obtained at a pressure drop of 24 KN/m^2. For the conservative analysis convection and radiation heat transfer is not considered at the outer walls.

A. Husain et al. [2013] studied the cooling system with jet impingement with the help of a finite volume solver. The aim was to dissipate the heat in case of Light emitting diodes used as arrays. The analysis was performed numerically in three dimensions for the turbulent flow conditions with steady state. Different combinations of array were selected to analyze and evaluate the drop in pressure and resistance. When the rate of flow was high, lower value of thermal resistance was obtained. For optimization four jet array combinations was selected and the design variables were analyzed.

A. Husain et al. [2016] forwarded a heat sink of hybrid nature with jet, pillar and micro- channel. Performance was studied and the high h was noticed in the case when ratio of jet pitch and diameter of jet was low. Also the pumping power was analyzed.

A. Husain et al. [2016] Different flow schemes were compared in case of jet impingement stem of cooling. Heat sink with different array combinations with the ratio of height of channel and diameter of nozzle as 2 was analyzed in terms of temperature increase; drop in pressure, thermal resistance and heat transfer coefficient. Lesser values of pressure drop and higher conformities were found in case of unconfined flow. In case of flow extraction h was found to be higher but low value of thermal resistance. A trend of increasing uniformity in temperature and decreasing performance was observed with increase in Reynolds number. As far as higher uniformity in temperature is concerned, the unconfined flow scheme seems to be better as compared with the other two.

Husain et al. [2016] introduced the novel concept of jet impingement heat sink with microchannel and pillars arrangement.

Husain, A. et al. [2016] differentiated the performance of a cooling system with impingement of jet. The comparison was made for different schemes of impingement of jet with confined and un confined wall. Study was made for three dimensional conditions for attributes in the form of temperature and drop in pressure. More uniformity in temperature and less drop in pressure was observed in case of unconfined flow. Positive relation was found in between Reynolds number and uniformity in temperature. Also inverse relation was detected in between Reynolds number and thermal sink performance. The rise in temperature and drop in pressure showed a negative relation with the number of jets. As the Reynolds number of jet is increased, thermal resistance deceased. Same was the case in relation to pumping power.

Bahaidarah, H. [2016] examined the PV system with impingent of jet in the two cases; PV system which was not cooled and cooling with impingement. The analysis was spotted in the warmer weather conditions. Six models of different characteristics were associated to determine the overall accomplishments of the system. The study was performed numerically as well as experimentally. The two exhibited sincere concurrence with each other. For the set conditions up to a certain value of h, performance increases but after this value no significant improvement was detected. The study was also concentrated for different months of a year. Maximum temperature in two different months were 342 K and 320 K for the uncooled case.

De Oliveira, P. A. & Barbosa, J. R [2017] presented the concept of heat sink with two phase jet. The end results of the design parameters were analyzed on the objective parameters. The diameter of orifice, applied load and the stroke of piston of the compressor were taken as parameters of design. It was explored that orifice with diameter 0.0005 m gives more thermodynamic

performance as compared with 0.0003 m diameter orifice. This was obtained when the length of jet and temperature of high temperature reservoir was fixed. In case of high diameter orifice pressure ratio obtained was low. And due to this reason there was less power consumption in compressor. For the 0.75 and 1 stroke of the compressor IInd law ratio was quite higher.

Chiu, H.-C. et al. [2017] fabricated heat sink prototypes with pin fin of micro nature. Both numerical and experimental studies carried out to benchmark the performance of thermal sink. Two geometrical parameters were included in the study. These were radius of fin and porosity of fin. Investigation was done for geometrical parameters and drop in pressure Vs performance of sink for a constant heat flux = 30 W/cm^2. No significant role of sensitivity was found in case of thermal resistance. Increasing trend was observed in case of flow rate with increase in porosity.

Zunaid, M. et al. [2017] studied heat characteristics using different heat sink materials. Study was performed for different Reynolds numbers.

Zunaıd, M. et al. [2017] Introduced the proposed structure of micro channel which helped in fluid mixing and hence increase in heat transfer rate.

Abo-Zahhad, E. M et al. [2019] Compared the jet impingement cooling with micro channel to simple jet impingement without micro channel. The study was made in case of photovoltaic structure of high concentration in both with and without micro channel. Five different designs of heat sink were analyzed for cell temperature. From the findings it was concluded that the hybrid scheme is more effective in contrast with simple jet impingement in terms of cell temperature reduction as well as in the uniformity of temperature. A temperature reduction of around 13 ^{0}C was observed for one of the case and in another case it was 20 ^{0} C when the rate of mass flow was increased at the inlet. Also there was an improvement in the efficiency of cell.

Abo-Zahhad, E. et al. [2019] Compared the case of jet impingement with the same case with microchannel. For the analysis zone of impingement and width of channel had been taken as the parameters. It was estimated from the study that in case of microchannel effectiveness was more as compared with impingement only. Also temperature uniformity was detected in microchannel with impingement. Friction losses were negligible and the overall efficiency of the system was increased. For low values of rate of flow increase was found in terms of effectiveness.

Wiriyasart, S. & Naphon, P. [2020] Presented the jet impinging technique with several fin shapes. Taking circular, rectangular and conical fins parametric study was performed. The inlet temperature of the coolant, mass flow rate of liquid was also taken for parametric analysis. Circular fin was observed to be giving high thermal performance as compared to the other two. For rectangular fin it was 12 percent higher and 25 percent for the conical fin. So this study can be implemented which taking care of design of thermal systems using different fin shapes.

2.2.3 NANOFLUID

Chein, R. & Huang, G. [2005] executed the Nanofluid consequences on the effectiveness of sink with micro channel of silicon. Water -copper was used as coolant. One phase fluid based study was undertaken. Relations based on the experimental work were discussed. Two different geometries of microchannel sink were compared in the investigation. Nanofluid consequences on the performance were noticed in the positive form.

Shalchi-Tabrizi, A. & Seyf, H. R. [2012] deliberated the properties of heat in a micro sink using Aluminum – water as Nanofluid. Two design criterion were selected These were concentration and radius of particle. Numerical interpretation was aimed. It was found from the interpretation that as the radius of particle was decreased, thermal properties increased. Also increasing fashion was noticed when particle concentration was increased. But with the use of Nano fluid negative

reaction was the outcome with change in concentration. Disorderness was also noted as surged with growing trend of Reynolds number and concentration. FVM was used to solve the governing equations in three dimensions.

Naphon, P. & Nakharintr, L. [2012] explored the thermal attributes of a heat sink with mini fins of rectangular shape with the Nanofluid. Aluminum was taken as the sink material. For the preparation of Nano fluid, water and titanium oxide were taken. The results were distinguished for the case with water and with Nano fluid. The characteristics of thermal sink were studied with the design parameters. Higher value of Nu was observed with Nano fluid. Enhancement in drop in pressure was noted.

Selvakumar, P. & Suresh, S. [2012] executed experimental study for 0.1 and 0.2 % volumetric concentration of copper oxide – water Nanofluid in a copper heat sink. With the application of Nano fluid surge in convection coefficient was observed for different concentrations. Almost thirty percent increment was noticed for 0.2 % concentration. Also surge in pumping power was detected using Nano fluid. The increase was almost fifteen percent.

Karami, N. & Rahimi, M. [2014] done experimental investigation to describe the effectiveness of PV cell using Nano fluid. Plate with micro channels of rectangular shape was captured. The effectiveness of the Nano fluid was assessed. An improvement of about twenty-seven percent was noticed at 0.01 % of concentration. In this study friction factor and Reynolds number were determined. The flow is found to be laminar in the channel. Extraordinary results were seen for reduction in temperature due to the presence of nanoparticles.

Selimefendigil, F. & Öztop, H. F. [2014] predicted the flow and heat characteristics for different variables like frequency, Re and concentration of Nano particles. Unsteady state conditions were adopted for the solution using FVM. Heat transfer augmentation was found from the results. The

results were found better at a Reynolds number of hundred. Also the Nusselt number was augmented.

Lelea, D. & Laza, I. [2014] Performed numerical investigation based on the finite volume method using Nanofluid in case of a micro heat sink. The results of Nano fluid were compared with the water. The geometry of the heat sink was considered for more than one inlet with tangential flow. Low velocity conditions were assumed for the examination of the simulation. The range of the Reynolds number was in between 15 to 100. Constant value of heat flus was taken at the base. With the increase in the flow rate of mass, decreasing trend was noticed in temperature of substrate. Pressure fall was more in case of Nano fluids for a constant value of pumping power.

Lelea, D. & Laza, I. [2014] executed numerical analysis in thermal sink with micro channel with the application of swirl flow and water- aluminum oxide in different concentrations as coolant. The outcome was compared with the simple water case. K and μ were higher in case of Nanofluid but c was lower as compared to water. Multiple inlets in sink were used for the exploration of the study. The highest temperature of the surfaces was noticed better with Nano fluid for a constant value of Reynolds number.

Miry, S. et al. [2015] employed the sink performance using aluminum oxide and titanium oxide based Nanofluid. The achievements were noted for different Reynolds number. With the rate of flow, fourteen percent increment was noticed in the surface coefficient with the use of Nano fluid in contrast to water. The increase in pumping power and resistance could be neglected in balancing with the performance. Eight percent augmentation in Nu was detected with Nanofluid. Also the application of Nanofluid caused the uniformity in temperature for the sink.

Lam, P. A. K. & Prakash, K. A [2016] presented optimization technique for impingement cooling using Nanofluid. The objective was to maximize rate of heat transfer and minimize generation of

entropy. Total three design variables and three response parameters were selected. With an increase in Reynolds number, increasing pattern was seen in Nusselt number and generation of entropy. Similar type of pattern was detected in case of concentration of nanoparticles. Also the flow pattern was investigated. Algorithm was used for the optimization.

Radwan, A. et al. [2016] adopted a new scheme using MCHSWNF in case of LCPVT systems using aluminum oxide and silicon carbide with water as coolant. Numerical simulations were predicted to determine the cell efficiency. From the outcomes the use of Nanofluid determined to be very effective as compared to the without Nanofluid. This was dependent on the concentration ratio. Nineteen percent increase was predicted in the efficiency and the temperature was reduced to 311 K.

Sun, B., Qu, Y. & Yang, D. [2016] used copper water Nanofluid which was prepared experimentally. Positive correlation detected between fraction and heat dissipation performance. At a height of 0.006 m influence was maximum. Pressure drop was not significant. Circular shape was found more effective as compared to the square for the nozzle. Angle of jet was positive effect on the performance.

Rehman, M. M. U. et al. [2017] evaluated the behavior of impinging jets on a heated plate. The material of the plate was copper. Different coolants were used for the study. Turbulence model was used for the equations in three dimensions. The properties were found in case of water, Nano fluid and phase change material. Results were correlated with experimental values. Aluminum oxide and phase change material was mixed with water and the results of this mixing were evaluated. The properties were detected best in case of phase change material. Improvement in attributes was also observed in case of Nano fluid but was less as compared to phase change material. The value of stress was more in case of Nano fluid and PCM.

Hasan, H. A. et al. [2017] assessed the execution of collector with impingement of jet in terms of thermal and electrical parameters. Thirty-six jets were used to push the water in the collector. Three cases were taken for study. These were silicon carbide –water, titanium oxide – water and silicon dioxide – water combinations. From the results the efficiency in the first case was detected maximum. Also it was noticed that the efficiency with nanoparticles was increase as compared with a conservative collector.

Zahmatkesh, I. & Ali Naghedifar, S. [2017] concluded that the response in terms of oscillation depends on the Re, Gr and Dr. It has no relevance for porosity and proportion of nanoparticles. The phenomenon of convection was used in the impingement cooling. The plate was horizontal and heated not completely. But the rate of heat transfer is high with surge in porosity and nanoparticles proportion. Situations was reviewed in the conflicting case between flow jet and buoyancy.

Arshad, W. & Ali, H. M [2017] deduced from the experimental results that heating power change caused the increase in Nusselt number in the case of titanium oxide – water Nano fluid but the same was not the case in water. Inverse trend was detected in case of heating power and drop in pressure. The case was discussed in a heat sink with mini channel. TiO_2 was used with fifteen percent concentration.

Arshad, W. & Ali, H. M. [2017] analyzed the hydraulic behavior with water and graphene based nanoparticles in case of sink with integrated fin. The experiential study was performed for different values of heat flux and ten percent concentration of nanoparticles. From the results closest affinity was noticed between heat input and transfer of heat. Same was the case for pumping power. At the lower values Nano fluid attributes were observed better.

Ziaedin Miry, S. et al. [2017] executed water aluminum oxide based study in a novel heat sink for the performance advancement. Elliptical section of the heat sink was proposed as a novelty in the study. Relative analysis was discussed for the cylindrical and elliptical sections. Positive pattern was seen in between concentration of Nano particles and convection coefficient. Negative pattern was detected for the resistance and rate of flow. The base temperature and the concentration relation was found in the reverse trend. Due to the density drop in pressure and Nano fluid fraction were detected in a positive trend. Fall in pressure was very insignificant for very small values of the rate of flow.

Wang, R. et al. [2017] used grooves of trapezoidal shape arranged in a series in MCHS with water aluminum oxide as Nano fluid. The aim was to increase the efficiency with increasing PV systems. From the results two phase model was preferred over single phase model. Optimization for the geometrical variables was explored. Same was adopted for the physical parameters. The study was performed using numerical simulations for different Reynolds number. Temperature. Flow and viscosity correlations of Nano fluids were discussed. Thermal performance was noted in positive correlation with Re and fractional volume.

Selimefendigil, F. & Öztop, H. F. [2017] examined a surface which was curved party using GWRFEM and COBYLA with impinging jets. Isothermal conditions were adopted for the surface udder study. Curved effects were noted to be significant at higher value of Re. Higher Nusselt number was saved for the curved shape. Also linear correlation was detected between Nusselt number and Nano fluid fraction. Vortices were found at the jet inlet.

Ali, H. M. & Arshad, W. [2017] executed experimental study in case of channel heat sink with different angles of channel as 22.5^0, 45^0 and 90^0. The reference for these angles was taken as x direction. The study was done for water-GNP Nano fluids at constant value of heat per unit area.

Copper was taken as the material for the sink. In case of 22.5^0 resistance was low and hence highest performance was noticed. As the angle decreased, h increased. LMTD decreased with increase in rate of flow.

Wang, R.-T. & Wang, J.-C. [2017] prepared the aluminium oxide Nano fluid. Concentration influenced the efficiency.

Nakharintr, L. et al. [2018] presented the characteristics using titanium oxide Nano fluids using impinging jet. Heat sink was made from aluminum. Experimental study was undertaken to note the trend of Nusselt number, resistance and pressure fall with the use of Nano fluid. Nusselt number and fractions were found in the increasing trend.

Zunaıd, M. et al. [2018] studied the microchannel with different materials. Copper predicted the highest performance.

Naphon, P. et al. [2018] examined experimentally the different schemes to enhance the rate of heat transfer. Impinging jets in a channel of micro nature with titanium oxide Nano fluid were used to enhance the characteristics related to flow and temperature. The suspension, radius of nozzle and the rate of mass flow were selected as variables. The results indicated that with the use of Nano fluid heat transfer attributes were improved. No significant increase was noticed in drop in pressure. The elevation of jet also affected the performance. With the decrease in the elevation the coefficient of heat increased. So the suitable choice of different parameters is very crucial.

Siavashi, M. et al. [2018] scrutinized the heat sink of cylindrical shape and porous nature with flow impingement in the form of Nano fluid. Uniform flow condition was adopted. The conservative equations were solved numerically and supported with the help of CFD simulation. Results indicated enhancement in performance of sink with the adoption of Nano particles. Also the influence of aspect was discussed. In the study non-dimensional variables were formed for the

solution. The end result of non-dimensional variables like Reynolds number, Prandtl number, Nano fluid was studied and evaluated. The response variable was selected as Nusselt Number. Re and shear stress were found in positive trend. Inverse trend was found in between aspect ratio and heat. Nano particles increase the Nusselt number.

Selimefendigil, F. & Öztop, H. F [2018] assessed the effectiveness in the name of heat and movement of fluid in JIHSWNF. Hot surface was taken for study which was maintained at a constant temperature along with cylinder which was rotating and adiabatic. The boundary conditions used in the equation were solved with the help of finite volume solver. The relation between the rotation of the cylinder and the cooling performance was investigated. The minimum and maximum limits for the Reynolds number were assumed to be hundred and four hundred. The position of cylinder horizontally also affected the properties. When the two cases i.e. with and without rotation, Nu was assessed as increased by twenty percent in case of rotation which was clockwise. The whirl movement was squashed due to rotation.

Selimefendigil, F. & Öztop, H. F [2018] performed numerical investigation in case of JIHSWNF using two jets. Constant temperature conditions were taken for the surface. Equation were solved with GWR method. It was found from the studies that the convection coefficient deteriorates in the presence of magnetic field. It reduces the thermal attributes of heat sink. The use of Nano particles tried to improve the aspects of fluid and heat. In the absence of field, Nusselt number is higher at higher value of Reynolds number. The problem was solved with steady state conditions.

Alirezaie, A. et al [2018] Used two Nano fluids based on ethylene glycol for the study and comparative analysis had been made for the cost of preparation of Nano fluid with the thermal proportion. Results had been validated with the modeling of neural network. So the analysis presents idea about the economic concept of Nano fluid. A new relation was also proposed for the

thermal conductivity of Nano fluids. More focus is required on the environmental effects of Nano particles and their use by engineers due to the toxic nature of some of the particles.

Naphon, P. et al. [2019] explored the impingement phenomenon with the application of Nanofluid. Two techniques were employed to study the characteristics. One was computational fluid dynamics and the other one was artificial network. Results were detected in the reasonable limits with the experimental values. Error detected in the solution was about one percent. Different layouts of micro channel were studied. Results indicated for further improvement in performance of heat sink.

Izadi, A. et al. [2019] used the concept of non – dimensionalization and similarity to solve the Navier – Stokes equations of partial differentiation nature. Copper water based Nanofluid was used in the numerical exploration of fluid movement and heat transport characteristics. Concept of jet impingement with uniformity of velocity and without uniformity was taken care of in the study. Partial differentiation equations are changed in ordinary differential equations. The end result of parameters like suspension of Nano fluid was discussed on the accomplishments. The results were validated with the commercial simulation results. It was noticed from the results that Nano fluid concentration and the rate of heat were in direct relationship. The results of temperature and velocity were executed in non-dimensional form. The performance was found to more in case of non-uniformity as compared to uniformity. Flow and temperature were found to be in inverse relation with porosity.

Sarafraz, M. M. et al. [2019] prospected the outcome of Reynolds number and heat flux for the GNP –water Nano fluid in a channel. Experimental outcome was studied to measure the surface coefficient, factor of friction and surface coefficient. In this case coefficient was increased by eight

percent and same was found in the case of Nusselt number. The accomplishment of the channel system was found to be augmented. This was in spite of the pressure value drop.

Bahiraei, M. et al. [2019] recommended the use of Nano fluid instead of the pure water to increase the rate of heat transport with small increase in pumping power. For this three dimensional numerical study was performed. Higher swirl flow causes high rotational speed which in turn causes high exchange of heat. With the increase in concentration, at a rotational speed of zero radian/sec, almost 16 % improvement was seen in convection coefficient.

Ambreen, T. et al. [2019] demonstrated the plots for temperature and streamlines in a heat sink with pin fin of micro nature along with Nano fluid. Fixed value of flux 300000 W/m^2 was applied at the bottom. It was concluded from the findings that for a constant value of drop in pressure, nanoparticles increased the heat dissipation. For 1% concentration almost 16 % improvement was marked in the value of h. On the upstream and downstream side non-uniform and uniform flow was spotted respectively.

Sorour, M. et al. [2019] Conducted experimental study to investigate the Nusselt number as a function of Reynolds number, volume fraction of water dependent Nano fluid. It was predicted from the results that with an increase in Re, Nu also gets increased. Nu also increases with an increase in the volume fraction of Nano particles. The effect of influence ratio was found to be insignificant. A new correlation was also proposed for the Nusselt number. As compared to the water, positive effect of Nano fluid was observed in the investigation.

Datta, A. et al. [2019] modeled the stream function and contours of temperature using copper – water Nano fluid in a thermal sink with jet impingement. The plate considered for the study was moving and hot. At different velocities of the plate local and average heat exchange coefficient

was analyzed. Also the effect of Reynolds number in the turbulent region was studied on the rate of heat exchange. Relations for the Nusselt number has been represented. The study was carried out using numerical simulations. Re and Nu were found in positive relationship.

Ghanbari, S. & Javaherdeh, K. [2019] exploited the use of non –Newtonian Nano fluid to enhance the heat exchange coefficient. The Nano particles were used in different concentration. Different parameters like friction factor, Nu were determined for the analysis. For 0.2 % concentration of graphene, almost 39% increment was detected in heat exchange coefficient. Also 12 % increment was seen in thermal conductivity. The experimental work was performed for baffles of circular shape and perforated.

Wiriyasart, S. & Naphon, P. [2019] accomplished the experimental study in case of impingement of jet with water as well as Nanofluid. The geometry of fin was modified and the end result of the parameters like rate of mass flow, area of heat source and heat flux were studied. Inverse relation was observed in case of Re and thermal resistance. Low value of thermal resistance was found in case of Nano fluid as compared to the water. The conditions were taken for the turbulent flow.

Neyestani, M. et al. [2019] intended the novel sink of porous nature for analysis using Nanofluid experimentally. CPU unit was adopted for the experimental investigation. The consequences of volume fractions were studied on the efficiency of CPU unit. Three configuration of sink were used. One of them was inline configuration. In this configuration thermal surge was not noticed much. The second configuration for the heat sink was staggered in which heat transportation rate was noticed to be more in comparison with inline. The third configuration was porous heat sink. In this configuration highest improvement was detected. Thirty-five percent decrement in temperature was detected using porous configuration over inline.

Izadi, A. et al. [2019] exhibited analytical inspection for the application of magnetic field with Nanofluid. The same was done in case of a CPU considering viscosity effects. The base of the CPU was modelled as hot surface with jets at the top and Nano fluid passed through foam. The analytical outcomes were justified with experiment. The end results of the various parameters like Re, Da, Ec, Ha and porosity were analyzed in correlation with the thermal and fluid behavior. The first step in the analysis was to convert initial PDE into nonlinear ODE and solving these ODE for the solution. Positive correlation was detected for Da and h.

Yang, L. et al. [2020] demonstrated the application of laws of thermodynamics particularly first and second in case of sink with micro channel. Growth was established in terms of surface coefficient with the addition of Reynolds number and concentration of Nano particles. temperature, uniformity and rate of irreversibility found in decrement with the two parameters. But reverse movement was discovered in exhibition of pumping power. The Nano fluid was expressed superior in contrast with base fluid.

Anitha, S., Loganathan, K. & Pichumani, M. [2020] Investigated the performance of heat exchanger with the help of two Nanofluid. Carbon nanotube – Al_2O_3 and Fe_3O_4 were used as Nano particles in the base fluid. Reynolds number and fraction of Nano fluids were assumed to be design parameters and Nusselt number, rate of heat transfer etc. were taken as response parameters. Nusselt number and rate of heat exchange were detected to be increased with Reynolds number and rate of mass flow. Among the two Nano fluids, Carbon nanotube – Fe_3O_4 / water was noticed to be more effective. With this Nano fluid effectiveness was increased by fifty percent.

Mohammad pour, J. & Lee, A. [2020] Presented the review of impinging jets both experimental and numerical. Swirling impinging jets were examined to be more effective as compared to the conventional. When the Nano particles were added in the base fluid, increase in critical heat flux

was detected. Due to the higher values of viscosity of the fluid sedimentation type problems were observed.

Ambreen, T. et al. [2020] interpreted the heat sink with aluminum foam along with the application of Nanofluid for hydrothermal attributes. The attributes were studied in the form of Nusselt number, average heat exchange coefficient and power of pumping. Also the distribution of temperature was discussed in the form of contours. Dynamics had been explained in the form of velocity vectors and streamlines. It was noticed that the porosity of the substrate base plays an important role in the heat exchange property of Nano fluids.

Yang, L. et al. [2020] devoted his investigation for the case of two heat sink with the application of Ag Nanofluid. The effect of fraction of the Nanofluid and Reynolds number had been analyzed with the temperature of CPU and heat exchange coefficient. With the augmentation in Reynolds number, temperature of CPU was observed to be decreased. Also the temperature uniformity was more in case of Nanofluid as compared to the water. However, increase in pumping power was also seen due to the frictional effects. The investigation was performed from the 1^{st} and 2^{nd} law view of thermodynamics.

Bahiraei, M. et al. [2020] assessed the 2^{nd} law of thermodynamics in a microchannel thermal sink with water based hybrid Nanofluid. Microchannel was fitted with ribs of rectangular shape. At the interface of solid and fluid, the generation of entropy was found to be more as compared to the dead area. This generation was due to the friction and exchange of heat. Entropy generation had been observed to be more in the corners in case of solid area. The lowest value of entropy generation due to friction was detected at the center of sink. Entropy generation declined with the augmentation in Reynolds number and weight fraction of Nano particles.

Mahdavi, M. et al. [2020] computed the heat exchange attributes in a rotating disk which was circular and hot using the application of Nanofluid. Ansys fluent was employed to investigate the multiphase flow of air and Nano fluid. The end result of rotation and volume fraction of Nano particles were studied. It was predicted that at higher volume fraction of Nano particles large values of torque is required to enhance the heat exchange. The reason for the same was augmentation in the viscosity of Nano fluid. The value of heat flux was assumed to be constant.

Ramesh, K.N. et al. [2020] provided an overview of heat exchange in case of heat sink with different heat exchanging techniques both experimentally as well as numerically. The various heat exchange enhancing techniques with jet impingement, micro channel, Nanofluid, magnet hydrodynamics with the various parameters had been discussed in detail. It was suggested that there is a need for developing low cost microchannel devices as well as more work is required in case magnet hydrodynamics. Also use of artificial neural network in this type studies are less. So more attention is required.

Chen, W. & Cheng, J. [2020] analyzed the concave surface for the purpose of heat exchange using SiO_2 water as Nanofluid and the same was differentiated with the case with water only. For the case of Nano fluid 5.85 % rise was observed in the heat exchange coefficient as compared to the water. It was noted that with augmentation in the curvature of the surface, Nusselt number increased. The study was carried out for turbulent flow range.

M.S, A. & Venkata subbaiah, K. [2020] studied the impingement of jet with different Nanofluid using Fortran dependent solver. Governing equations were solved using FDM. Reynolds number, concentration of particles etc. were taken as design parameters. Twenty-five percent augmentation was seen in case of Al_2O_3 – water Nanofluid. Also in case of Cu- water Nanofluid sixty percent

improvement was detected in the heat exchange effectiveness. Results were validated with the available experimental results.

Pratap, A. et al. [2020] studied the relation between Nusselt number and dimensionless spacing with and without Nanofluid. For the investigation constant value of heat flux is assumed. In the case of water as well as Nanofluid, positive relationship was observed between Nu and dimensionless spacing. But the same is more in case of Nanofluid. Circular jet was taken for the analysis and Re was kept constant.

Izadi, A. et al. [2020] conducted numerical study to examine the heat and fluid characteristics of Nanofluid in a sink with foam of metal. The equations were used for the fully developed conditions. Magnetic force influence was also studied. The consequences of different parameters which were used in non-dimensional form was observed on the fluid and thermal attributes. Augmentation in concentration of Nano particles resulted in increase in transfer of heat. CFD approach was not adopted here.

Ho, C. J. et al. [2020] carried out experimental analysis for the decadence of heat in case of a heat sink with mini channel using water and alumina for divergent Nano particles fraction. The outcome of variables like Re, mean temperature and Nano particles was interpreted on the Nusselt number and friction. From the results it was interpreted that for Re = 483 and 968, negligible effect was thee on the friction factor in relation to entry temperature of Nano fluid. However, Re = 161, inverse shift established between the two variables. Higher temperature of the fluid decreased the Nusselt number.

CHAPTER - 3

OBJECTIVES OF THE STUDY

3.1 Introduction

This chapter deals with the research gaps for the current analysis. Based on the research gap research objectives have been formulated. The research methodology to solve the problem has been discussed.

3.2 Research Gaps

From the available literature it is found that less research has been conducted on the jet impingement heat sink with the use of pillars. Also it is noticed that no significant work has been made regarding the use of Nanofluid in combination with air foil pillars.

Based on the available literature, novel analysis has been proposed for the different combinations of jet-channel-air foil pillars with the application of CuO- water based Nano fluid. Also a novel air foil shape is used for the pillars to enhance the dissipation of heat with impingement and channel flow. So the airfoil pillars propose the novel concept for this analysis. Due to this in the current work analysis has been performed using airfoil pillars in heat sink with impingement of jet using a three dimensional model with the CuO and Al_2O_3 Nano particles with different concentration to enhance the thermal and fluid characteristics.

The objective of this study is to increase the rate of heat transfer with the use of combination of technologies like impingement of jet, use of airfoil pillars and Nanofluid in a heat sink.

At present, sufficient research work is available for increasing the heat transfer rate through free convection and forced convection. These works focused on heat transfer based on fluid through conduction and heat transfer based on air through convection. A few literatures are available based

on the application of Nanofluid. Also the concept of jet impingement heat sink with and without pillars needs further research. The concept of jet impingement with and without Nanofluid is also an important aspect of research. Nanofluid can also be analysed for different volume fraction of nanoparticles.

The application of Nano fluid technology offers several unique advantages such as

- requirement of much less volume of sample or reagents,
- reduces the costs;
- shorter time for the molecular products.
- High surface-to-volume ratios at the Nano scale lead to shorter heat and mass transfer times.
- For instance, it offers a way of screening and systematic testing in the domain of drug discovery.
- There is less literature based on enhancing the heat transfer in micro-channels.

3.3 Research Objectives

The main objective of this study is to increase the heat transfer rate using Nanofluid. Jet impingement heat sinks have a wide application in various fields like bio medical devices, electronics cooling, automobiles, aerospace etc. Increase in the heat transfer rate enhances the cooling rate of the system. This study mainly focuses on increasing the heat transfer with the use of pillars and Nanofluid.

Keeping in view of the gaps in the literature, the following objectives have been formulated for carrying the present research work.

1) Analysis of jet impingement heat sink without pillars.
2) Analysis of jet impingement heat sink with pillars

3) Thermal performance analysis of jet impingement heat sink with base fluid.
4) Thermal performance analysis of jet impingement heat sink with different Nanofluid.

3.4 Research Methodology

- Study and analysis of available literature in detail.
- The various parameters will be selected based on the literature review and based on the previous works made on the jet impingement heat sink.
- The selected geometry shape based on the literature survey will be modelled and analysed using Computational Fluid Dynamics.
- Validation of the results with the published literature.
- The effect of Nanofluid and volume fraction of the nanoparticles on the thermal performance of the system will be analysed.

CHAPTER - 4

GRID INDEPENDENCE TEST & VALIDATION

4.1 Introduction

This chapter deals with the independence test for the grid system. Validation of the problem based on the literature is discussed in detail with the help of contours and graph.

4.2 Grid Independence Test

Figure 4.1 to 4.5 shows the grid independence test for the rise in maximum temperature, overall pressure drop, heat transfer coefficient, Nusselt number and thermal resistance respectively. The grid independence test is performed for variables like rise in maximum temperature, overall drop in pressure, heat transfer coefficient, Nusselt number and thermal resistance. The test is performed for the height ratio = 1 and pitch ratio = 6.

4.2.1 Grid Independence Test for Rise in Maximum Temperature

Figure 4.1 shows the grid test for rise in maximum temperature. The test is performed for the height ratio = 1 and pitch ratio = 6. In this system 120000 nodes are found to be sufficient for the values to be stabilized. When the nodes are changed from 100000 to 120000, the error in the value of rise in maximum temperature is found to be less than 1percent. Further increase in nodes do not have any significant effect on the parameters. Also when the nodes are changed from 200000 to 300000, error of around 5 percent is noticed.

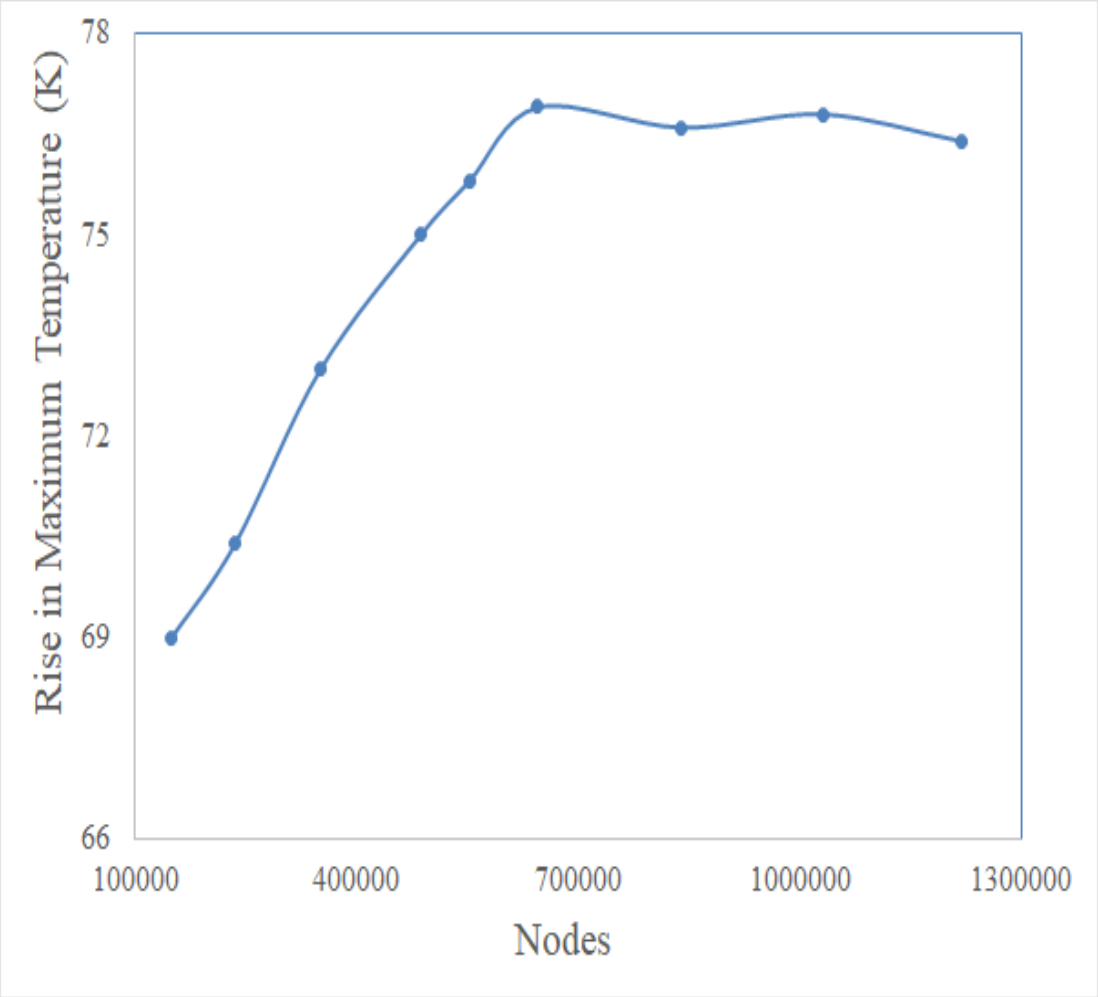

Figure 4.1: Grid Independence Test for Rise in Maximum Temperature

4.2.2 Grid Independence Test for overall pressure drop

Figure 4.2 shows the grid test for overall pressure drop. The test is performed for the height ratio = 1 and pitch ratio = 6. In this system 120000 nodes are found to be sufficient for the values to be stabilized. When the nodes are changed from 100000 to 120000, the error in the value of rise in maximum temperature is found to be less than 1percent. Further increase in nodes do not have any significant effect on the parameters. Also when the nodes are changed from 486471 to 552200, error of around 10 percent is noticed.

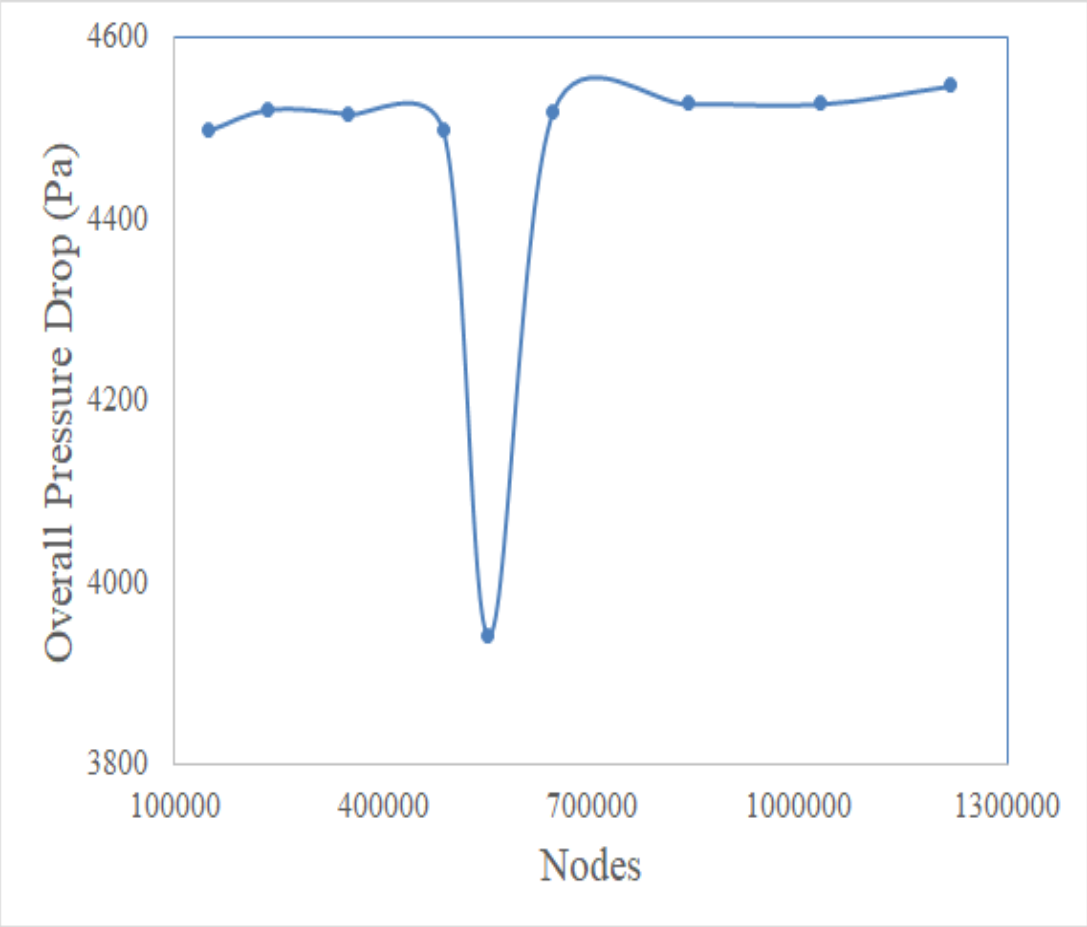

Figure 4.2: Grid Independence Test for Overall Pressure Drop

4.2.3 Grid Independence Test for heat transfer coefficient

Figure 4.3 shows the grid test for heat transfer coefficient. The test is performed for the height ratio = 1 and pitch ratio = 6. In this system 120000 nodes are found to be sufficient for the values to be stabilized. When the nodes are changed from 100000 to 120000, the error in the value of rise in maximum temperature is found to be less than one percent. Further increase in nodes do not have any significant effect on the parameters. Also when the nodes are changed from 235032 to 350643, error of around five percent is noticed.

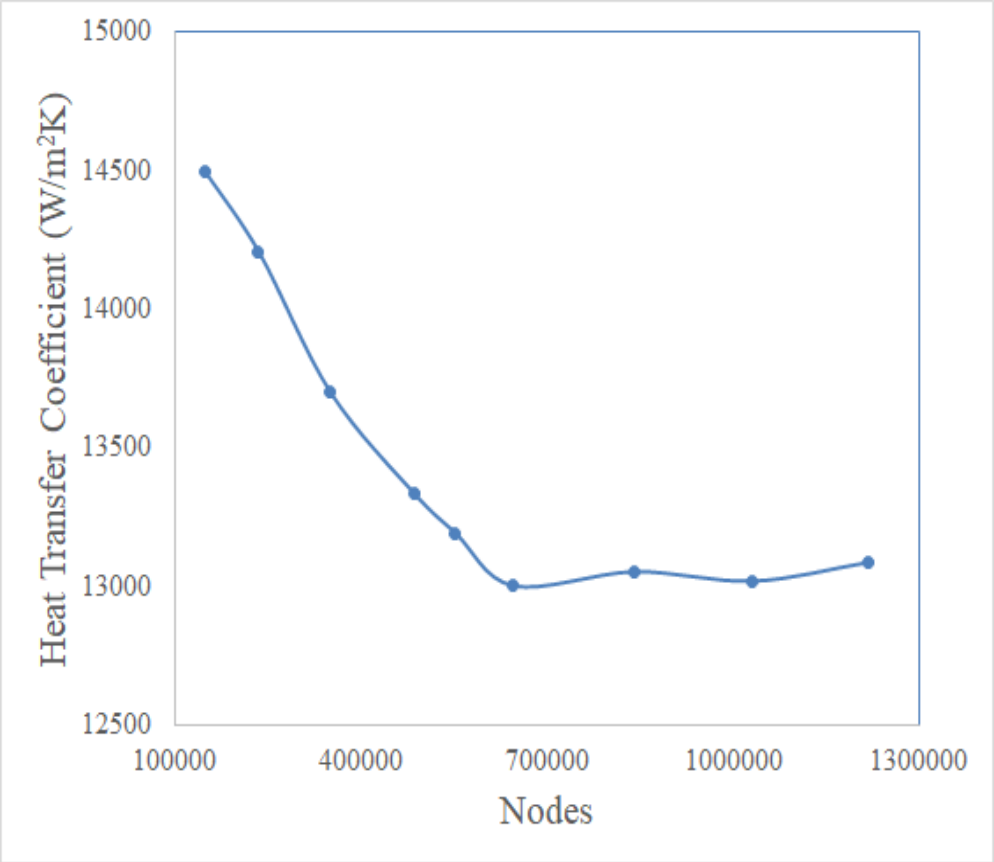

Figure 4.3: Grid Independence Test for Heat Transfer Coefficient

4.2.4 Grid Independence Test for Nusselt Number

Figure 4.4 shows the grid test for Nusselt number. The test is performed for the height ratio = 1 and pitch ratio = 6. In this system 120000 nodes are found to be sufficient for the values to be stabilized. When the nodes are changed from 100000 to 120000, the error in the value of rise in maximum temperature is found to be less than 1percent. Further increase in nodes do not have any significant effect on the parameters. Also when the nodes are changed from 235032 to 350643, error of around five percent is noticed

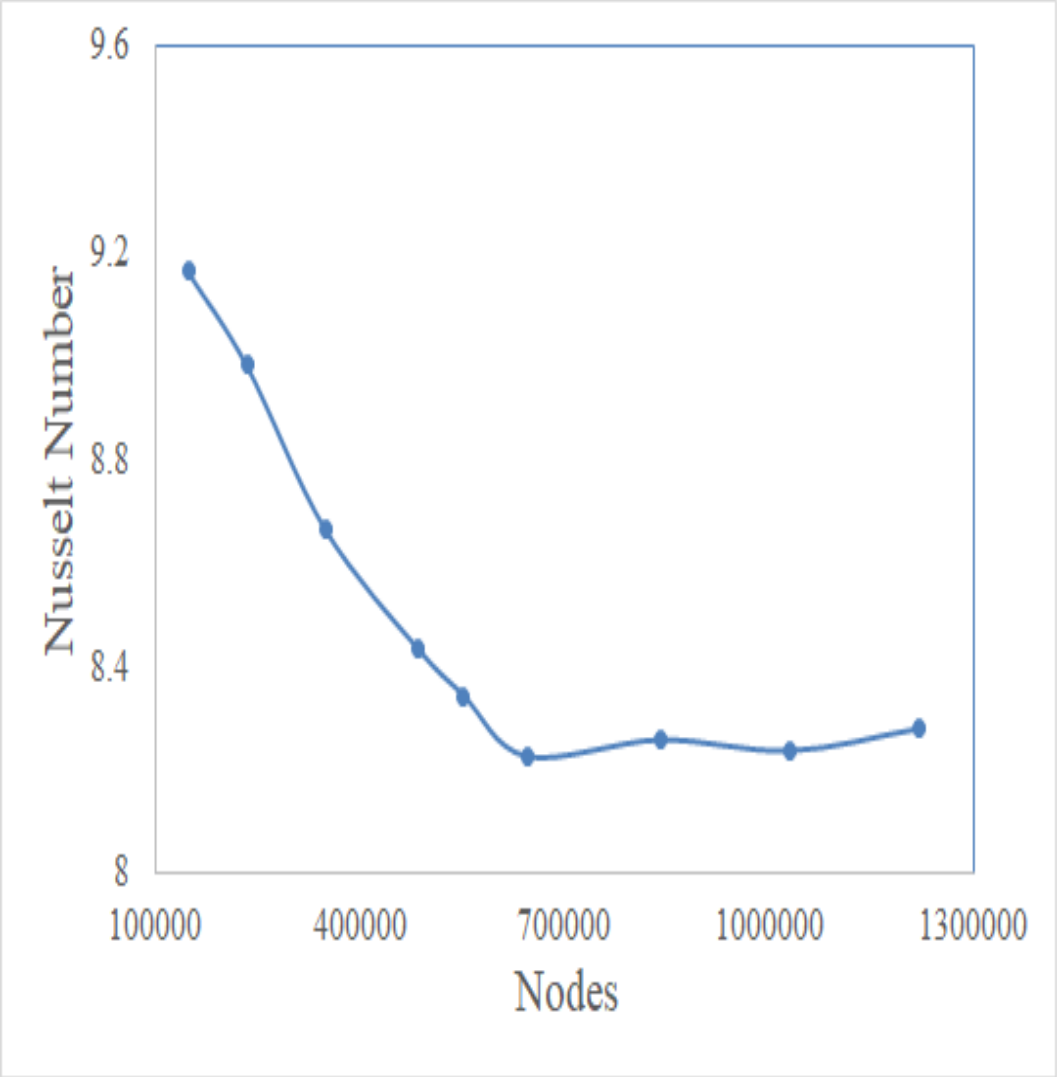

Figure 4.4: Grid Independence Test for Nusselt Number

4.2.5 Grid Independence Test for thermal resistance

Figure 4.5 shows the grid test for thermal resistance. The test is performed for the height ratio = 1 and pitch ratio = 6. In this system 120000 nodes are found to be sufficient for the values to be stabilized. When the nodes are changed from 100000 to 120000, the error in the value of rise in maximum temperature is found to be less than one percent. Further increase in nodes do not have any significant effect on the parameters. Also when the nodes are changed from 235032 to 350643, error of around five percent is noticed.

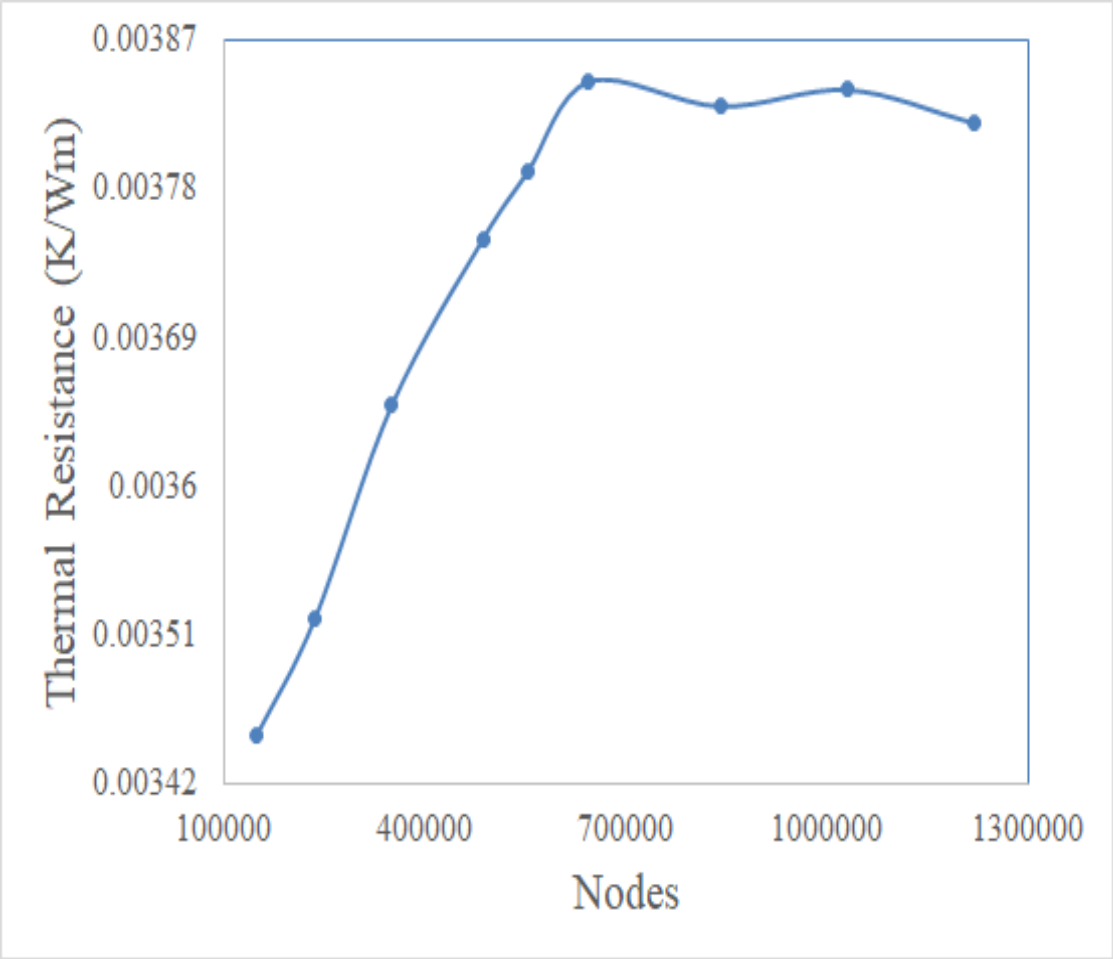

Figure 4.5: Grid Independence Test for Thermal Resistance

4.3 Validation

4.3.1 Introduction

In this study validation is performed using computational fluid dynamics. For validation work performed by Husain et al [2016] is considered. First of all, the geometry is drawn using solid works as a tool. The file of geometry is imported in Ansys for simulation. The geometry consists of heat sink as well as micro channel. Heat sink and channel is drawn according to the dimensions as specified earlier. Mate command of Solid works is used to combine different parts into a single entity. Meshing is done finer and finer for the improvement and accuracy of results. Using the

boundary conditions simulation is performed and the results are validated.

4.3.2 Geometry for Validation

The geometry which is considered for validation is shown in the figure below.

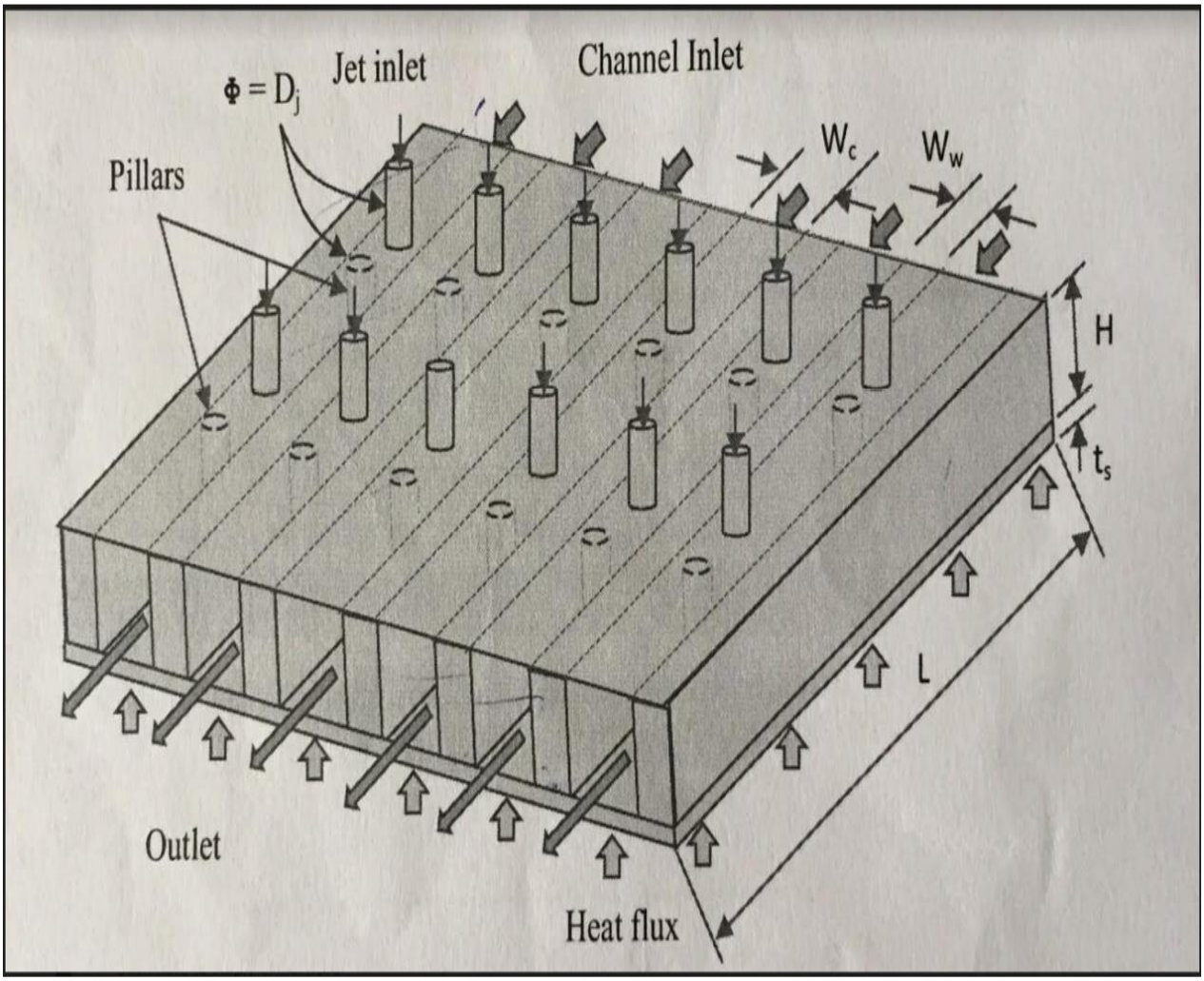

Figure 4.6: Geometric configuration of micro channel heat sink for validation Husain et al. [2016]

4.3.3 Validation Results

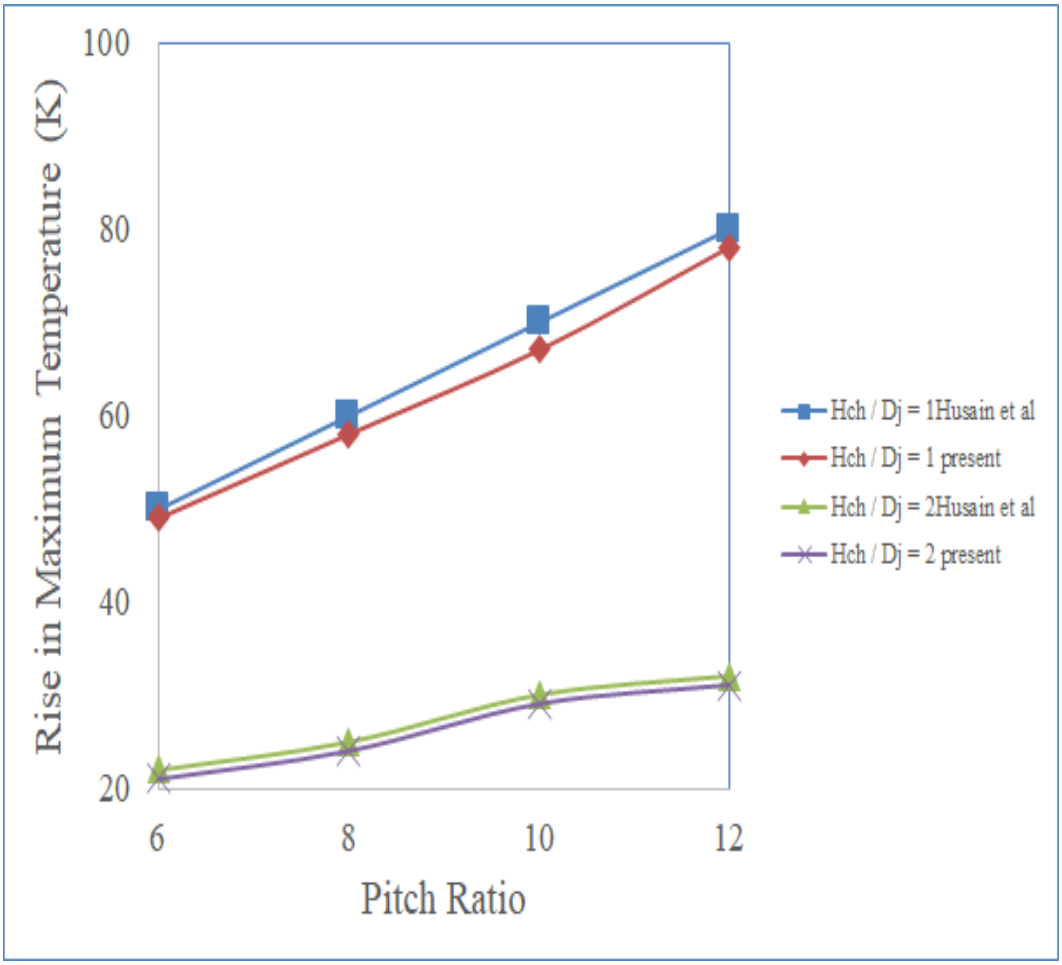

Figure 4.7: Comparison of simulation results with the results of Husain et al [2016]

Figure 4.13 shows the comparative analysis of present simulation results and the results obtained from available literature Husain et al. [2016]. The validation has been performed for the rise in maximum temperature with pitch ratio for height ratio of 1 and 2. The two results are found to be in good concurrence with each other.

CHAPTER - 5

PROBLEM SPECIFICATION

5.1 Introduction

The study of the jet impingement heat sink with airfoil pillars with and without Nanofluid begins with the generation of simulation “data”. This is accomplished by defining the problem and then using “Ansys “to do the simulation using details such as dimensions of channel and governing equations, the initial velocity and pressure fields and fluid properties.

5.2 The Problem

In order to solve the flow of a viscous, incompressible fluid in a channel with jet impingement heat sink with water and Nanofluid some assumptions are necessary, since mathematical expressions become simpler and the solutions are still close to real cases. A 3-Dimensional model is considered in this thesis.

5.3 Assumptions

- 3-Dimensional numerical model is considered
- The fluid is water which is considered incompressible and Newtonian
- Steady state conditions are assumed.
- Flow is not affected by the gravity field

Although some of the values depend on temperature, they can be considered constants when the variation in temperature is small. For water average values are:

$$\rho = 998 \ [Kg/m^3]$$

$$\mu = 0.001 \ [Kg/m\ s]$$

$$k = 0.6 \ [W/mk]$$

5.4 Geometric representation of impinging jet heat sink

The arrangement regarding impinging jet heat sink with airfoil shaped pillars is exhibited in figure 5.1. It consists of heat sink with jet of water. The inlet and outlet of channel are shown. Pillars are used to increase the heat exchange rate. The model is used with combinations like Jet flow, Channel flow, Jet – channel flow, channel-pillar flow and jet- channel-airfoil pillars flow. Airfoil pillars are placed in between the jets of impingement. The fluid enters from the channel inlet and leaves from the channel outlet as shown in the figure 5.2. Jet of water are used at equal spacing. Pillars are placed in between the jets. Pillars are acting as an inactive structure. Laminar flow and steady state condition has been assumed for the investigation. The model is first validated with the experimental results of Tuckerman & Pease [1981], Wang et al. [2004]. The model has been used in different cases. First case with pure water and second case with water – CuO Nano fluid with 0.5 % and 1% concentration. Also water – Al_2O_3 with 5% concentration is used for another case.

The measurement of the heat based sink as base of substrate is taken as 1 cm X 1 cm. The height of channel (H_{ch}) is taken as 0.4 cm. Substrate base thickness is taken as 0.2 cm. A plate of thickness 0.4 cm is taken on which nozzles are fitted is known as nozzle plate and thickness of this plate is named as nozzle plate thickness (t_{nz}). Total five design dimensionless variables are selected for design and analysis. Dimensionless variables are ratio of diameter of jet (D_j) and diameter of pillar (D_{pl}) named as diameter ratio, proportion of width of channel (W_{ch}) and width of wall of channel (W_{chw}) named as width ratio, proportion of width of channel (W_{ch}) and diameter of jet (D_j) named

as width diameter ratio, ratio of height of channel (H_{ch}) and diameter of jet (D_j) named as height ratio and ratio of pitch of jet (Ph) and diameter of jet (D_j) named as pitch ratio. For analysis diameter ratio and width ratio are assumed to be constant and the value of height ratio, width ratio and pitch ratio are jumbled.

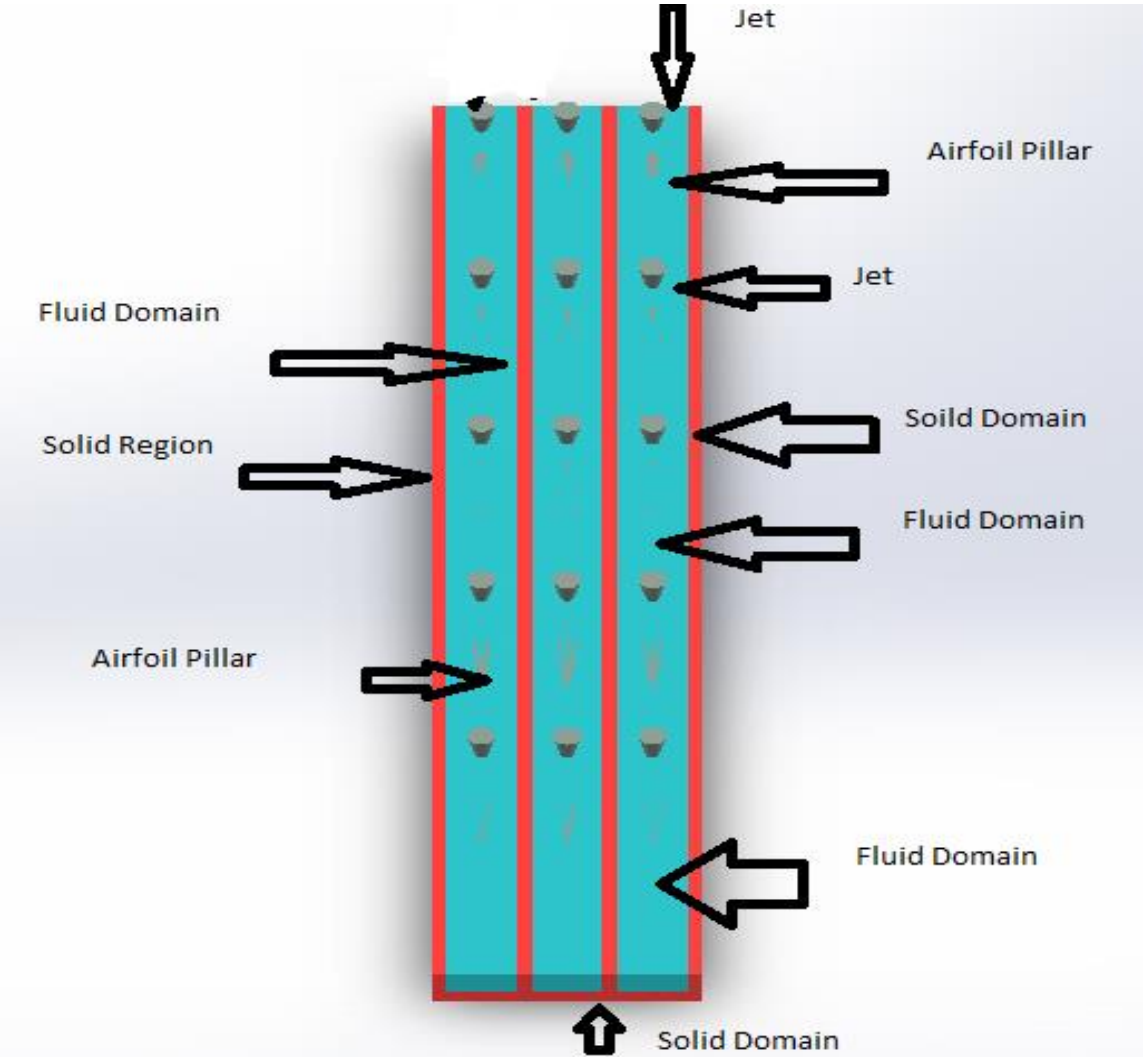

Figure 5.1: Various Domains of Model

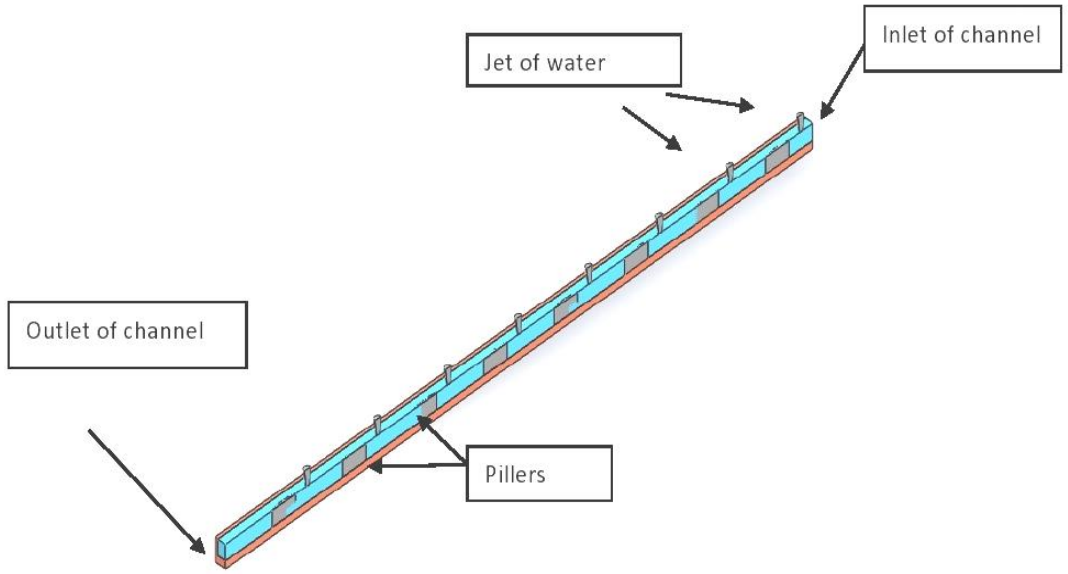

Figure 5.2: Representation of Model

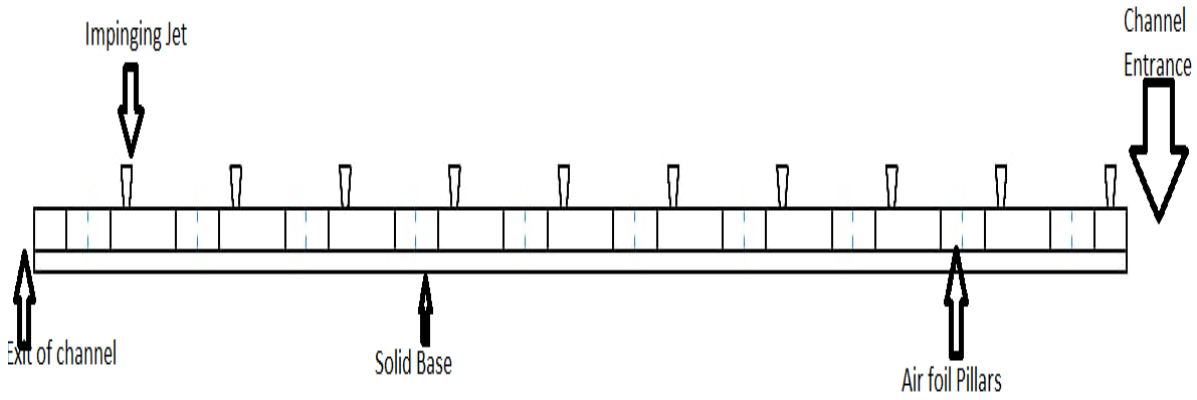

Figure 5.3: Computational Model

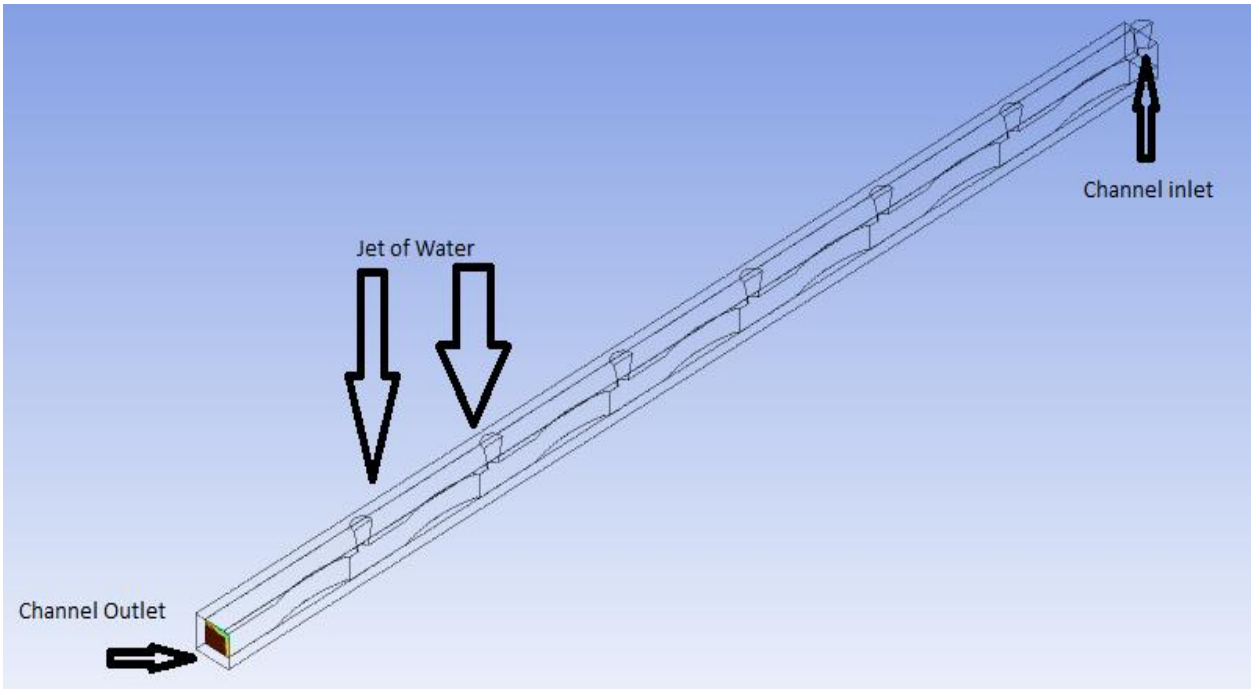

Figure 5.4: Channel inlet and outlet

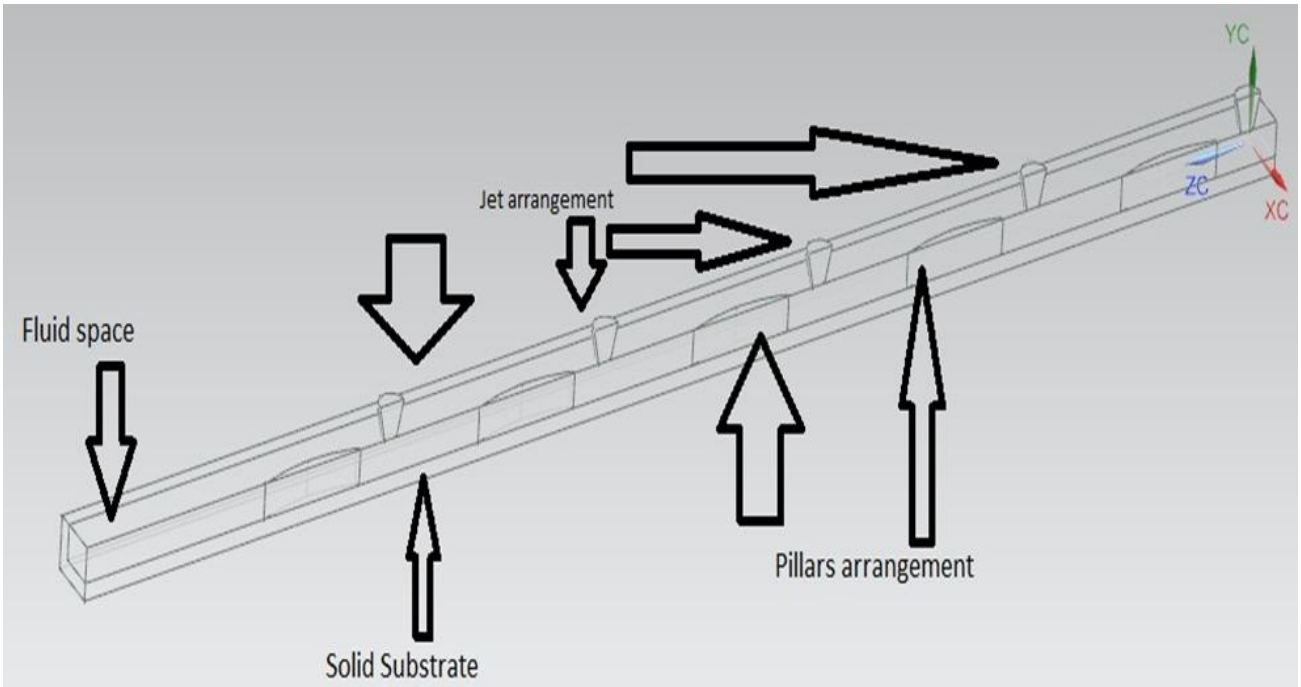

Figure 5.5: Jet and Pillars

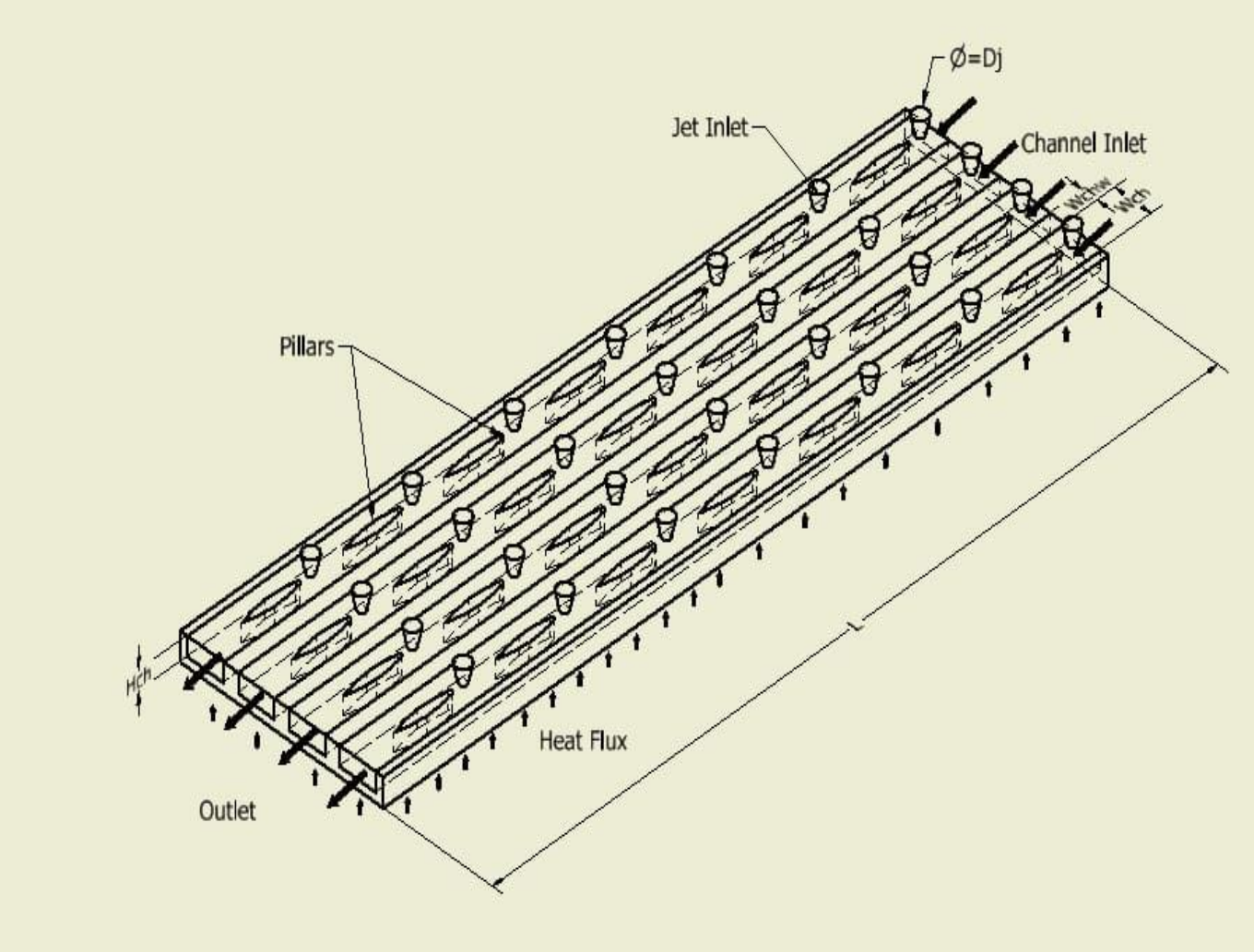

Figure. 5.6 Geometrical Representation

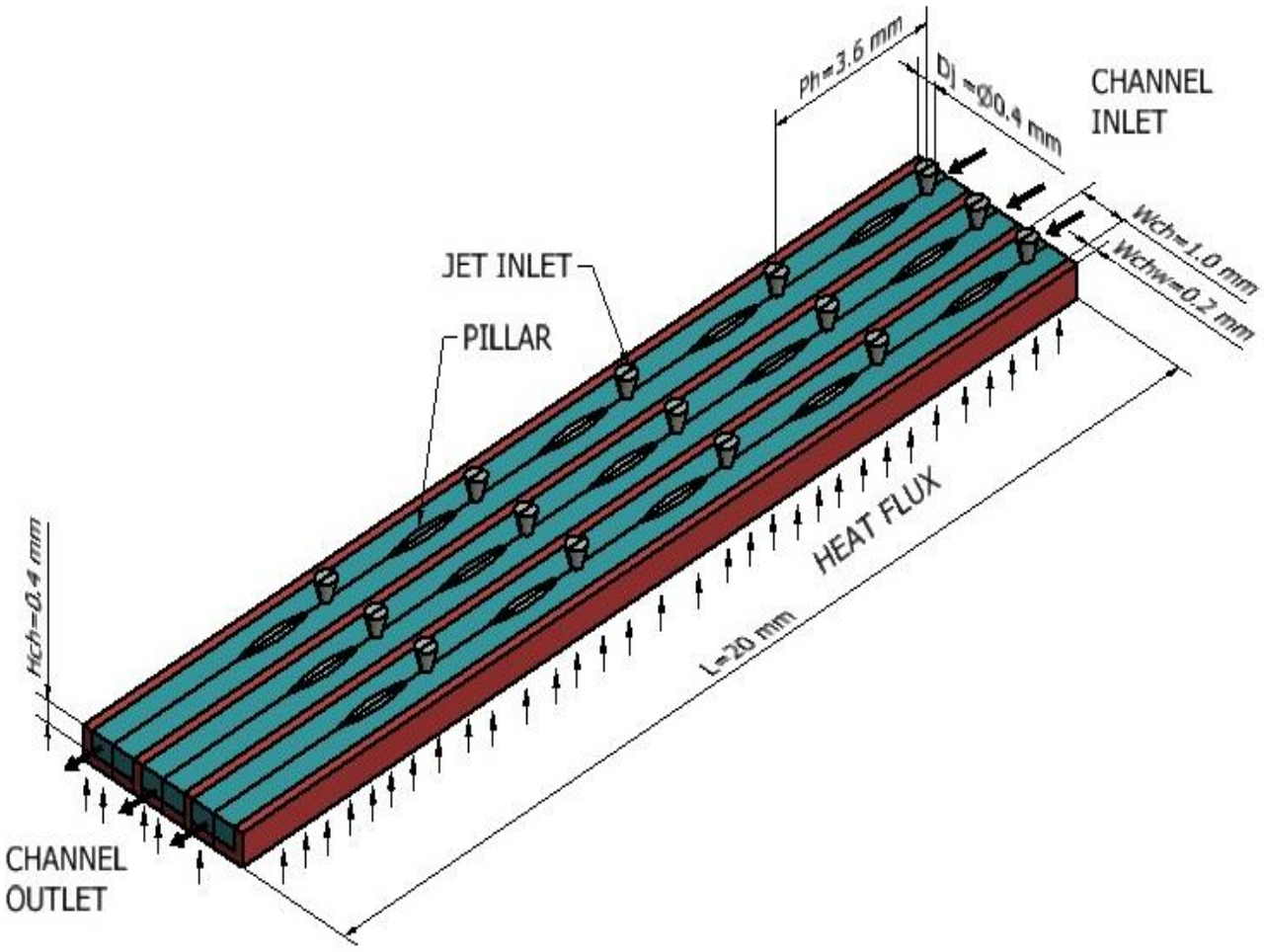

Figure. 5.7 Geometrical Arrangement

5.5 Mathematical Formulation

The flow domain is shown in the figure 5.4. The governing equations used for the solutions are based on the conservation of mass, conservation of momentum and conservation of energy. The numerical simulation is performed with the help of computational fluid dynamics. Water, water – CuO Nano fluid and water - Al_2O_3 Nano fluid is taken as a coolant in different cases which flows through the channel and jet.

$$\frac{\partial \rho}{\partial t} + \frac{\partial (\rho u)}{\partial x} + \frac{\partial (\rho v)}{\partial y} + \frac{\partial (\rho w)}{\partial z} = 0 \qquad \text{(Kumar, D. 2014)} \qquad (1)$$

$$\frac{\partial (\rho u)}{\partial t} + u\frac{\partial (\rho u)}{\partial x} + v\frac{\partial (\rho u)}{\partial y} + w\frac{\partial (\rho u)}{\partial z} = -\frac{\partial p}{\partial x} + \frac{\partial}{\partial x}[\lambda \nabla . V + 2\mu \frac{\partial u}{\partial x}] + \frac{\partial}{\partial y}[\mu (\frac{\partial v}{\partial x} + \frac{\partial u}{\partial y})] + \frac{\partial}{\partial z}[\mu (\frac{\partial u}{\partial z} + \frac{\partial w}{\partial x})] + \rho f_x \qquad \text{(Kumar, D. 2014)} \qquad (2)$$

$$\frac{\partial (\rho v)}{\partial t} + u\frac{\partial (\rho v)}{\partial x} + v\frac{\partial (\rho v)}{\partial y} + w\frac{\partial (\rho v)}{\partial z} = -\frac{\partial p}{\partial y} + \frac{\partial}{\partial y}[\lambda \nabla . V + 2\mu \frac{\partial v}{\partial y}] + \frac{\partial}{\partial x}[\mu (\frac{\partial v}{\partial x} + \frac{\partial u}{\partial y})] + \frac{\partial}{\partial z}[\mu (\frac{\partial v}{\partial z} + \frac{\partial w}{\partial y})] + \rho f_y \qquad \text{(Kumar, D. 2014)} \qquad (3)$$

A constant value of heat flux is taken and is initiated as source of heat at the bottom side of substrate. Reynolds number is given by

$$\mathrm{Re} = \frac{\rho v d}{\mu} \qquad \text{(Husain et al. 2016)} \qquad (4)$$

Local heat transfer coefficient is

$$h = \frac{Q}{A\Delta T} \qquad \text{(Husain et al. 2016)} \qquad (5)$$

Nusselt number is given by

$$Nu = \frac{hd}{k} \qquad \text{(Husain et al. 2016)} \qquad (6)$$

Rise in Maximum temperature is

$$(\Delta T)_r = T_{s,max} - T_{f,i} \qquad \text{(Husain et al. 2016)} \qquad (7)$$

Pumping power is

$$P_p = q_j \times p_j + q_{ch} \times p_{ch} \qquad \text{(Husain et al. 2016)} \qquad (8)$$

5.6 Properties of Nanofluid

Table 1: Thermo-Physical properties of the (Al_2O_3-water) Nanofluid

Sr No	Material	Density (Kg/m^3)	Specific Heat (J/KgK)	Thermal Conductivity (W/mK)	Viscosity (Kg/ms)
1	Pure water (concentration= 0)	981.3	4189	0.643	0.000598
2	Al_2O_3	3600	765	36	-
3	Al_2O_3 –water (Concentration = 1%)	1007.4	4154.7	0.661	0.000612
4	Al_2O_3 –water (Concentration = 2%)	1033.6	4120.5	0.68	0.000627
5	Al_2O_3 –water (Concentration = 3%)	1059.8	4086.2	0.699	0.000642
6	Al_2O_3 –water (Concentration = 4%)	1086	4052	0.719	0.000657
7	Al_2O_3 –water (Concentration = 5%)	1112.2	4017.8	0.739	0.000672

(Mushtaq I. Hasan et al. 2012)

CHAPTER - 6

METHOD OF SOLUTION

6.1 Introduction

In the present analysis the problem is solved using computational fluid dynamics. Some basic details regarding Computational fluid dynamics is represented in this chapter.

The branch of mechanics of fluids which ensures a cost effective way of real flows simulation by the numerical results of the governing equations is known as Computational Fluid Dynamics (CFD.). The Navier–Stokes formulations, one of the governing equations for Newtonian fluid dynamics have been utilized for over hundred years. In spite of this the advancement of reduced form of these formulations is an active area of research, particularly the turbulent problem of Re averaged Navier-Stokes formulations. But in case of non-Newtonian fluid dynamics, two phase flows and chemically reacting flows, theoretical development is at a lesser advanced stage. In this method i.e. Computational technique, the governing differential equations has been replaced by algebraic equations which can be easily solved by the computers. One of the major reasons for the rise and emergence of CFD is the steady enhancement in computer power since 1960s.It allowed testing of situations which are very tough or impossible to be measured experimentally and are not amenable to analytic solution. Experimental methods play a major role in analyzing and validating the limits of different approximations to the governing equations, mainly rig tests and wind tunnel thus providing a cost effective alternative. The analytic solutions cannot be achieved for most practical applications due to the extreme complexity of flow governing equations. In the computational fluid dynamic problem, we used different code in authorized Ansys. In this

condition the CFD conclude problem to problem as per data given. The method constraint in the alternative testing scale. In using the thermal design problem CFD provided the simulation on the various flow technique as per the problem. CFD base on different problem on different situation on grid data it noted that fluid flow condition in micro channel. It is noted the segment of analytic solution describe the condition of fluid flow condition.

6.2 Applications of CFD

6.2.1 Aerospace

Various methods of CFD are used in different applications (flow around an aircraft etc.) related to aerospace for the role of predicting part effectiveness.

6.2.2 Automotive

In the field of automotive applications CFD is used for modeling the cars aerodynamics to reduce drag in different operating conditions and also in other fields like auxiliary systems, engine components etc.

6.2.3 Biomedical

CFD is used to design and simulate the blood flow in the heart vessels, inhalers, flow in heart aid systems.

6.2.4 Chemical Engineering

Applications of CFD in the field of chemical engineering are vast and surplus such as petrochemicals, pollution control, fertilizers, food processing, waste treatment recycle etc.

6.2.5 Power Generation

In the field of power sector CFD finds applications in the analysis of economizer, super heaters, pulverized coal combustion, low NOx burner design and in other areas to improve performance and efficiency of the plant.

6.2.6 Electronic systems

The various thermal challenges faced by manufactures highlights the increasing applications for accurate and cheap computational design tools to overcome complex thermal problems related to their cooling. It is the thermal analysis of electronic system by thermal management solution(TMC).

6.3 Steps of CFD

- Divide the fluid volume (surface) up into manageable chunks (gridding)
- Equation to be simplify at required condition
- boundary condition must be set
- Initialization of grid values
- Simplify the equation through the step grid at the required set point.

6.4 Advantages

In CFD process there are following advantage carried out. It dominates the various step process but it quite effective for 3-D volume. The generation process takes less time as time take manually operated proses.

- In CFD process carried out great time reduction and reduction in cost.
- There is a possibility analyze different problem which are very difficult and dangerous.
- CFD technique offer analyze the problem in capacity of limit in over its limit.
- Practical unlimited in level of detail.
- For analyze the result plot various graph for validation the result in deferent purpose use.
- For the good result simplification has been quite simple in mode of process.
- Several incomplete modals to describe the turbulence, multiphase and other difficult problems.

6.5 Disadvantages

- . Easy to excess and low investment lead to over trading.
- Initially cost provided through the set up more as par data

6.6 CFD code

CFD code use in different category in various applications. The use of these code we can apply in the generation tool which an associate in CFD analysis.

6.6.1 CFD commercial code

STAR CD, FLUIENT, CFX, CFDESIGN, FLUIDYN etc.

6.6.2 CFD research code

COOLFLUID, CFDSHIP IOWA etc.

6.6.3 CFD public code

WINPIPED, HYDRO etc.

6.6.4 Other CFD codes

Other Codes used in generation software as GAMBIT and grid visualization such as ADINAAUI CFX-Post, COMSO, ENSIGHT, FIELDVIEW, Hyper View ETC.

6.7 CFD PROCESS

- The purpose of CFD use with respect to the code applies in various applications such as separated the bubbly flow through domain.
- In the application we seen the massive flow, uniform flow and unsteady flow. In the proses which provide the conjugate configuration rate in the code assign.
- With respect to the code we can apply various other application such that multiphase fluid. Marine, biomedical etc.
- The flow tendency in various manner judges by the code applies on it. It is configuring the step in apply the code.
- It leads to apply the code as per the step required in generation process. During the process configuration said the next step to lead. If their drawback than post process to apply.

6.8 Steps

- Layout the geometry
- Apply the physics
- Generate mesh
- Solution
- Report
- Feedback

6.9 Background Information

The science and practice of achieving approximate numerical solution using digital computers is known as Computational Mechanics. When this approach is applied in the field of problems concerned with thermal and fluid, it is generally termed as CFD. Thus CFD is primarily a field of continuum mechanics which deals with numerical simulation of heat transfer and fluid flow problems. The basic fundamental of CFD problems is Naiver–Stokes formulations, which helps in defining many single-phase (gas or liquid, but not both) fluid flows. The Euler equations are achieved by simplifying these equations by removing terms defining viscous action. The full potential equations can be obtained by doing further simplification by eliminating terms describing vorticity. Historically, a method was first developed to solve the linearization potential equations. Two dimensional (2D) methods were developed using flow over a cylinder by taking air foil as reference selection. Even though they failed, these calculations establish the support for modern CFD. The computer power available leads to development of 3-D methods. Los Alamos National Lab can be considered as the place where the first work using computers to model fluid flow governed by the Navier-Stokes equation happened. Francis H. Harlow, who is considered as one

of the pioneers of CFD led this group and they developed various types of numerical methods in order to simulate transient two-dimensional fluid flows. Today different codes are used in the development of many submarines, helicopters, surface ship and more recently wind turbines. Many codes have also been used for modelling such things as high speed trains and also in jet impingement and micro-channel cooling technology. Now days in to achieve greater high heat flux removal and thereby reducing the high temperature and pressure gradient along channel flow, a new field of research is trying to harness the two cooling technologies (microchannel and jet impingement cooling). The characteristics of fluid flow are investigated by modelling single-phase fluid flow and heat transfer in a micro-channel jet impingement with the help of CFD. Numerical model has been used to analyze the three dimensional micro-channel jet impingement fluid flows by assuming the flow to be fully developed flow. Different parameters such as Re, channel configuration, substrate material, and working fluid effects on the performance were analyzed and results thus obtained were used to differentiate available literatures. Optimum values of some of the important variables used during the examination were reported and more steps were also noted to recognize the model. Reduction of flow analysis complexity is also done by applying the fully developed flow assumption. Most recently in order to achieve higher temperature uniformity and improvement in electronics items of hot spot management, the use of micro jet impingements on substrates has also discussed. The value of characteristics equation more precise the optimum condition in simulation of given data. It is the synthesized the various dimension on the factor of micro channel design. The function can be excluded the flow parameter in micro channel which the flow condition satisfied.

6.10 Numerical Procedure

The following flow chart clearly explains the numerical procedure used for the study.

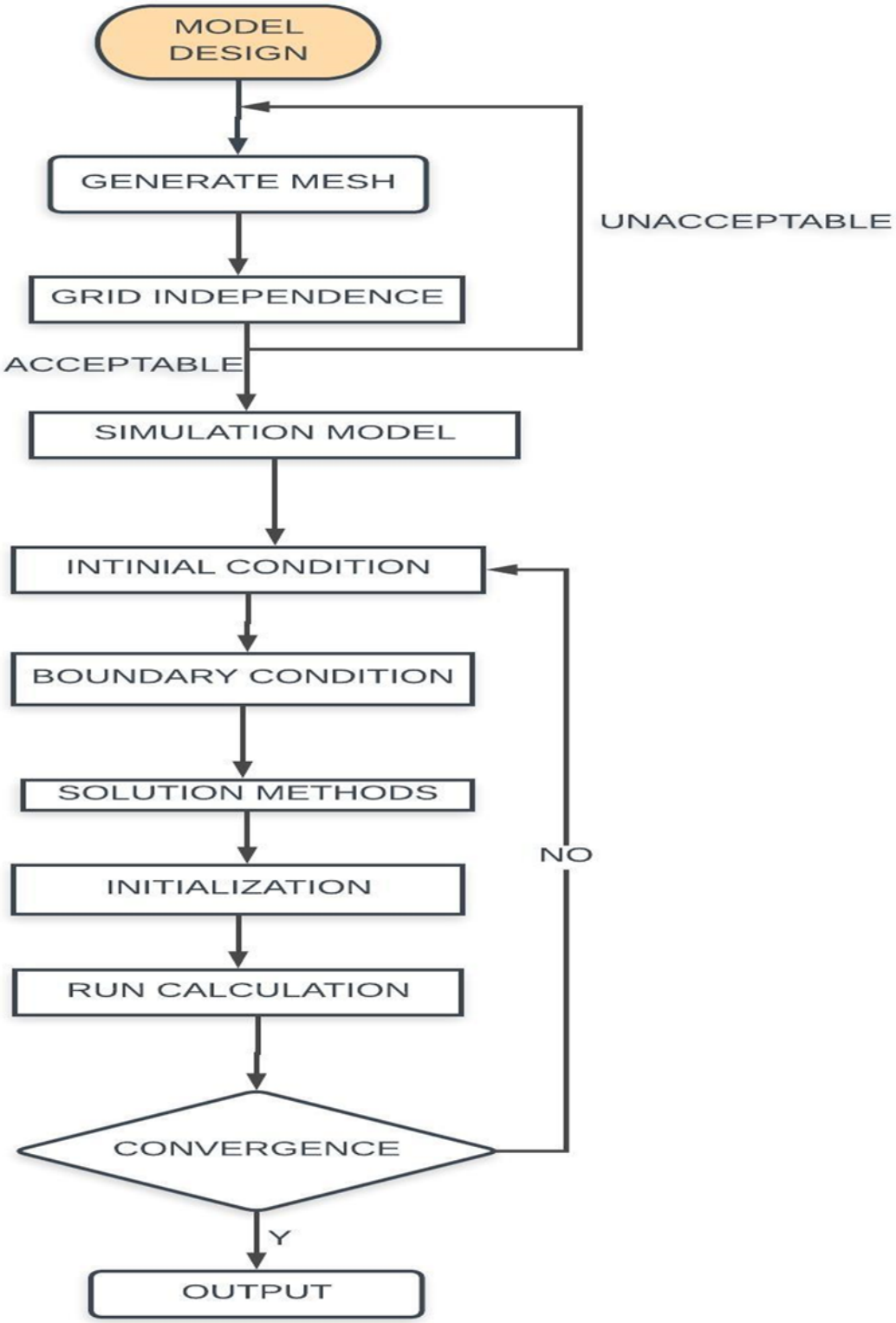

Figure 6.1: Flow chart for procedure

6.11 Ansys Mesh File

The Ansys file is shown in the figure 6.1. The figure represents the meshing used in the Ansys. Ten Lakh nodes are used. Tetrahedral meshing is used in the Ansys for the current study.

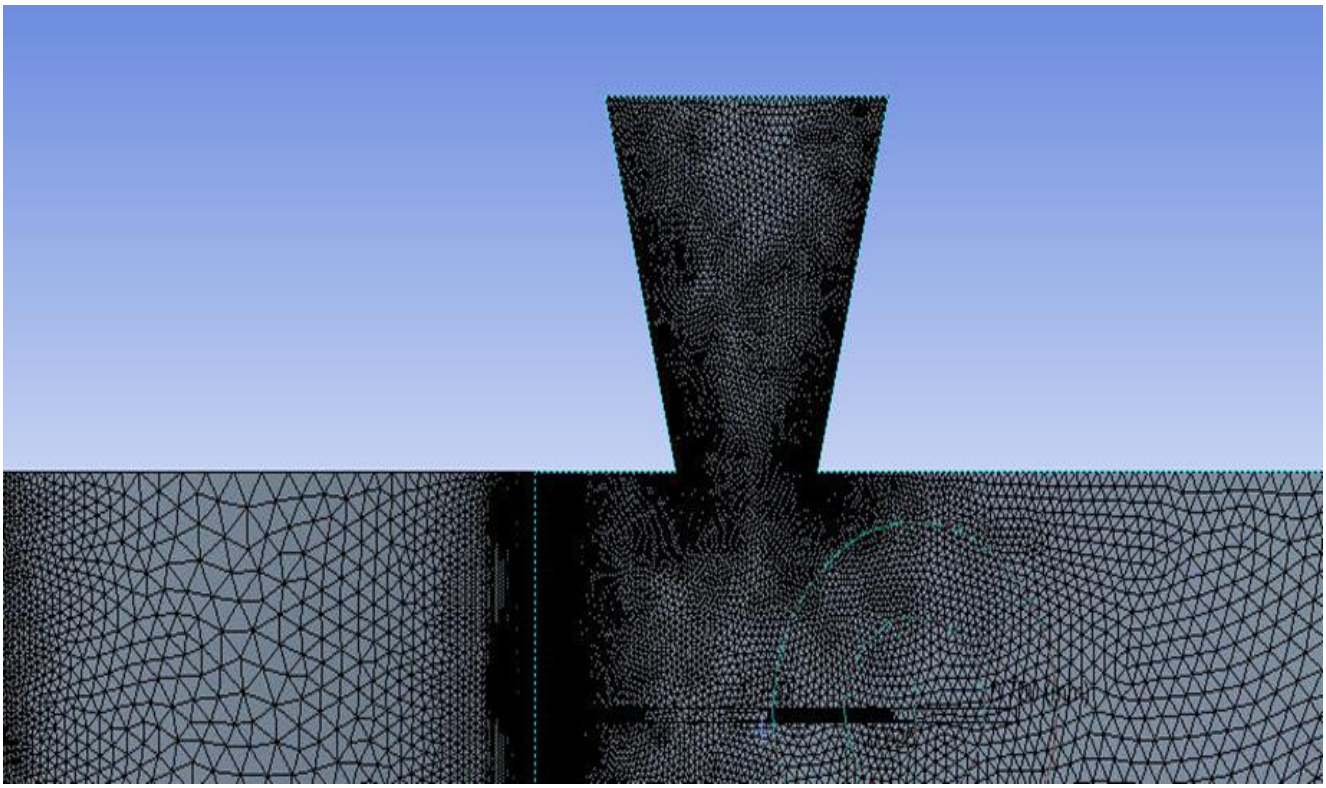

Figure 6.2: Ansys Mesh file

CHAPTER - 7

RESULTS AND DISCUSSION

7.1 Introduction

Concept of jet impingement is found to be very interesting techniques in the dissipation of heat. Then use of pillars as an inactive structure also found to be an aid in surging the attributes of heat transfer. Now in the current study air foil shape of the pillars is identified. Computational fluid dynamics is used to solve the problem.

The three dimensional model of heat sink with airfoil pillars has been utilized for the study based on the pure water, water – CuO Nanofluid with 0.5% and 1% concentration and water – Al_2O_3 Nanofluid with 5% concentration. The numerical model has been tested for grid independence test. The analysis has been performed for 1000000 nodes for the negligence of error due to grid dependence. The three dimensional model was validated with the help of available literature in the form of simulation and experimental. The results obtained are in straight accordance with experimental outcomes available Husain et al [2016], Husain et al [2013], Tuckerman & Pease [1981], Wang et al. [2004].

Computational fluid dynamics analysis has been accomplished to control thermal attributes of model. The comparative execution has been carried out for the water and water - CuO Nanofluid in terms of different characteristics parameters. The results were found using parameters of rise in temperature, drop in pressure, thermal resistance, coefficient of heat transfer and Nusselt number. Analysis of heat sink for different combinations has been studied in the form of temperature, pressure drop, coefficient of heat exchange, Nusselt number, thermal resistance and pumping

power for fixed value of mass flow rate. Four values of Height ratio (HR) (1,2,3 and 4) has been taken for the performance evaluation. Pitch ratio (PR) is varied from 6 to 12.

7.2 Water – Al_2O_3 Nano fluid (5%)

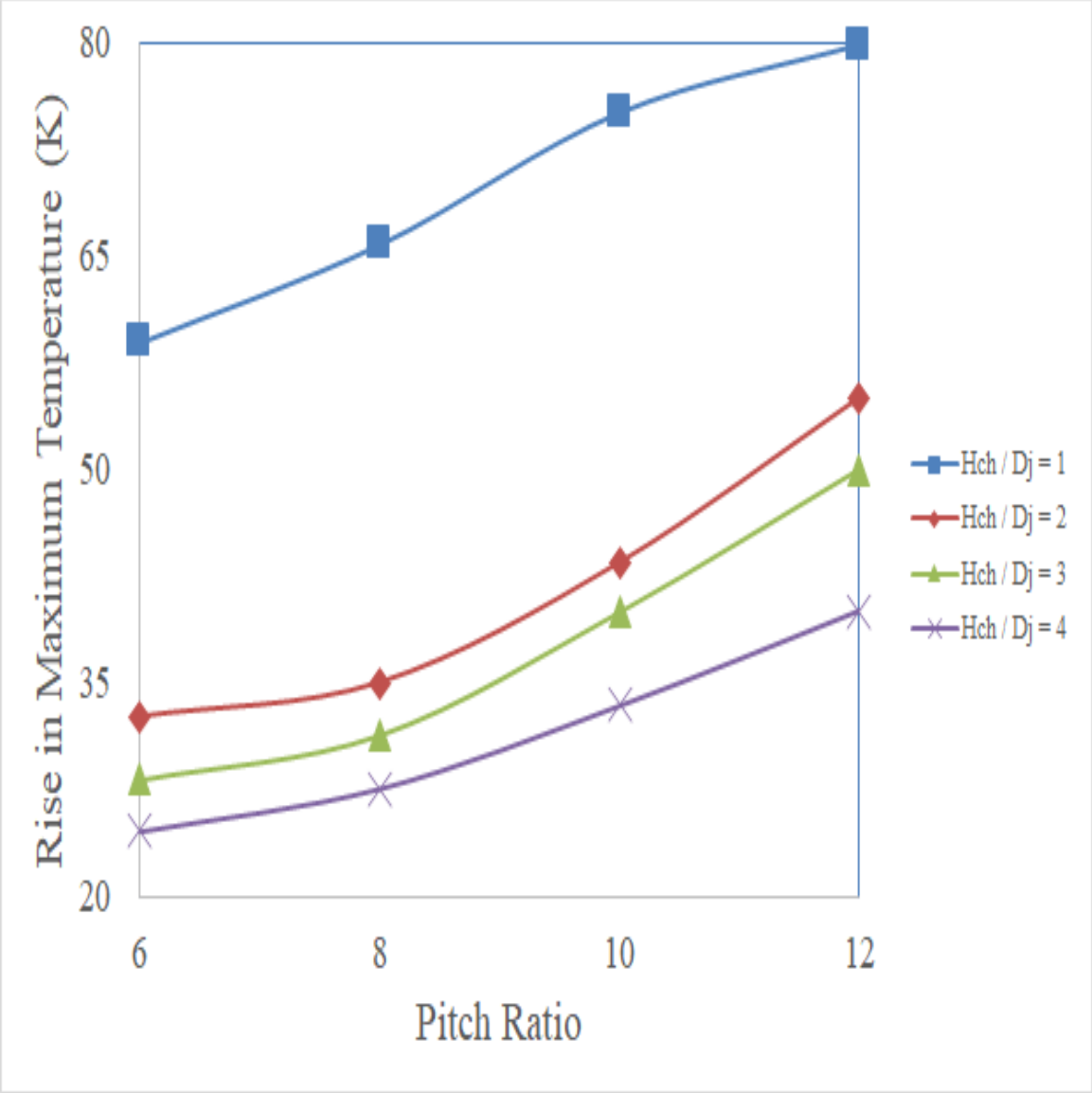

Figure 7.1: Effect of Pitch ratio $(\frac{Ph}{D_j})$ on rise in maximum temperature$(\Delta T)_r$ for water based Al_2O_3 Nanofluid

Figure 7.1 indicates the relation between maximum temperature rise and pitch ratio for different values of height ratio (1,2,3 and 4). The values of temperature are detected for pitch ratio values

6,8,10 and 12. With the increase in pitch ratio, from 6 to 12, maximum temperature also increases for a particular value of height ratio. Rise in maximum temperature is maximum for height ratio =1 and minimum for height ratio = 4. With an increase in the pitch ratio, rise in temperature is detected. This is because of the decrease in the number of impingements which results due to increase in the pitch ratio and due to thermophysical properties of Nanofluid.

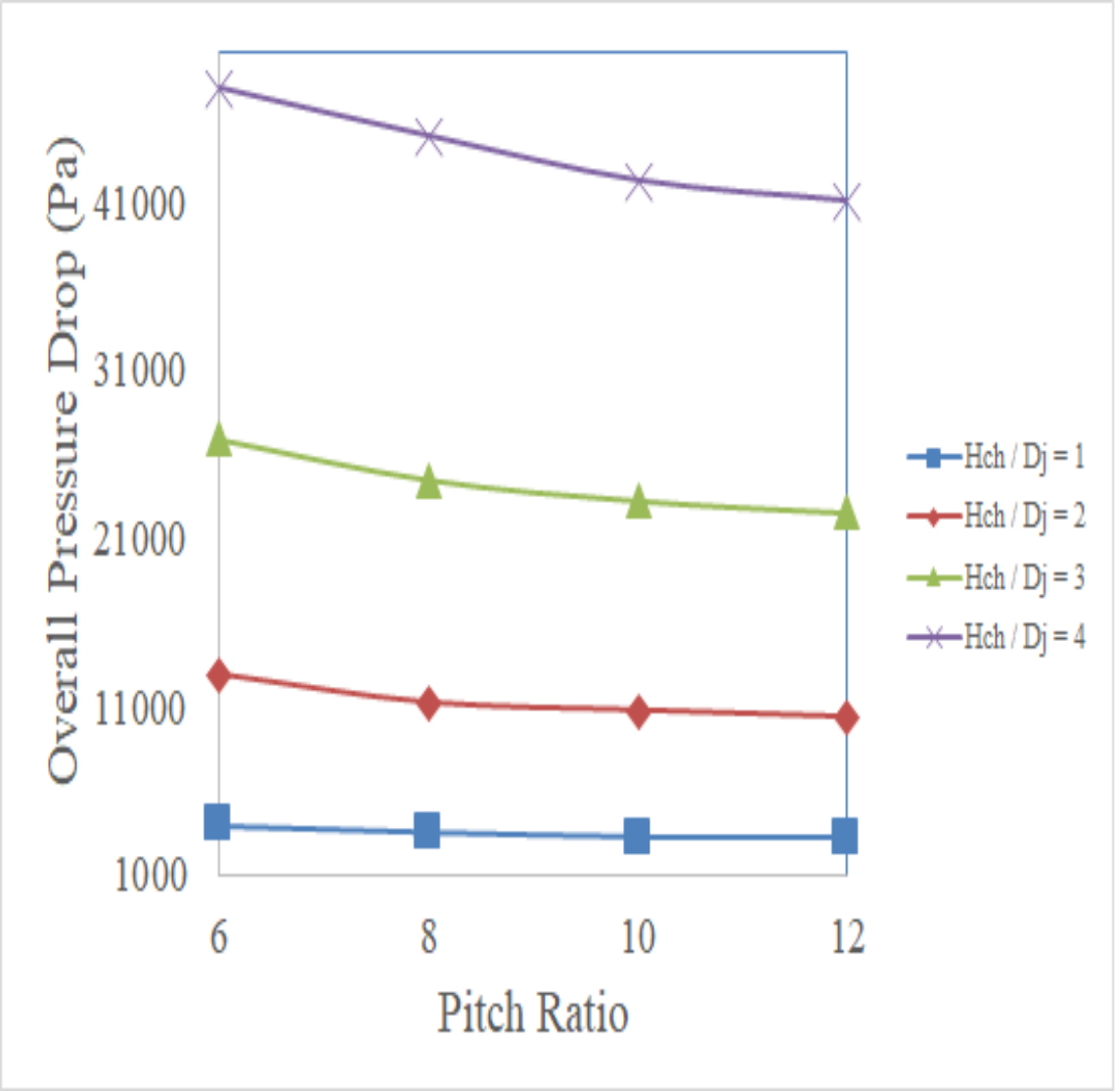

Figure 7.2: Effect of Pitch ratio($\frac{Ph}{D_j}$) on overall pressure drop$(\Delta P)_o$ for water based Al_2O_3 Nanofluid

Figure 7.2 indicates the relation between overall pressure drop and pitch ratio for different values

of height ratio (1,2,3 and 4). The values of pressure drop are detected for pitch ratio values 6,8,10 and 12. With the increase in pitch ratio, from 6 to 12, pressure drop decreases for a particular value of height ratio. Minimum pressure drop is observed for height ratio =1 and maximum for height ratio = 4. Increase in pitch ratio from 6 to 12 also results in decrease in the velocity of fluid and hence discharge. Since this reduction is from jet inlet to the outlet of channel, overall pressure drop also decreases from jet inlet to the channel outlet.

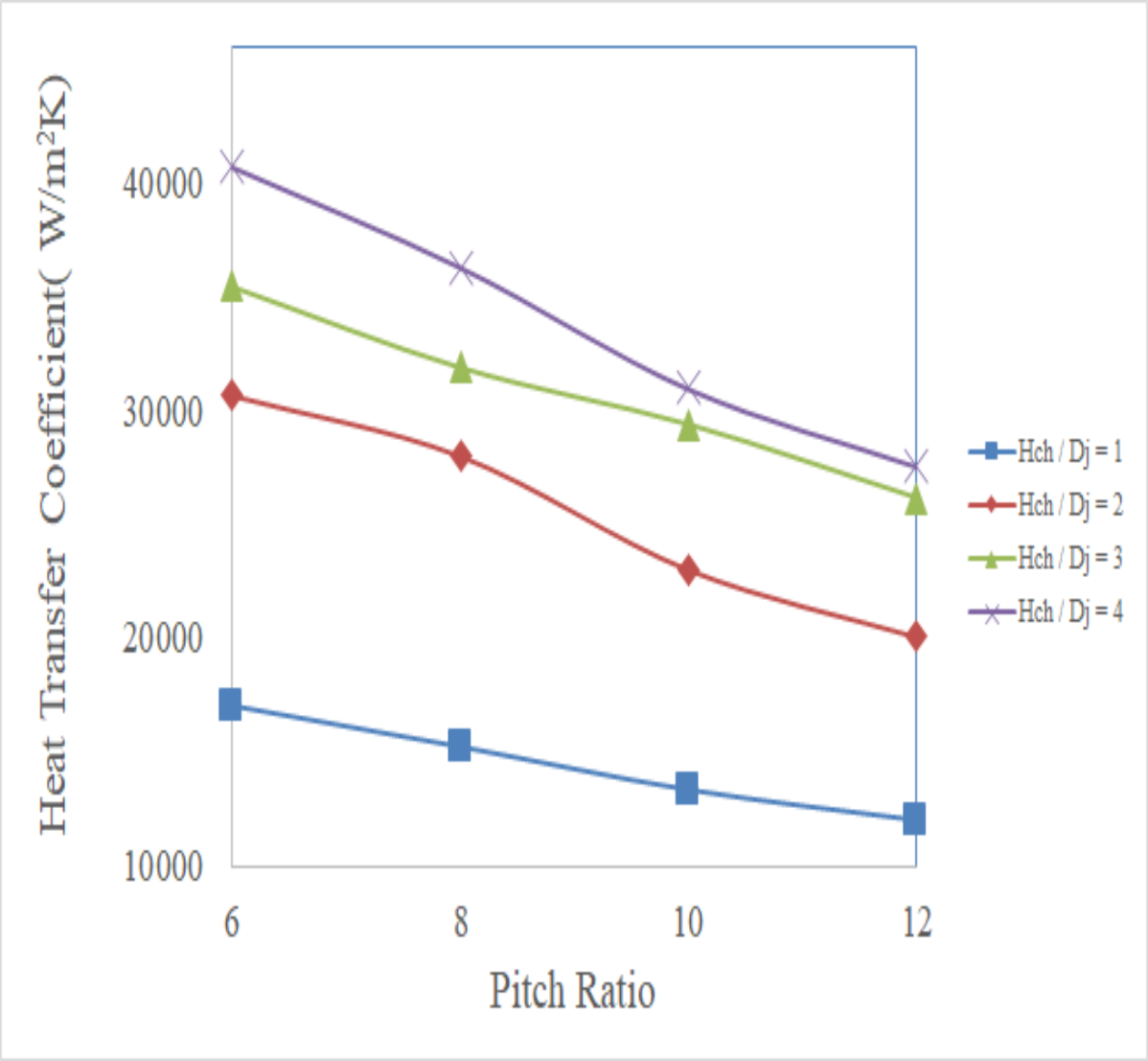

Figure 7.3: Effect of Pitch ratio $\left(\frac{Ph}{D_j}\right)$ on heat transfer coefficient (h) for water based Al_2O_3 Nanofluid

Figure 7.3 indicates the relation between coefficient of heat transfer and pitch ratio for different values of height ratio (1,2,3 and 4). The values of heat transfer coefficient are detected for pitch ratio values 6,8,10 and 12. With the increase in pitch ratio, from 6 to 12, heat transfer coefficient decreases for a particular value of height ratio. Heat transfer coefficient is maximum for height ratio =4 and minimum for height ratio = 1. With an increase in the pitch ratio, convection heat transfer is reduced. The reason for the same is increase in the boundary layer thickness. Because with an increase in the pitch ratio, the counting of jets decreases. And hence the wall jet gets more space to spread in the radial direction. And finally the interaction with the other jets decreases.

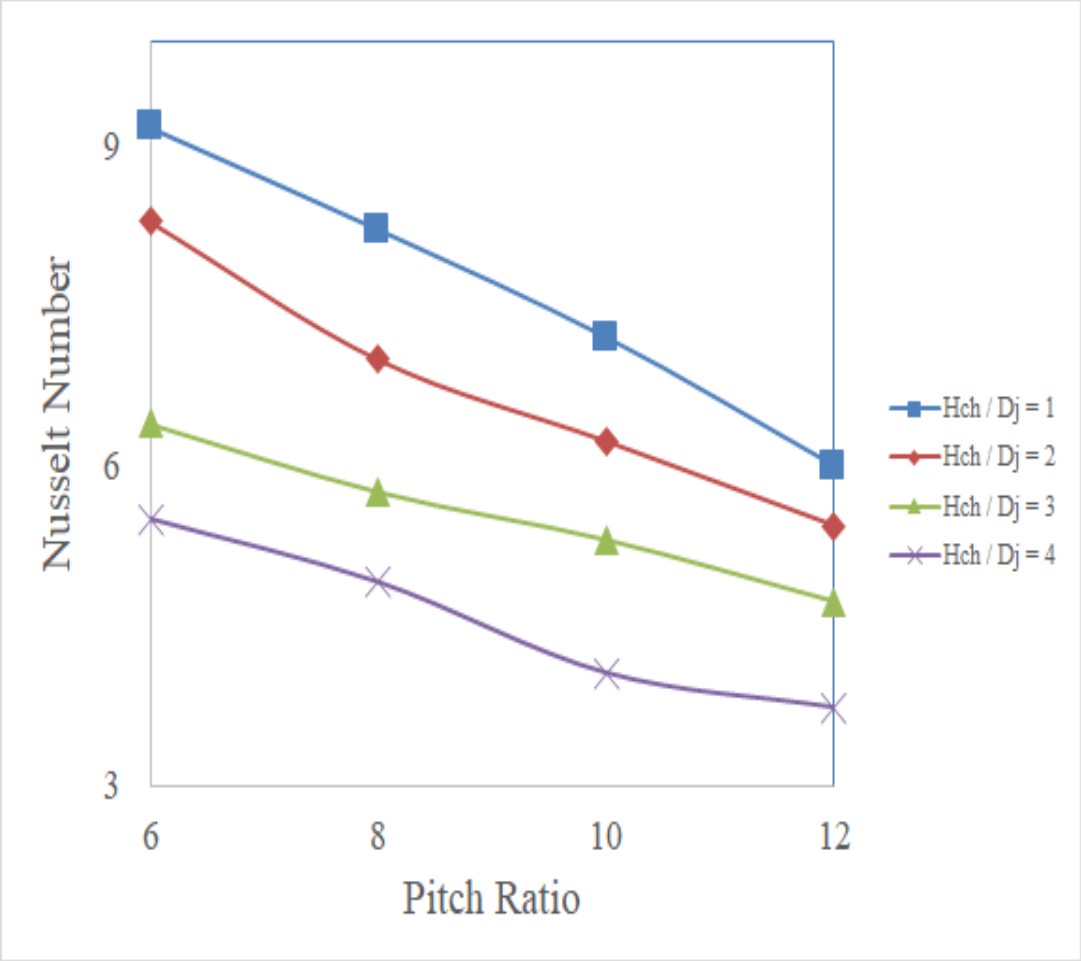

Figure 7.4: Effect of Pitch ratio $\left(\frac{Ph}{D_j}\right)$ on Nusselt Number (Nu) for water based Al_2O_3 Nanofluid

Figure 7.4 indicates the relation between Nusselt number and pitch ratio for different values of height ratio (1,2,3 and 4). The values of heat transfer coefficient are detected for pitch ratio values 6,8,10 and 12. With the increase in pitch ratio, from 6 to 12, Nusselt number decreases for a particular value of height ratio. Nusselt number is found to be maximum for height ratio =1 and minimum for height ratio = 4. With an increase in the pitch ratio, Nu is reduced. The reason for the same is increase in the boundary layer thickness. Because with an increase in the pitch ratio, the counting of jets decreases. And hence the wall jet gets more space to spread in the radial direction. And finally the interaction with the other jets decreases

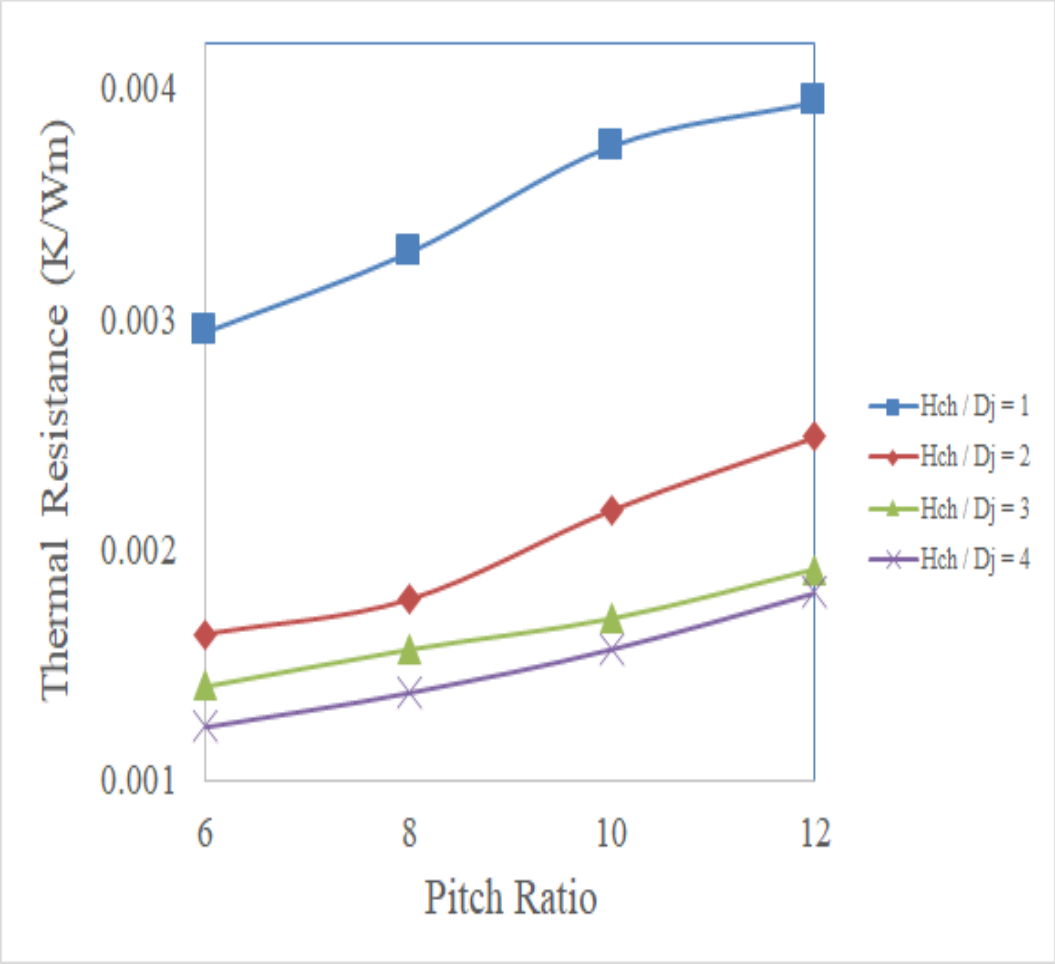

Figure 7.5: Effect of Pitch ratio $(\frac{Ph}{D_j})$ on Thermal resistance$(R)_T$ for water based Al_2O_3 Nanofluid

Figure 7.5 indicates the relation between thermal resistance and pitch ratio for different values of height ratio (1,2,3 and 4). The values of thermal resistance are detected for pitch ratio values 6,8,10 and 12. With the increase in pitch ratio, from 6 to 12, thermal resistance increases for a particular value of height ratio. Thermal resistance is found to be maximum for height ratio =1 and minimum for height ratio = 4. But due to the frictional losses thermal resistance has a tendency to increase with an increase in the pitch ratio.

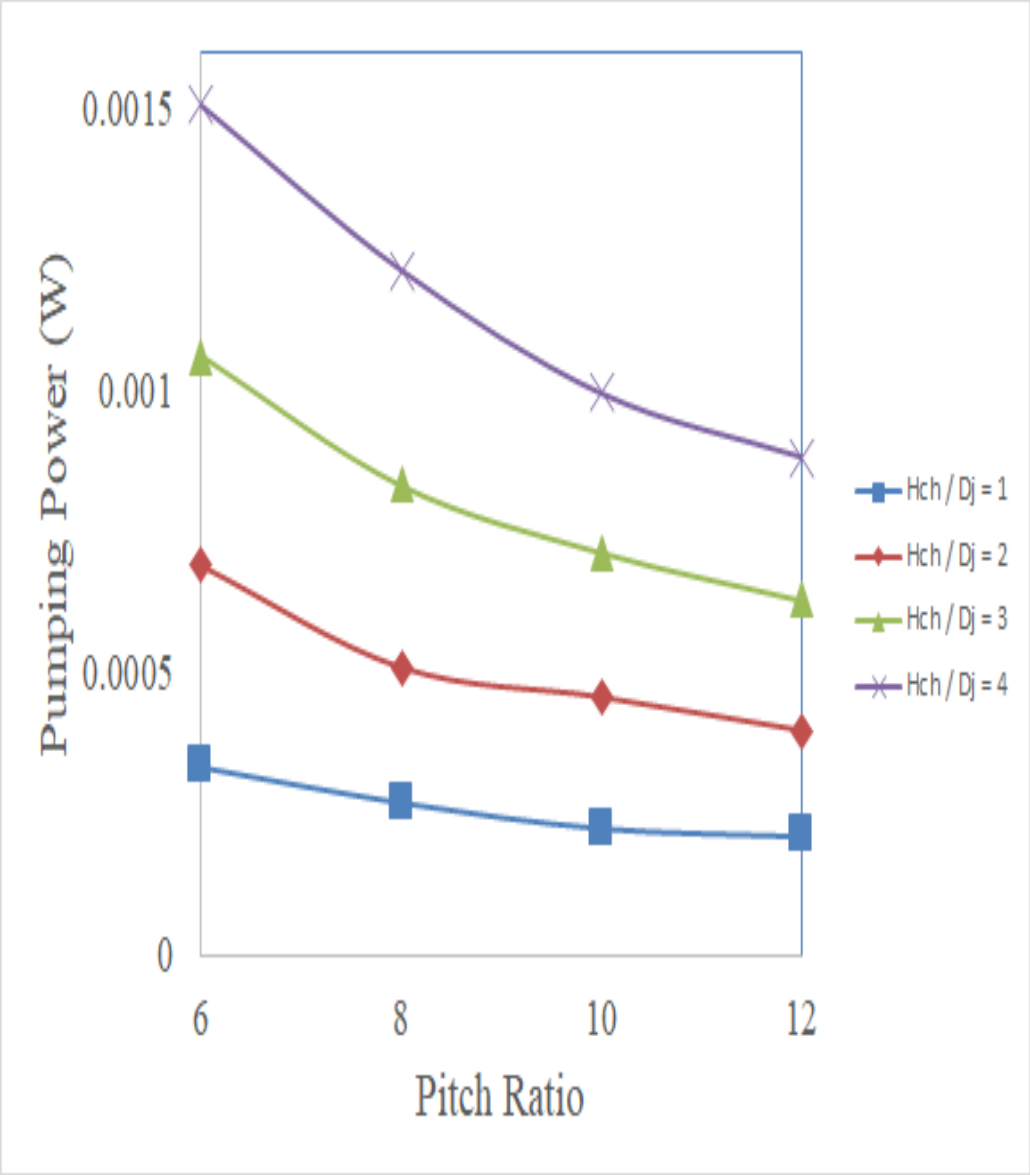

Figure 7.6: Effect of Pitch ratio ($\frac{Ph}{D_j}$) on Pumping power (P_p) for water based Al_2O_3 Nanofluid

Figure 7.6 indicates the relation between pumping power and pitch ratio for different values of height ratio (1,2,3 and 4). The values of pumping power are detected for pitch ratio values 6,8,10 and 12. With the increase in pitch ratio, from 6 to 12, pumping power decreases for a particular value of height ratio. Pumping power is found to be maximum for height ratio =4 and minimum for height ratio = 1. The thermophysical properties of Nanofluid has an advantage of decreasing trend in pumping power.

7.3 Water-CuO (0.5%) and water-Al_2O_3 Nano fluid (5%)

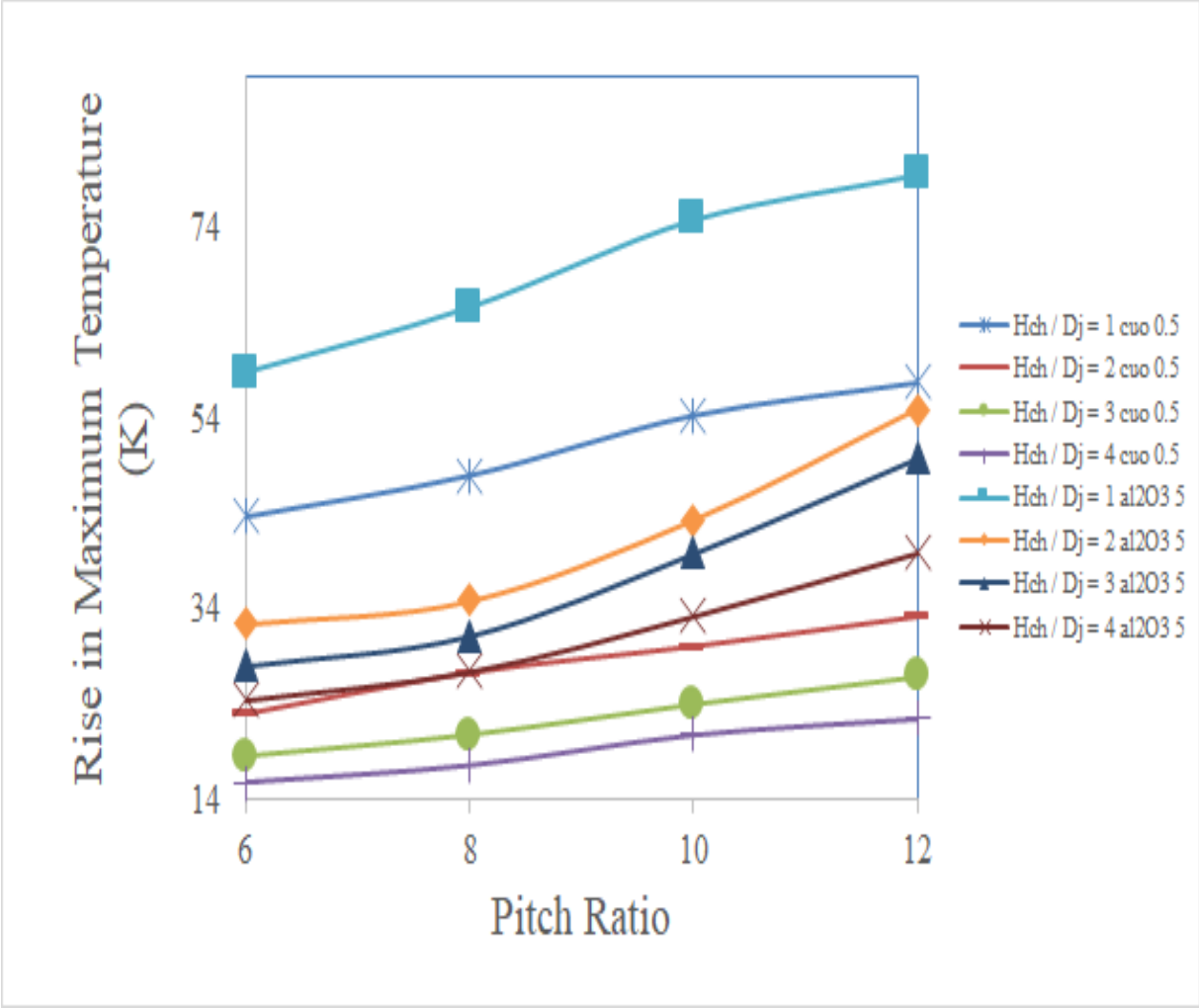

Figure 7.7: Effect of Pitch ratio $(\frac{Ph}{D_j})$ on rise in maximum temperature$(\Delta T)_r$ for water based CuO and Al_2O_3 Nanofluid

Figure 7.7 shows the comparative analysis for the rise in maximum temperature with pitch ratio for water based CuO and Al_2O_3 Nano fluids. CuO is used with 0.5% concentration and Al_2O_3 is used with 5% concentration. With an increase in the pitch ratio, rise in temperature is detected. This is because of the decrease in the number of impingements which results due to increase in the pitch ratio. The thermophysical properties of Nanofluid plays an important role in decreasing the temperature of the base and attainment of the uniformity.

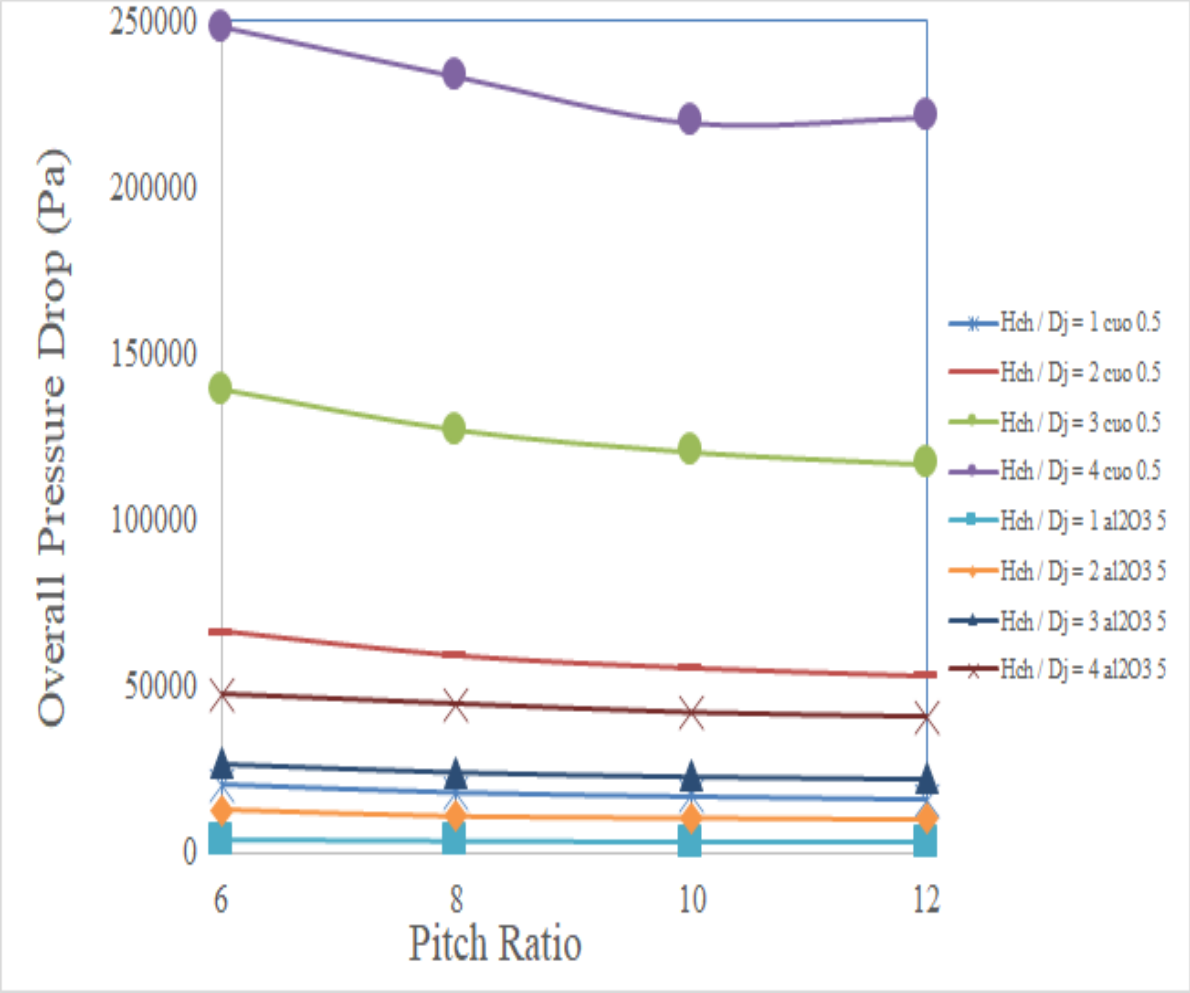

Figure 7.8: Effect of Pitch ratio($\frac{Ph}{D_j}$) on overall pressure drop($\Delta P)_o$ for water based CuO and Al_2O_3 Nanofluid

Figure 7.8 shows the comparative analysis for the drop in pressure with pitch ratio for water based CuO and Al_2O_3 Nano fluids. CuO is used with 0.5% concentration and Al_2O_3 is used with 5% concentration. Drop in pressure is found to be more in case of CuO as compared to Al_2O_3. The same is due to the lower thermal conductivity of CuO- water as Compared to the other Nanofluid.

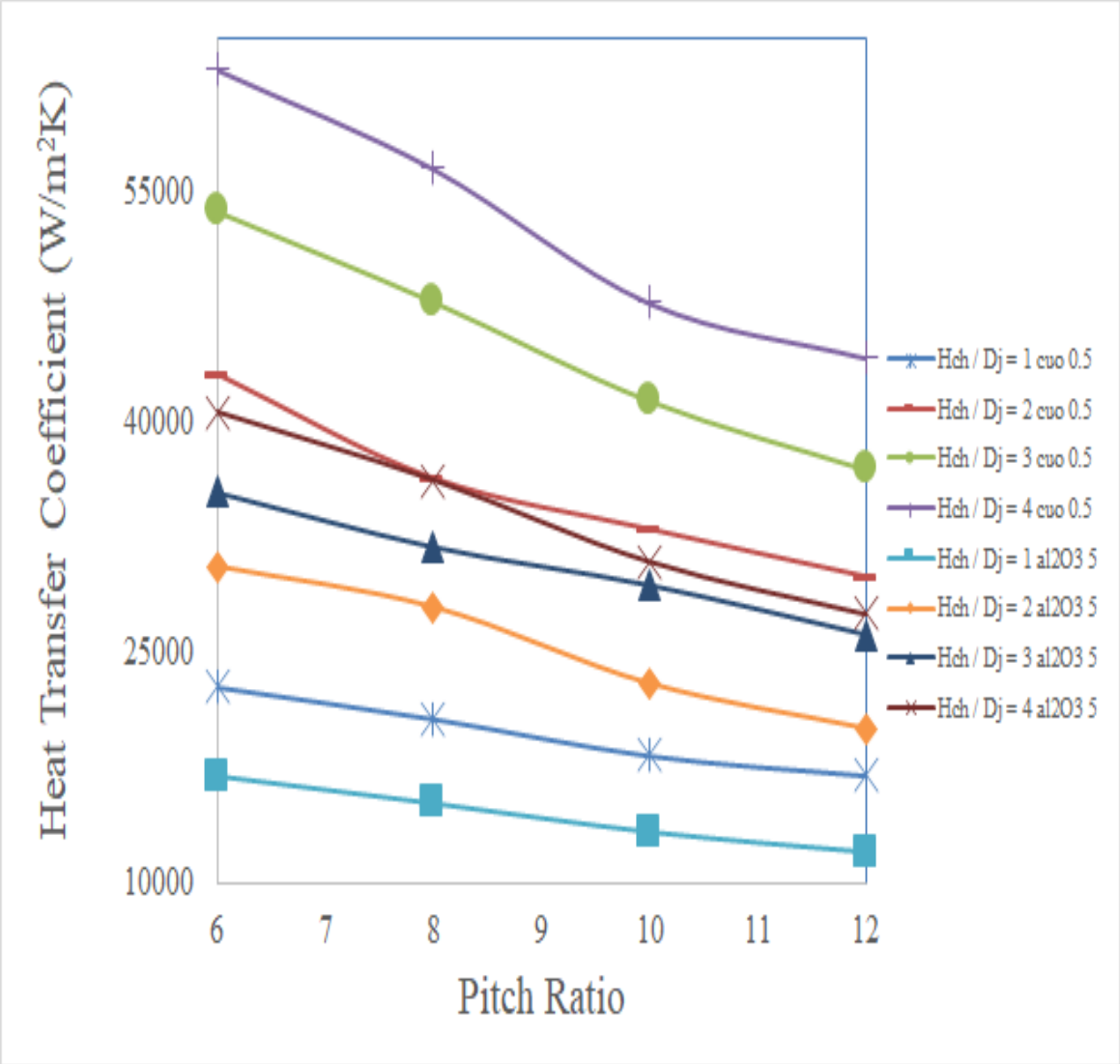

Figure 7.9: Effect of Pitch ratio $\left(\frac{Ph}{D_j}\right)$ on heat transfer coefficient (h) for water based CuO and Al_2O_3 Nanofluid

Figure 7.9 shows the comparative analysis for the coefficient of heat transfer with pitch ratio for water based CuO and Al_2O_3 Nano fluids. CuO is used with 0.5% concentration and Al_2O_3 is used with 5% concentration. With an increase in the pitch ratio, convection heat transfer is reduced. The reason for the same is increase in the boundary layer thickness. Because with an increase in the pitch ratio, the counting of jets decreases. And hence the wall jet gets more space to spread in the radial direction. And finally the interaction with the other jets decreases

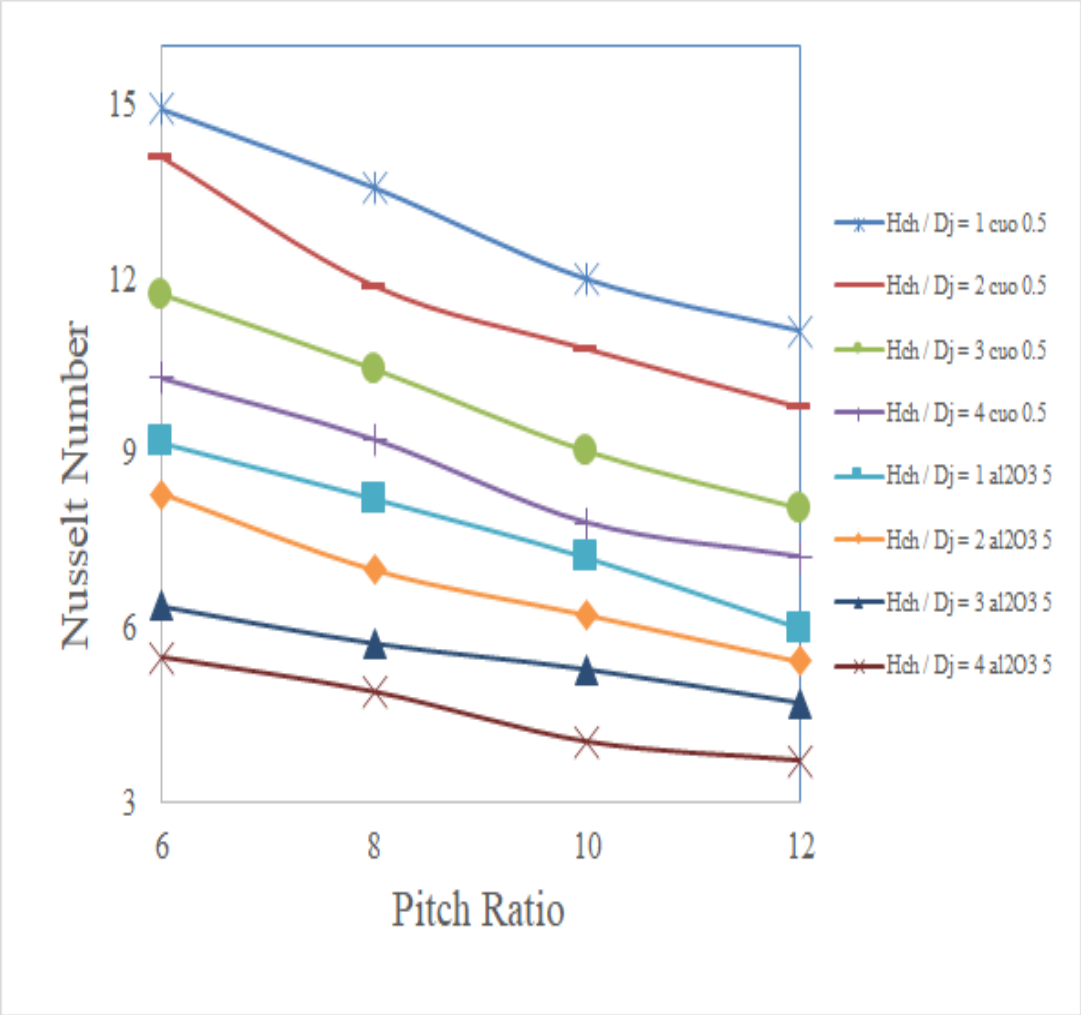

Figure 7.10: : Effect of Pitch ratio $\left(\frac{Ph}{D_j}\right)$ on Nusselt Number (Nu) for water based CuO and Al_2O_3 Nanofluid

Figure 7.10 shows the comparative analysis for the Nusselt number with pitch ratio for water based CuO and Al_2O_3 Nano fluids. CuO is used with 0.5% concentration and Al_2O_3 is used with 5% concentration. Decreasing trend is observed with an increase in the pitch ratio for both the cases. The reason for the same is increase in the boundary layer thickness. Because with an increase in the pitch ratio, the counting of jets decreases.

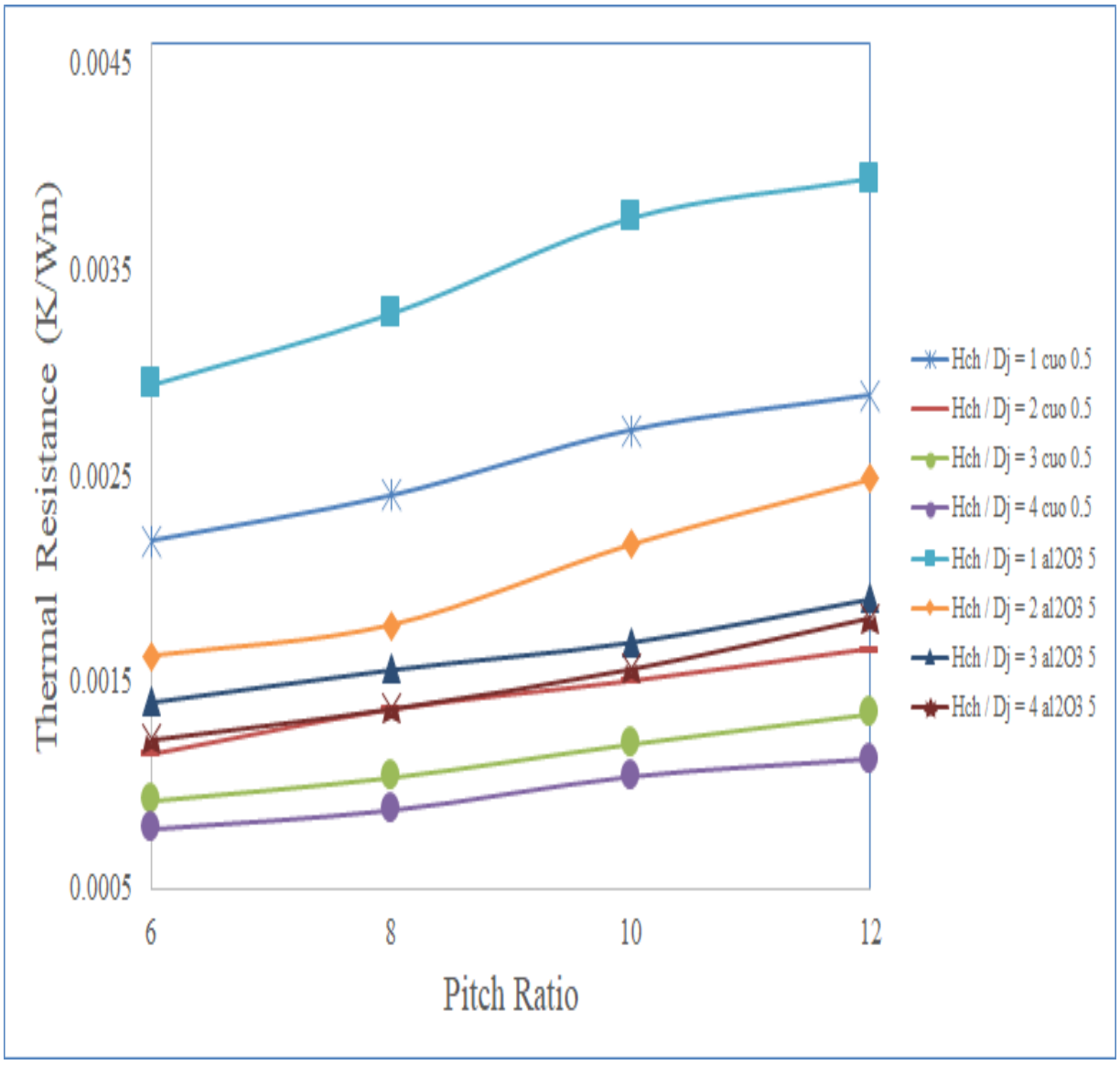

Figure 7.11: Effect of Pitch ratio $(\frac{Ph}{D_j})$ on Thermal resistance$(R)_T$ for water based CuO and Al_2O_3 Nanofluid

Figure 7.11 shows the comparative analysis for the thermal resistance with pitch ratio for water based CuO and Al_2O_3 Nano fluids. CuO is used with 0.5% concentration and Al_2O_3 is used with 5% concentration. Increasing trend is detected in both the cases because of the frictional losses in between the jets.

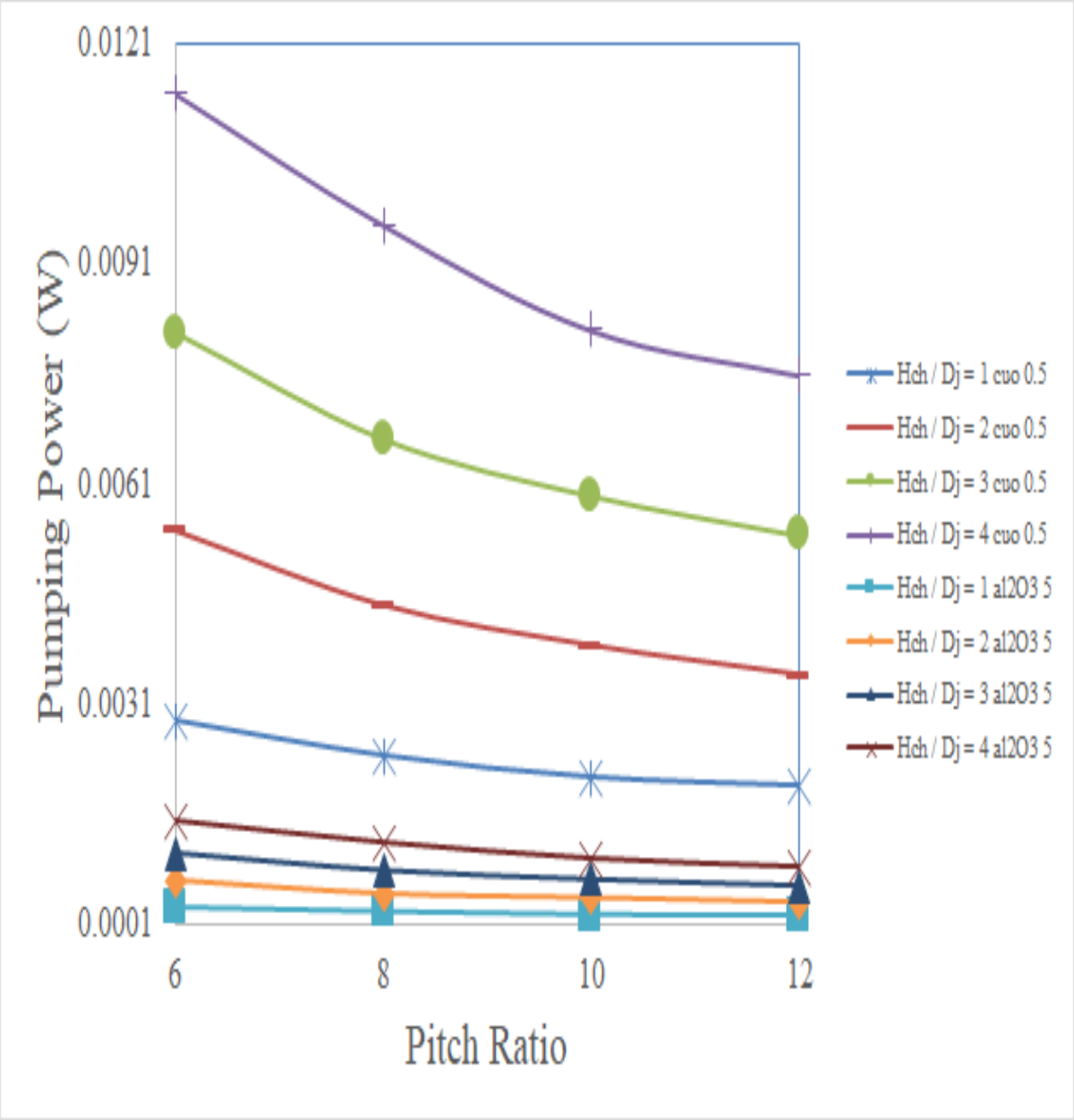

Figure 7.12: Effect of Pitch ratio ($\frac{Ph}{D_j}$) on Pumping power (P_p) for water based CuO and Al_2O_3

Nanofluid

Figure 7.12 shows the comparative analysis for the pumping power with pitch ratio for water based CuO and Al_2O_3 Nano fluids. CuO is used with 0.5% concentration and Al_2O_3 is used with 5% concentration. In this case also decreasing trend is detected because of the thermophysical properties of the Nanofluid.

7.4 Graph for different parameters with height ratio using water

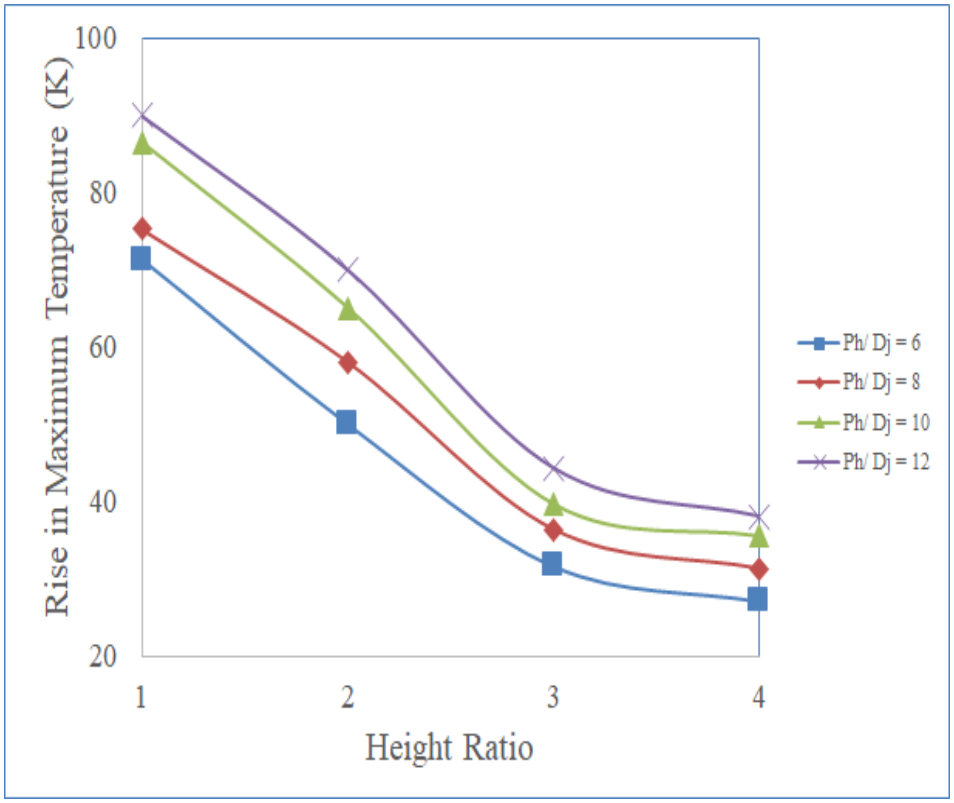

Figure 7.13: Effect of Height ratio $(\frac{H_{ch}}{D_j})$ on Rise in maximum temperature$(\Delta T)_r$ for water

From the figure 7.13 it is clearly understood that lowest value of temperature is at height ratio = 4 and pitch ratio = 6.

Figure 7.13 depicts the temperature rise with the ratio of channel height and diameter of channel for different values of pitch ratio. Inverse trend is observed between the two variables. For Ph/Dj = 6, $(\Delta T)_r$ for Hch/Dj= 1,2,3 and 4 is noticed to be 71.29 K,50 K, 31.62 K and 27.1 K. This shows

that as the design parameter is increased, the response parameter is decreased. For Ph/Dj = 8, $(\Delta T)_r$ for Hch/Dj= 1,2,3 and 4 is noticed to be decreased. The maximum value is found to be 75 K. Similar type of pattern is seen for Ph/Dj = 10 and 12. From the graph it is concluded that the maximum temperature is detected at Ph/Dj = 12 and Hch/Dj=1 Also the optimum value is 90 K. Hence for all values of Ph/Dj (6,8,10 and 12), Hch/Dj = 1, is noticed to be the optimum parameter.

With an increase in HR, the velocity of jet increases which in result create thinner boundary layer and hence decreasing trend is observed.

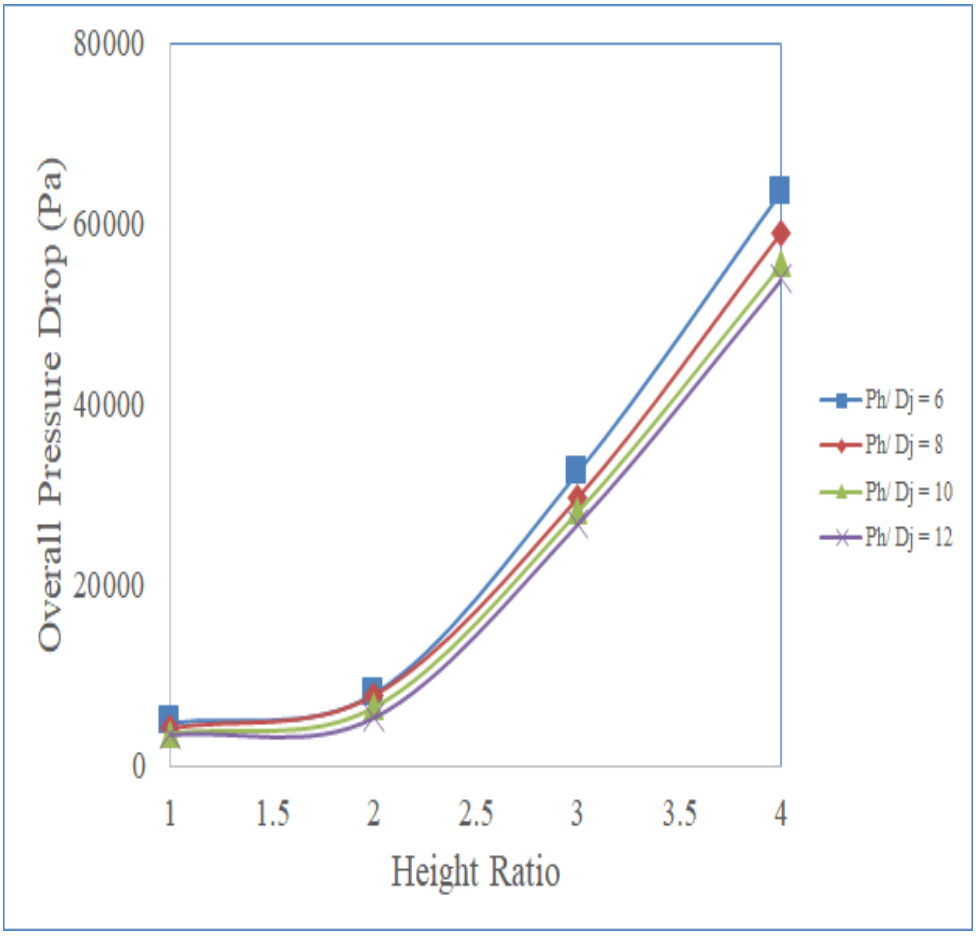

Figure 7.14: Effect of Height ratio $(\frac{H_{ch}}{D_j})$ on Overall pressure drop $(\Delta P)_o$ for water

Figure 7.14 communicates the moderation in fall in pressure with Hch/ Dj for various values of Ph/Dj. At Ph/Dj = 6 and Hch/Dj= 1, the value of response parameter was recognized as 4811 Pa.

The value escalates as the value of Hch/Dj is increased. And the extreme value is marked at Hch/Dj = 4. For Ph/Dj= 8 the extreme value is marked at Hch/Dj= 4. Also the extreme value is noted to be 59000 Pa. So it is concluded that positive pattern is analysed between the design and response variables. The minimum value of fall in pressure is concluded to be 3508 corresponding to Ph/Dj =12 and Hch/Dj = 1. So it is deduced from the figure 7.14 that for all values of Ph/Dj (6,8,10 and 12), Hch/Dj = 1is detected as the optimum parameter. With an increase in height ratio from 1 to 4, the velocity of jet and hence discharge is increased. This results in advancement in the frictional losses, which further results in an increase in the OPD.

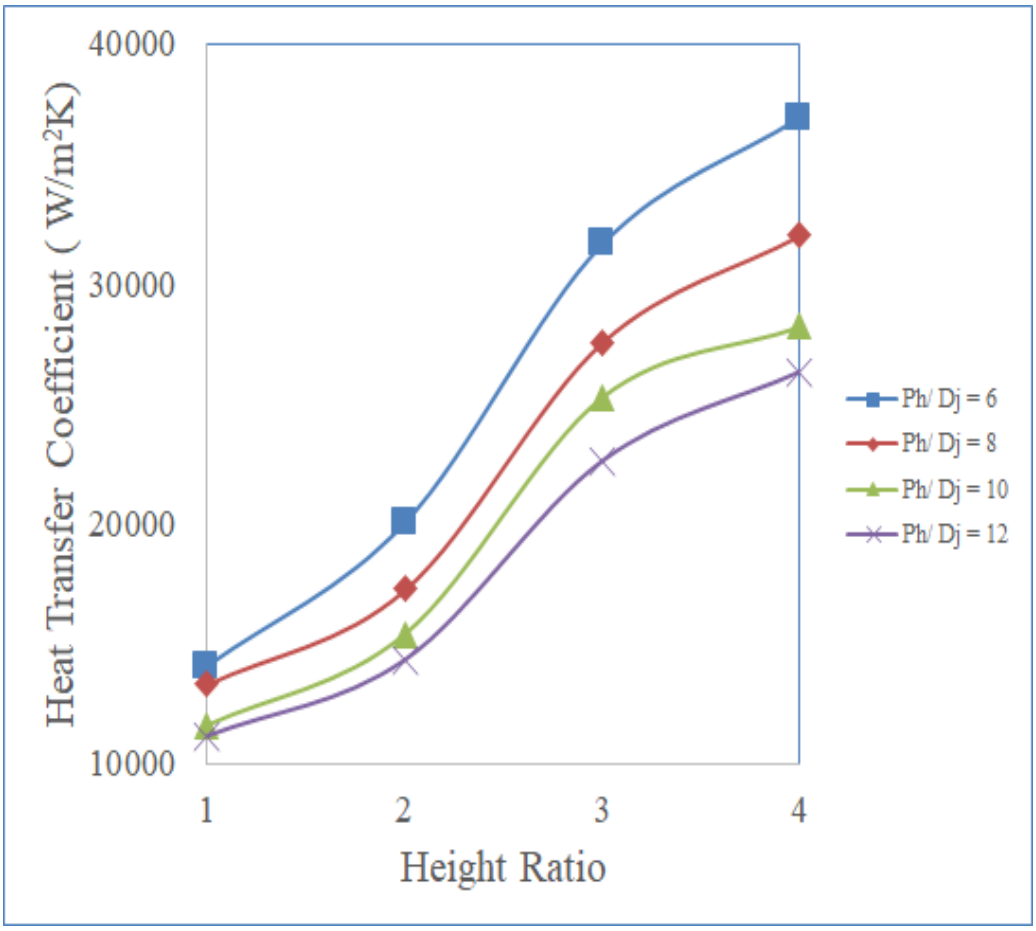

Figure 7.15: Effect of Height ratio ($\frac{H_{ch}}{D_j}$) on Heat transfer coefficient (h) for water

Figure 7.15 shows the moderation in coefficient of heat transfer with Hch/Dj for various values of

Ph/Dj respectively. For Ph/Dj = 6 and Hch/Dj= 1, the value of response parameter is marked as 14000. Now as the value of Hch/Dj is surged from 1 to 4, escalation is marked in the value of response variable. Homogeneous pattern is marked for Ph/Dj = 8 10 and 12 as Hch/Dj is increased from 1to 4. Hence from the figure 7.15 the optimum value of response variable is marked at Ph/Dj = 6, Hch/Dj= 1. It is deduced from the figure 7.15 that positive pattern is noticed between the two variables. The increase in coefficient is due to the fall in temperature rise, with an increase in Hch/Dj.

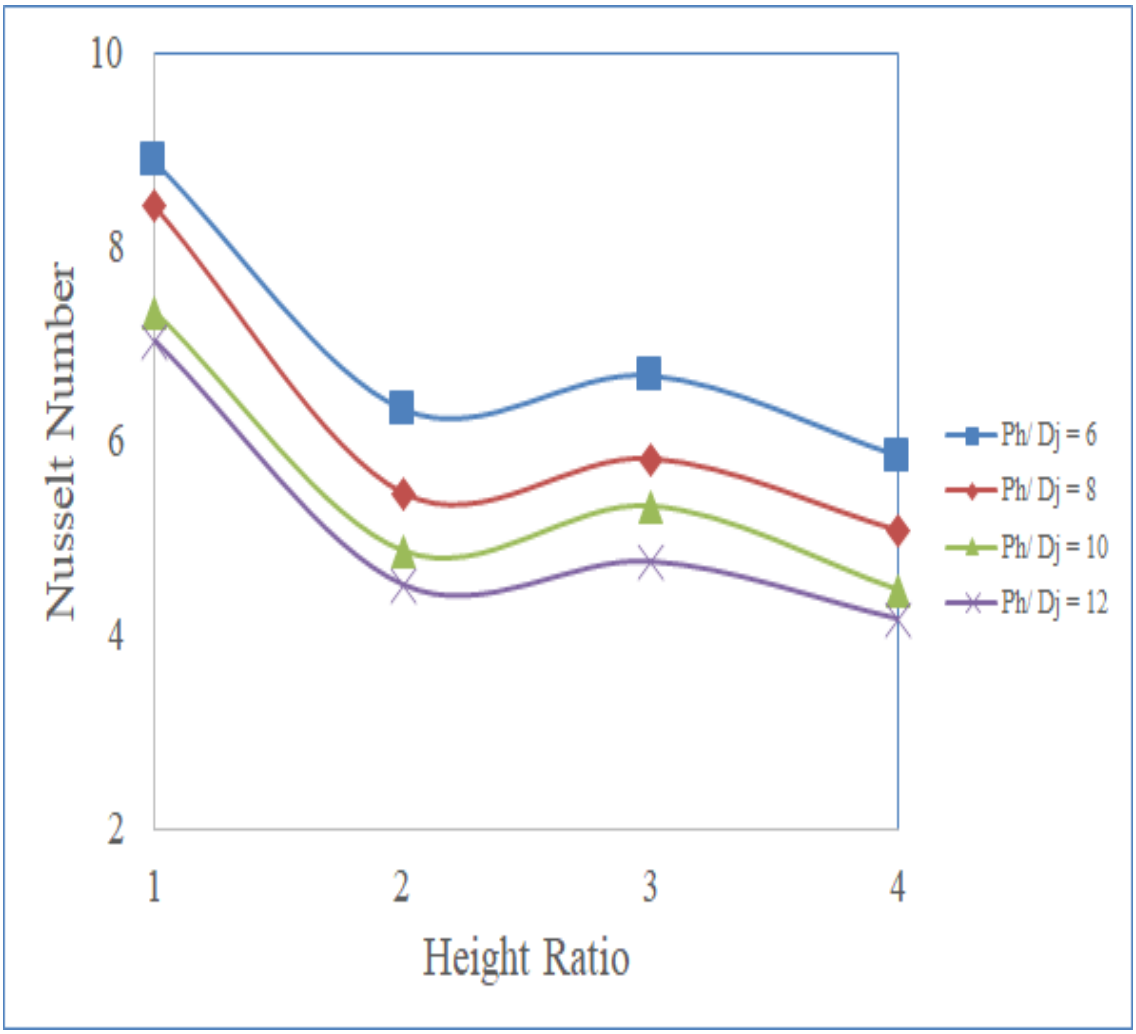

Figure 7.16: Effect of Height ratio ($\frac{H_{ch}}{D_j}$) on Nusselt Number (Nu) for water

Figure 7.16 exhibits the relation between Nu and Hch/Dj. For Ph/Dj= 6 and Hch/Dj = 1, the value

of Nu is marked as 8.8. Lowest value is marked at Hch/Dj = 4. For Ph/Dj= 8, the extreme value is marked at Hch/Dj = 1. So from the figure it is concluded that the optimum value is 8.8 which is communicating to Ph/Dj= 6 and Hch/Dj = 1. As the value of Hch/Dj is surged, reducing trend in Nu is noticed. In case of Nusselt number reducing pattern is noticed. The reason for the same is related to the decrease in diameter of jet.

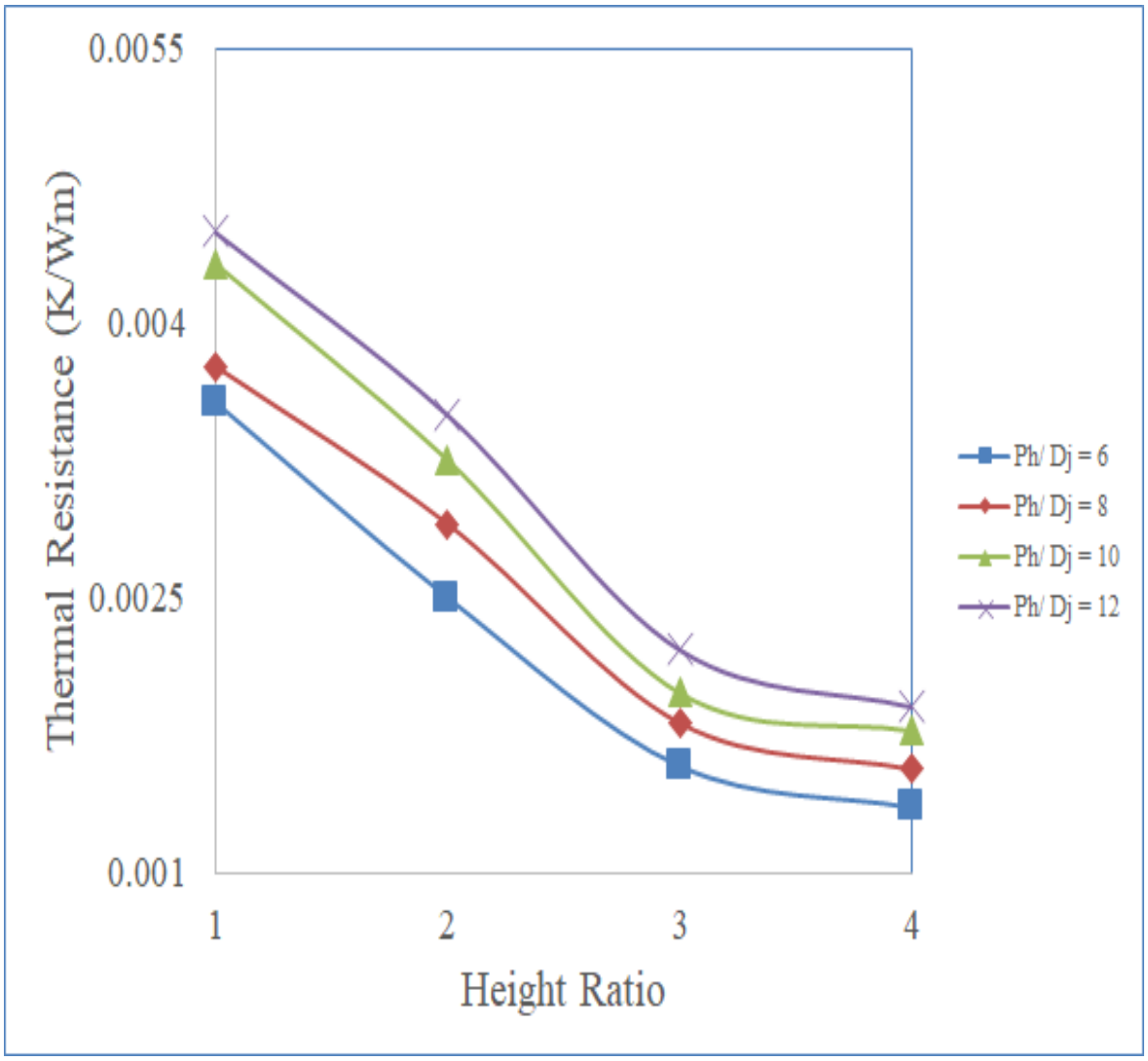

Figure 7.17: Effect of Height ratio $(\frac{H_{ch}}{D_j})$ on Thermal resistance$(R)_T$ for water

Figure 7.17 exhibits the characteristics of resistance for design variable Hch/Dj = 1 to 4. For Ph/ Dj = 6, Hch/Dj = 1, the value of resistance is marked as 0.0035645. This value dwindles as Hch/Dj

is surged from 1 to 4. For Ph/ Dj = 8, Hch/Dj = 1, R_T = 0.0037595. As Hch/Dj is increased the value of resistance decreases. This is due to decrease in the diameter of jet, which increases the velocity of jet and causes turbulence. For Ph/ Dj = 10, Hch/Dj = 1, R_T = 0.00432. Similar trend is detected in the case of Ph/Dj = 12.

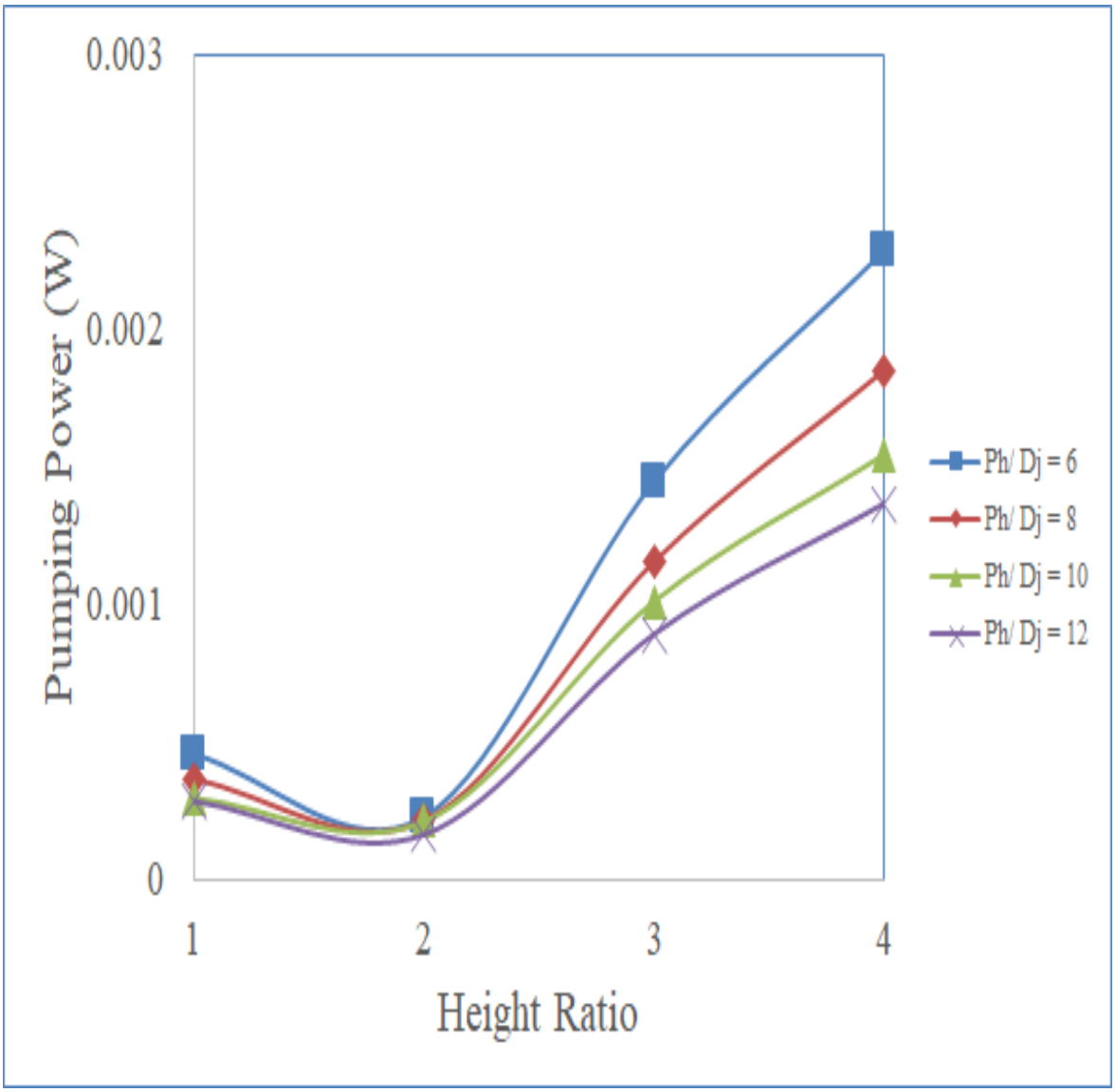

Figure 7.18: Effect of Height ratio ($\frac{H_{ch}}{D_j}$) on Pumping Power (P_p) for water

Figure 7.18 depicts the correlation between the design variable which is taken as pumping power and response variable which is proportion of height and diameter for different values of proportion

of pitch and diameter. For ph/Dj = 6 and Hch/Dj = 1, the value of power is noted to be 0.00044933 W. Lowest value of power is marked at Hch / Dj = 2. For For ph/Dj = 8, lowest value is at Hch/Dj = 2. So the conclusion drawn from the figure 18 is that as the proportion of height and diameter is increased, power also increases. This increase in power is not desirable and this results in the decrease in the performance of the system. This is due to the increase in the friction forces.

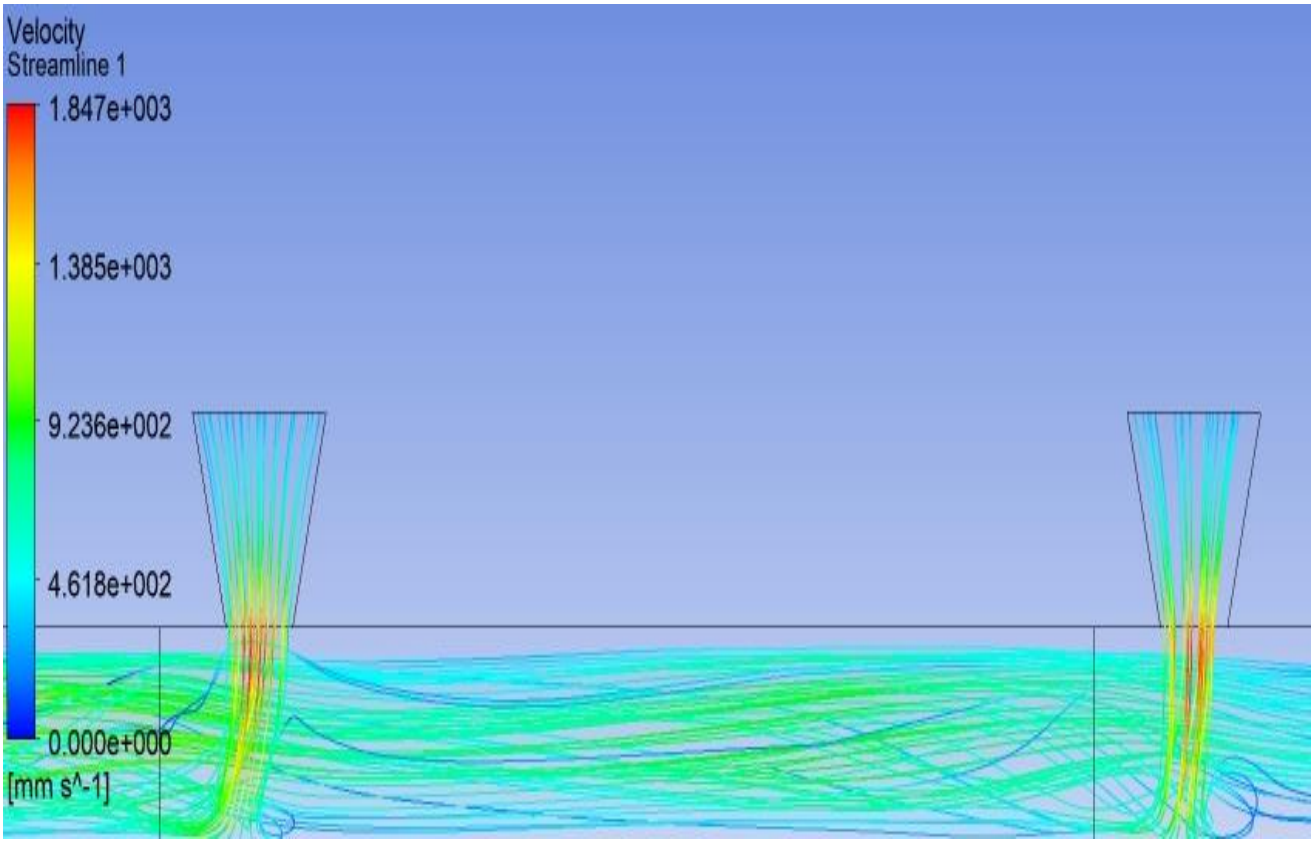

Figure 7.19: Streamlines at HR = 1, PR = 6 for water

From the results it was conclude that use of air foil pillars has helped in reducing the thermal resistance. This definitely aids to the improvement in the transfer of heat. Figure 7.19 shows the pattern of streamlines.

7.5 Water and water – CuO Nano fluid (1%)

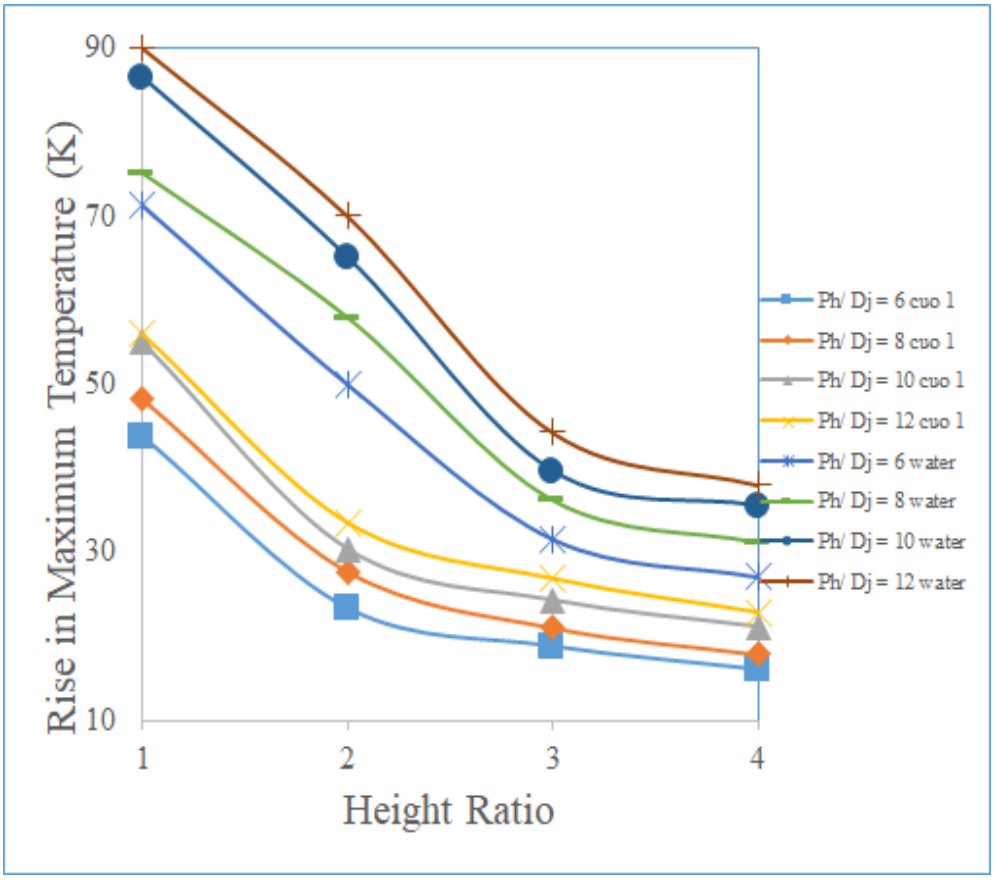

Figure 7.20: Effect of Height ratio $(\frac{H_{ch}}{D_j})$ on Rise in maximum temperature$(\Delta T)_r$ for water and water based CuO Nanofluid

Figure 7.20 indicates the revision in the temperature of substrate with change in the height ratio (1,2,3 and 4) for pitch ratio = 6,8,10 and 12 in case of water and Nanofluid (NFL) with 1% concentration. From the figure 20 it is clear that at PR = 8 for NFL temperature rise is marked as 48.19 K, analogous to HR = 1. For the similar conditions for the water, it is marked as 75.19 K. At HR = 2, temperature is reduced to 27.7 K in case of NFL and58 K in case of pure water. At HR = 3, temperature values are found to be 21.04 K and 36.3 K for NFL and water respectively in analogous to PR = 8. At HR = 4, the values are noted to be 31.25 K and 17.86 K for water and NFL respectively. So at PR = 8, increase in HR leads to decrease in temperature rise. For PR = 10

and HR = 1, temperature for NFL and water is noted to be 86.4 K and 55.02 K respectively. For HR = 2,3 and 4 and PR = 10, temperature is marked as 64 K,39.6 K, 35.48 K for water and 30.39 K, 24.31 K, 21.15 K for NFL sequentially. Similarly, for PR = 12, HR = 1,2,3 and 4, the values are found to be in decreasing order. With an increase in HR, the velocity of jet increases which in result create thinner boundary layer and hence decreasing trend is observed.

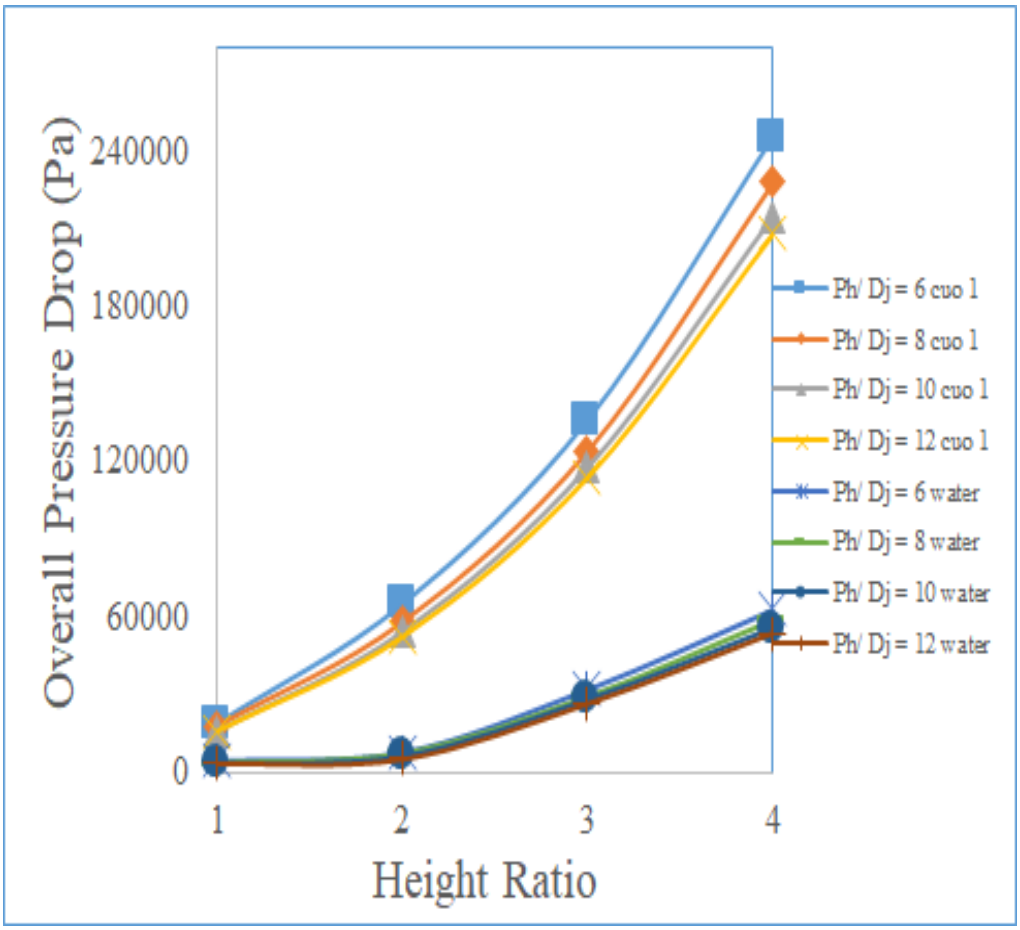

Figure 7.21: Effect of Height ratio $(\frac{H_{ch}}{D_j})$ on Overall pressure drop$(\Delta P)_o$ for water and water based CuO Nanofluid

Figure 7.21 intimates the relation between HR and overall pressure drop (OPD) for distinct values of PR for water and NFL. At PR = 8 and HR = 1, OPD is marked as17813 Pa and 4166 Pa for NFL and water sequentially. Now as HR is increased 2,3 and 4, OPD is also increased in both the cases

with values 7826 Pa, 29683 Pa and 59020 Pa in case of water sequentially. At PR = 10 and HR = 1,2,3 and 4, OPD = 3553 Pa, 6489 Pa, 28173 Pa and 55565 Pa respectively for water and in case of NFL higher values of OPD is noted. As HR is increased, OPD also gets increased, which is not a desirable condition. So the model for HR = 1gives optimum conditions both in case of water and NFL. The minimum values of OPD are 3508 Pa and 15844 Pa in water and NFL corresponding to HR = 1 and PR = 12. With an increase in height ratio from 1 to 4, the velocity of jet and hence discharge is increased. This results in advancement in the frictional losses, which further results in an increase in the OPD.

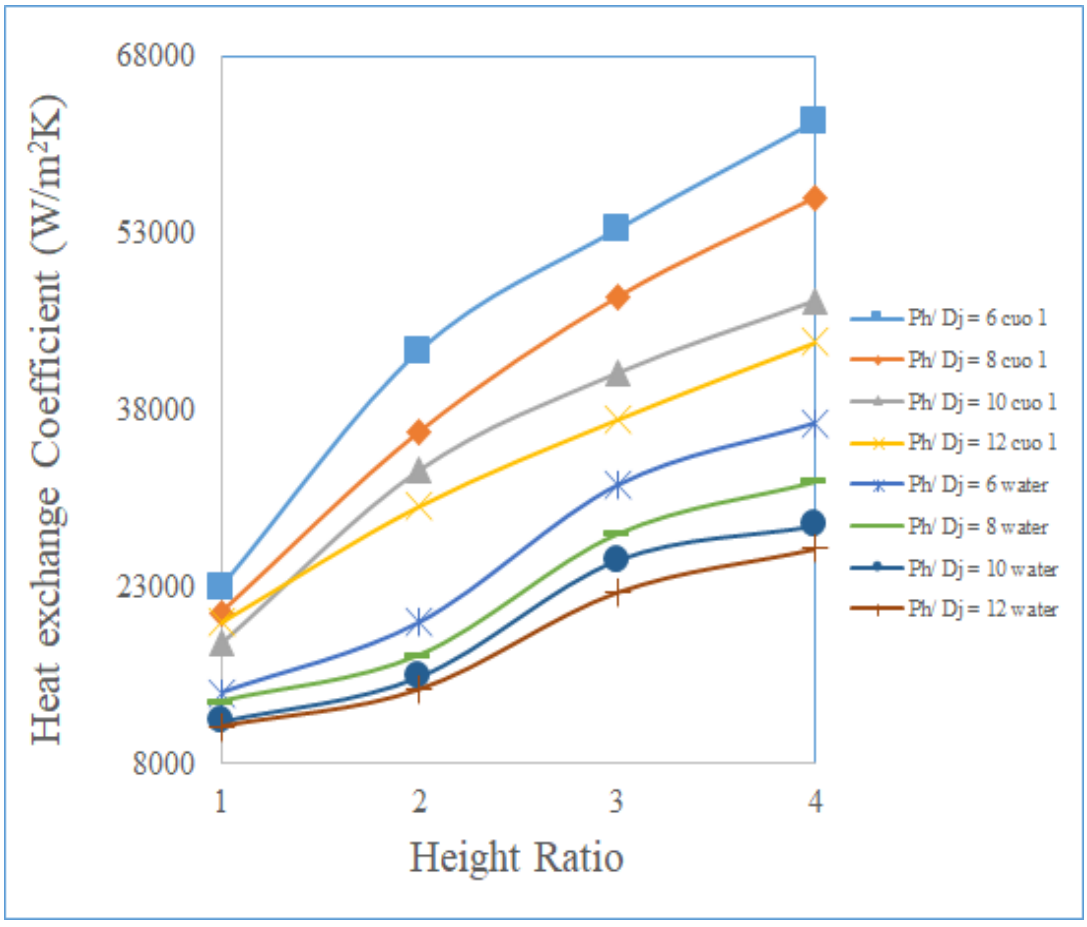

Figure 7.22: Effect of Height ratio ($\frac{H_{ch}}{D_j}$) on Heat transfer coefficient (h) for water and water based CuO Nanofluid

Figure 7.22 intimates the connection between HR and Coefficient of heat exchange (h) for distinct values of PR in case of water and water- CuO Nano fluid with 1% concentration. It is predicted from the figure 7.22 that with the use of NFL, h is increased in differentiation to pure water. At PR = 8 and HR = 1, h is marked as 13299 for pure water and 20751 for NFL. At HR =2, h is marked as 17241 and 36101 for water and NFL sequentially. At HR = 3, h is noticed to be 27548 for water and 47528 for NFL analogous to PR = 8. At HR = 4, h is increased to 32000 for pure water and 55991 for NFL. For PR = 10 and HR = 4, h is found to be 28184 and 47281 for water and NFL. This indicates that h is detected to be more with NFL in contrast to pure water. For PR = 12 the extreme value of h is detected to be 26288 for water and 43744 for NFL, which is analogous to HR = 4. So with the augmentation in HR, h is also augmented for a particular value of PR. The lowest value of h is marked corresponding to PR = 6 and HR = 1. The increasing trend in coefficient is due to the fall in temperature rise, with an increase in Hch/Dj.

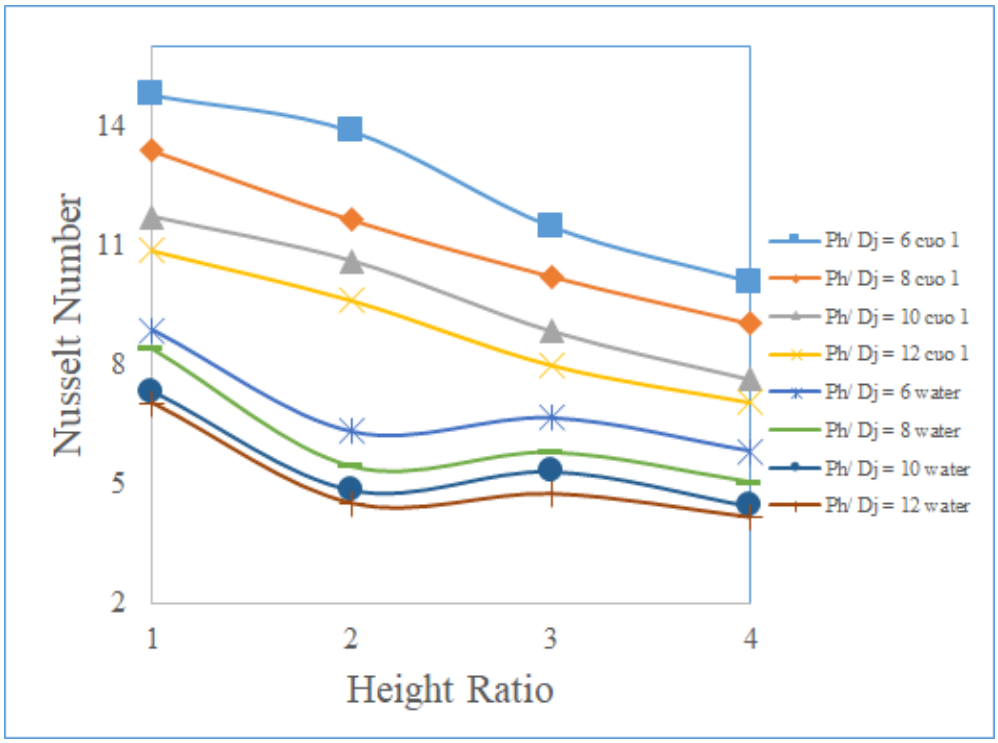

Figure 7.23: Effect of Height ratio ($\frac{H_{ch}}{D_j}$) on Nusselt Number (Nu) for water and water based CuO Nanofluid

In figure 7.23, connection between the HR and Nusselt number (Nu) has been executed for different values of PR for pure water and NFL with 1% concentration. At PR = 8 and HR = 1, Nu = 13 for NFL and 8 for water which is lower than NFL. So the use of water – CuO NFL with 1 % concentration increased the value of Nu. At HR =2, Nu is marked as 11 and 5.45 for NFL and water sequentially. With the increase in the value of HR, decreasing fashion is predicted in the value of Nu both for water and NFL. The extreme value of Nu is noticed in case of NFL corresponding to HR = 1 and PR = 6. The lowest value of Nu is obtained corresponding to PR = 12 and HR = 4.

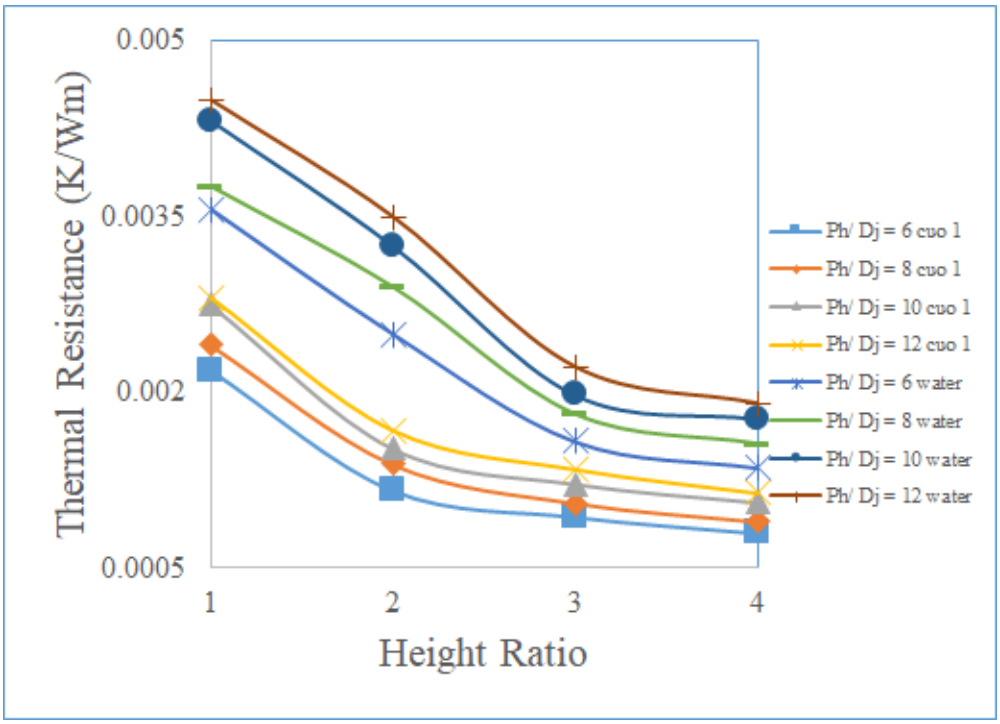

Figure 7.24: Effect of Height ratio ($\frac{H_{ch}}{D_j}$) on Thermal resistance$(R)_T$ for water and water based CuO Nanofluid

Figure 7.24 outlines the interconnection between HR and thermal resistance in case of heat sink with impinging jet with airfoil pillars with and without NFL. Thermal resistance is detected to be 0.0024 and 0.0037 with and without NFL respectively for PR = 8 and HR = 1. For HR = 2, resistance is noticed to be 0.0013 for NFL and 0.0029 for water at PR = 8. Similarly, for HR = 3 and 4, resistance is 0.001,0.00089 for NFL and 0.0018, 0.0015 without NFL at PR = 8. So it is concluded from the figure 7.24 that the value of resistance is more without NFL. Also with an advancement in the HR, resistance dwindles in both the cases with and without NFL. This is due to decrease in the diameter of jet, which increases the velocity of jet and causes turbulence.

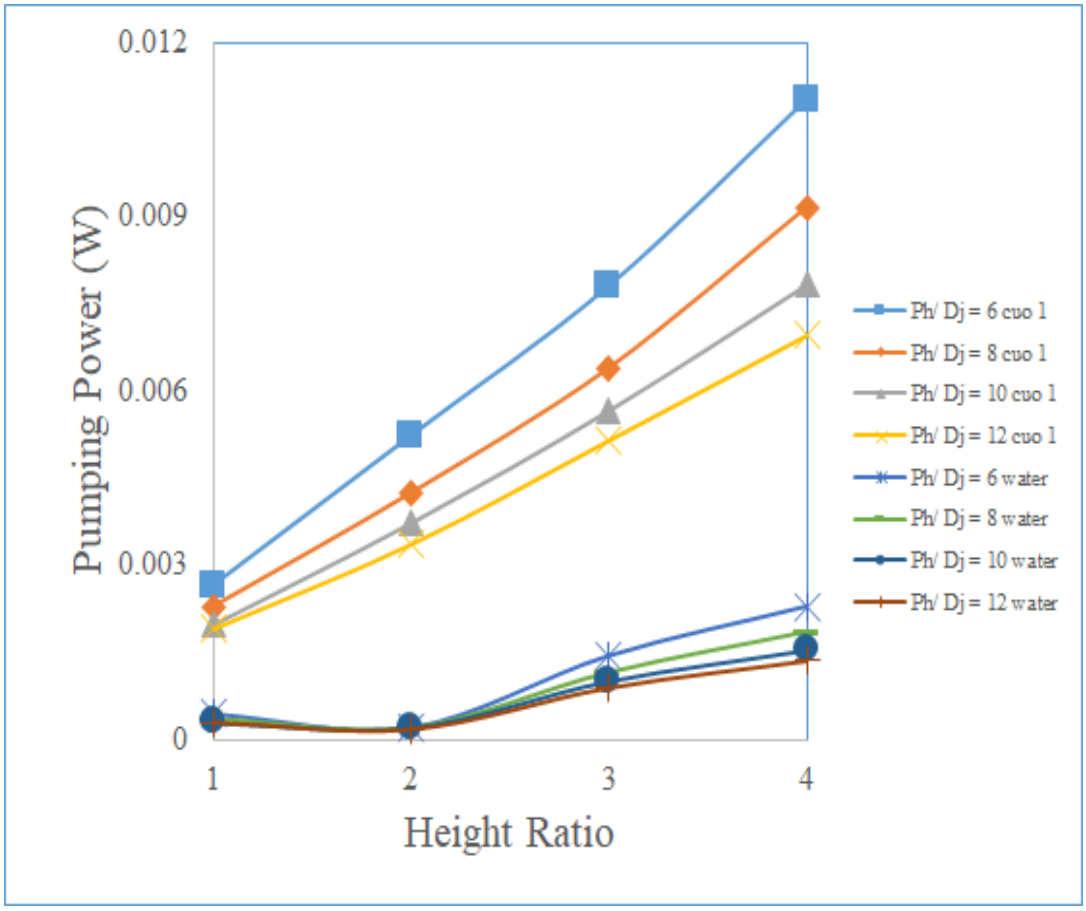

Figure 7.25: Effect of Height ratio ($\frac{H_{ch}}{D_j}$) on Pumping Power (P_p) for water and water based CuO Nanofluid

The connection between Height ratio and pumping power in case of impinging jet with airfoil pillars with and without Nano fluid is represented in the figure 7.25. For PR = 12 and HR = 1, pumping power is noticed to be 0.001 W and 0.0002 W with and without NFL respectively. With an advancement in HR to 2, power requirement increased to 0.003 W and 0.00016 W in case of water and NFL respectively at PR = 12. Similar trend is detected for HR = 3 and 4 for PR = 12. For PR = 6,8 and 10, it is noted from the figure that with an increment in the HR, power requirement also gets increased. So the pumping power is higher with Nano fluid as compared without Nano fluid. This is due to the increase in the frictional resistance due to increased velocity.

7.6 Graph for different parameters with pitch ratio using water

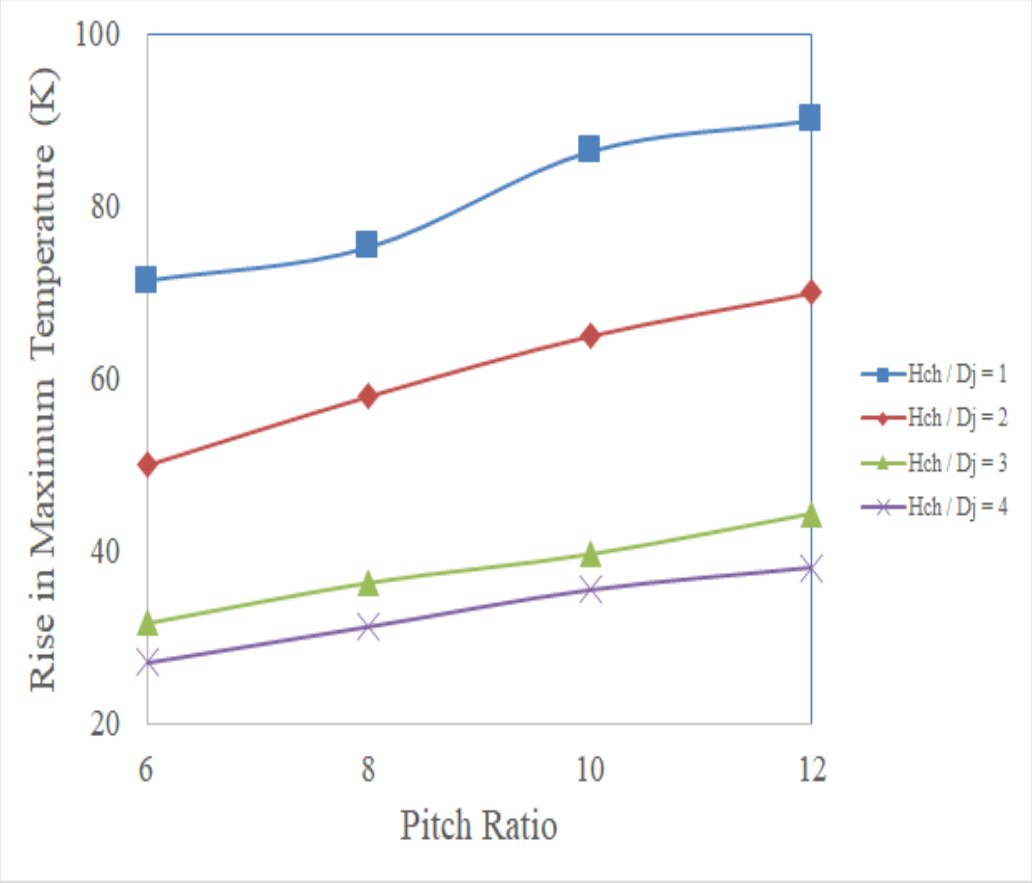

Figure 7.26: Effect of Pitch ratio $(\frac{Ph}{D_j})$ on rise in maximum temperature$(\Delta T)_r$ for water

Figure 7.26 shows the comparative analysis of modification in the temperature rise of fluid $(\Delta T)_r$ with Ph/D_j corresponding to H_{ch}/D_j = 4, 3, 2 and 1. For H_{ch}/D_j =1, It is observed from the graph that as the Ph/D_j is increased the rise in maximum temperature also increases. This trend is observed up to pitch ratio is 12. Also corresponding to H_{ch}/D_j =2, It is observed from the graph that as Ph/D_j is increased the rise in maximum temperature also increases. This trend is observed up to Ph/D_j is 12. In case of H_{ch}/D_j = 3, increasing trend is observed in the temperature profile in contrast to surge in Ph/D_j. From graph the minimum value of temperature rise is observed to be 27 k at Ph/D_j = 6 and the peak value to be 38 k at Ph/D_j = 12 for of H_{ch}/D_j = 4. The maximum rise in temperature is observed at H_{ch}/D_j = 1 and Ph/D_j = 12. So it can be concluded that the as the Ph/D_j increases, the $(\Delta T)_{r\ also}$ increases. The augmentation in $(\Delta T)_r$ is due to the less number of impingements with augmentation in P/D_j.

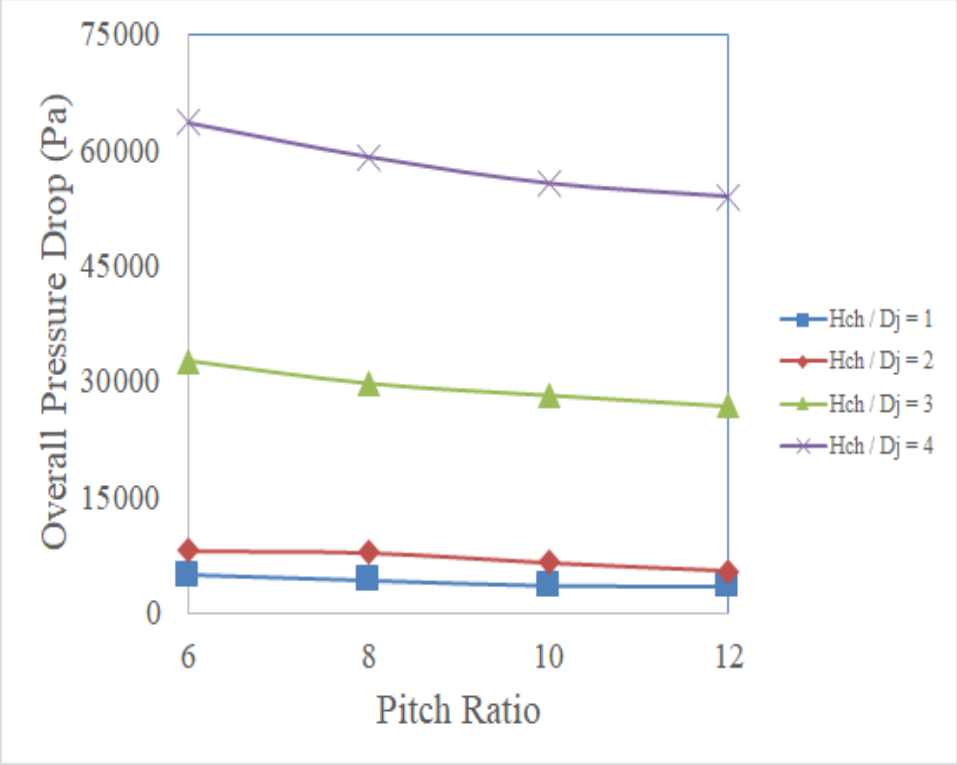

Figure 7.27: Effect of Pitch ratio$(\frac{Ph}{D_j})$ on overall pressure drop$(\Delta P)_o$ for water

Figure 7.27 shows the comparative analysis of variation in the overall pressure drop (OPD) with the pitch ratio (6, 8, 10 and 12) corresponding to height ratio (H_{ch}/D_j) = 1, 2, 3 and 4. Ph/D_j is varied from 6 to 12 and the variation in pressure drop is analyzed. Corresponding to $H_{ch}/D_j = 1$, It is observed from the graph that there is an inverse relation between Ph/D_j and overall drop in pressure. The minimum and maximum value of OPD is observed to be 3508 and 4811 respectively which are corresponding to $Ph/D_j = 12$ and $Ph/D_j = 6$. In case when the height ratio (H_{ch}/D_j) is kept constant and is equal to 2 and pitch ratio is varied from 6 to 12, It is observed from the graph that OPD decreases with increase in Ph/D_j. The minimum and maximum value of OPD is observed to be 5401 and 8069 respectively which are corresponding to $Ph/D_j = 6$ and $Ph/D_j = 12$. For $H_{ch}/D_j = 3$ which is kept constant, the results show the minimum and maximum value is at $P/D_j = 12$ and $Ph/D_j = 6$. Large pressure drop is found from the results at $Ph/D_j = 6$ and $Ph/D_j = 12$ at $H_{ch}/D_j = 4$. Form the results it is concluded that Large values of OPD are found corresponding to $H_{ch}/D_j = 4$. Increase in pitch ratio from 6 to 12 also results in decrease in the velocity of fluid and hence discharge. Since this reduction is from jet inlet to the outlet of channel, overall pressure drop also decreases from jet inlet to the channel outlet.

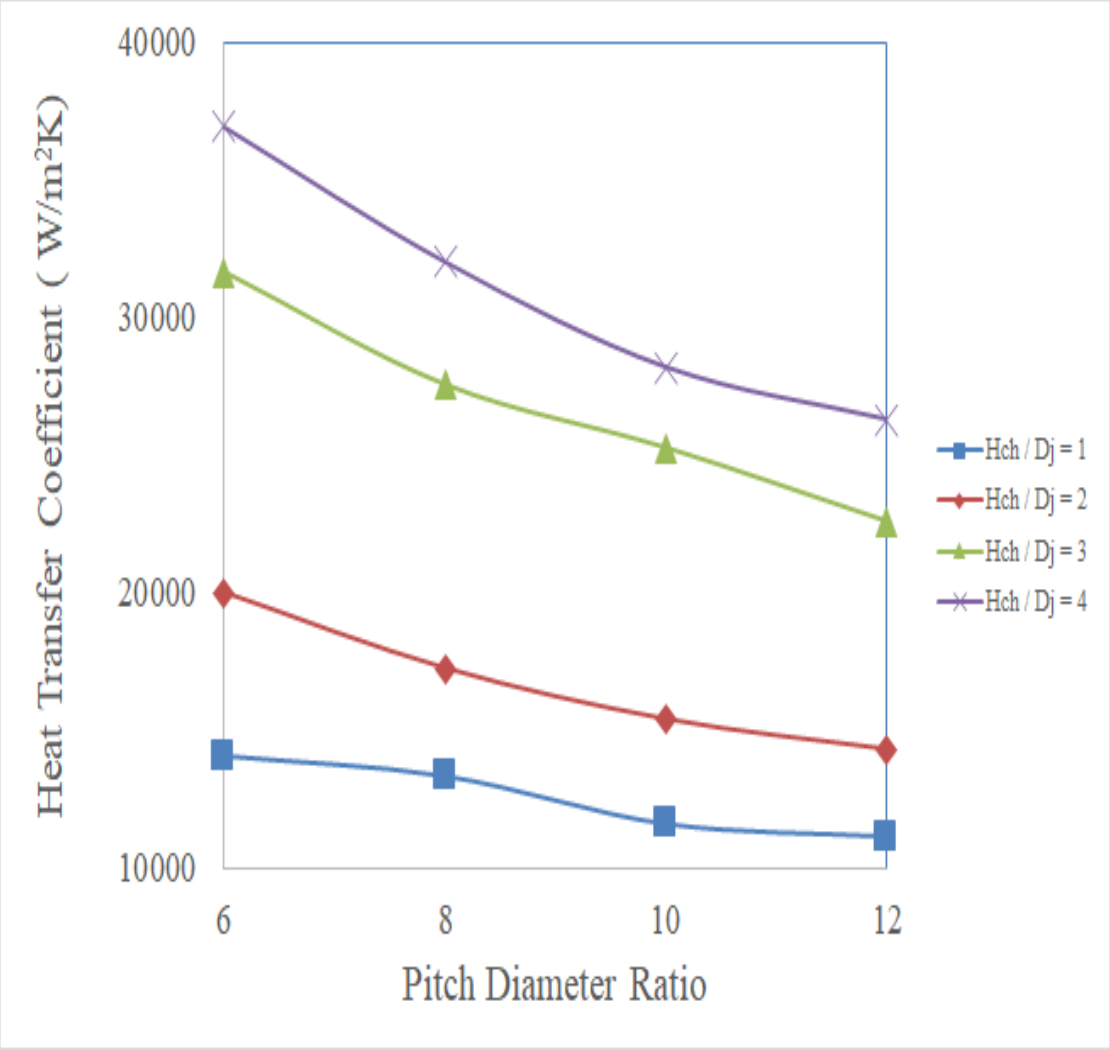

Figure 7.28: Effect of Pitch ratio $\left(\frac{Ph}{D_j}\right)$ on heat transfer coefficient (h) for water

This is a fact that coefficient of heat transfer plays an important role in case of heat transfer. Coefficient of heat transfer is found using heat flux = 100 X 10^4 W/m^2. Figure 7.28 depicts the comparative analysis of development in the heat transfer coefficient (h) with the pitch ratio (6, 8, 10 and 12) corresponding to H_{ch}/D_j = 1, 2, 3 and 4. The curve in figure 7.28, in case when the height ratio (H_{ch}/D_j) is kept constant and is equal to 1shows the modification in coefficient of heat transfer (h) with (Ph/D_j). Ph/D_j is varied from 6 to 12 and the variation in h is analyzed. The minimum and maximum value of h is observed to be 11111 and 14027 respectively which are

corresponding to Ph/D_j = 12 and Ph/D_j = 6. For H_{ch}/D_j = 2, h minimum is 14285 at Ph/D_j =12. Also the maximum value of h is found to be 20000 at Ph/D_j = 6. One of the curve in figure 4, depicts the variability of h with the Ph/D_j for H_{ch}/D_j = 3. The minimum value of h is observed to be 22578 at Ph/D_j =12. Also the maximum value of h is found to be 31625 at Ph/D_j = 6. Decreasing trend is observed from the results for h with an increase in pitch diameter ratio. Also for H_{ch}/D_j = 4, minimum value of h is observed to be 26288 at Ph/D_j =12 and maximum value of h is found to be 36900 at Ph/D_j = 6. Decreasing trend is observed from the results for h with an increase in Ph/D_j. Now from the figure 4 it was concluded that h is found to be maximum in case of H_{ch}/Dj = 4 and Ph/D_j = 6. Larger value of heat transfer coefficient will help in higher heat transfer rate so this case is preferred over the other ones. With a surge in Ph/D_j, number of impingements decreases which results in diminishing of h. With an increase in the pitch ratio, convection heat transfer is reduced. The reason for the same is increase in the boundary layer thickness. Because with an increase in the pitch ratio, the counting of jets decreases. And hence the wall jet gets more space to spread in the radial direction. And finally the interaction with the other jets decreases

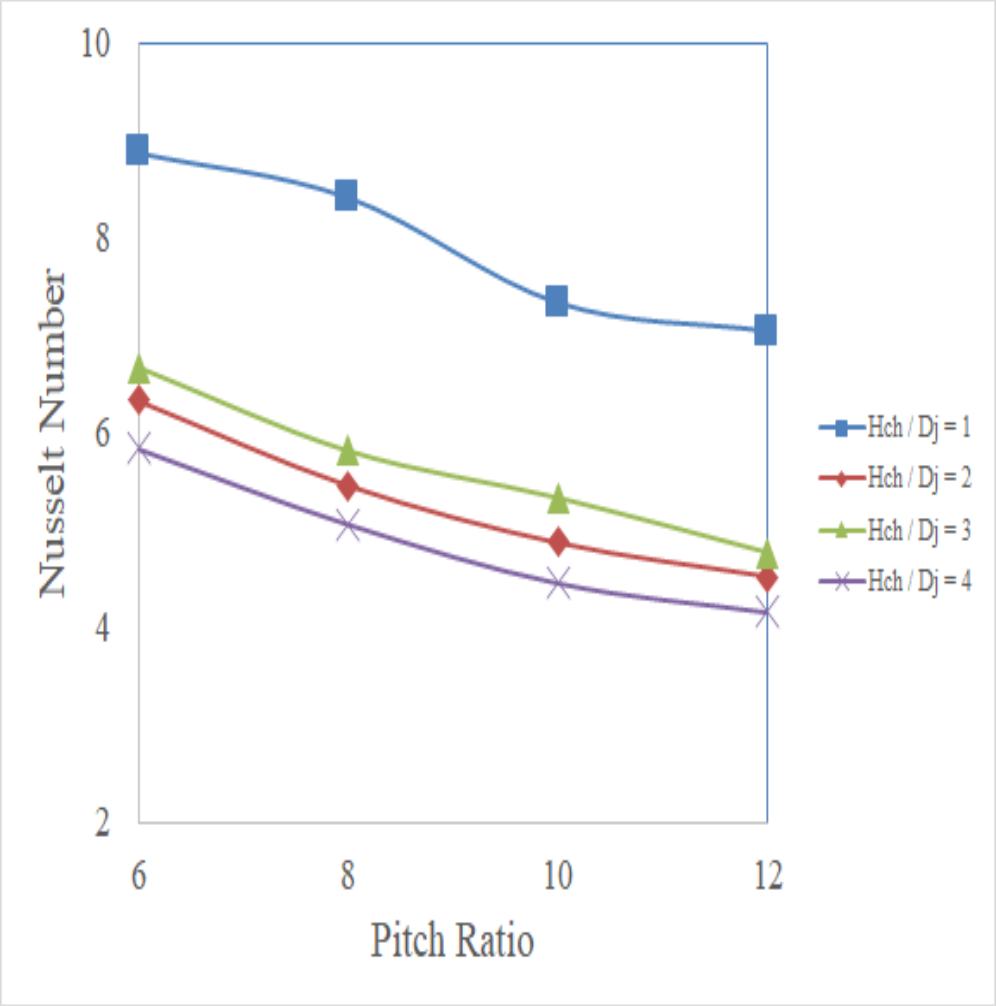

Figure 7.29: Effect of Pitch ratio $\left(\frac{Ph}{D_j}\right)$ on Nusselt Number (Nu) for water

Nusselt number is an important parameter in case of heat transfer A comparative study was made for the Nu and pitch ratio for different height ratio (1, 2, 3, and 4) and is shown in the figure 7.29. The alteration of Nusselt number (Nu) with pitch ratio for height ratio = 1 is shown in the one of the curve in figure 729. The value of Nu is found to be maximum at pitch ratio = 6 and minimum value of Nu is found from the results at pitch ratio = 12. Corresponding to $H_{ch}/D_j = 2$, After a value of pitch ratio = 10 no significant change in the value of Nusselt number is observed in the results. Also from the results it can be concluded that the maximum value of Nu is at $Ph/D_j = 6$. The

minimum value of Nu is observed at pitch ratio = 12. For a constant value of height ratio = 3, Inverse relation is predicted from the results in between the two variables. The maximum value of Nu is predicted at pitch ratio = 6 and minimum value at Ph/D_j = 12. As is seen from the graph with an increase in the value of pitch ratio from 6 to 12, there is a decrease in the value of Nu. So the case with Ph/D_j = 6 is preferred when H_{ch}/D_j = 4. From the results it is clear that the same type of trend is observed in case of height ratio = 3 and 4. The maximum value of Nusselt number is found in case of height ratio = 1 and pitch ratio =6. With an increase in the pitch ratio, Nu is reduced. The reason for the same is increase in the boundary layer thickness. Because with an increase in the pitch ratio, the counting of jets decreases. And hence the wall jet gets more space to spread in the radial direction. And finally the interaction with the other jets decreases.

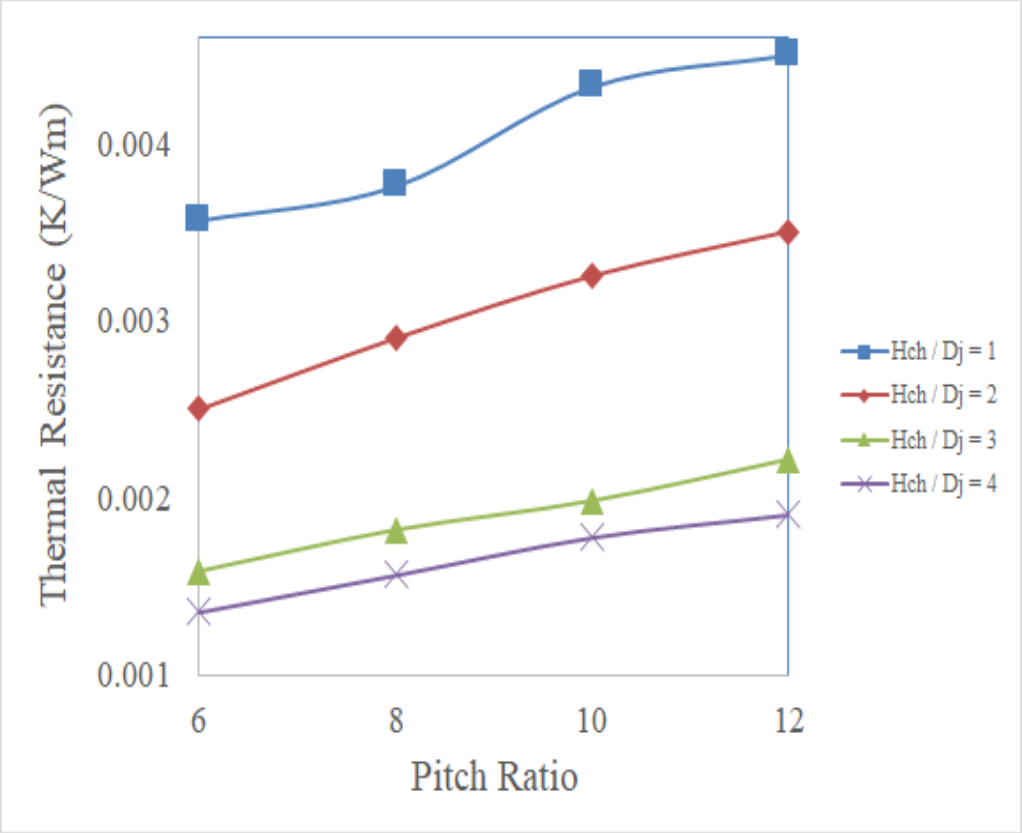

Figure 7.30: Effect of Pitch ratio $(\frac{Ph}{D_j})$ on Thermal resistance$(R)_T$ for water

Thermal resistance (R_T) is the resistance to the flow of heat transfer. Higher thermal resistance will result in lesser heat transfer rate. Differentiating analysis between the thermal resistance and pitch ratio for different values of height diameter ratio (1, 2, 3 and 4) is shown in the figure 7.30. From the curve in figure 7.30, Lesser R_T is obtained from the results at pitch ratio = 6 and H_{ch}/D_j = 1. Maximum value of R_T is found at Ph/D_j = 12 corresponding to H_{ch}/D_j = 1. At a constant value of H_{ch}/D_j = 2, the modification in thermal resistance with the change in the pitch ratio is shown in the figure 7.30. Higher R_T is obtained from the results at Ph/D_j = 12. This implies that at this condition less rate of heat transfer will be there as compared to the heat transfer rate at pitch ratio = 8. Corresponding to height ratio = 3, as the value of pitch ratio increases the thermal resistance also increases which is not a favorable condition for the rate of heat transfer. The maximum R_T is observed from the results at pitch ratio = 12. At a height ratio = 4, an increasing trend is detected in R_T with an increase in the value of pitch ratio. Maximum R_T is found from the results at Ph/D_j = 12. So it was concluded from the figure 7.30 that highest R_T is predicted at proportion of height and diameter =1 and proportion of pitch and diameter = 12. Also the lowest value of thermal resistance is predicted at H_{ch}/D_j = 4 and Ph/D_j = 6. The surge in the R_T is due to increased velocity, which further increases the frictional losses.

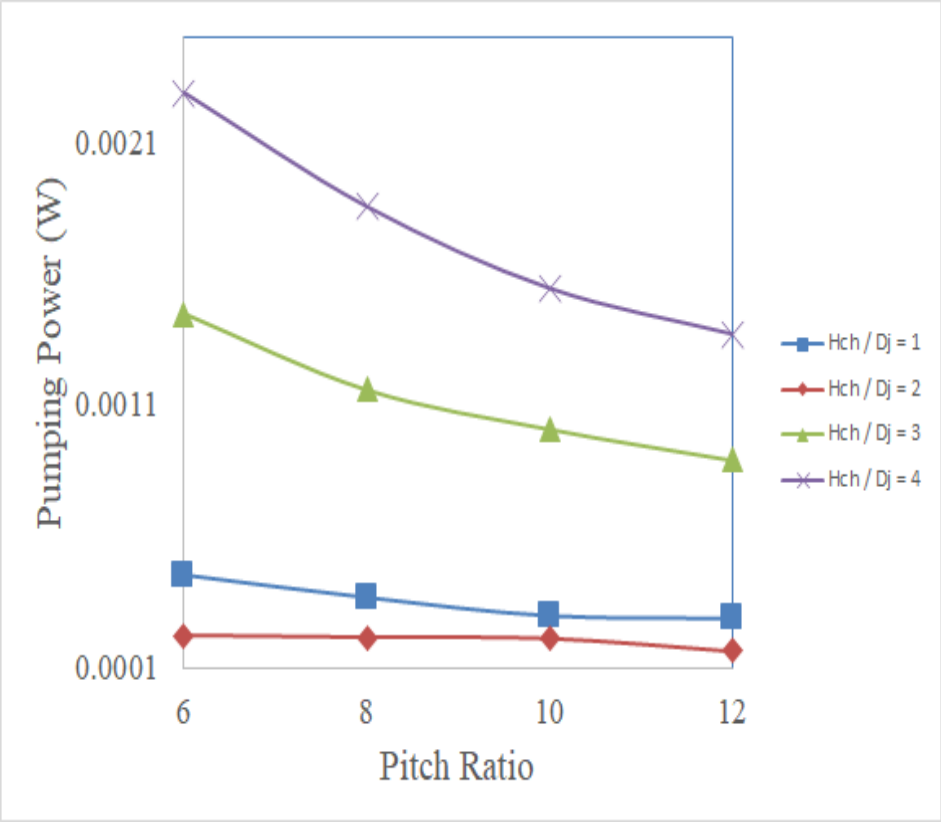

Figure 7.31: Effect of Pitch ratio ($\frac{Ph}{D_j}$) on Pumping power (P_p) for water

Pumping power (PP) is power which is needed for the fluid to flow through the heat sink. Comparative exploration of PR with pitch ratio for different values of height ratio as $Hch/D_j = 1$, $H_{ch}/D_j = 2$, $H_{ch}/D_j = 3$ and $H_{ch}/D_j = 4$ has been shown in figure 7.31. At a height ratio = 1, from the results maximum value of PR is found at a pitch ratio of 6 and minimum value is at a pitch ratio of 12. In the case $H_{ch}/D_j = 2$, maximum value of PR is found at a pitch ratio of 6 while the minimum value of PP is observed at a pitch ratio of 12. Higher pumping power is not desirable. For a constant value of height ratio = 3, From the results it has been noted that as the pitch ratio is increased from 6 to 12, Pumping power gets decreased. The minimum value of pumping power is observed corresponding to pitch ratio of 12 while the highest value is obtained at 6. for $H_{ch}/D_j = 4$, lowest observation of PR is obtained corresponding to pitch ratio =12 while the highest value is

corresponding to 6. So It was concluded that the lowest pumping power is predicted in case of the combination with pitch ratio = 12 and height ratio = 2.

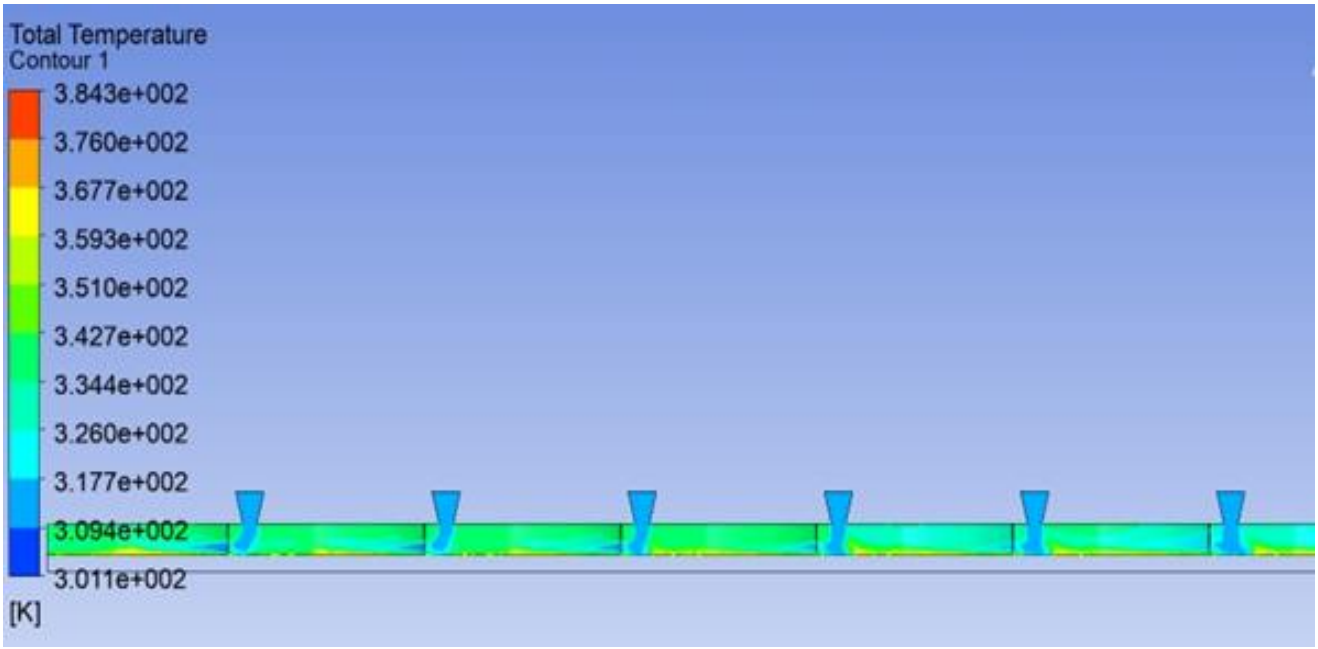

Figure 7.32(a): Temperature Distribution at Height ratio $\left(\frac{H_{ch}}{D_j}\right) = 1$, Pitch ratio $\frac{Ph}{D_j} = 6$ for water

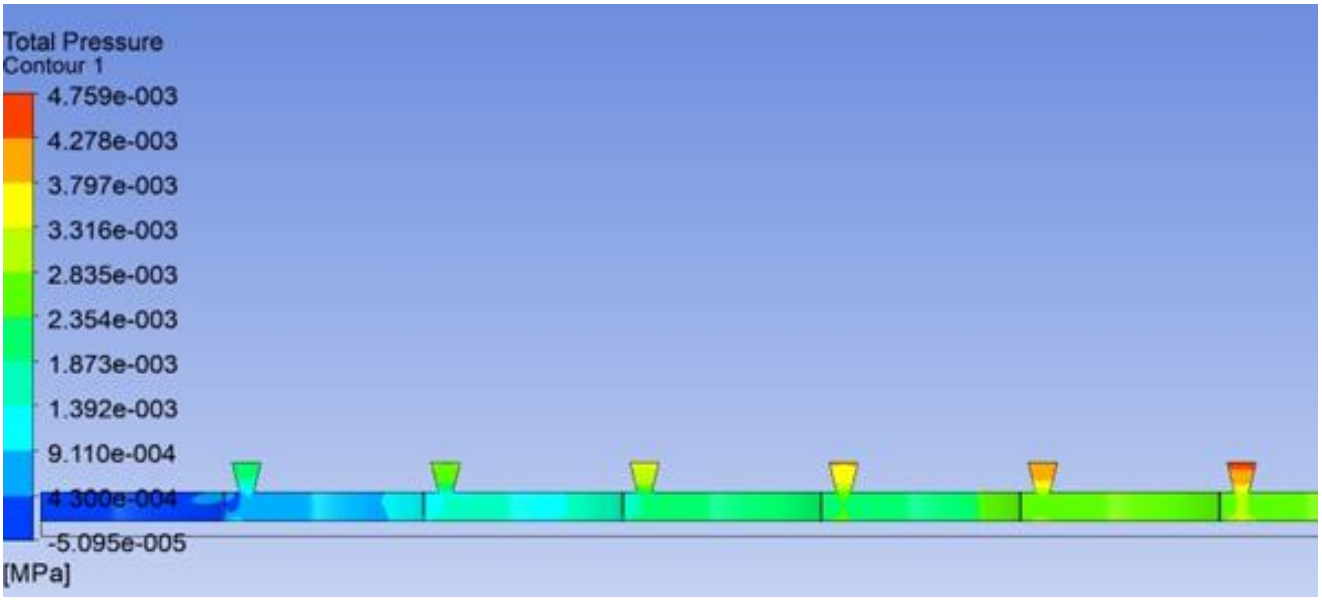

Figure 7.32(b): Pressure Distribution at Heightratio $\left(\frac{H_{ch}}{D_j}\right) = 1$, Pitch ratio $(\frac{Ph}{D_j})$ = 6 for water

Figure 7.32(a) depicts the distribution of temperature in impingement of jet in a heat sink with the air foil pillars. Temperature contours are shown in the figure in case of height ratio = 1 and pitch ratio = 6. The distribution of temperature for the fluid domain shows the minimum and maximum values of temperature. In the figure 7.32(b) distribution of pressure is depicted with the help of simulation using CFD.

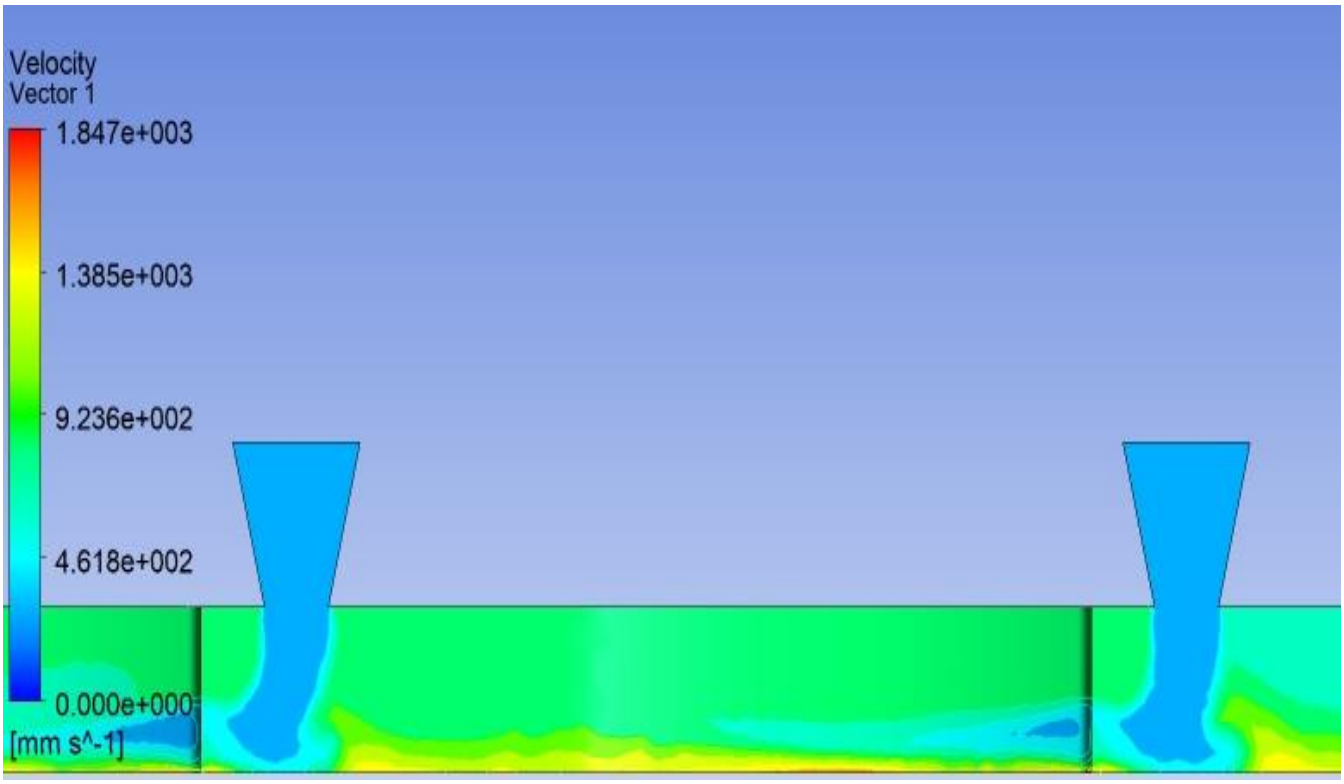

(C) : Side View

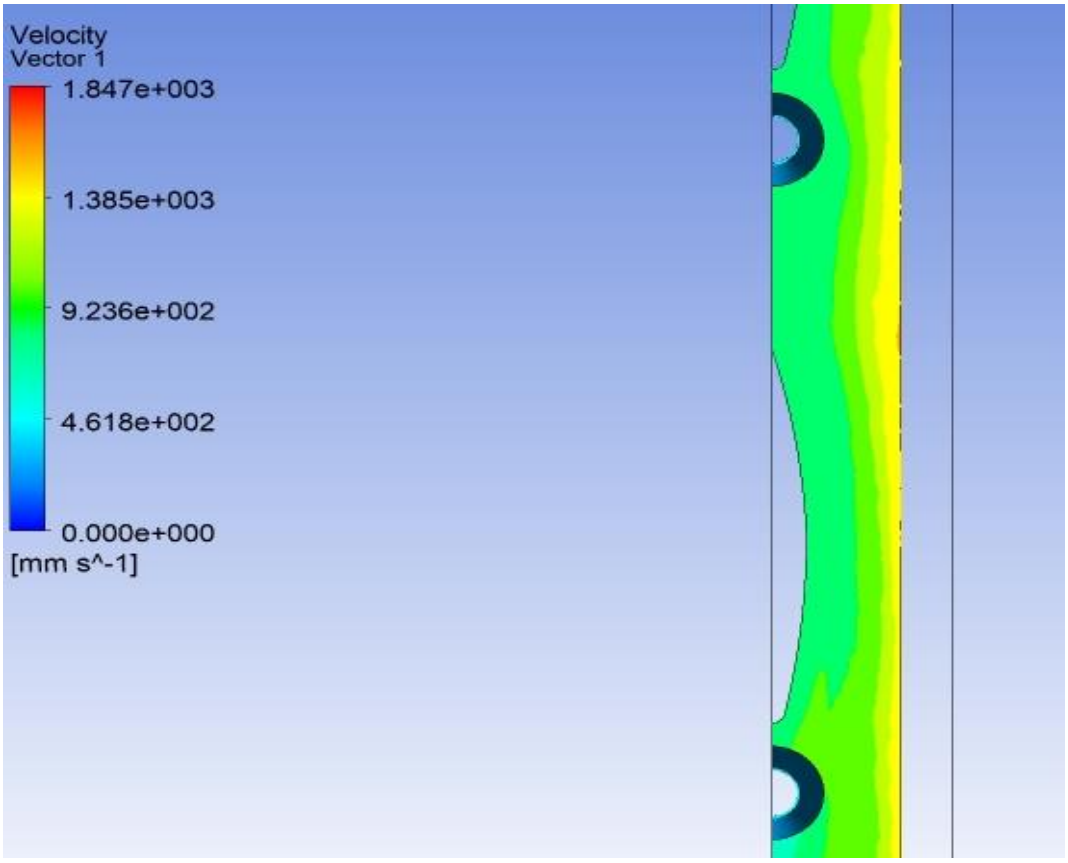

(d): Top View

Figure 7.32 (c, d): Flow Pattern at Height ratio $\left(\frac{H_{ch}}{D_j}\right) = 1$, Pitch ratio $(\frac{Ph}{D_j})$ = 6 for water

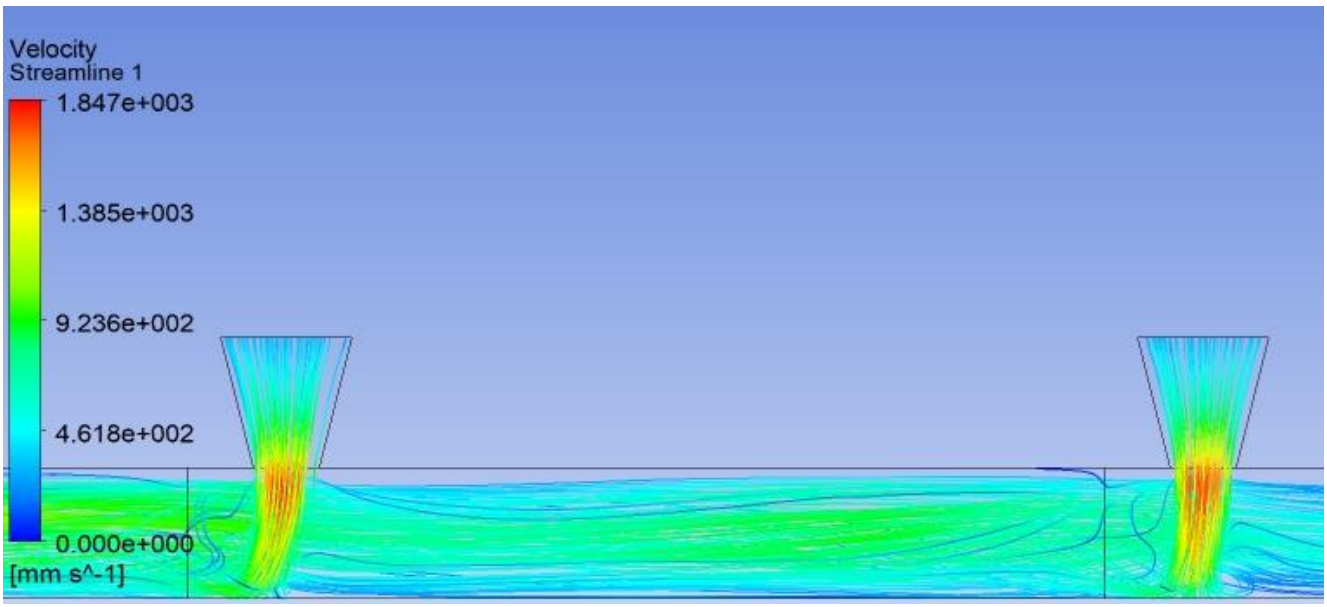

(e): Side View

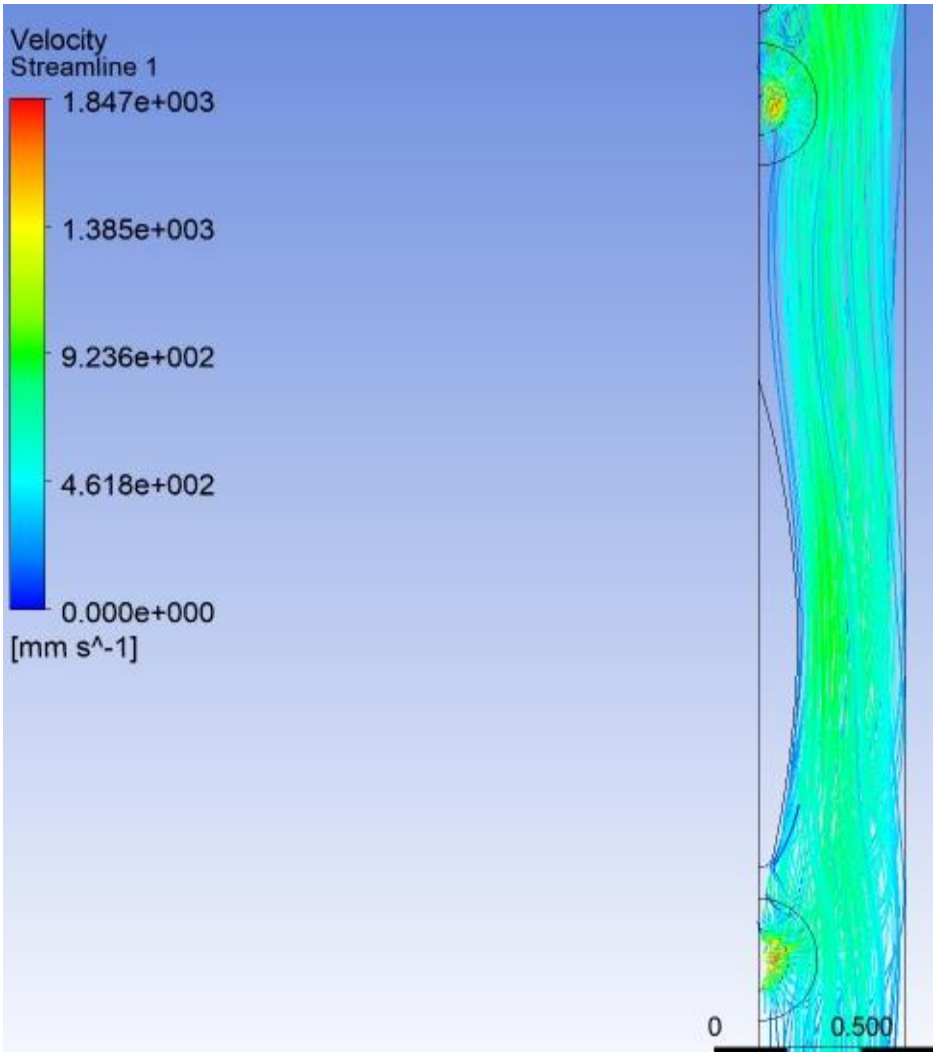

(f): Top View

Figure 7.32(e, f): Stream lines at Height ratio $\left(\frac{H_{ch}}{D_j}\right) = 1$, Pitch ratio $(\frac{Ph}{D_j})$ = 6 for water

Figure 7.32(c,d) shows the flow patter in the form of velocity vector at $\frac{H_{ch}}{D_j} = 1$ and pitch ratio = 6. Also the streamlines are shown in the figure 7.32(e,f). Vortices are noticed behind the impingement of jet. The end result of jet is noticed to be somewhat destroyed due the flow in the channel.

7.7 Water and water– CuO Nano fluid (0.5%)

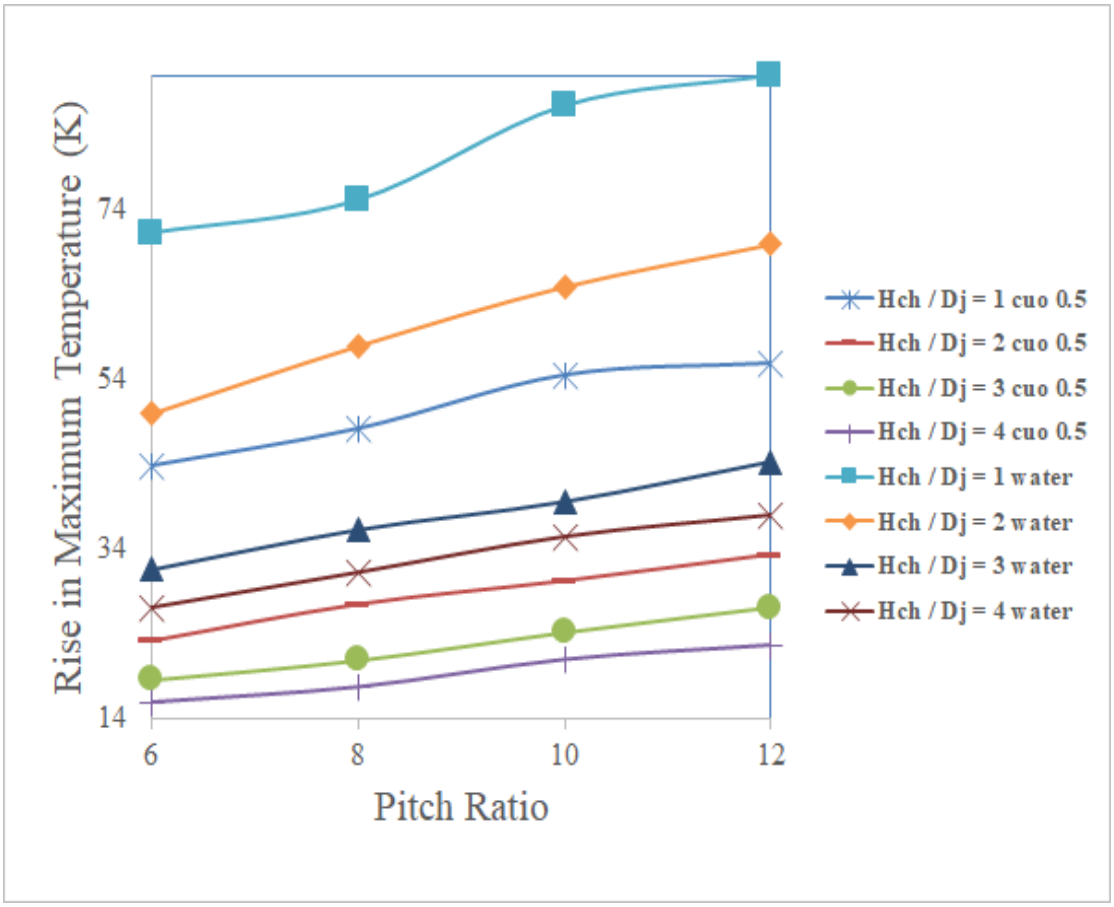

Figure 7.33: Effect of Pitch ratio $(\frac{Ph}{D_j})$ on rise in maximum temperature$(\Delta T)_r$ for water and water– CuO Nanofluid (0.5%)

Figure 7.33 indicated the distinction in rise in maximum temperature (RIMT) with pitch ratio (PR). PR is varied as 6,8,10 and12. The same has been noticed for different values of height ratio (HR). HR is taken as 1,2,3 and 4. RIMT with PR for different values of HR has been compared for water and water –copper oxide (CuO) Nano fluid. The comparative analysis has been made for 0.5 % concentration. For HR = 1 and PR = 6, RIMT = 71.29 and 43.83 for water and Nano fluid respectively. For PR= 8, RIMT = 75.19 for water and 48.2 for Nano fluid. For PR= 10, RIMT = 86.4 for water and 54.53 for Nano fluid. For PR= 12, RIMT =90 and 55 For water and Nano fluid

respectively. As the PR grows, RIMT also grows. For HR = 2,3 and 4, RIMT has been observe in direct proportion with PR. The RIMT is lower in case of Nano fluid as compared to simple water. The same is due to the increase in the thermal conductivity of the working fluid (Nano fluid).

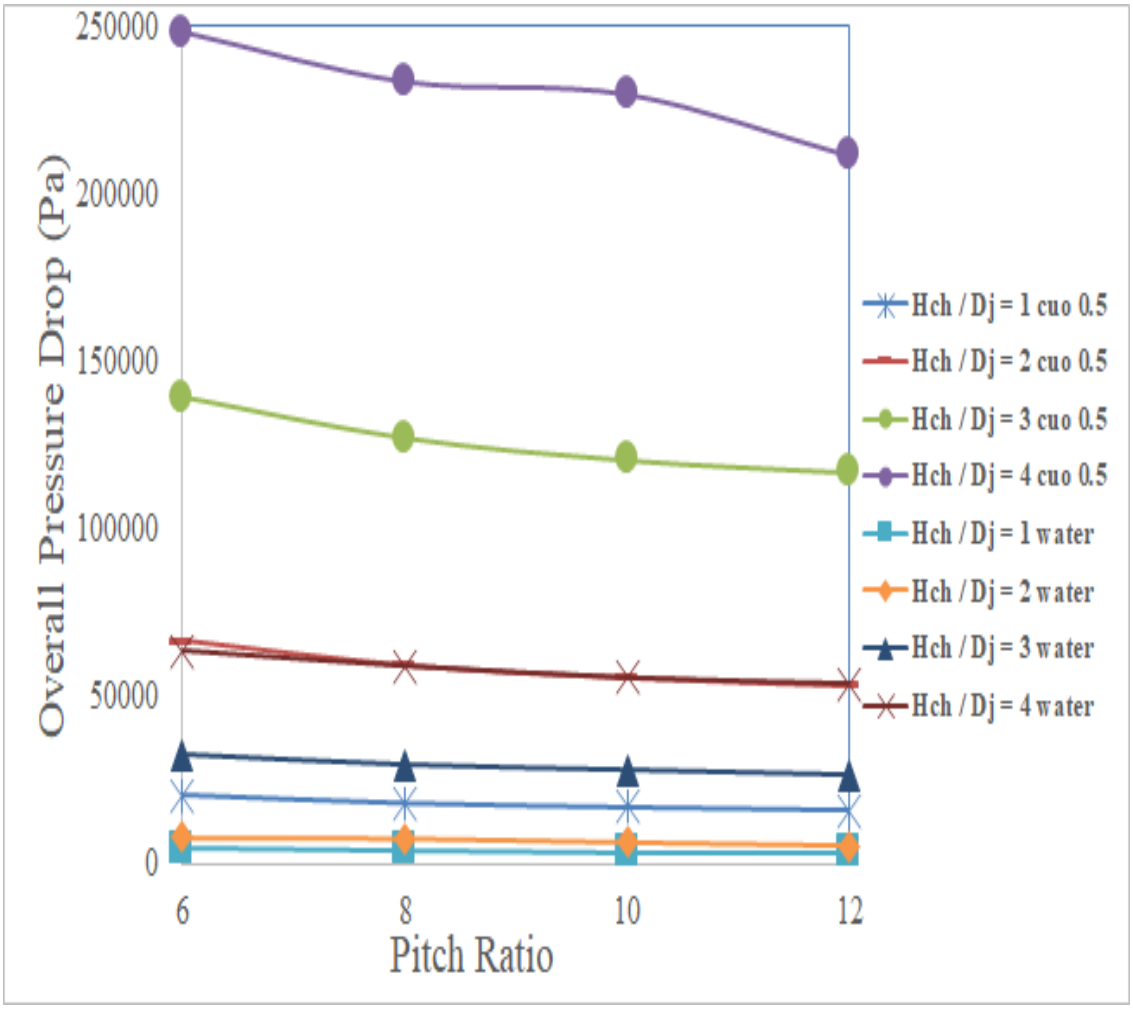

Figure 7.34: Effect of Pitch ratio($\frac{Ph}{D_j}$) on overall pressure drop$(\Delta P)_o$ for water and water– CuO Nanofluid (0.5%)

Figure 7.34 projects the interconnection between overall pressure drop (OPD) with pitch ratio (PR) for different values of height ratio (HR) for water and Nanofluid. For HR = 1, PR= 6, OPD was found to be =4811 for water and 20524 for Nano fluid. At PR= 8, OPD = 4166 and 18208 for water

and Nano fluid respectively. At PR= 10, OPD = 3553 for water and 17040 for Nano fluid. OPD = 3508 and 16213 for water and Nano fluid respectively corresponding to PR = 12 and HR =1. As PR increases, OPD decreases. For HR = 2 and PR =6, the value of OPD for water and Nano fluid is noticed to be 8069 and 66817 respectively. Similarly, at PR = 8, OPD = 7826 and 59478 for the water and Nano fluid. From the figure 7.34, it is recognized that with increase in PR for different values of HR, OPD decreases. Also OPD is noticed to be more in case of Nano fluid as compared to the water. The reason for the high pressure drop in Nano fluid is due to higher due to increased viscosity of Nano fluid as compared to water.

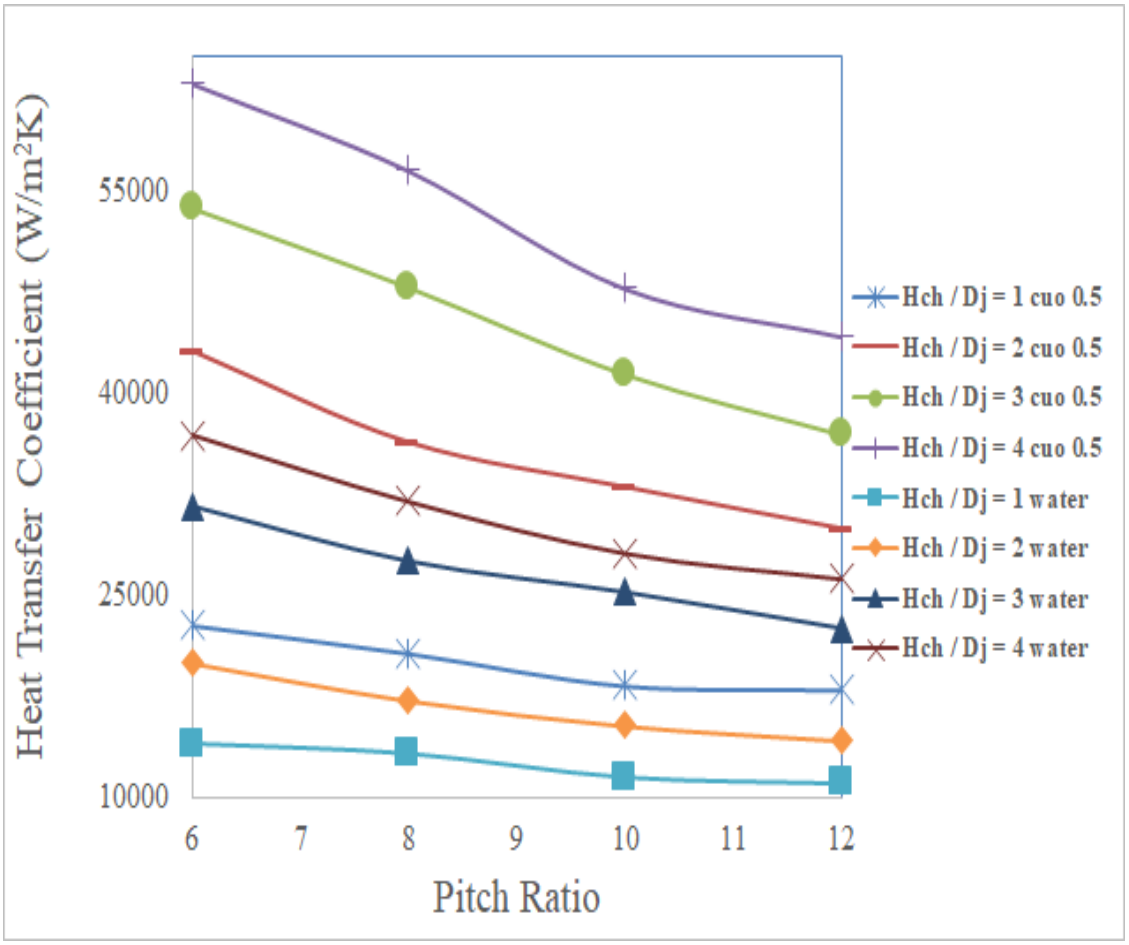

Figure 7.35: Effect of Pitch ratio $\left(\frac{Ph}{D_j}\right)$ on heat transfer coefficient (h) for water and water–CuO Nanofluid (0.5%)

The interconnection of Heat Transfer Coefficient (h) with Pitch ratio (PR) for water and Nano fluid for various values of HR = 1,2,3 and 4 is projected in the figure 7.35. For HR = 1and at PR = 6, the value of h is to be noted as 14027 and 22815 for water and Nano fluid respectively. For PR = 8, h = 13299 and 20746 for water and Nano fluid respectively. For PR = 10, h = 11574 and 18338 for water and Nano fluid. Also h is observed to be 18000 for Nano fluid and 11111 for water corresponding to PR = 12. For HR =2, PR= 6, value of h= 17556 and 43122 for water and Nano fluid respectively. For water as the value of PR is increased, h is decreased for constant values of HR. In case of Nano fluid also with increase in PR, h is decreased. The maximum value of h = 36900, at HR= 4 and PR= 6 in case of water while in case of Nano fluid extreme value of h = 62972 at HR = 4 and PR = 6. So the higher value of h is noted in case of Nano fluid as compared to water. The higher value of the h is justified because of the increase in the velocity. Since for a constant Re, viscosity of Nano fluid is more than water.

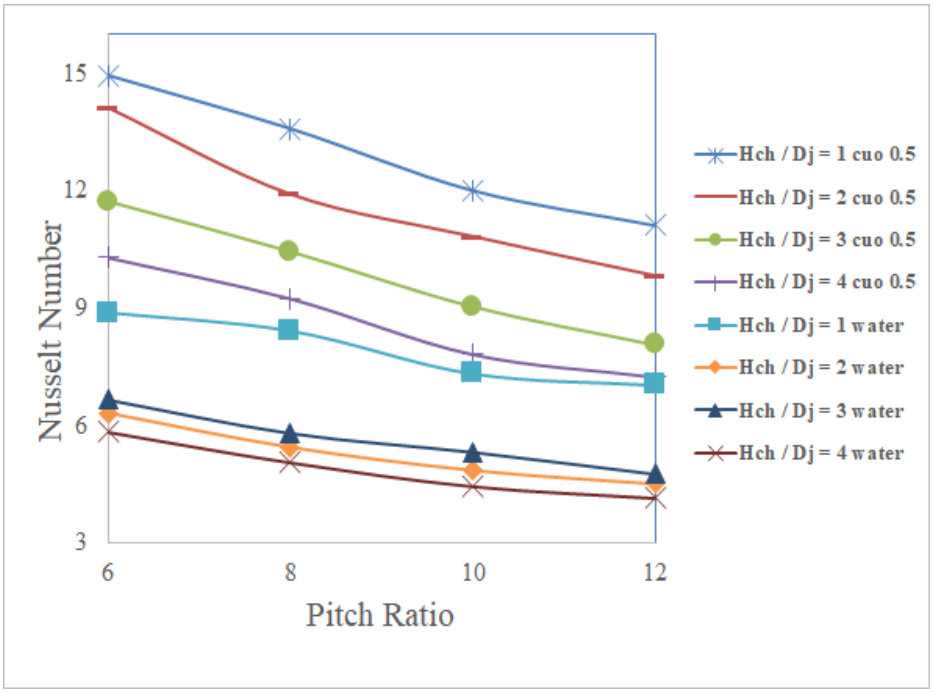

Figure 7.36: Effect of Pitch ratio $\left(\frac{Ph}{D_j}\right)$ on Nusselt Number (Nu)for water and water– CuO Nanofluid (0.5%)

In figure 7.36, the interrelation between Nusselt Number (Nu) and Pitch ratio (PR) is deduced for four different values of height ratio (HR) using water and the same has been compared with the case using Nano fluid as working fluid. For HR = 1, at PR =6, the value of Nu is noticed to be 8.871 for water and 14.93 for Nano fluid. As the value of PR is increased from 6 to 8, Nu is detected to be 8.4 for water and 13.58 for Nano fluid. At PR = 10, the value of Nu is 12 and 7 in case of Nano fluid and water respectively. Nu = 11, at PR= 12 which is higher as compared to Nu = 7 in case of water. For HR = 2, Nu = 6 for water and 14.11 for Nano fluid corresponding to PR = 6. From the figure 7.36 it is clear that as PR is increased from 6 to 12, Nu gets decreased for both water and Nano fluid. The maximum value of Nu is detected to be 14.93 in case of Nano fluid and the minimum value of Nu is 4.15 in case of water. The same is due to thermophysical properties of Nano fluid as compared to the base fluid.

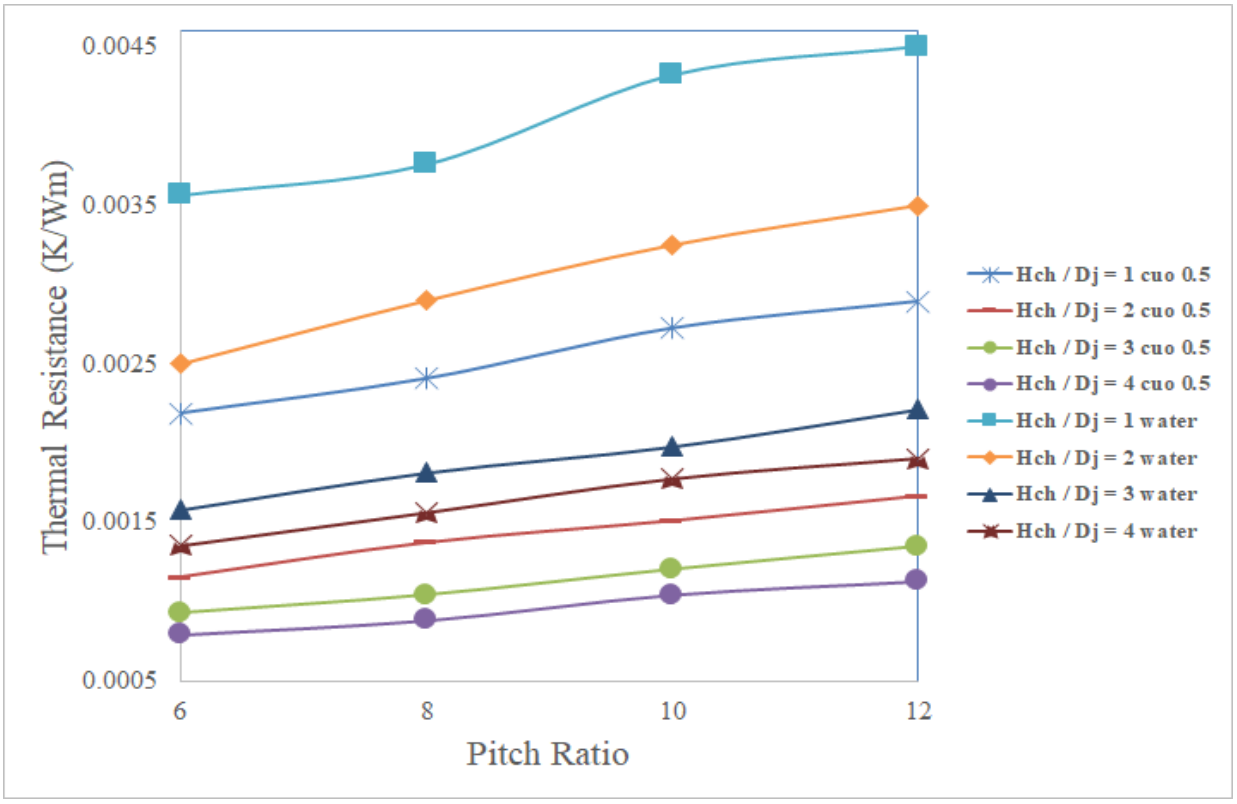

Figure 7.37: Effect of Pitch ratio $(\frac{Ph}{D_j})$ on Thermal resistance$(R)_T$for water and water– CuO Nanofluid (0.5%)

The correlation between the thermal resistance (R_T) and pitch ratio is shown in the figure 7.37. The correlation was discussed for PR values from 6 to 12 at constant values of HR = 1,2,3 and 4 for the water and Nano fluid. AT HR = 1 and PR = 6, R_T is noticed to be 0.0035 and 0.0021 for water and Nano fluid respectively. Lower value of R_T is noticed in case of Nano fluid with 0.5 % concentration. For PR= 8, R_T is detected to be 0.00241 for 0.5 % concentration and 0.00375 for water. R_T = 0.00272 and 0.00432 at PR = 10 in case of Nano fluid and water respectively. Similarly, at pitch ratio = 12, the value of resistance is noted to be 0.0028 in case of 0.5 % concentration and 0.0045 in case of pure water. As the value of PR is increased, increasing trend is seen for resistance in both the cases with water and Nano fluid. Increasing trend is observed due to increased frictional forces due to the airfoil pillars.

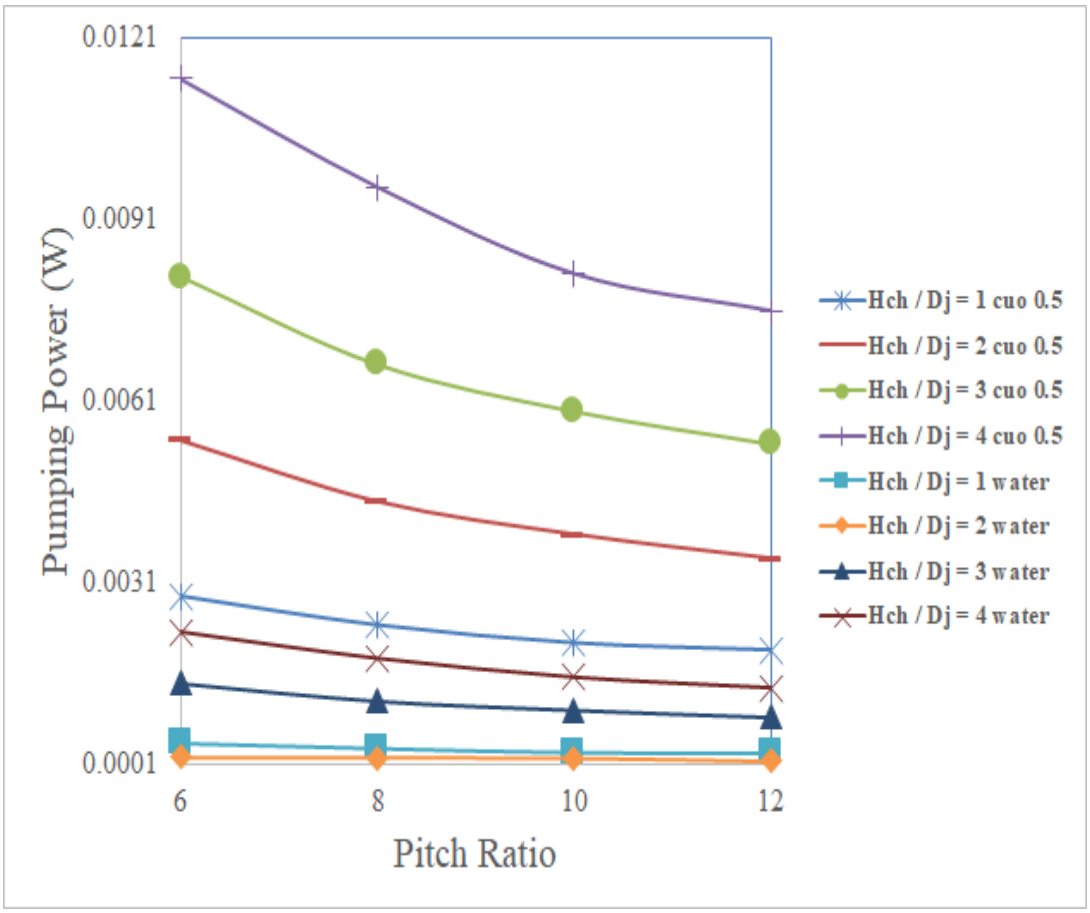

Figure 7.38: Effect of Pitch ratio ($\frac{Ph}{D_j}$) on Pumping power (P_p) for water and water– CuO Nanofluid (0.5%)

Figure 7.38 presents the relation between pumping power (PP) and pitch ratio for different value of height ratio (1,2,3 and 4). At HR = 1 and PR = 6 for water the value of pumping power is found to be 0.00044. For the same condition PP = 0.0028 in case of Nano fluid. At HR= 1 and PR = 8, PP = 0.00036 and 0.00239 for water and Nano fluid respectively. PP = 0.000294 and 0.0021 at HR= 1, PR = 10 For water and Nano fluid respectively. AT HR = 1, PR = 12, PP is noted to be 0.0002838 and 0.001987 for simple water and Nano fluid respectively. Higher value of PP is found in case of Nano fluid which is due to the increase in the velocity and frictional resistance.

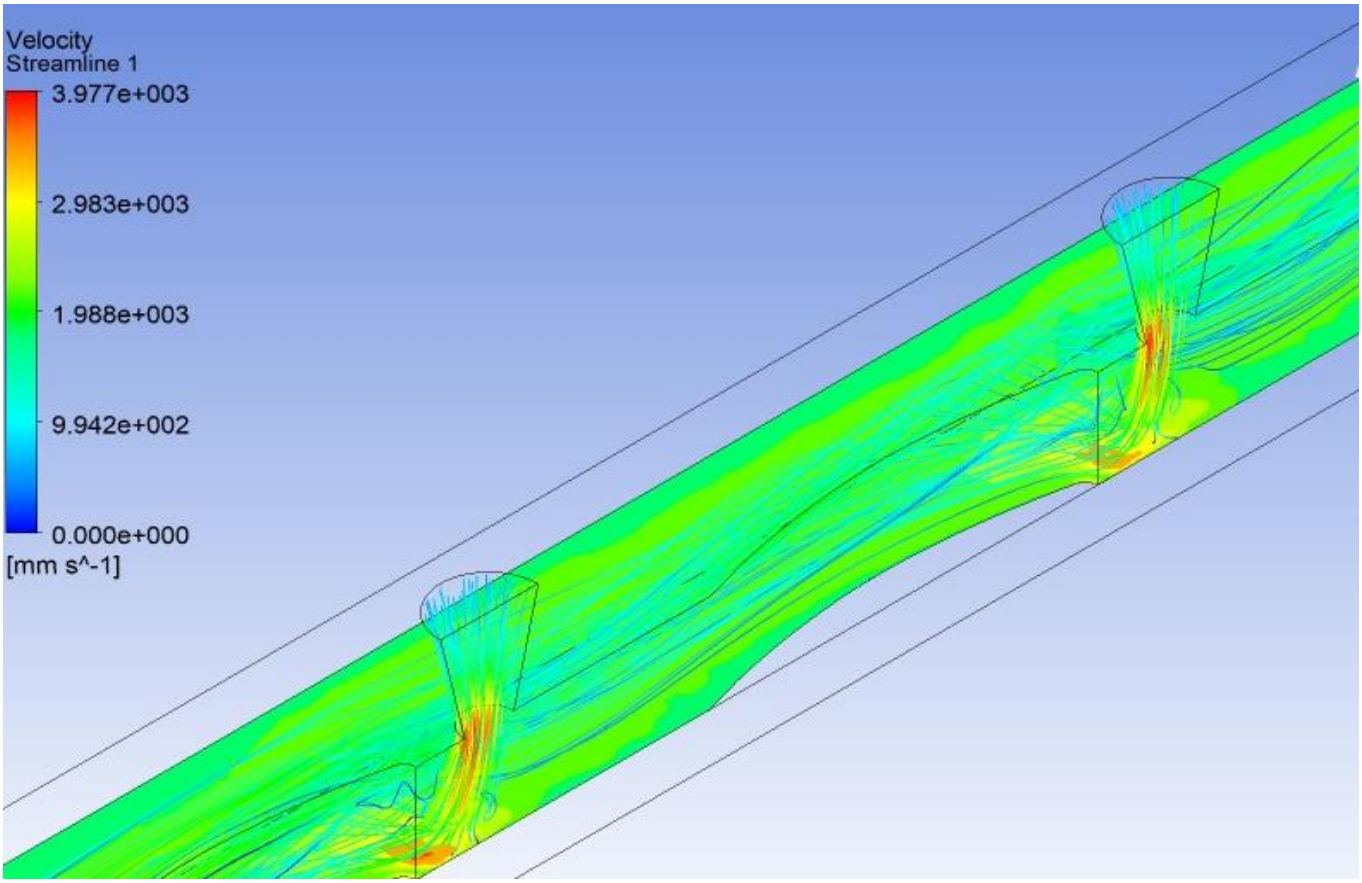

Figure 7.39: Streamlines at Pitch ratio (PR) = 6, Height ratio (HR) = 1 for water and water– CuO Nanofluid (0.5%)

Figure 7.39 presents the fashion of streamlines corresponding to PR =6 and HR= 1 in case of water – CuO Nano fluid. The fashion of streamlines before and after the jet position is represented. The fashion of stream lines gets affected in the vicinity of jets. Vortices have been noted after the jet.

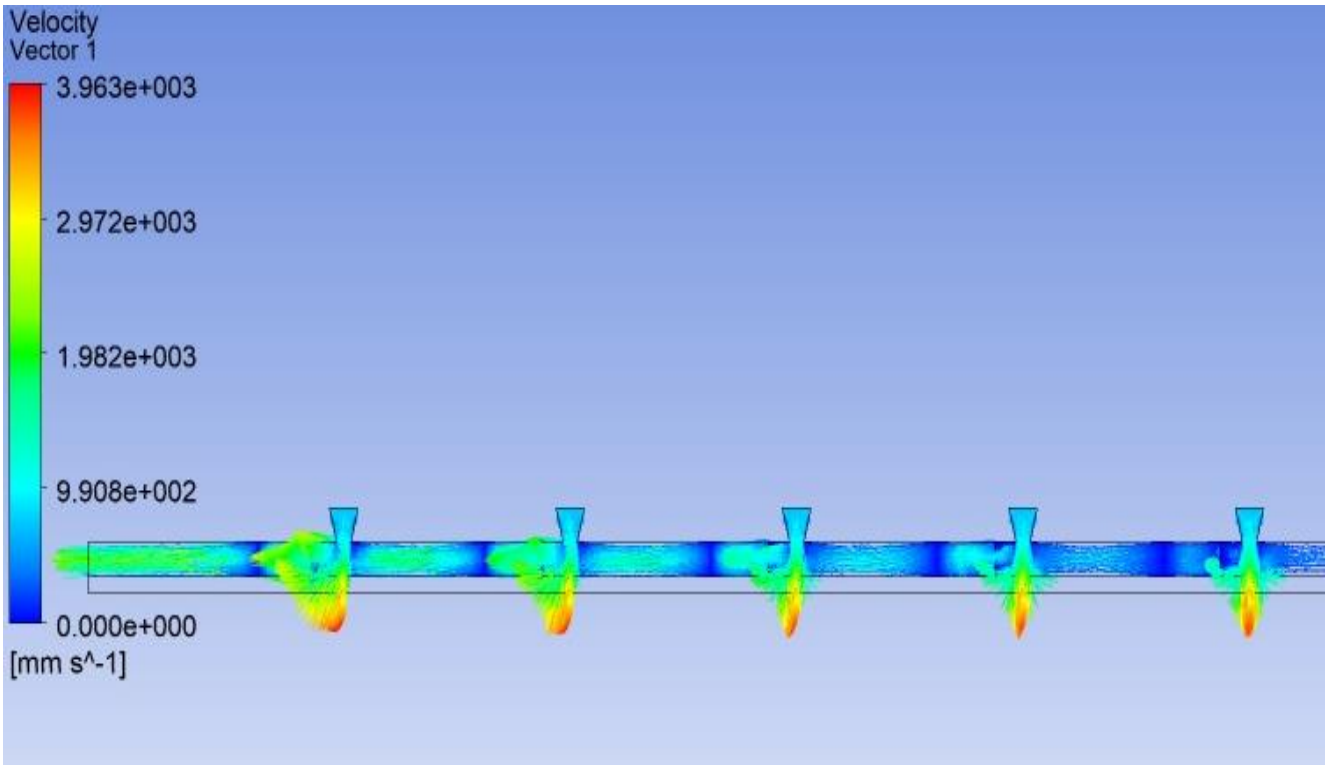

Figure 7.40: Velocity Vector at Pitch ratio (PR) = 8, Height ratio (HR) = 1 for water and water–CuO Nanofluid (0.5%)

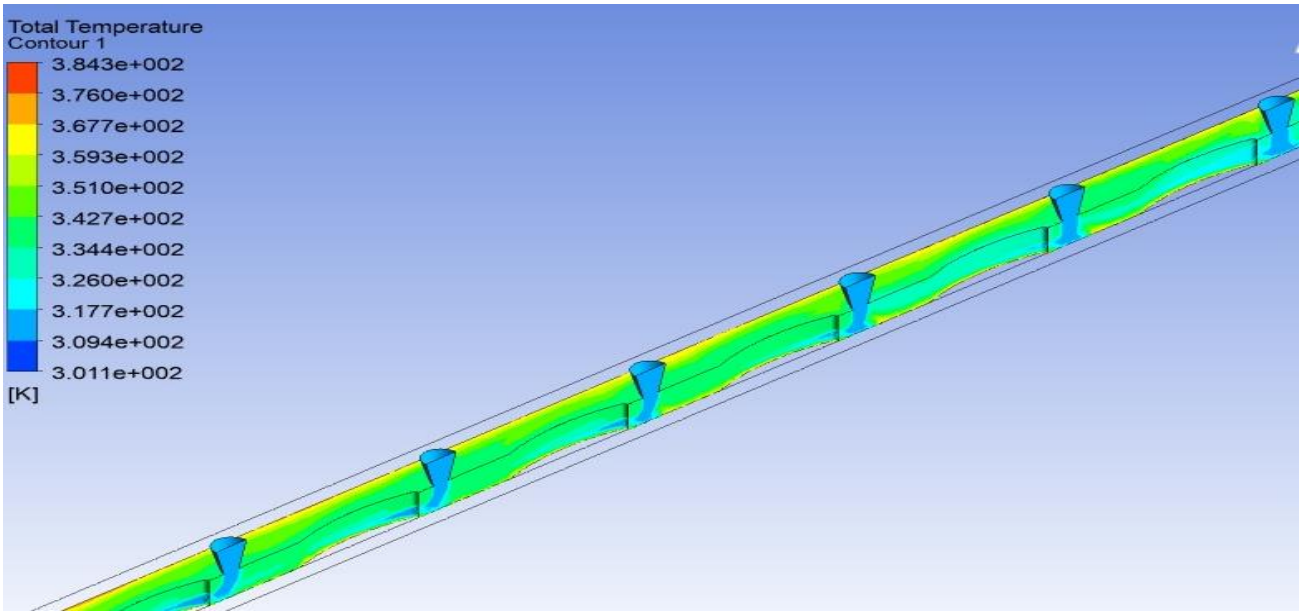

Figure 7.41: Temperature contour at Pitch ratio (PR) = 6, Height ratio (HR) = 1 for water

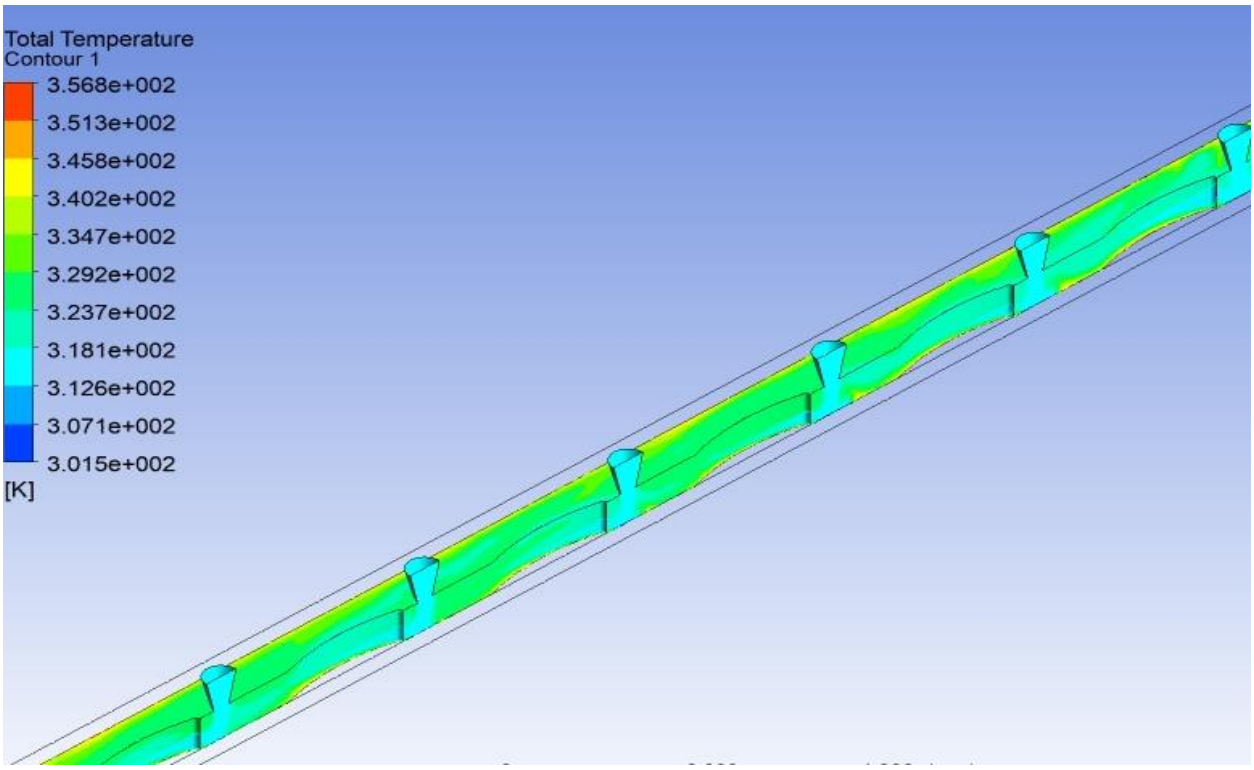

Figure 7.42: Temperature contour at Pitch ratio (PR) = 6, Height ratio (HR) = 1 for water– CuO Nanofluid (0.5%)

In the figure 7.40, for the water and CuO Nano fluid the velocity vector is represented for PR= 8 and HR = 1. The magnitude of velocity is also shown in the contours. The maximum and minimum value is shown in the figure.

Figure 7.41 and figure 7.42 represents the temperature contours in case of water and Nano fluid. The same has been presented for the same conditions (HR = 1 and PR = 6). The temperature of the substrate is reduced with the use of Nano fluid. The temperature is reduced from 384.3 in case of pure water to 356.8 in case of Nano fluid.

7.8 Different combinations using water-CuO Nano fluid (0.5%)

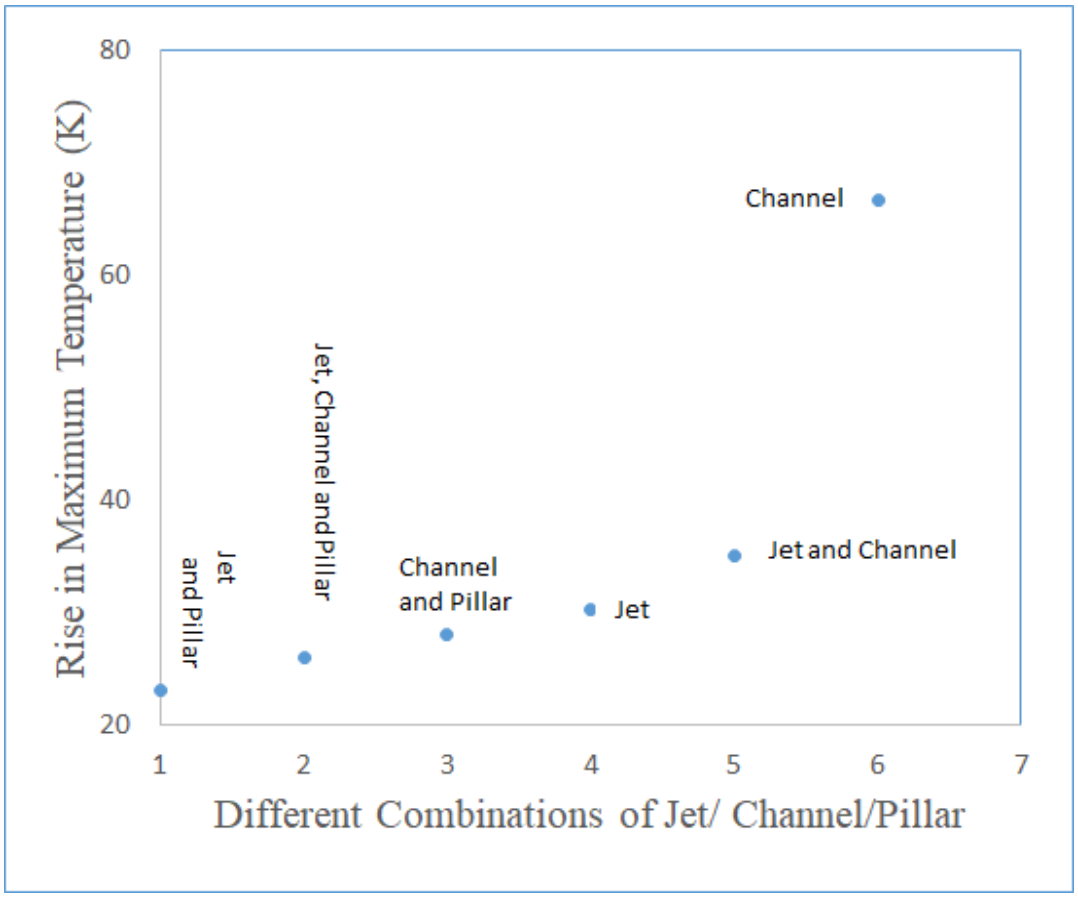

Figure 7.43:Rise in Maximum temperature $(\Delta T)_r$ for Different combinations of jet channel and pillar (DCOJCP) for water-CuO Nanofluid (0.5%)

Figure 7.43 depicts the variations in the temperature of heat sink with different combinations of Jet, channel and pillars with the use of CuO – water Nano fluid. RIMT has been found minimum in case of jet and pillar coalition. The presence of pillars leads to division of the boundary layer. Also the jet flow caused high impingement resulting the lower temperature. Max value is established for the channel flow. The reason for the same is due to advancement of boundary layer.

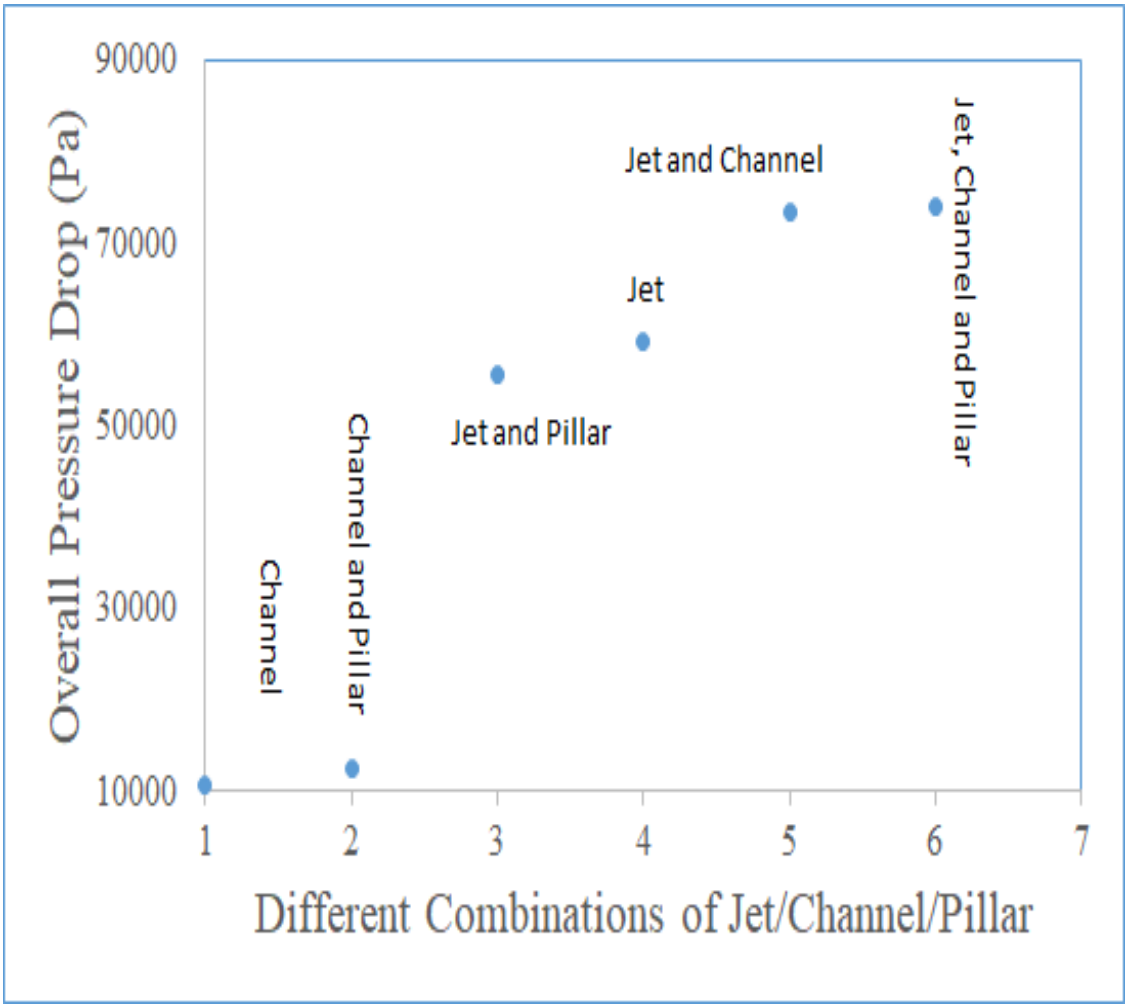

Figure 7.44:Overall Pressure drop $(\Delta P)_o$ for Different combinations of jet channel and pillar DCOJCP for water-CuO Nanofluid (0.5%)

Figure 7.44 outlined the variance in pressure drop for separate composition of jet, pillar and channel flow. For the amalgamation of flow in a channel with jet impingement and pillars, higher drop in pressure is noticed. Due to the increased velocity of the jet and discharge, in this combination drop in pressure augmented.

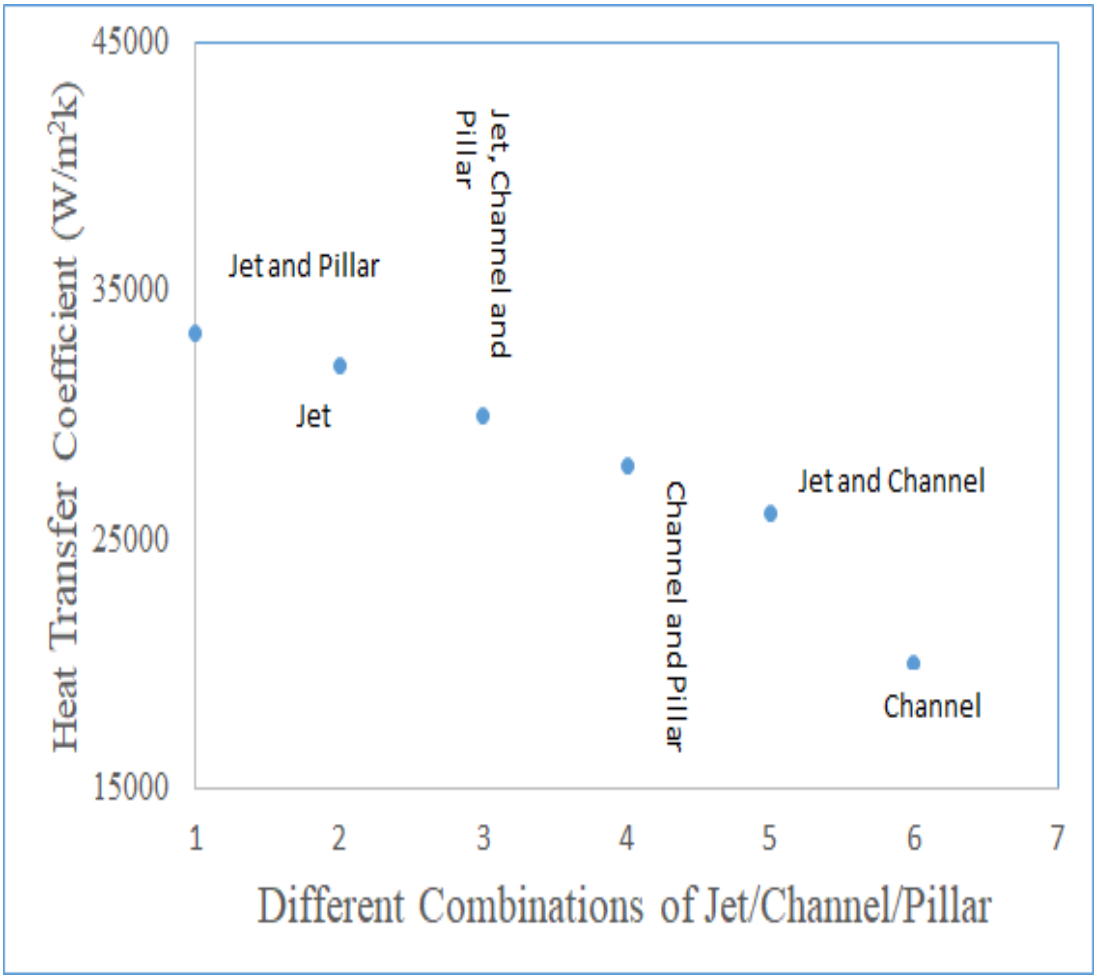

Figure 7.45: Heat Transfer coefficient (h) for Different combinations of jet channel and pillar (DCOJCP) for water-CuO Nanofluid (0.5%)

The variation of coefficient of heat transfer for the distinct combinations with the application of CuO- water Nano fluid is depicted in figure 7.45. Jet and pillars of air foil shape combination resulted in to increased value of Coefficient of heat exchange while the lower value is found in case of flow in channel. The use of air foil pillars with jet impingement in microchannel flow resulted high heat exchange coefficient. In contrast to the jet flow, channel flow exhibited lower values. Due to the presence of channel flow vortices diminished which resulted into lower heat exchange coefficient.

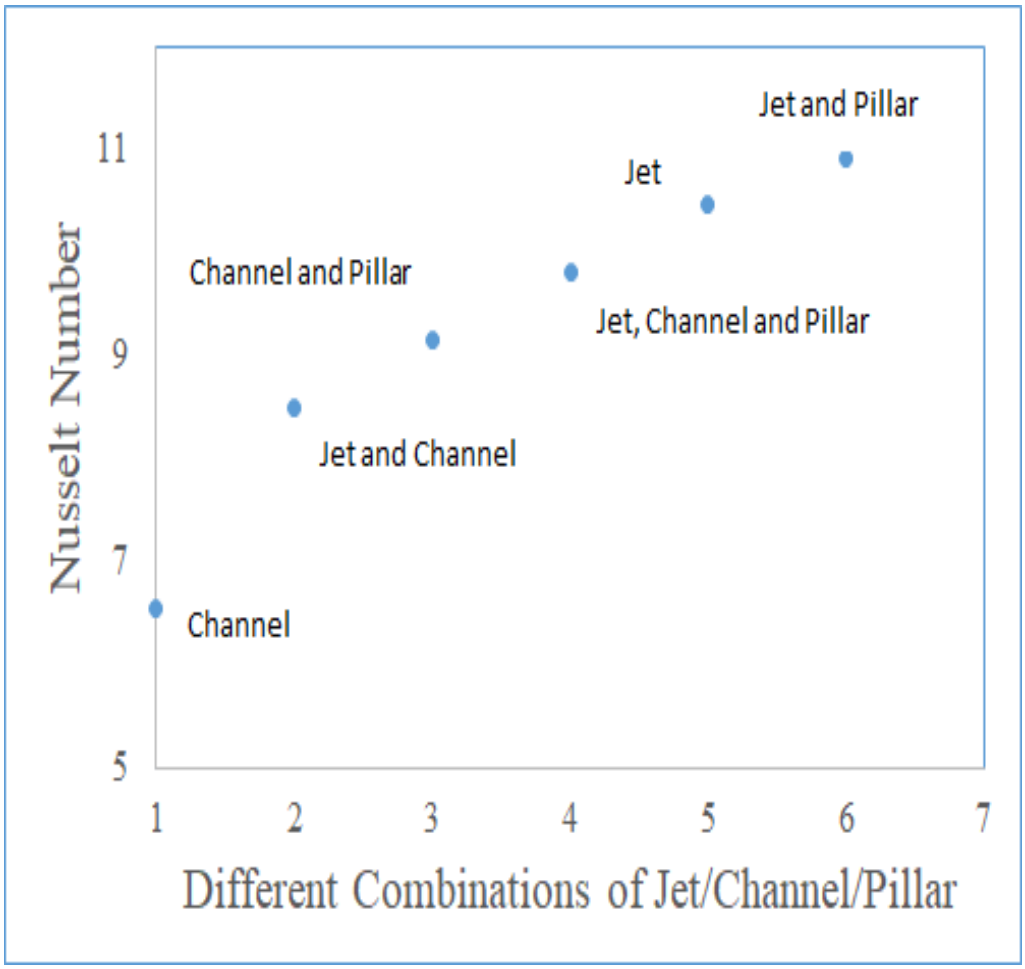

Figure 7.46: Nusselt Number(Nu) for Different combinations of jet channel and pillar (DCOJCP) for water-CuO Nanofluid (0.5%)

The variation in Nu with DCOJCP has been outlined in the figure 7.46. The combination of CuO – water Nano fluid with different combinations augmented the Nu. Jet and pillar showed more Nu as compared to the other arrangements. The combinations like jet and channel, channel and pillar, jet, channel and pillars, and jet flow lies in between channel and jet-pillar.

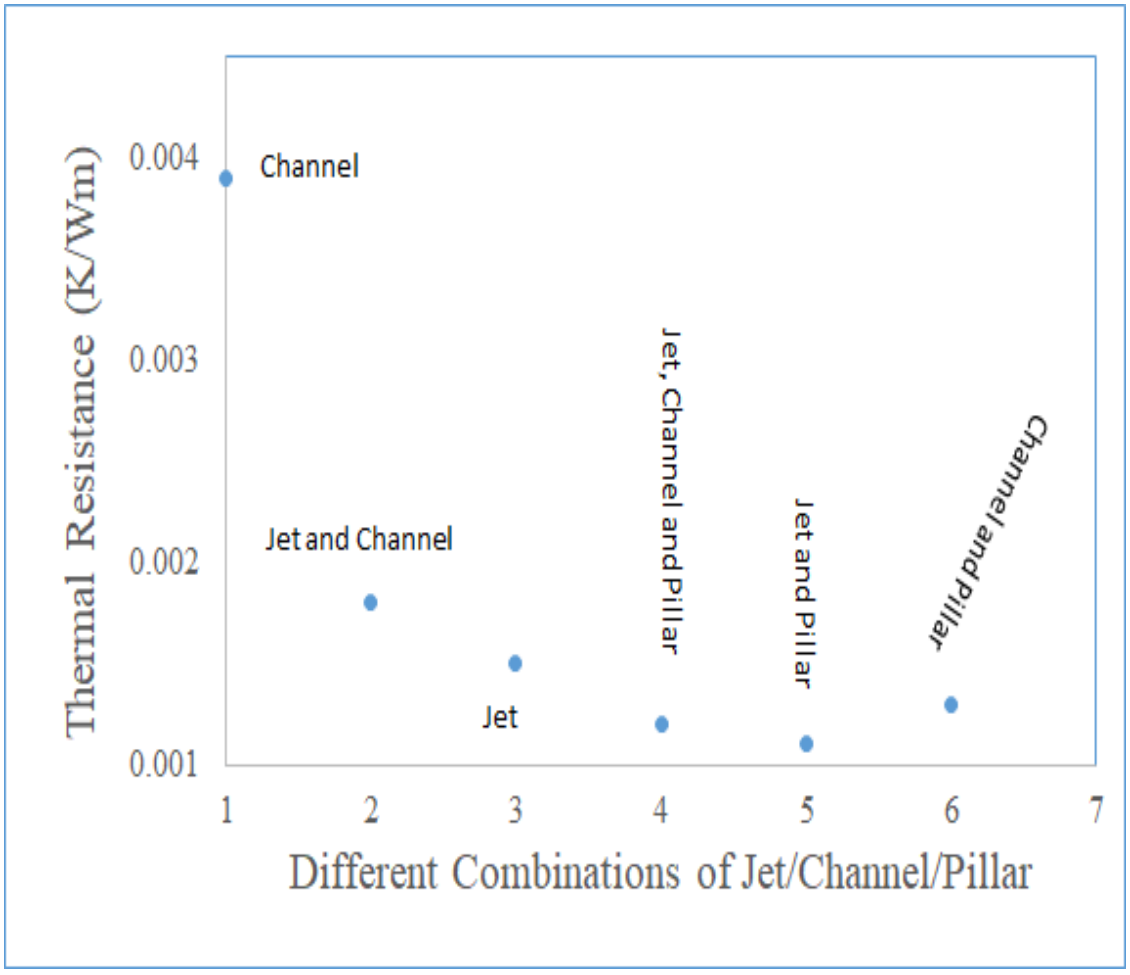

Figure 7.47: Thermal resistance (R_T) for Different combinations of jet channel and pillar (DCOJCP) for water-CuO Nanofluid (0.5%)

The relation of thermal resistance for several arrangements of jet-channel- pillar is explained with the help of figure 7.47. Thermal resistance is higher for channel flow and minimum for channel-pillar arrangement. Due to the augmentation in velocity, friction losses are increased resulting into higher Thermal resistance.

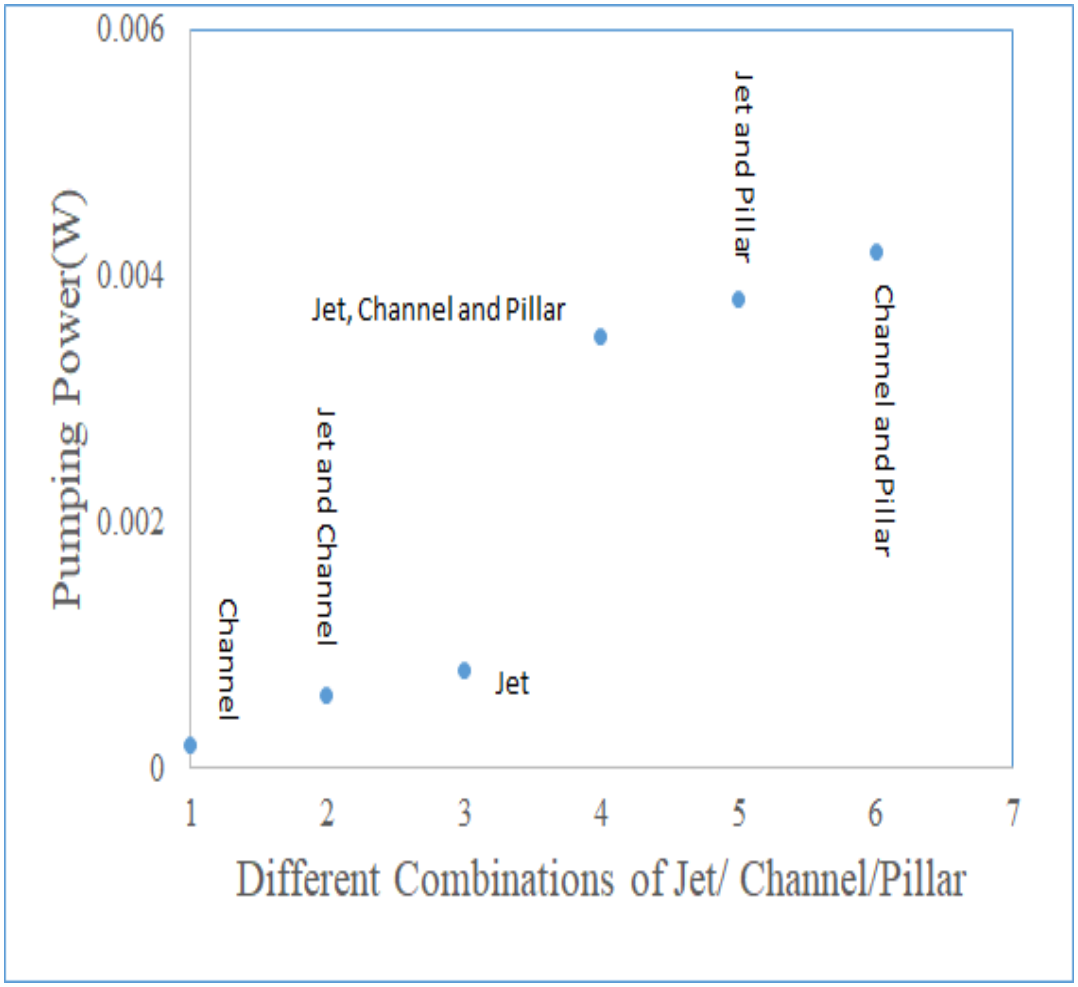

Figure 7.48: Pumping Power $(P)_p$ for Different combinations of jet channel and pillar (DCOJCP) for water-CuO Nanofluid (0.5%)

For the distinct arrangements of jet-channel and pillars, change in the pumping power (PP) has been depicted in the figure 7.48. This power is on the higher side for the case of channel- pillar and on the lower side for channel flow. The other combinations lie in the intermediate positions.

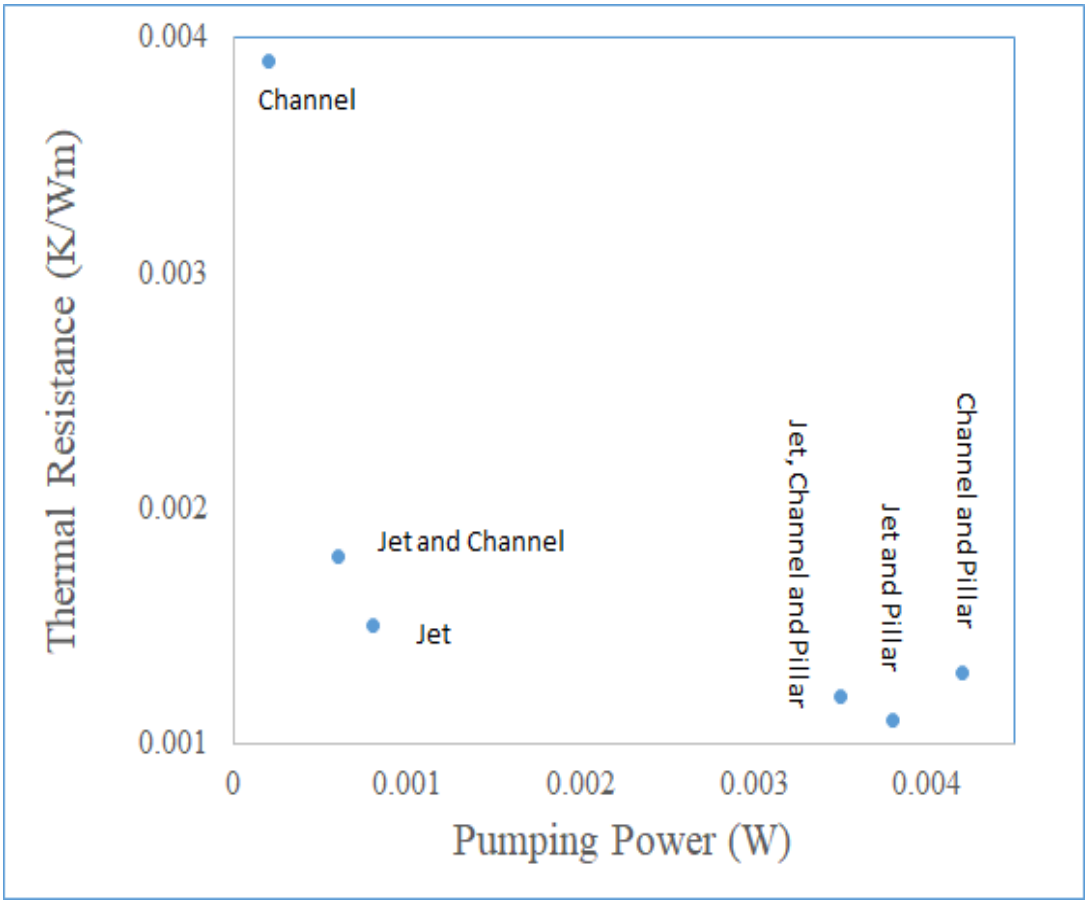

Figure 7.49: Relation between Thermal resistance (R_T)and Pumping Power $(P)_p$ for water-CuO Nanofluid (0.5%)

The association between thermal resistance and pumping power (PP) is shown in the figure 7.49 for different combinations of jet-channel and pillar along with the application of CuO- water Nano fluid. It has been recognized that for the for the highest value of Thermal resistance, PP is lowest and vice-versa. Jet- pillar flow corresponds to higher pumping power and low Thermal resistance due to the bifurcation of the boundary layer caused by air foil pillars.

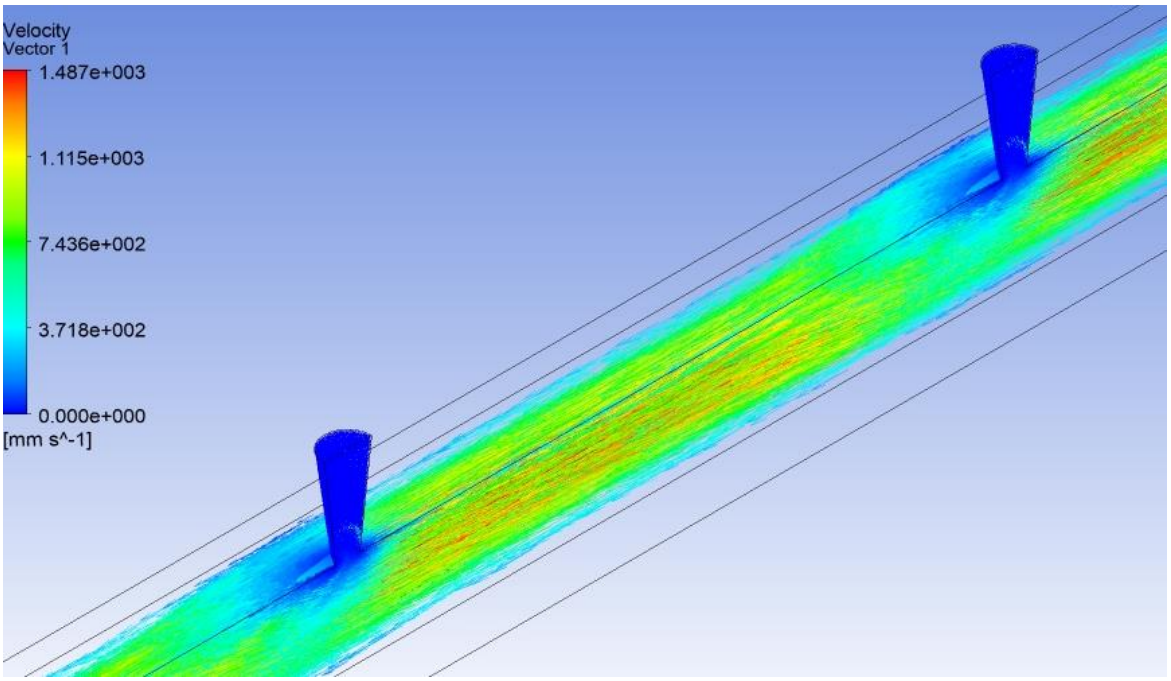

Figure 7.50 (a) Channel

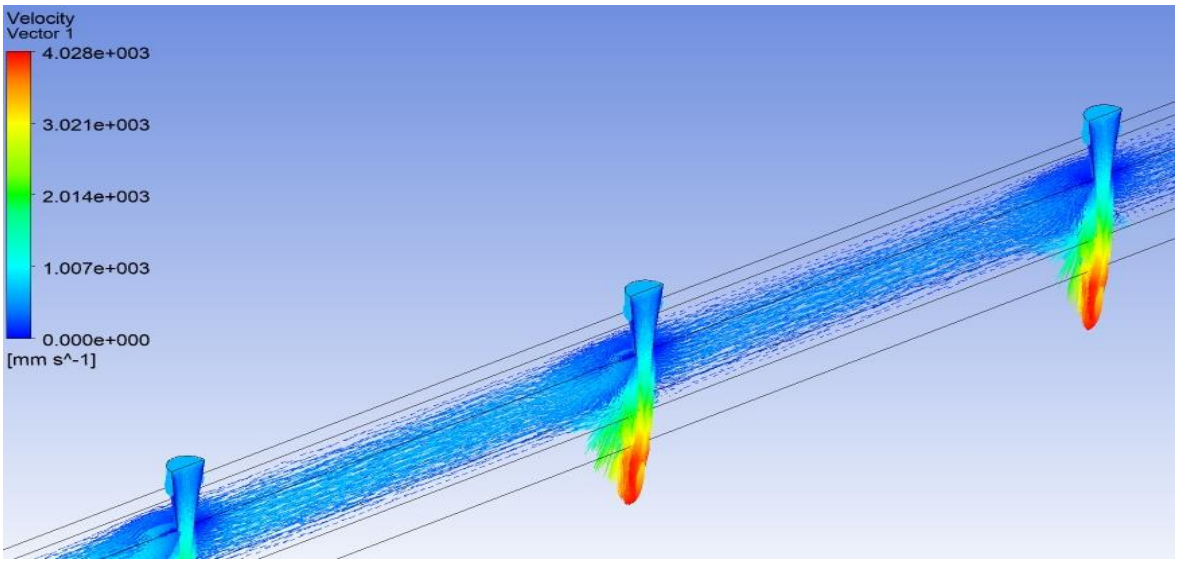

Figure 7.50 (b) Jet

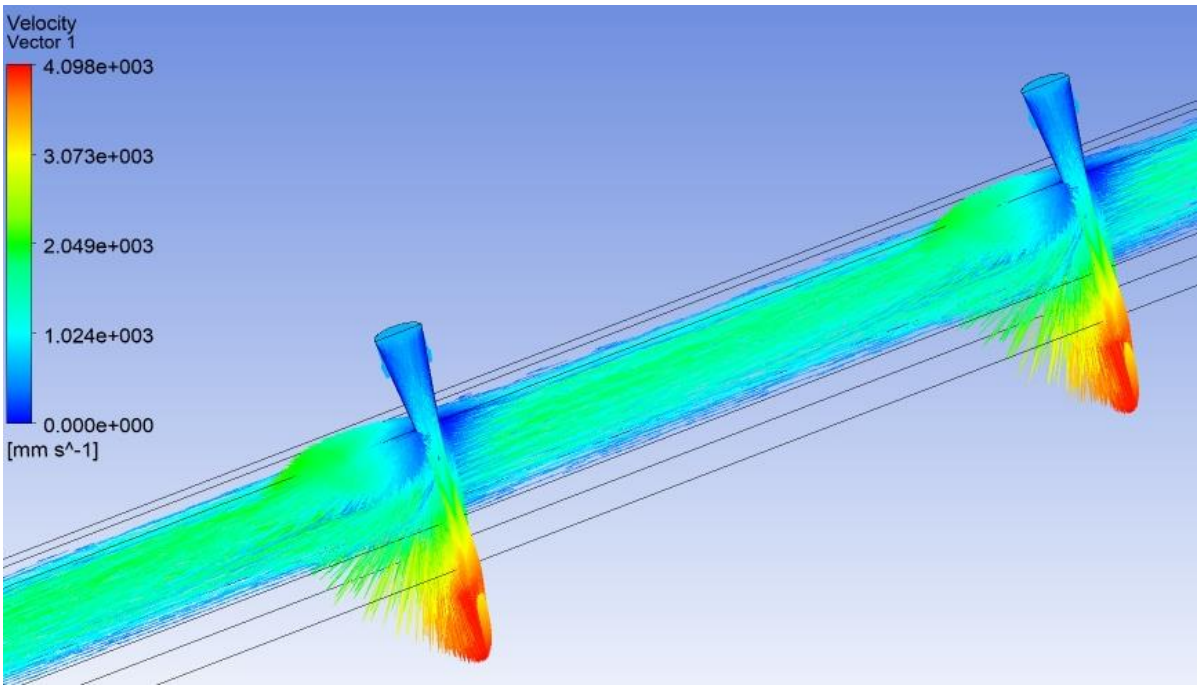

Figure 7.50 (c) Jet and Channel

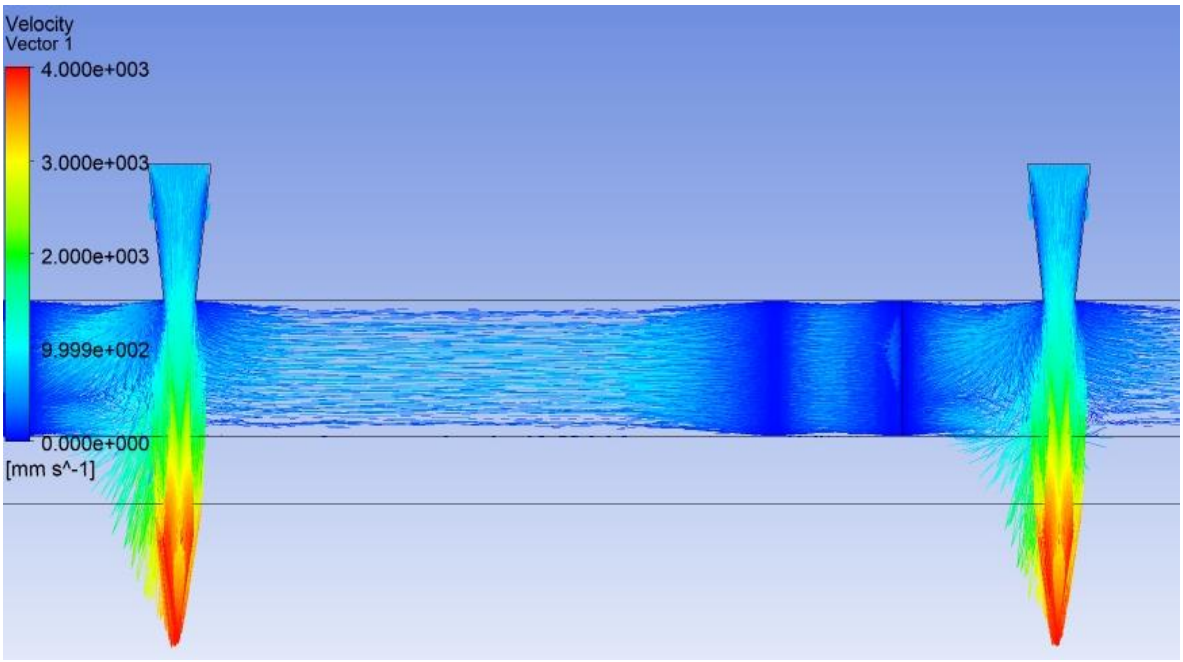

Figure 7.50 (d) Jet and Pillar

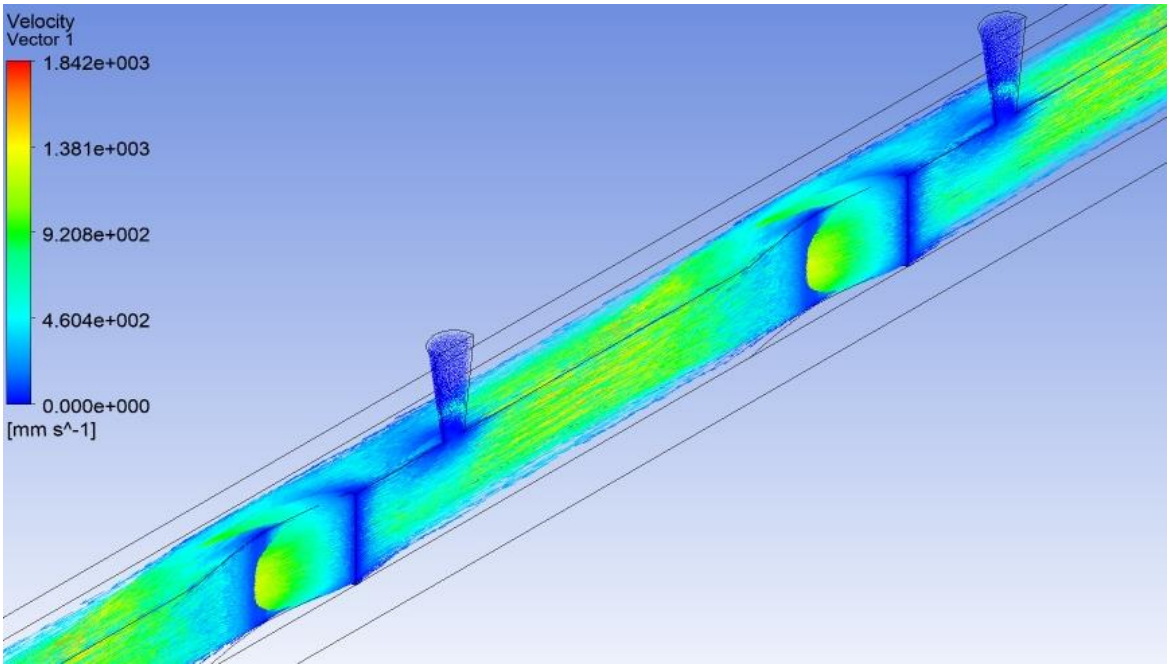

Figure 7.50 (e) Channel and Pillar

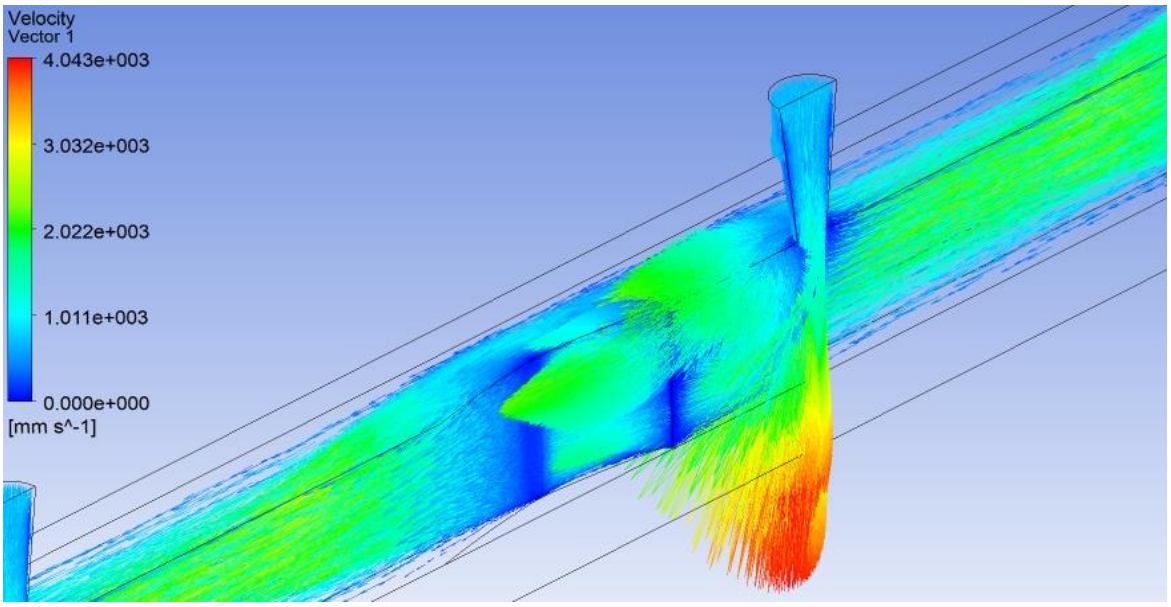

Figure 7.50 (f) Jet, Channel and Pillar

Figure 7.50: Velocity vector in different Combinations for water-CuO Nano fluid (0.5%)

Figure 7.50 presents the velocity vector for different combinations. For all the cases mass flow rate is taken as constant. In the case of impingement of jet in figure 7.50 (b), vortex formation is

detected which helps in increasing the heat exchange coefficient. In figure 7.50 (a), the flow in the channel tried to lessen the effect of jet impingement and hence reduction in coefficient. Figure 7.50 (c) represented the combined effect of jet and channel flow. In figure 7.50 (d), the effect of air foil pillars on the flow pattern is noticed which has provided an augmentation in the helix movement. Figure 7.50 (e) and (f) describes the effect of the combination of channel- air foil pillar and jet-channel-air foil pillars.

7.9 Different combinations using water – Al_2O_3 Nano fluid (5%)

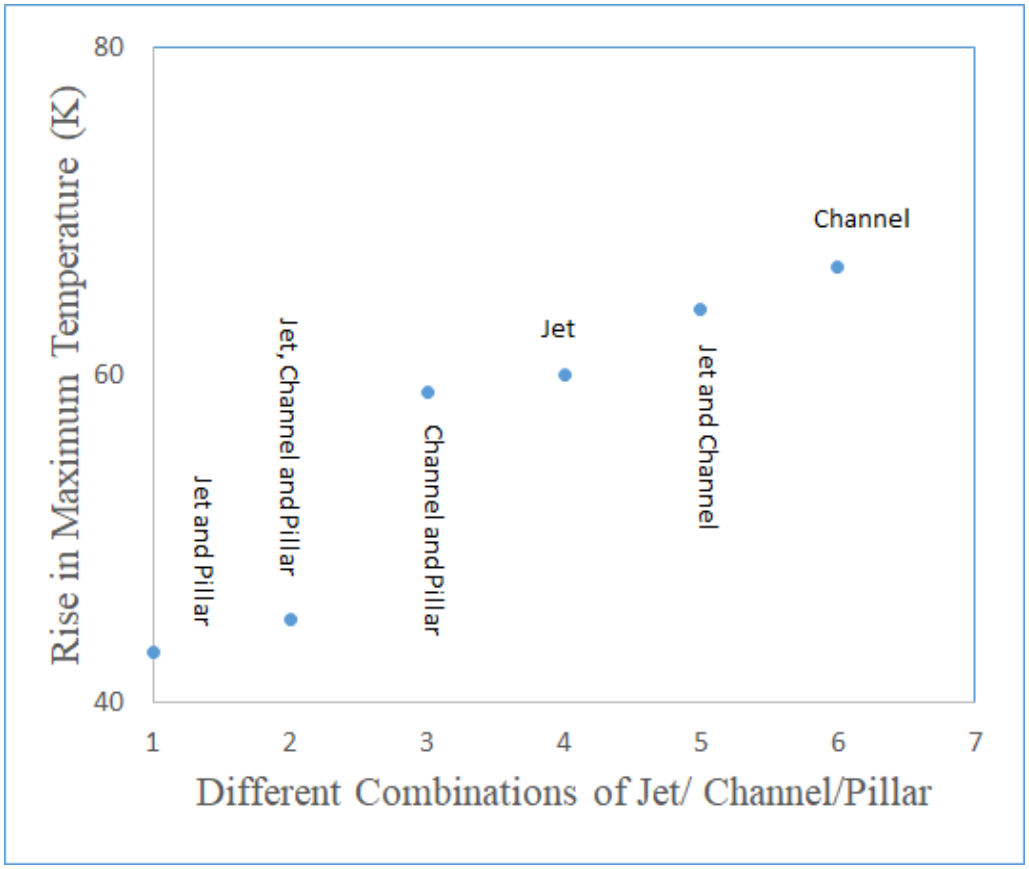

Figure 7.51: Rise in Maximum temperature $(\Delta T)_r$ for Different combinations of jet channel and pillar (DCOJCP) for water – Al_2O_3 Nanofluid

Figure 7.51 depicts the variations in the temperature rise with different combinations of Jet, channel and pillars with the use of Al_2O_3 – water Nano fluid with 5% concentration. RIMT has been found minimum in case of jet and pillar coalition. The presence of pillars leads to division of the boundary layer. Also the jet flow caused high impingement resulting the lower temperature. Max value is established for the channel flow. The reason for the same is due to advancement of boundary layer.

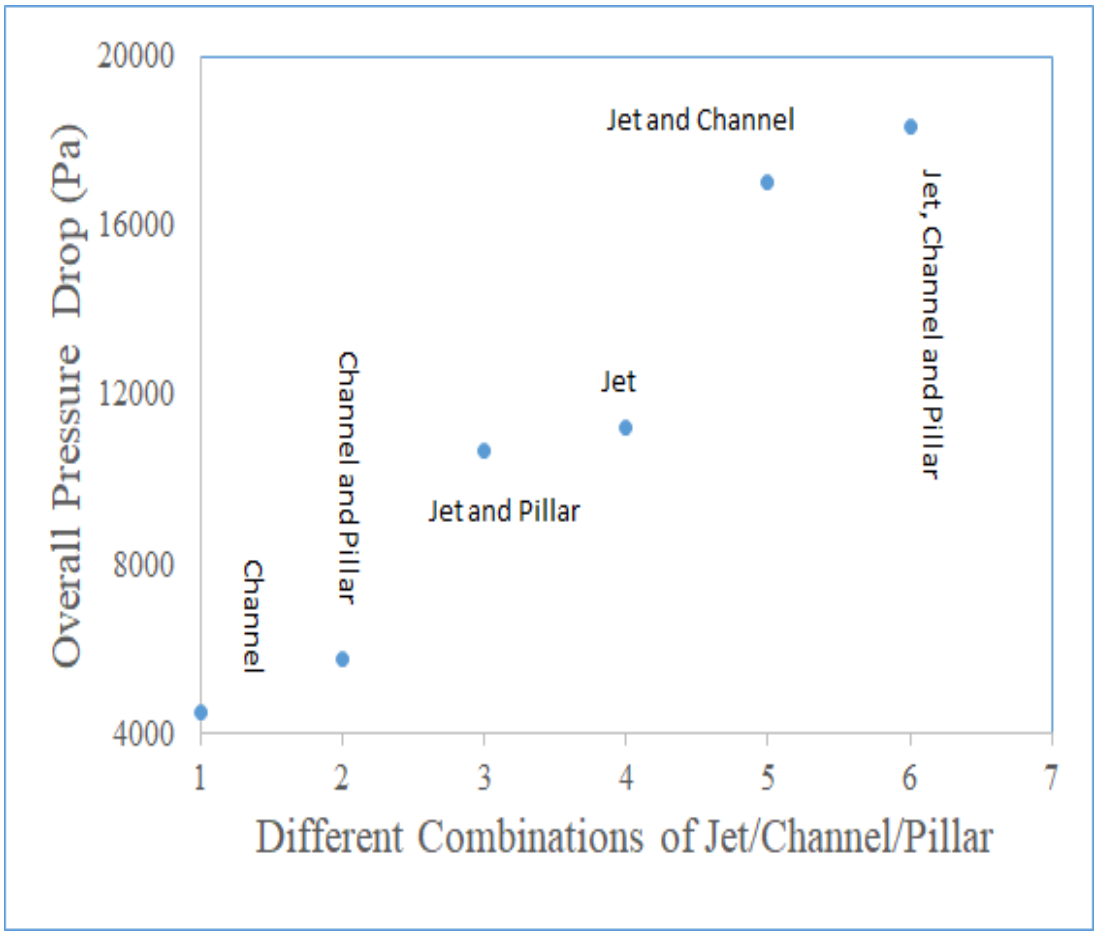

Figure 7.52: Overall Pressure drop $(\Delta P)_o$ for Different combinations of jet channel and pillar (DCOJCP) for water – Al_2O_3 Nanofluid

Figure 7.52 outlined the variance in pressure drop for separate composition of jet, pillar and channel flow. For the amalgamation of flow in a channel with jet impingement and pillars, higher

drop in pressure is noticed. Due to the increased velocity in this combination drop in pressure augmented. Another important aspect of the increase in the pitch ratio is that less space will be there and the counting of airfoil pillars for a particular space decreases. And the same thing happens with the number of nozzles. Due to the less number of pillars, loss of momentum will be less for the heat sink. This would finally result in lower pressure drop in case of channel flow.

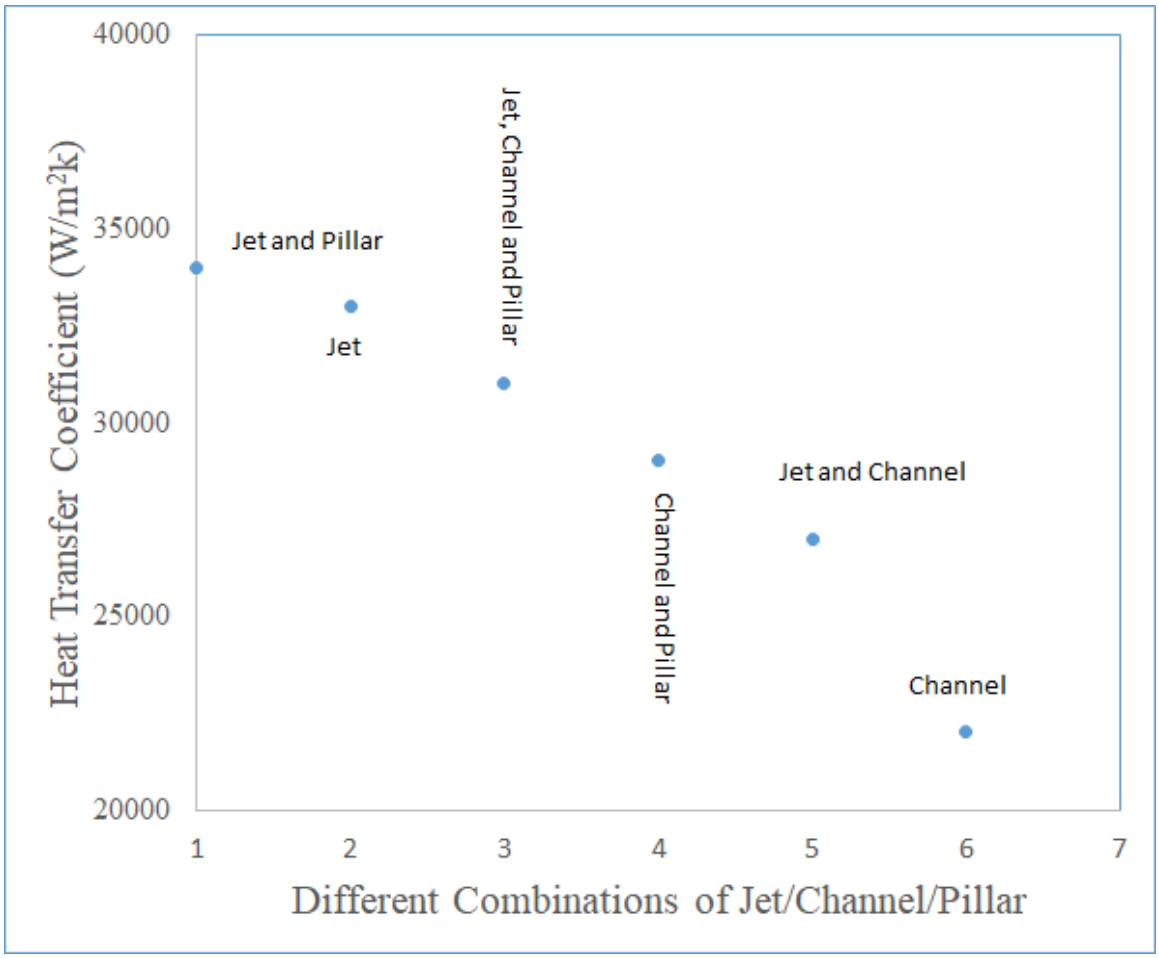

Figure 7.53: Heat Transfer coefficient (h) for Different combinations of jet channel and pillar (DCOJCP) for water – Al_2O_3 Nanofluid

The variation of coefficient of heat transfer for the distinct combinations with the application of Al_2O_3- water Nano fluid is depicted in figure 7.53. Jet and pillars of air foil shape combination

resulted in to increased value of Coefficient of heat exchange while the lower value is found in case of flow in channel. The use of air foil pillars with jet impingement in microchannel flow resulted high heat exchange coefficient. In contrast to the jet flow, channel flow exhibited lower values. Due to the presence of channel flow vortices diminished which resulted into lower heat exchange coefficient. Another important advantage of airfoil pillars is that it leads to boundary layer bifurcation. Due to this reason the two combinations (Jet- channel- airfoil pillars and Jet- airfoil pillars) results in less increase in the temperature. And this results in high convection heat transfer. For the jet – pillar combination heat transfer coefficient is found to be highest because of the more distractions

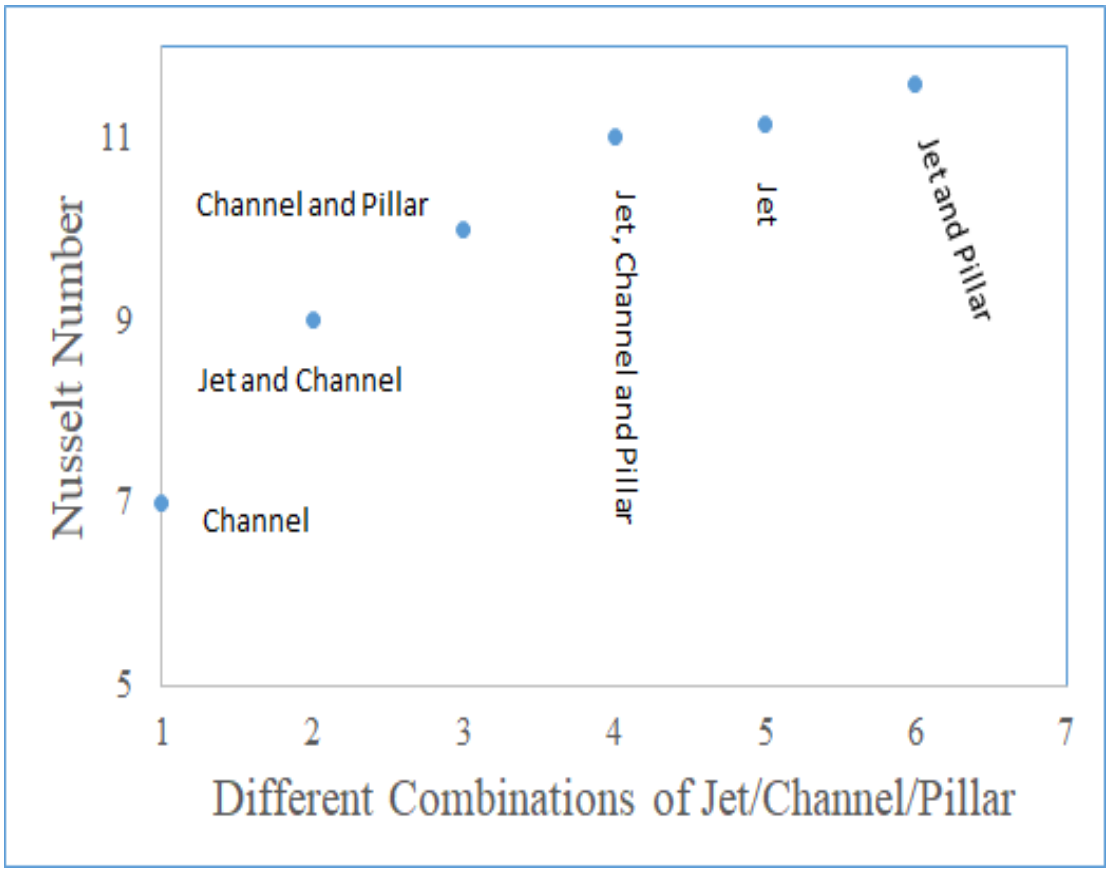

Figure 7.54: Nusselt Number (Nu) for Different combinations of jet channel and pillar (DCOJCP)for water – Al_2O_3 Nanofluid

The variation in Nu with DCOJCP has been outlined in the figure 7.54. The combination of Al_2O_3 – water Nano fluid with different combinations augmented the Nu. Jet and pillar showed more Nu as compared to the other arrangements. The combinations like jet and channel, channel and pillar, jet, channel and pillars, and jet flow lies in between channel and jet-pillar.

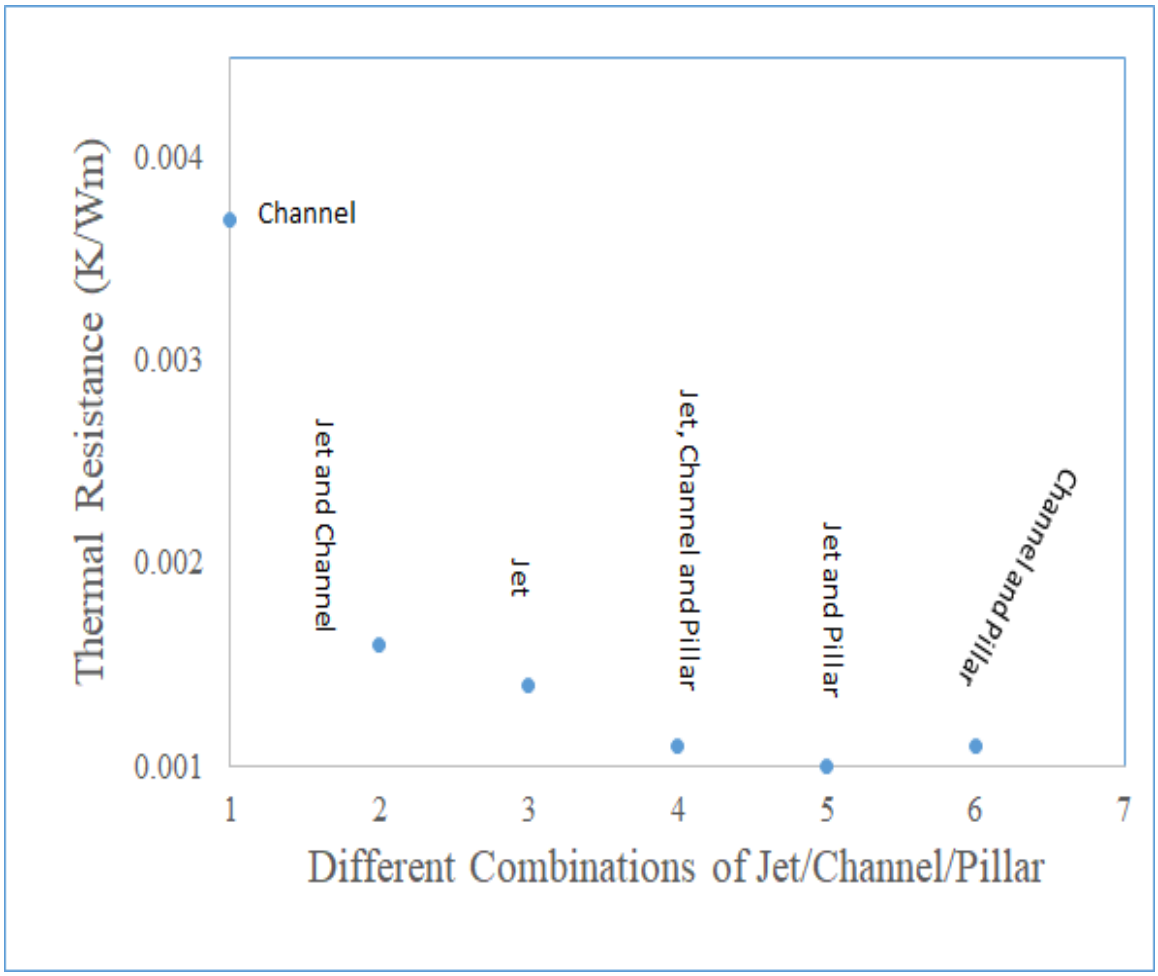

Figure 7.55: Thermal resistance (R_T) for Different combinations of jet channel and pillar (DCOJCP) for water – Al_2O_3 Nanofluid

The relation of thermal resistance for several arrangements of jet-channel- pillar is explained with the help of figure 7.55. Thermal resistance is higher for channel flow and minimum for channel-pillar arrangement. Due to the augmentation in velocity, friction losses are increased resulting into

higher Thermal resistance. Thermal dispersion of the Nanofluid is the main reason for the decrease in the thermal resistance of the channel combinations.

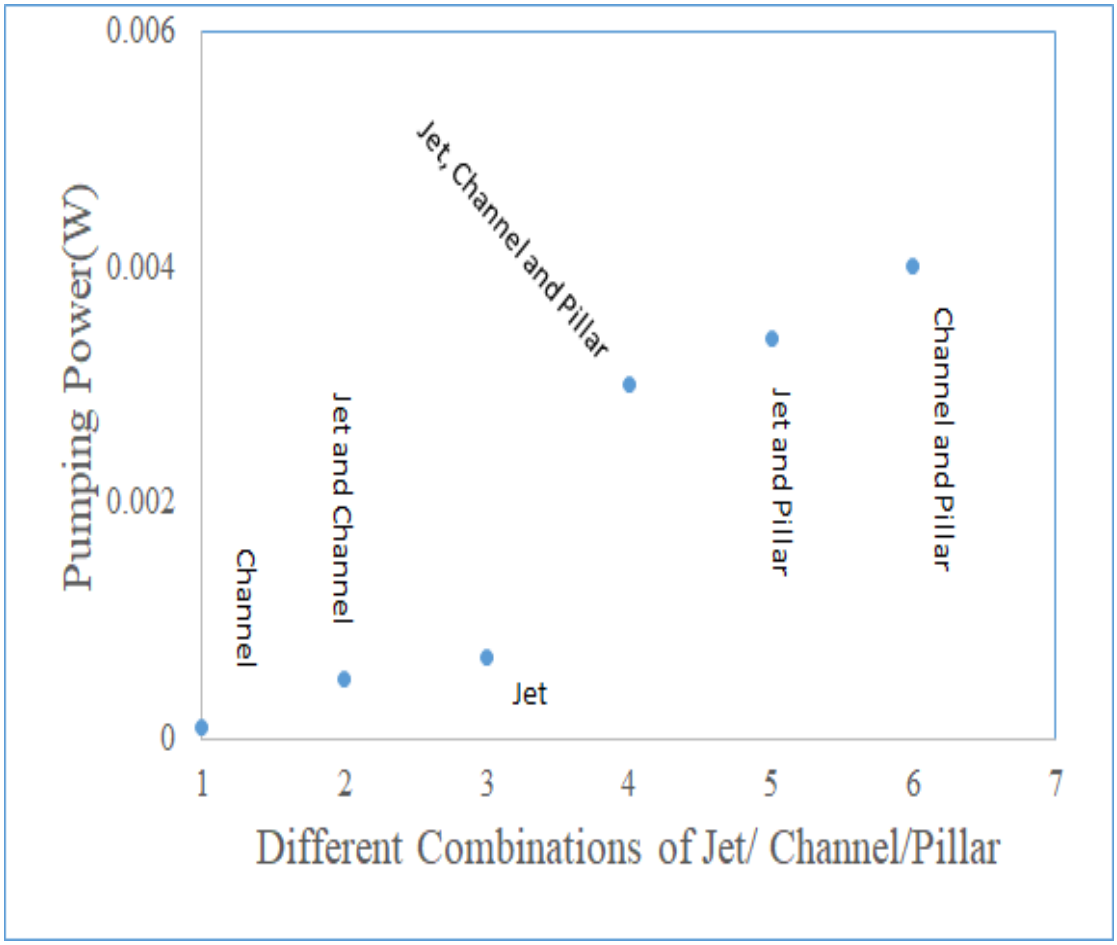

Figure 7.56: Pumping Power $(P)_p$ for Different combinations of jet channel and pillar (DCOJCP) for water – Al_2O_3 Nanofluid

For the distinct arrangements of jet-channel and pillars, change in the pumping power (PP) has been depicted in the figure 56. This power is on the higher side for the case of channel- pillar and on the lower side for channel flow. The other combinations lie in the intermediate positions.

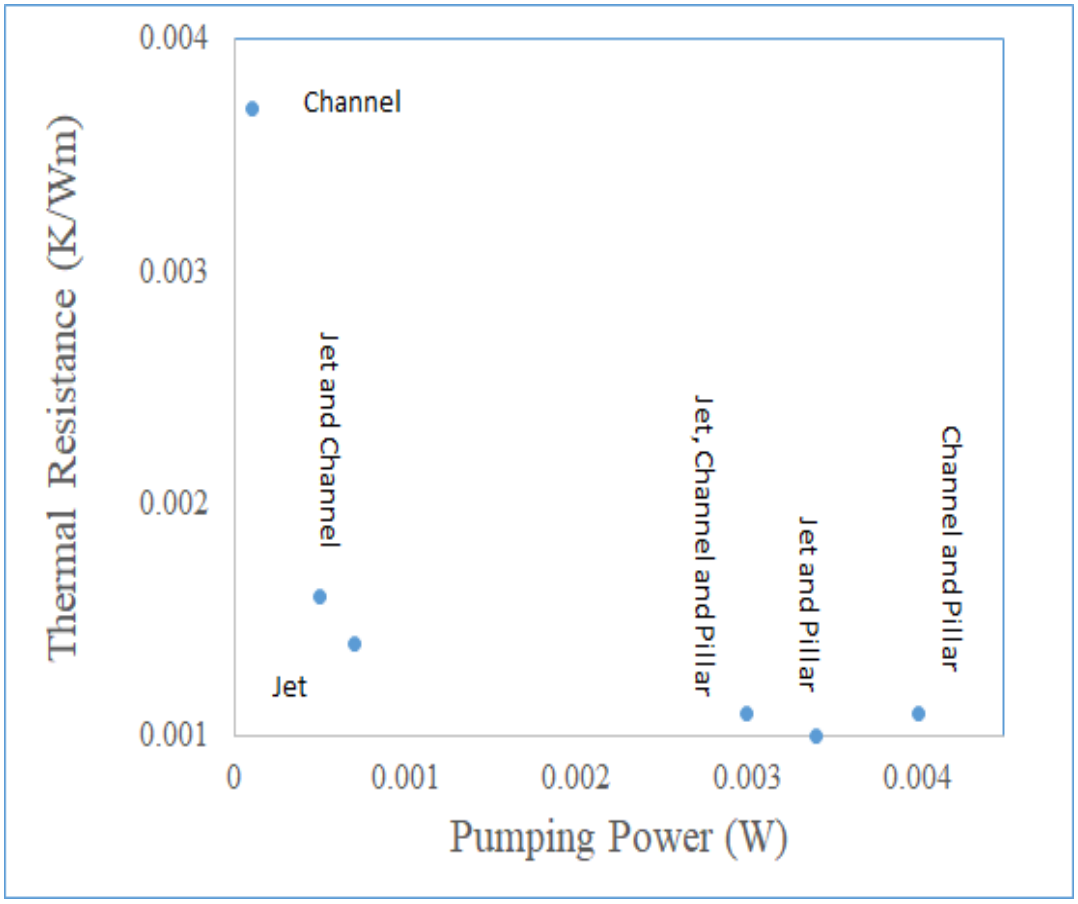

Figure 7.57: Relation between Thermal resistance (R_T)and Pumping power $(P)_p$ for water – Al_2O_3 Nano fluid

The association between thermal resistance and pumping power (PP) is shown in the figure 7.57 for different combinations of jet-channel and pillar along with the application of Al_2O_3 - water Nano fluid. It has been recognized that for the for the highest value of Thermal resistance, PP is lowest and vice-versa. Jet- pillar flow corresponds to higher Pumping power and low Thermal resistance. Thermal dispersion of the Nanofluid is the main reason for the decrease in the thermal resistance of the channel.

7.10 Velocity Vector using Al_2O_3-water Nano Fluid (5%)

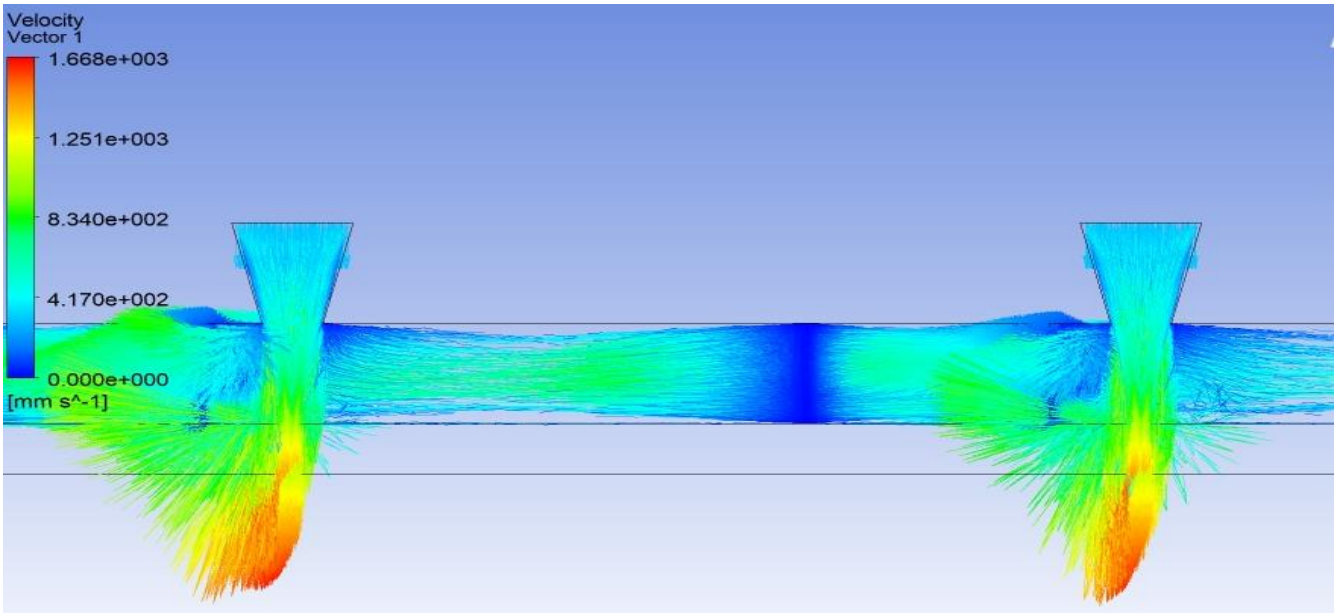

Figure 7.58: Flow Pattern at Height ratio $\left(\frac{H_{ch}}{D_j}\right) = 1$, Pitch ratio $\left(\frac{Ph}{D_j}\right) = 6$ for Al_2O_3-water Nanofluid

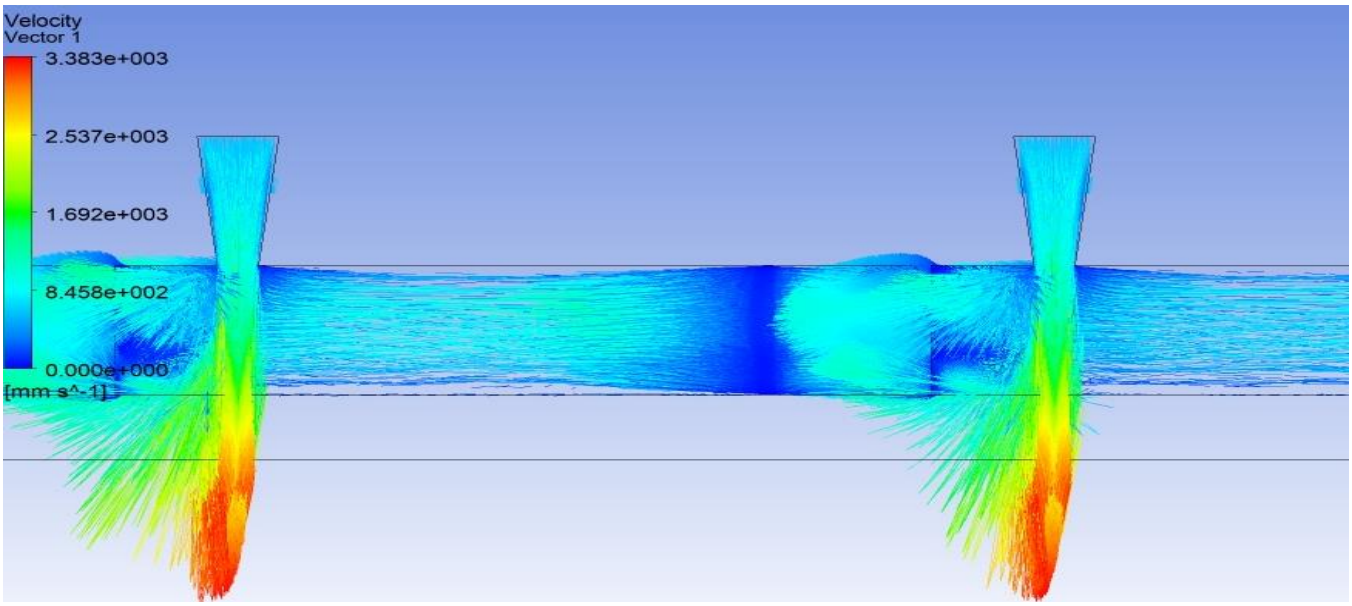

Figure 7.59: Flow Pattern at Height ratio $\left(\frac{H_{ch}}{D_j}\right) = 2$, Pitch ratio $\left(\frac{Ph}{D_j}\right) = 6$ for Al_2O_3-water Nanofluid

Figure 7.58 and 7.59 shows the flow pattern contours using Al_2O_3 – water Nano fluid for $\frac{H_{ch}}{D_j} = 1, \frac{Ph}{D_j} = 6$ and $\frac{H_{ch}}{D_j} = 2, \frac{Ph}{D_j} = 6$ respectively.

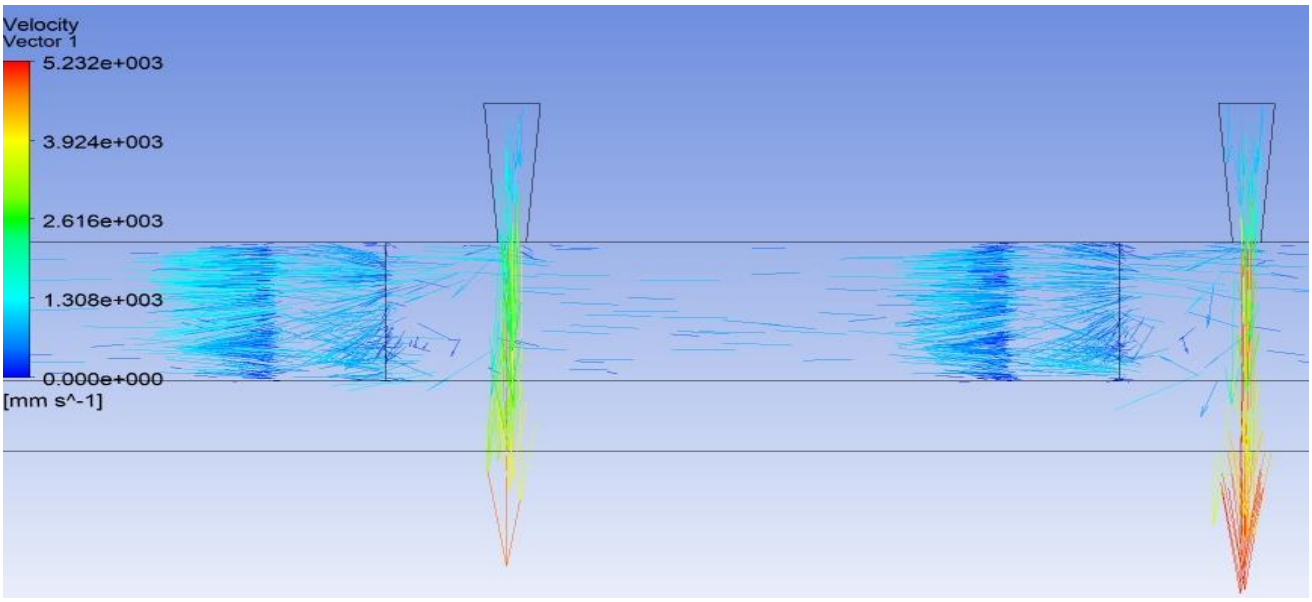

Figure 7.60: Flow Pattern at Height ratio $\left(\frac{H_{ch}}{D_j}\right) = 3$, Pitch ratio $(\frac{Ph}{D_j}) = 6$ for Al_2O_3-water Nanofluid

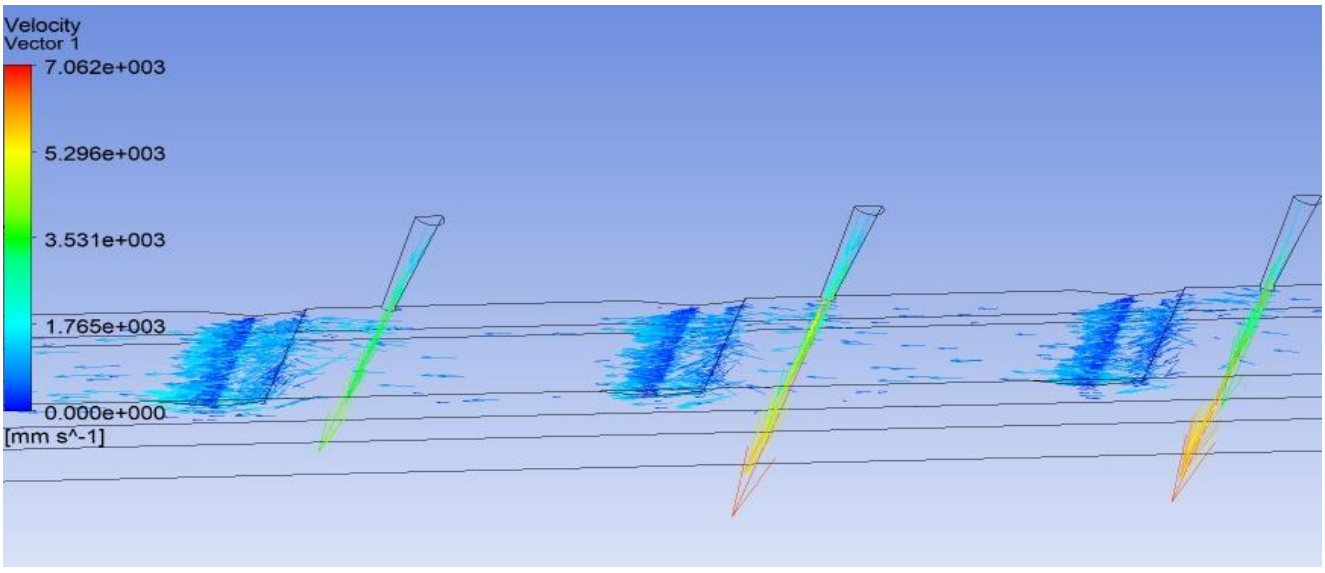

Figure 7.61: Flow Pattern at Height ratio $\left(\frac{H_{ch}}{D_j}\right) = 4$, Pitch ratio $(\frac{Ph}{D_j}) = 6$ for Al_2O_3-water Nanofluid

Figure 7.60 and 7.61 shows the flow pattern contours using Al_2O_3 – water Nano fluid for $\frac{H_{ch}}{D_j} = 3, \frac{Ph}{D_j} = 6$ and $\frac{H_{ch}}{D_j} = 4, \frac{Ph}{D_j} = 6$ respectively.

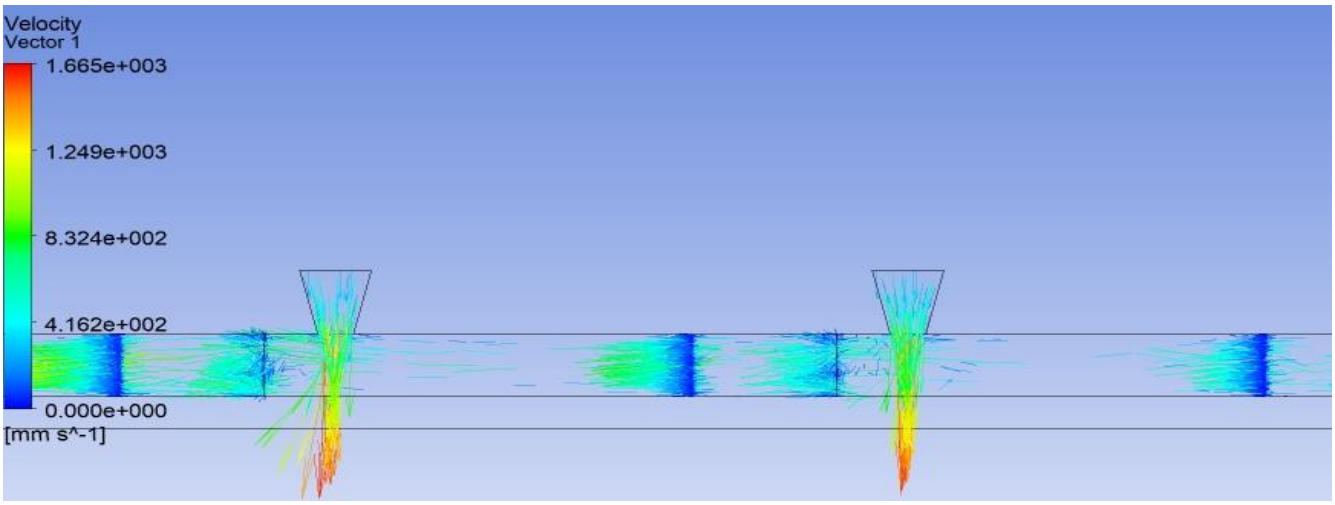

Figure 7.62: Flow Pattern at Height ratio $\left(\frac{H_{ch}}{D_j}\right) = 1$, Pitch ratio $(\frac{Ph}{D_j}) = 8$ for Al_2O_3-water Nanofluid

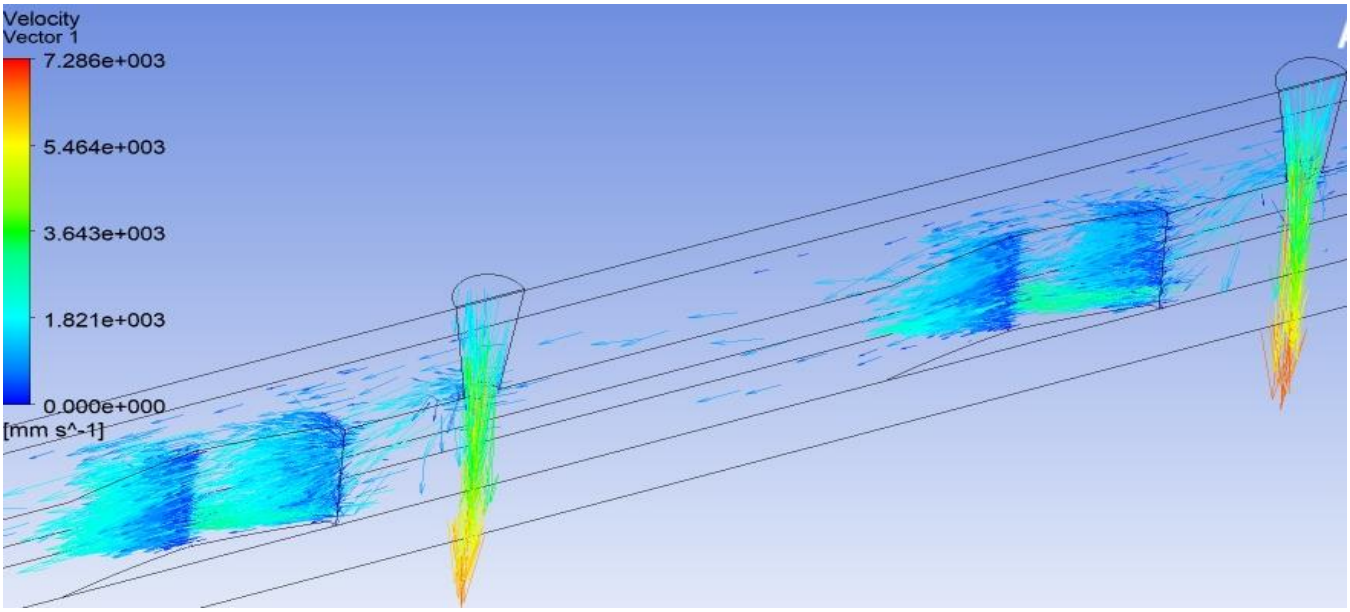

Figure 7.63: Flow Pattern at Height ratio $\left(\frac{H_{ch}}{D_j}\right) = 2$, Pitch ratio $(\frac{Ph}{D_j}) = 8$ for Al_2O_3-water Nanofluid

Figure 7.62 and 7.63 shows the flow pattern contours using Al_2O_3 – water Nanofluid for $\frac{H_{ch}}{D_j} = 1, \frac{Ph}{D_j} = 8$ and $\frac{H_{ch}}{D_j} = 2, \frac{Ph}{D_j} = 8$ respectively.

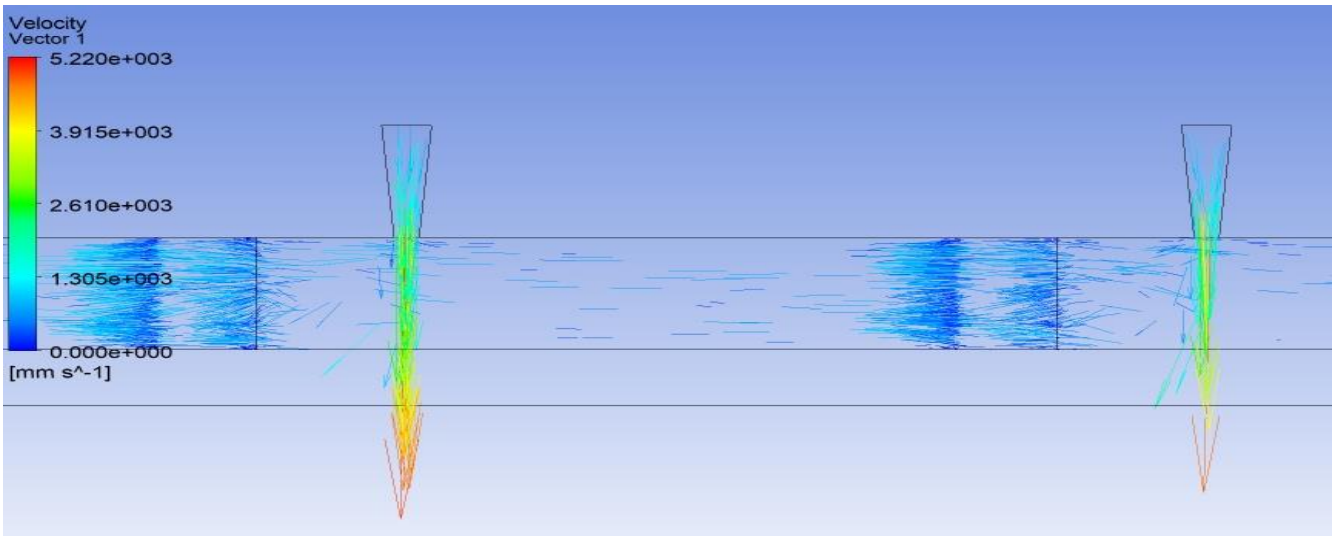

Figure 7.64: Flow Pattern at Height ratio $\left(\frac{H_{ch}}{D_j}\right) = 3$, Pitch ratio $\left(\frac{Ph}{D_j}\right) = 8$ for Al_2O_3-water Nanofluid

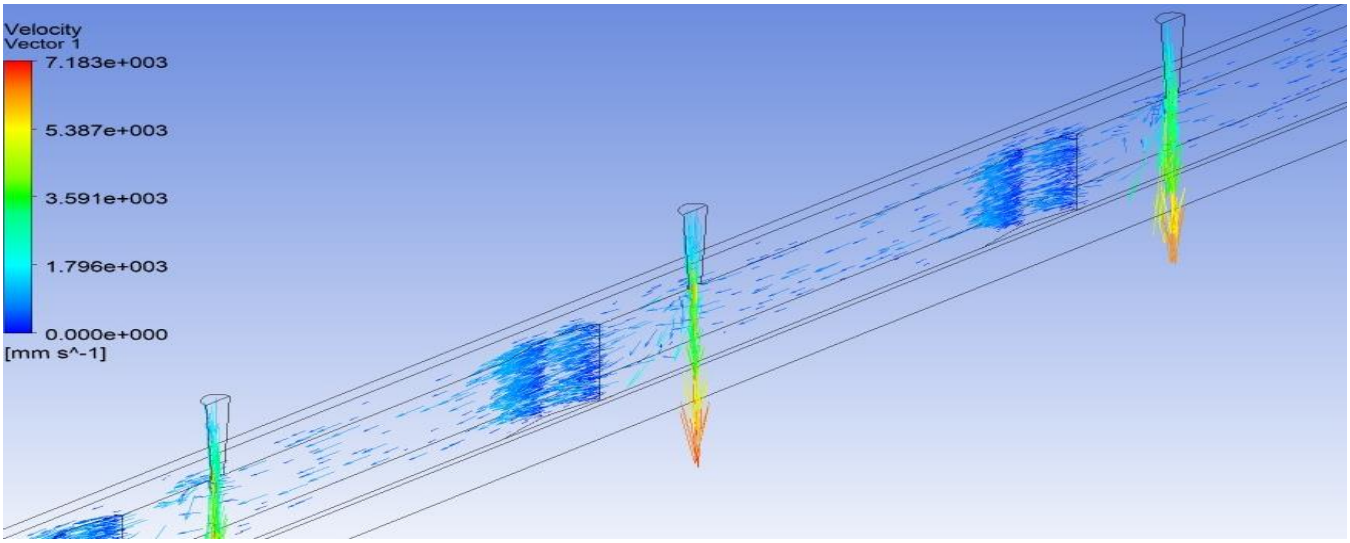

Figure 7.65: Flow Pattern at Height ratio $\left(\frac{H_{ch}}{D_j}\right) = 4$, Pitch ratio $\left(\frac{Ph}{D_j}\right) = 8$ for Al_2O_3-water Nanofluid.

Figure 7.64 and 7.65 shows the flow pattern contours using Al_2O_3 – water Nano fluid for $\frac{H_{ch}}{D_j} = 3, \frac{Ph}{D_j} = 8$ and $\frac{H_{ch}}{D_j} = 4, \frac{Ph}{D_j} = 8$ respectively. The minimum and maximum value of velocity vector is shown in the above figures.

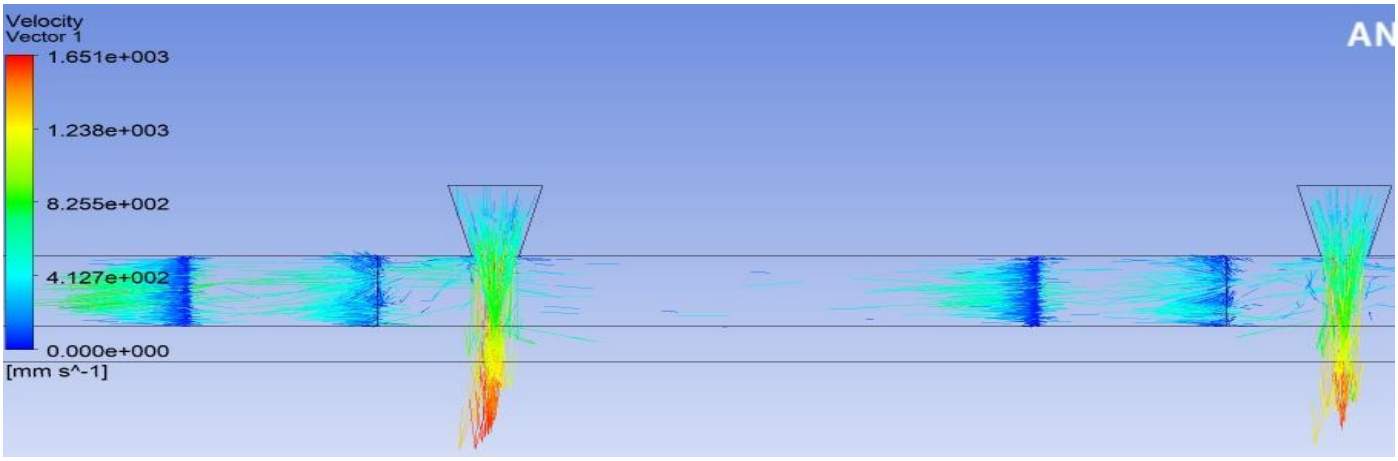

Figure 7.66: Flow Pattern at Height ratio $\left(\frac{H_{ch}}{D_j}\right) = 1$, Pitch ratio $(\frac{Ph}{D_j})$ = 10 for Al_2O_3-water Nanofluid

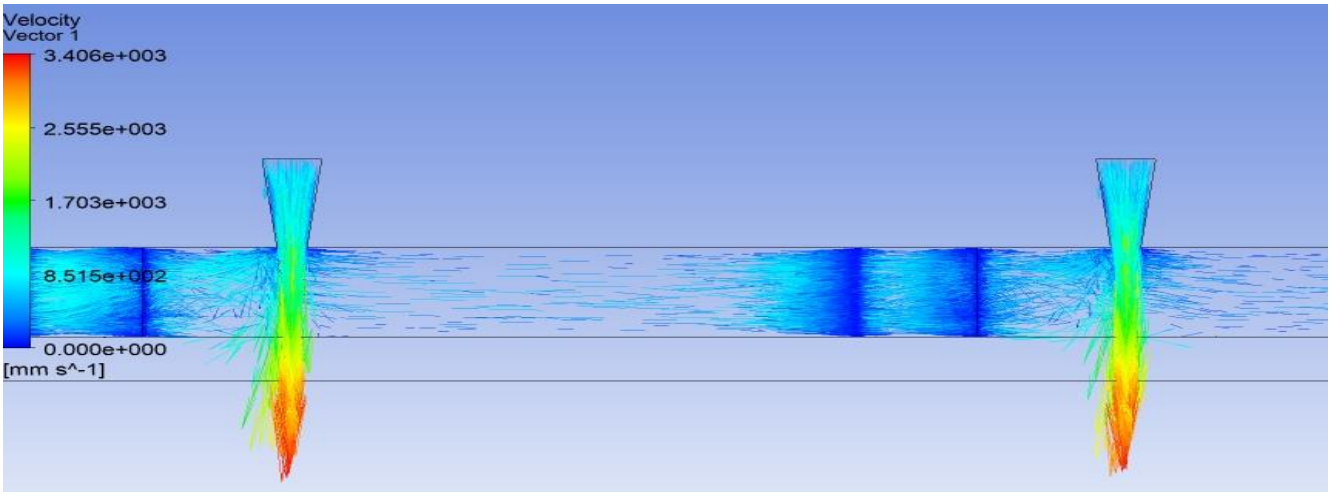

Figure 7.67: Flow Pattern at Height ratio $\left(\frac{H_{ch}}{D_j}\right) = 2$, Pitch ratio $(\frac{Ph}{D_j})$ = 10 for Al_2O_3-water Nanofluid

Figure 7.66 and 7.67 shows the flow pattern contours using Al_2O_3 – water Nano fluid for $\frac{H_{ch}}{D_j} = 1, \frac{Ph}{D_j} = 10$ and $\frac{H_{ch}}{D_j} = 2, \frac{Ph}{D_j} = 10$ respectively. The minimum and maximum value of velocity vector is shown in the above figures.

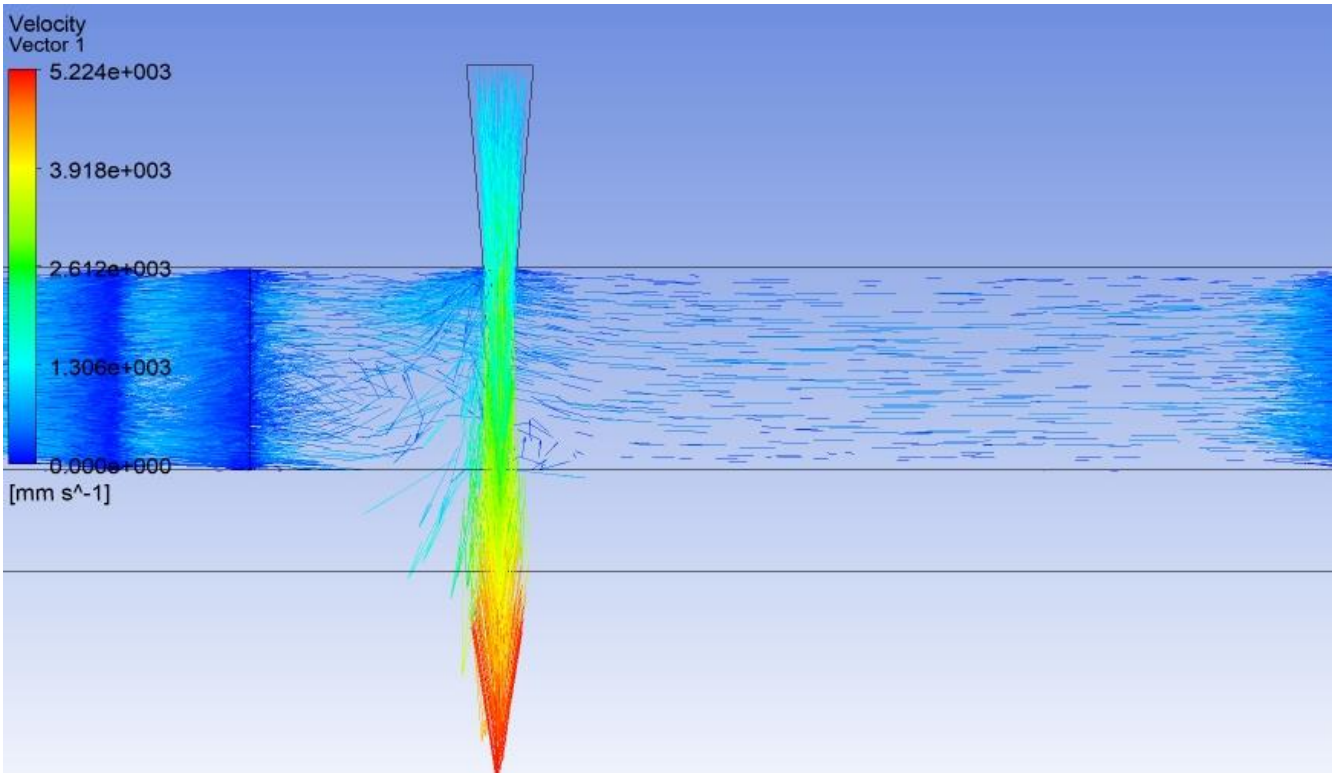

Figure 7.68: Flow Pattern at Height ratio $\left(\frac{H_{ch}}{D_j}\right) = 3$, Pitch ratio $\left(\frac{Ph}{D_j}\right) = 10$ for Al_2O_3-water Nanofluid

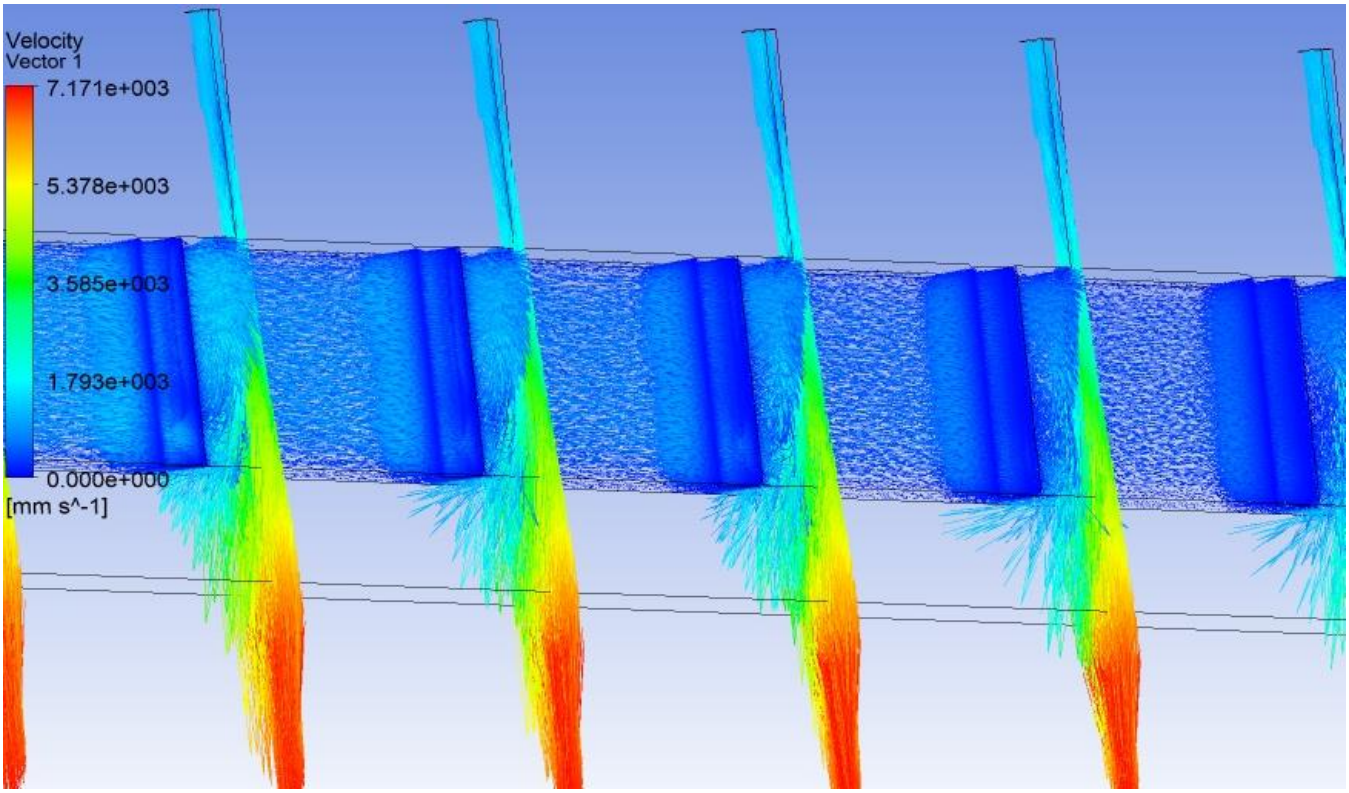

Figure 7.69: Flow Pattern at Height ratio $\left(\frac{H_{ch}}{D_j}\right) = 4$, Pitch ratio $(\frac{Ph}{D_j})$ = 10 for Al_2O_3-water Nanofluid

Figure 7.68 and 7.69 shows the flow pattern contours using Al_2O_3 – water Nano fluid for $\frac{H_{ch}}{D_j} = 3, \frac{Ph}{D_j} = 10$ and $\frac{H_{ch}}{D_j} = 4, \frac{Ph}{D_j} = 10$ respectively. The minimum and maximum value of velocity vector is shown in the above figures.

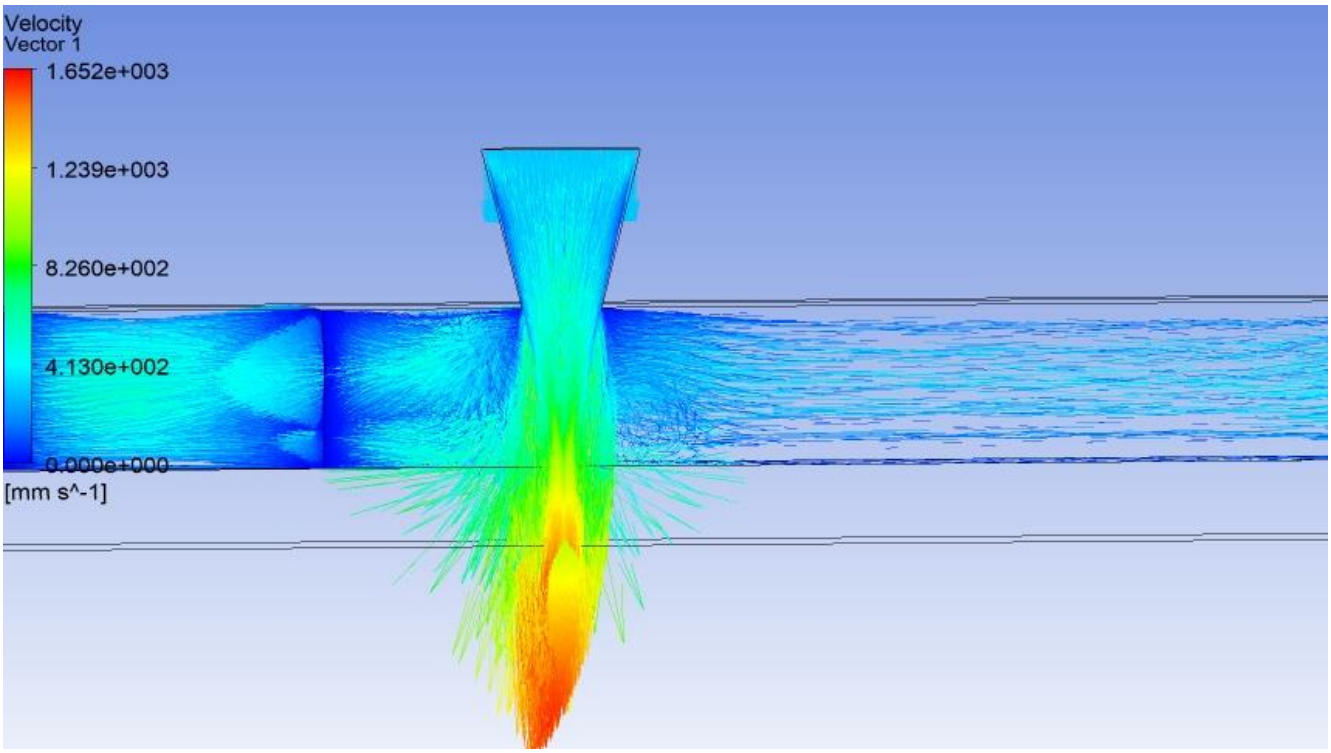

Figure 7.70: Flow Pattern at Height ratio $\left(\frac{H_{ch}}{D_j}\right) = 1$, Pitch ratio $(\frac{Ph}{D_j}) = 12$ for Al_2O_3-water Nanofluid

Figure 7.70 and 7.71 shows the velocity vector contours using Al_2O_3 – water Nano fluid for $\frac{H_{ch}}{D_j} = 1, \frac{Ph}{D_j} = 12$ and $\frac{H_{ch}}{D_j} = 2, \frac{Ph}{D_j} = 12$ respectively. The minimum and maximum value of velocity vector is shown in the above figures.

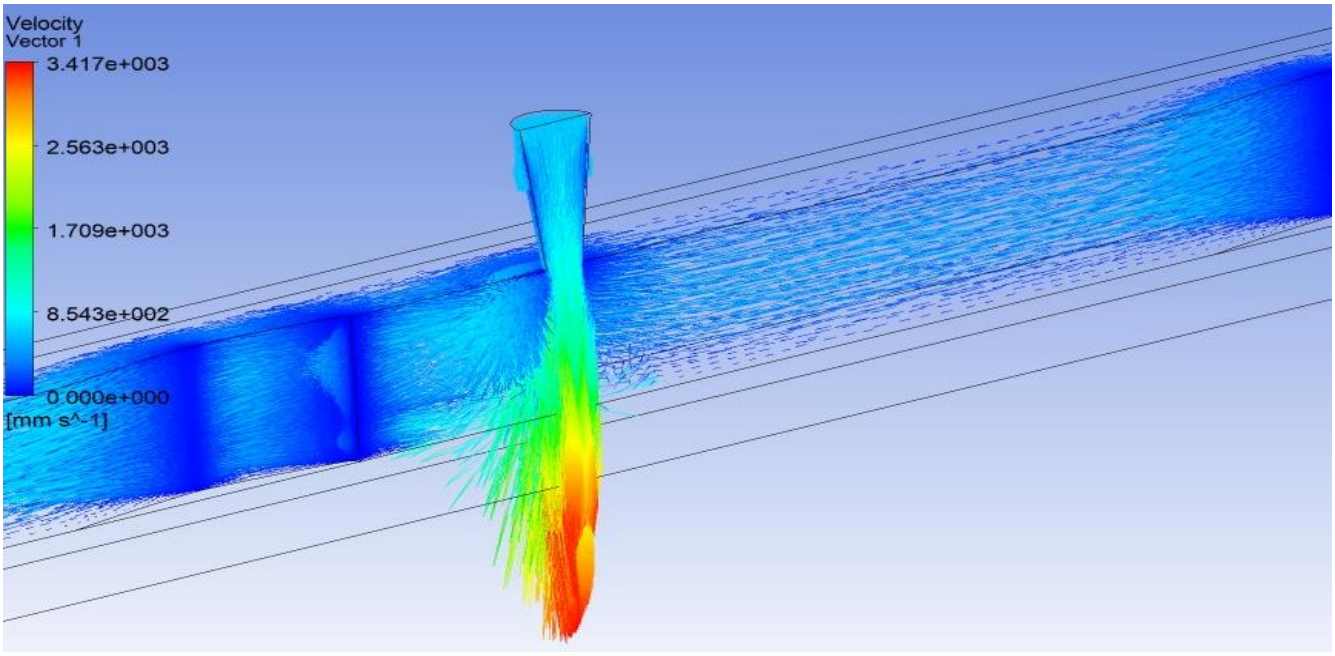

Figure 7.71: Flow Pattern at Height ratio $\left(\frac{H_{ch}}{D_j}\right) = 2$, Pitch ratio $(\frac{Ph}{D_j}) = 12$ for Al_2O_3-water Nanofluid

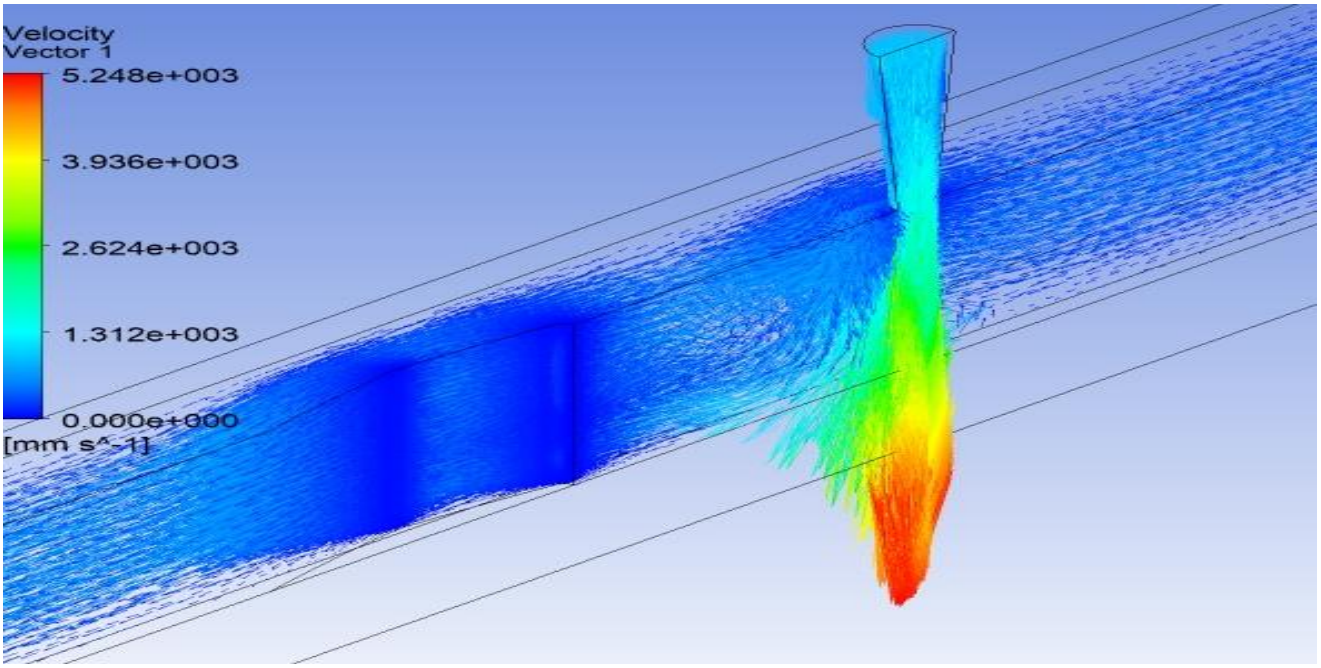

Figure 7.72: Flow Pattern at Height ratio $\left(\frac{H_{ch}}{D_j}\right) = 3$, Pitch ratio $(\frac{Ph}{D_j}) = 12$ for Al_2O_3-water Nanofluid

Figure 7.72 and 7.73 shows the velocity vector contours using Al_2O_3 – water Nano fluid for $\frac{H_{ch}}{D_j} = 3, \frac{Ph}{D_j} = 12$ and $\frac{H_{ch}}{D_j} = 4, \frac{Ph}{D_j} = 12$ respectively. The minimum and maximum value of velocity vector is shown in the figure 7.72 and 7.73.

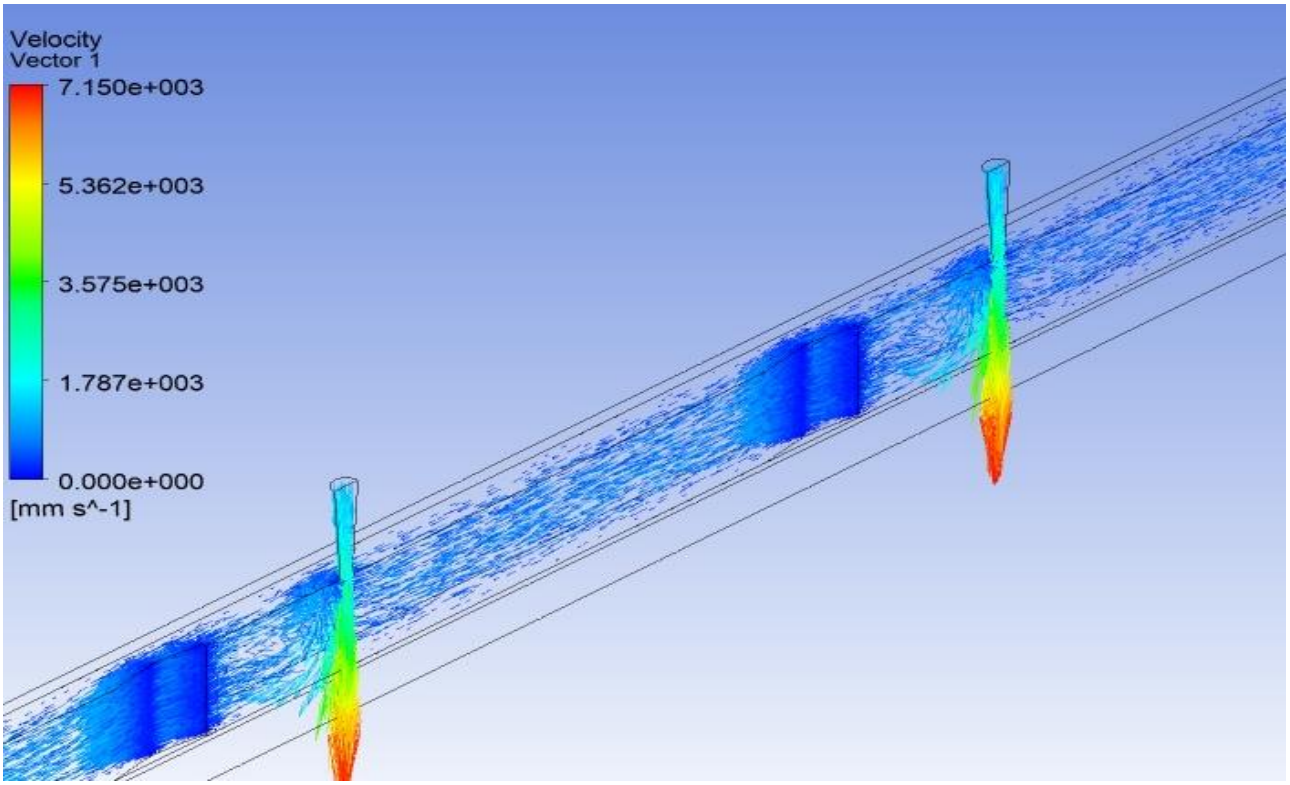

Figure 7.73: Flow Pattern at Height ratio $\left(\frac{H_{ch}}{D_j}\right) = 4$, Pitch ratio $(\frac{Ph}{D_j}) = 12$ for Al_2O_3-water Nanofluid.

Figure 7.74 shows the velocity vector contours in case of channel flow. Similarly figure 7.75 shows the flow pattern in the form of velocity vector in case of jet flow. The minimum and maximum value of velocity vector is shown in the figures 7.74 and 7.75.

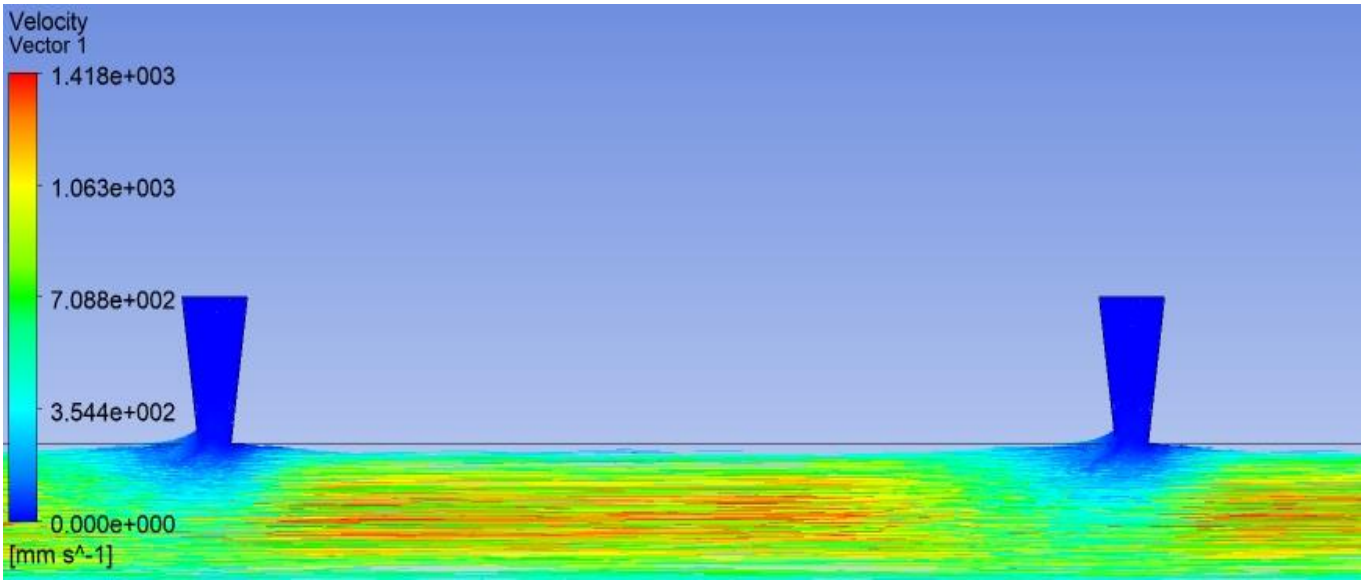

Figure 7.74: Flow Pattern for channel flow for Al_2O_3-water Nano Fluid

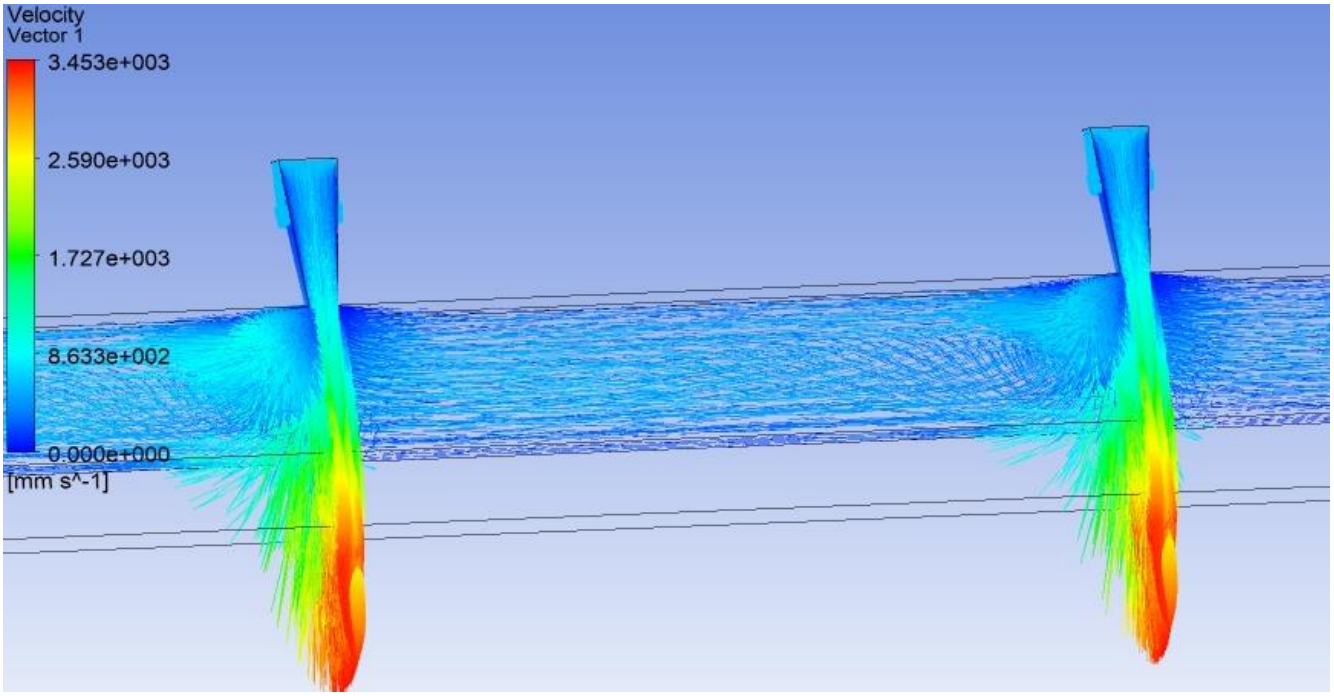

Figure 7.75: Flow Pattern for jet flow for Al_2O_3-water Nano Fluid

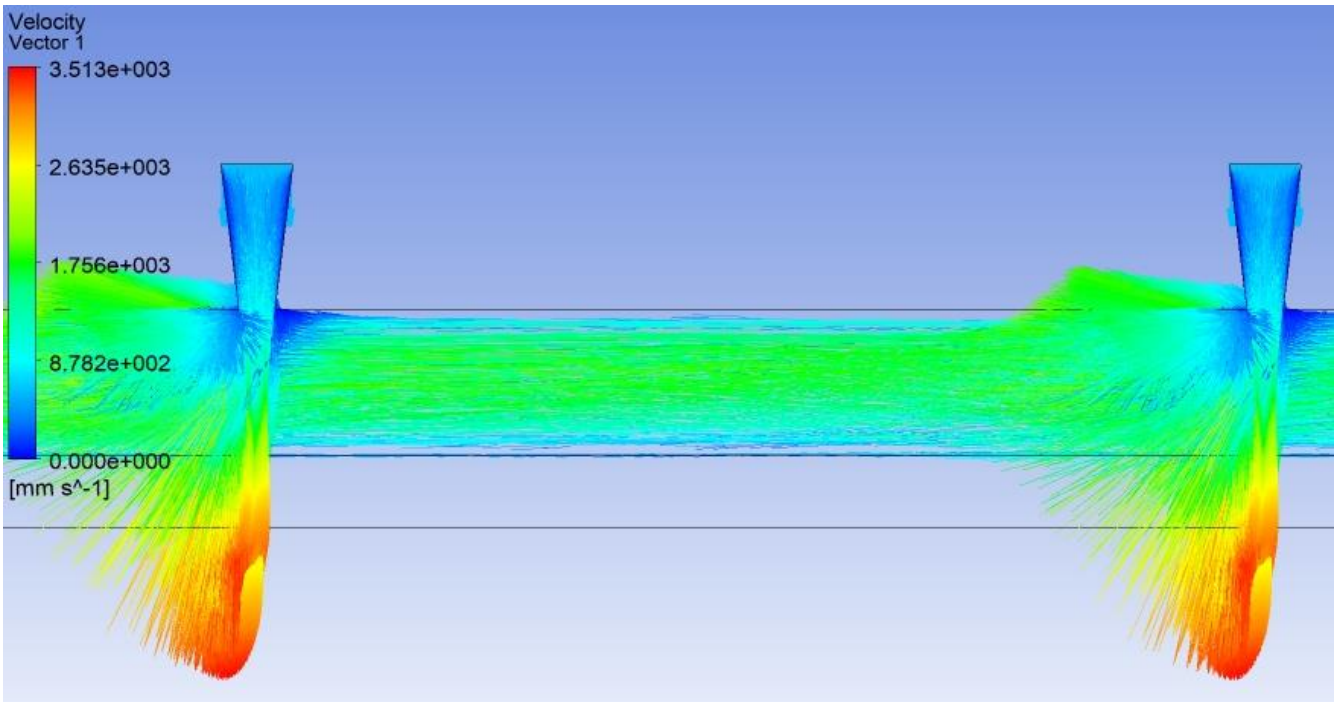

Figure 7.76: Flow Pattern for jet and channel flow for Al_2O_3-water Nano Fluid

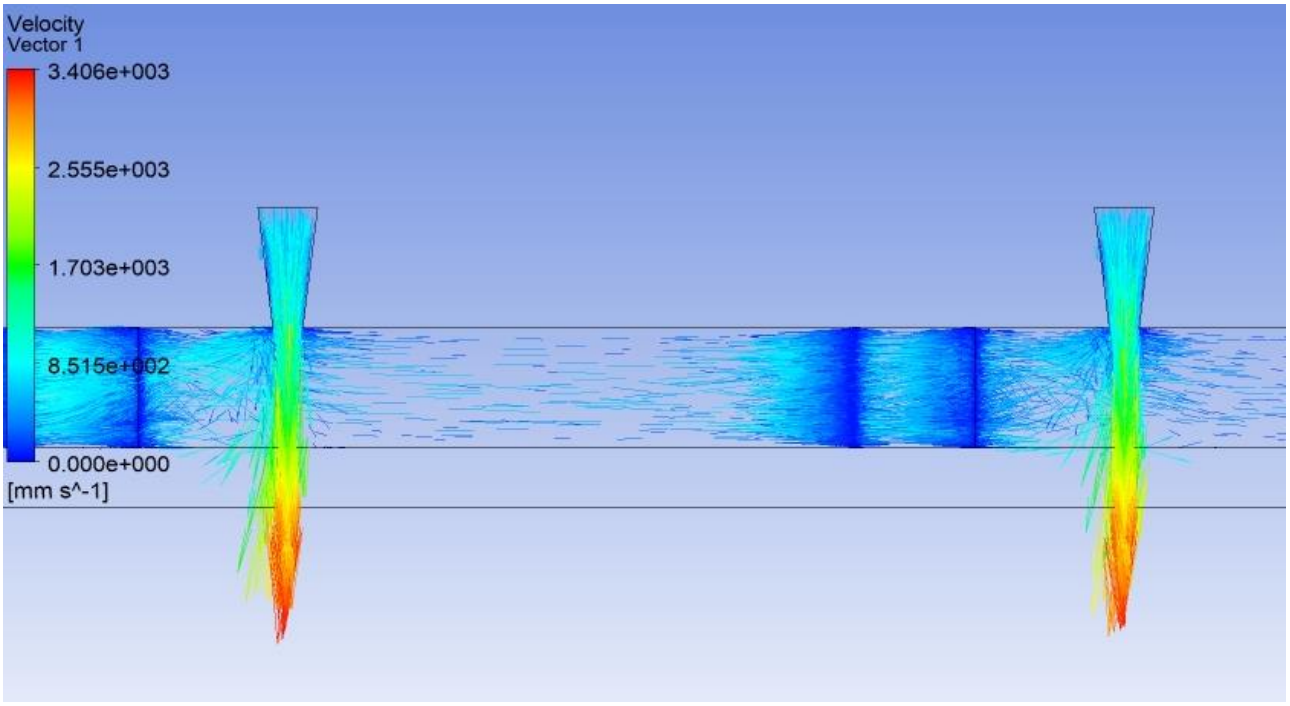

Figure 7.77: Flow Pattern for jet – pillar combination for Al_2O_3-water Nano Fluid

Figure 7.76 shows the velocity vector contours in case of channel and jet flow combination. Similarly figure 7.77 shows the flow pattern in the form of velocity vector in case of jet- pillar combination. The minimum and maximum value of velocity vector is shown in the above figures.

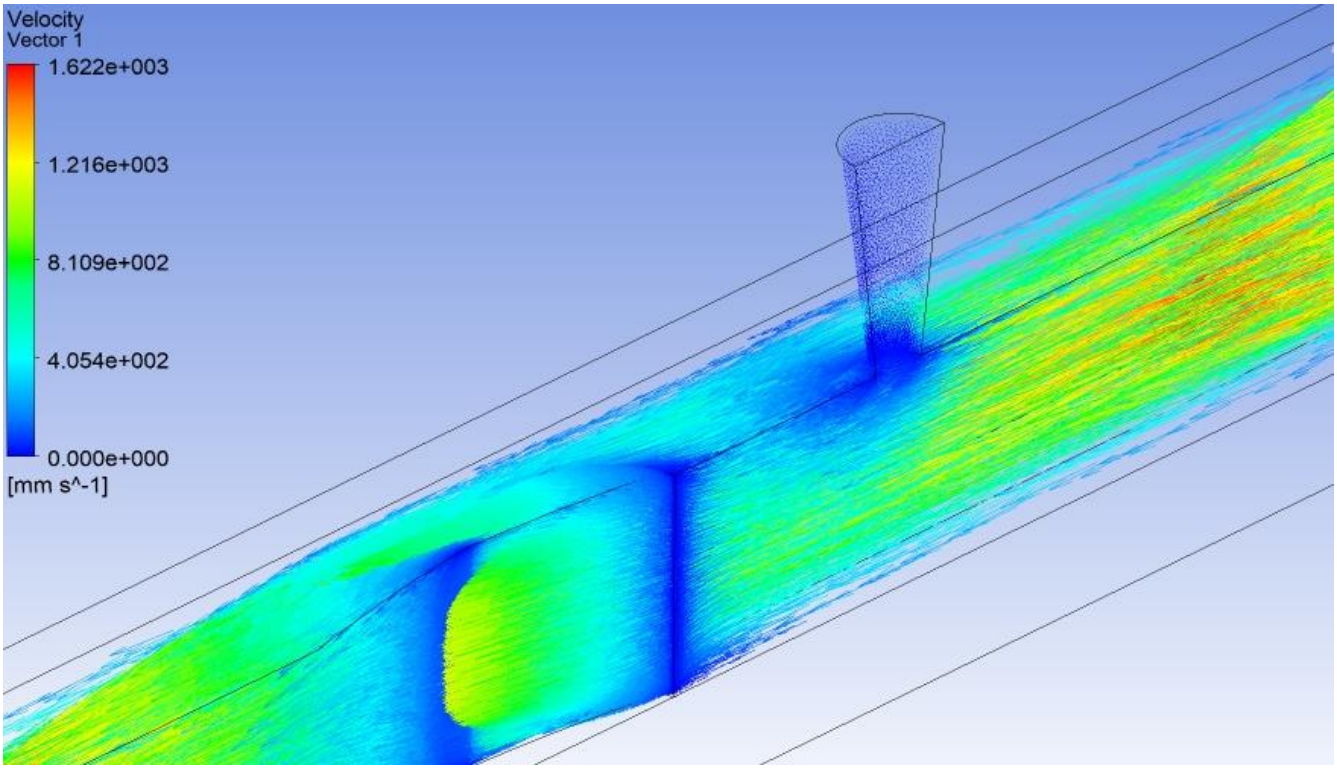

Figure 7.78: Flow Pattern for channel – pillar combination for Al_2O_3-water Nano Fluid

Figure 7.78 shows the velocity vector contours in case of channel - pillar flow combination. Similarly figure 7.79 shows the flow pattern in the form of velocity vector in case of jet- channel -pillar combination. The minimum and maximum value of velocity vector is shown in the figures 7.78 and 7.79.

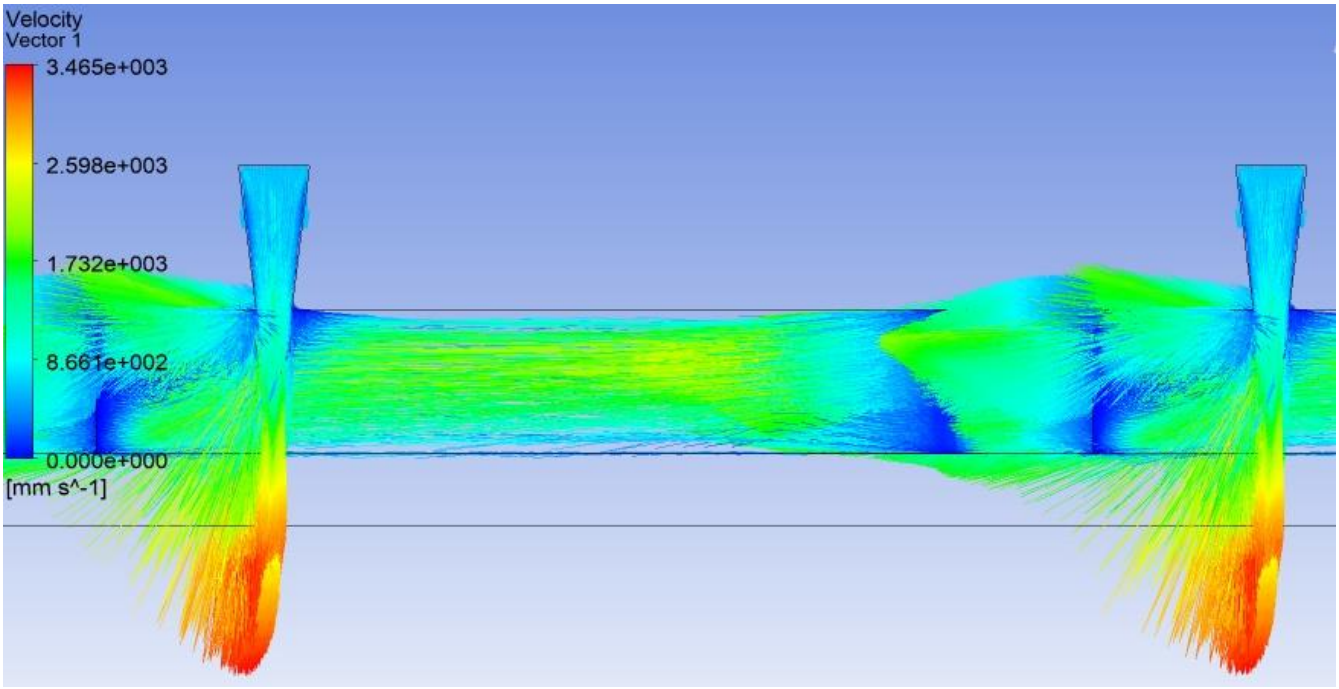

Figure 7.79: Flow Pattern for jet – channel – pillar combination for Al_2O_3-water Nano Fluid

7.11 Streamlines using Al_2O_3 – water Nano Fluid (5%)

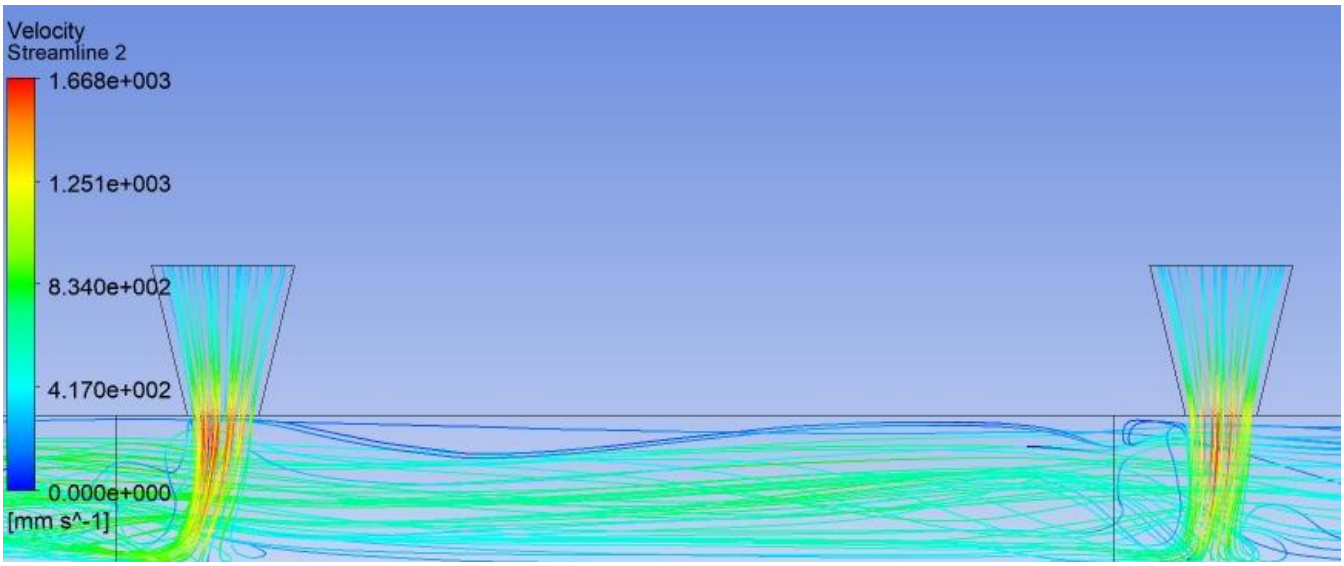

Figure 7.80: Streamlines at Height ratio $\left(\frac{H_{ch}}{D_j}\right) = 1$, Pitch ratio$(\frac{Ph}{D_j})$ = 6 for Al_2O_3-water Nanofluid

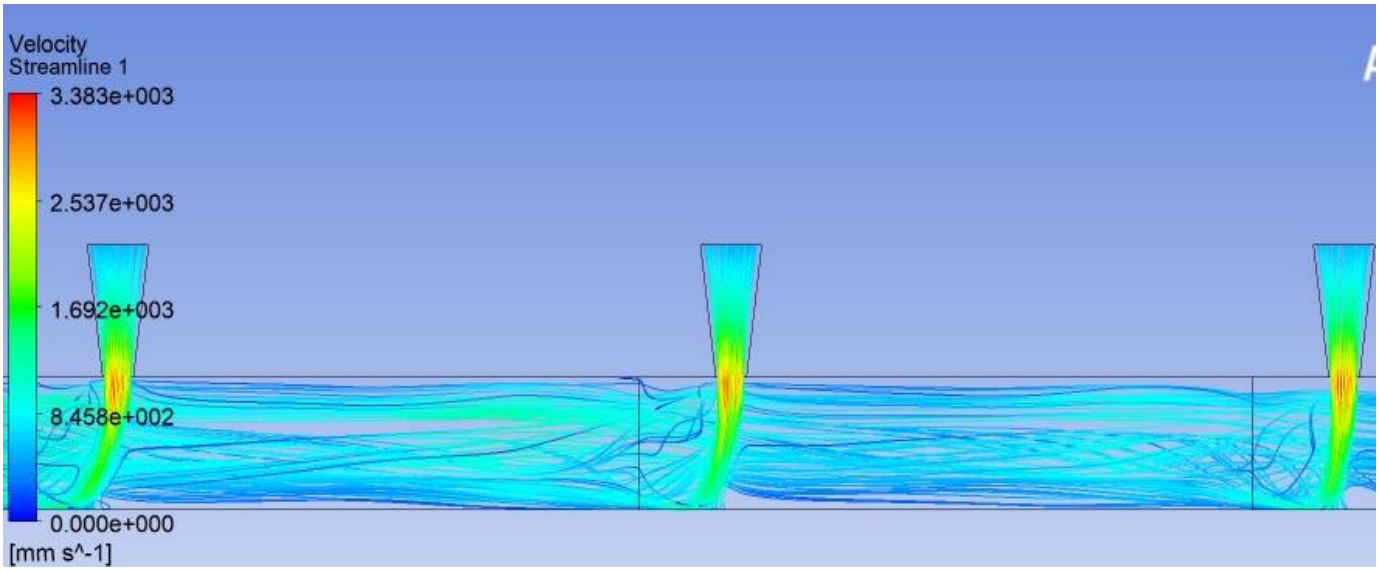

Figure 7.81: Streamlines at Height ratio $\left(\frac{H_{ch}}{D_j}\right) = 2$, Pitch ratio$(\frac{Ph}{D_j})$ = 6 for Al_2O_3-water Nanofluid

Figure 7.80 and 7.81 shows the streamlines contours using Al_2O_3 – water Nano fluid for $\frac{H_{ch}}{D_j} = 1, \frac{Ph}{D_j} = 6$ and $\frac{H_{ch}}{D_j} = 2, \frac{Ph}{D_j} = 6$ respectively.

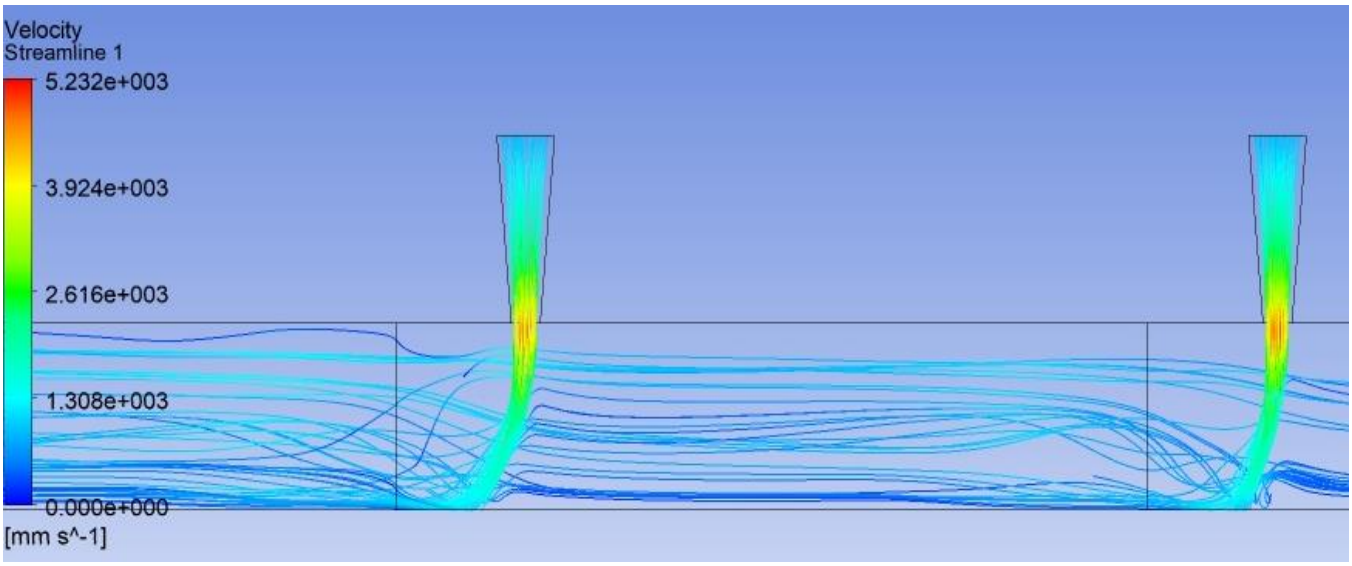

Figure 7.82: Streamlines at Height ratio $\left(\frac{H_{ch}}{D_j}\right) = 3$, Pitch ratio$(\frac{Ph}{D_j}) = 6$ for Al_2O_3-water Nanofluid

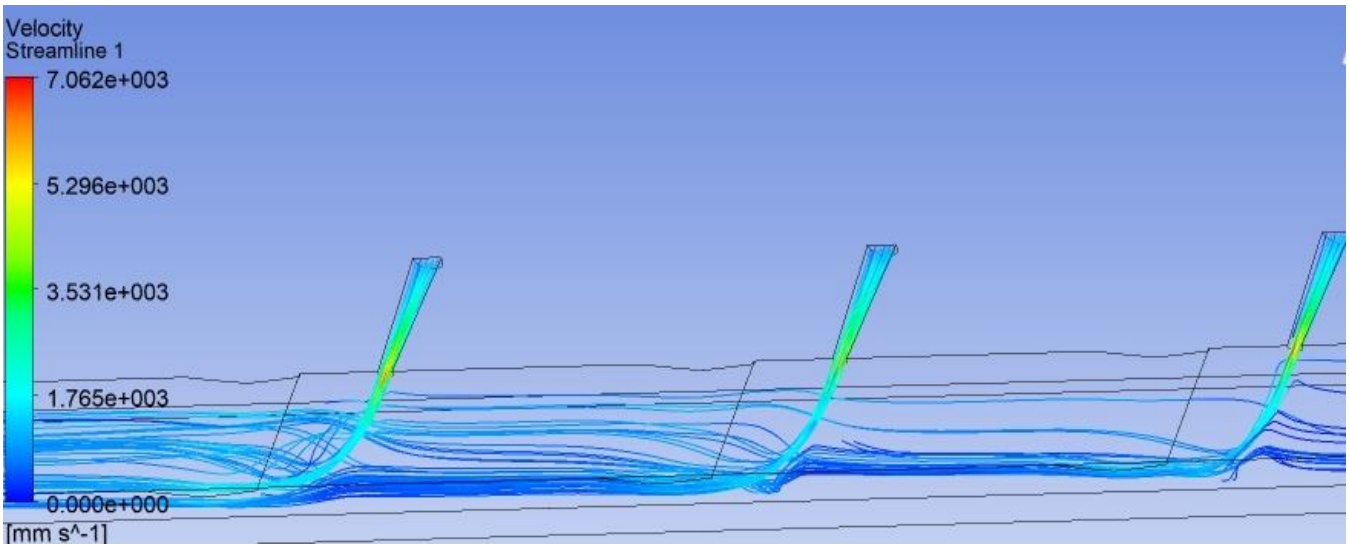

Figure 7.83: Streamlines at Height ratio $\left(\frac{H_{ch}}{D_j}\right) = 4$, Pitch ratio$(\frac{Ph}{D_j}) = 6$ for Al_2O_3-water Nanofluid

Figure 7.82 and 7.83 shows the streamlines contours using Al_2O_3 – water Nano fluid for $\frac{H_{ch}}{D_j} = 3, \frac{Ph}{D_j} = 6$ and $\frac{H_{ch}}{D_j} = 4, \frac{Ph}{D_j} = 6$ respectively.

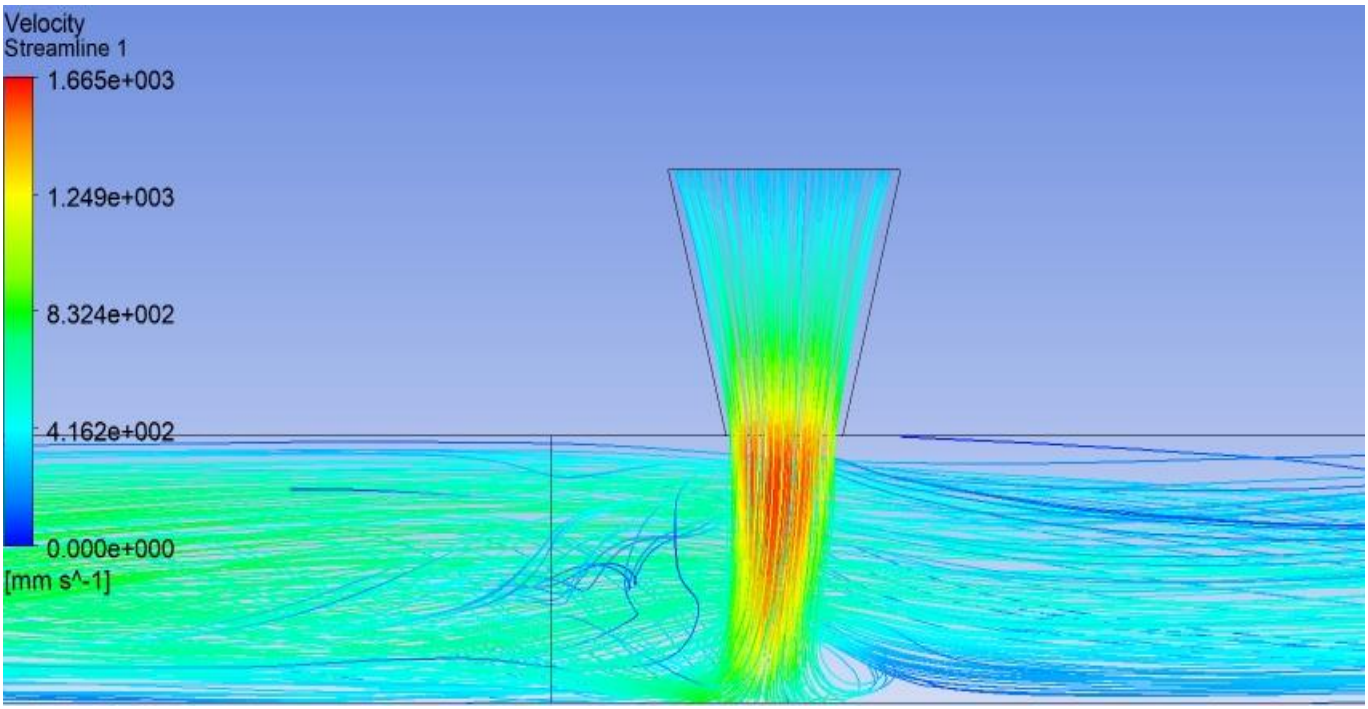

Figure 7.84: Streamlines at Height ratio $\left(\frac{H_{ch}}{D_j}\right) = 1$, Pitch ratio$\left(\frac{Ph}{D_j}\right) = 8$ for Al_2O_3-water Nanofluid

Figure 7.84 and 7.85 shows the streamlines contours using Al_2O_3 – water Nano fluid for $\frac{H_{ch}}{D_j} = 1, \frac{Ph}{D_j} = 8$ and $\frac{H_{ch}}{D_j} = 2, \frac{Ph}{D_j} = 8$ respectively. Figure 86 and 87 shows the streamlines contours using Al_2O_3 – water Nano fluid for $\frac{H_{ch}}{D_j} = 3, \frac{Ph}{D_j} = 8$ and $\frac{H_{ch}}{D_j} = 4, \frac{Ph}{D_j} = 8$ respectively.

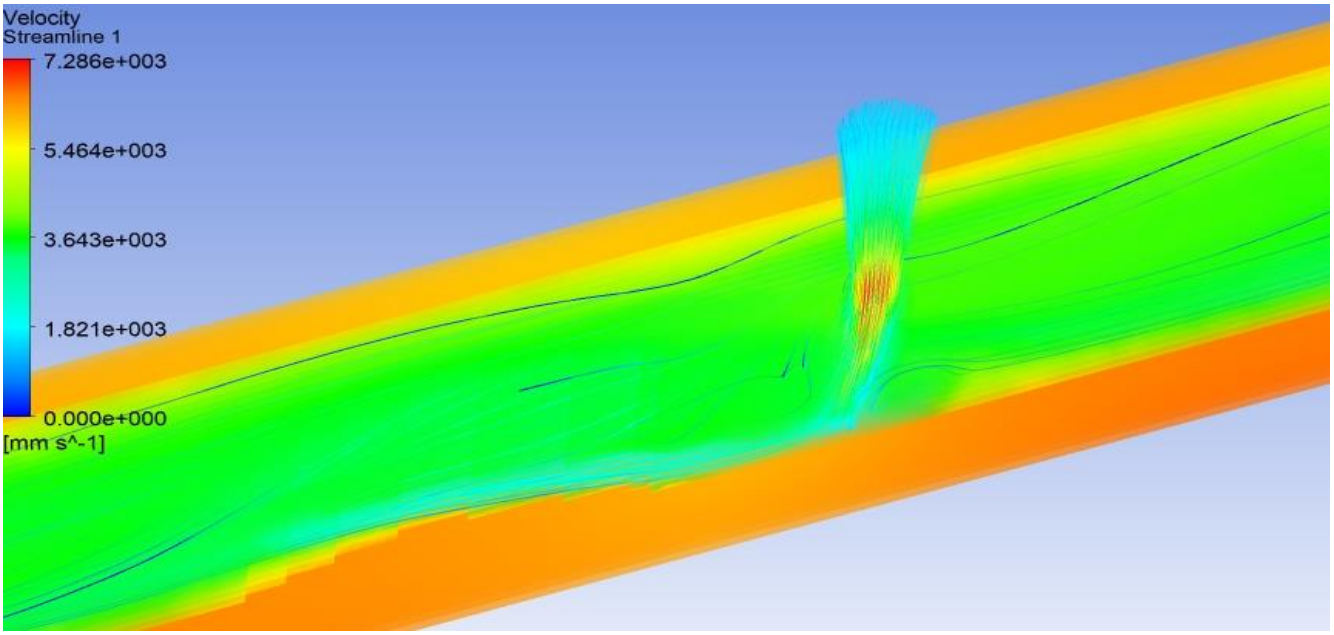

Figure 7.85: Streamlines at Height ratio $\left(\frac{H_{ch}}{D_j}\right) = 2$, Pitch ratio$\left(\frac{Ph}{D_j}\right) = 8$ for Al_2O_3-water Nanofluid

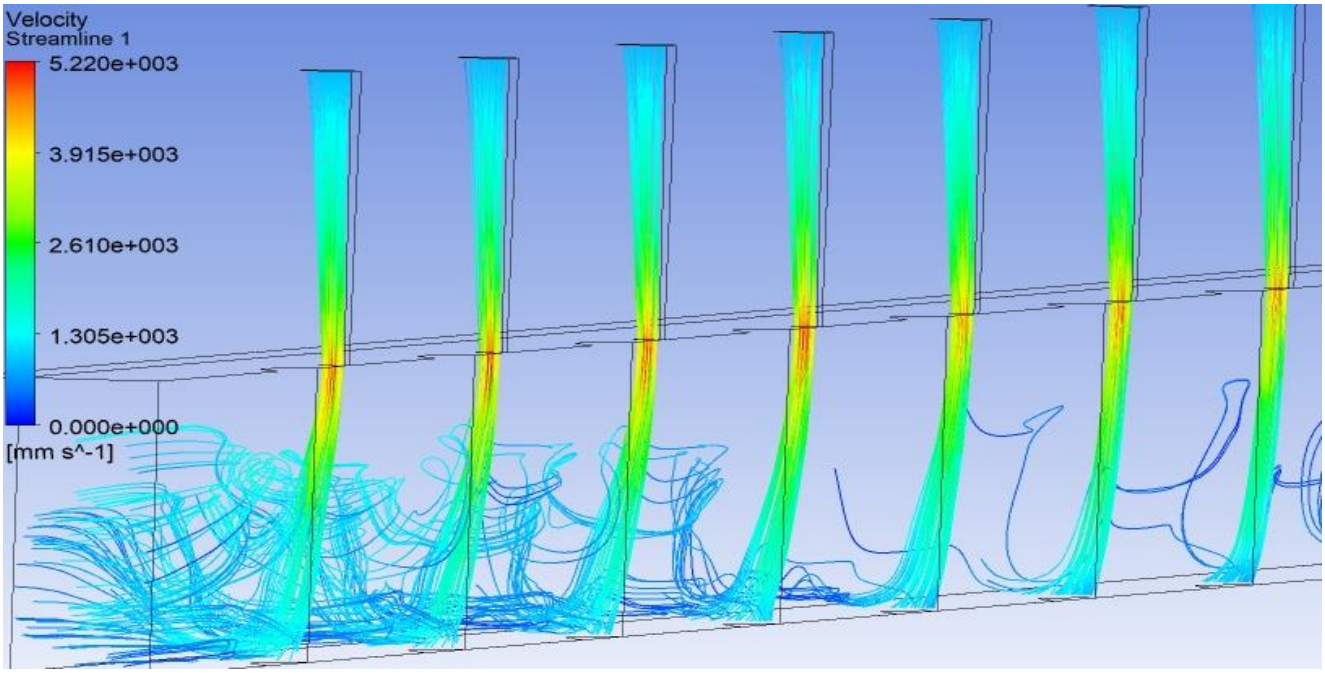

Figure 7.86: Streamlines at Height ratio $\left(\frac{H_{ch}}{D_j}\right) = 3$, Pitch ratio$\left(\frac{Ph}{D_j}\right) = 8$ for Al_2O_3-water Nanofluid

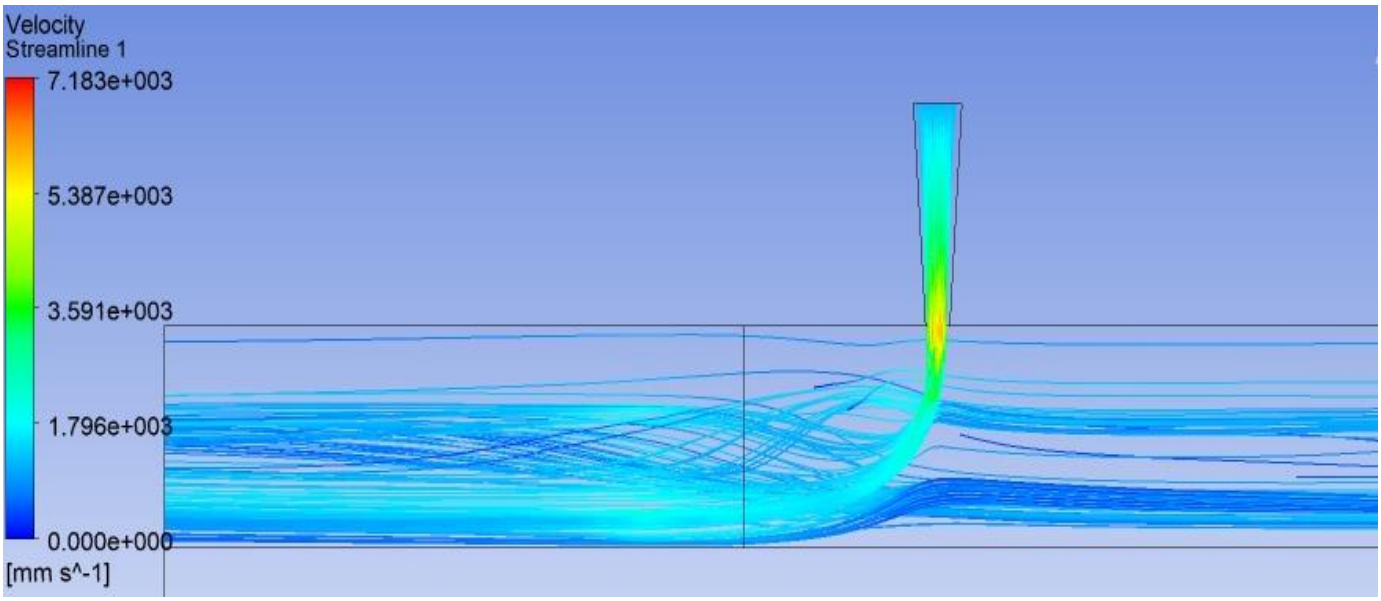

Figure 7.87: Streamlines at Height ratio $\left(\frac{H_{ch}}{D_j}\right) = 4$, Pitch ratio$\left(\frac{Ph}{D_j}\right)$ = 8 for Al_2O_3-water Nanofluid

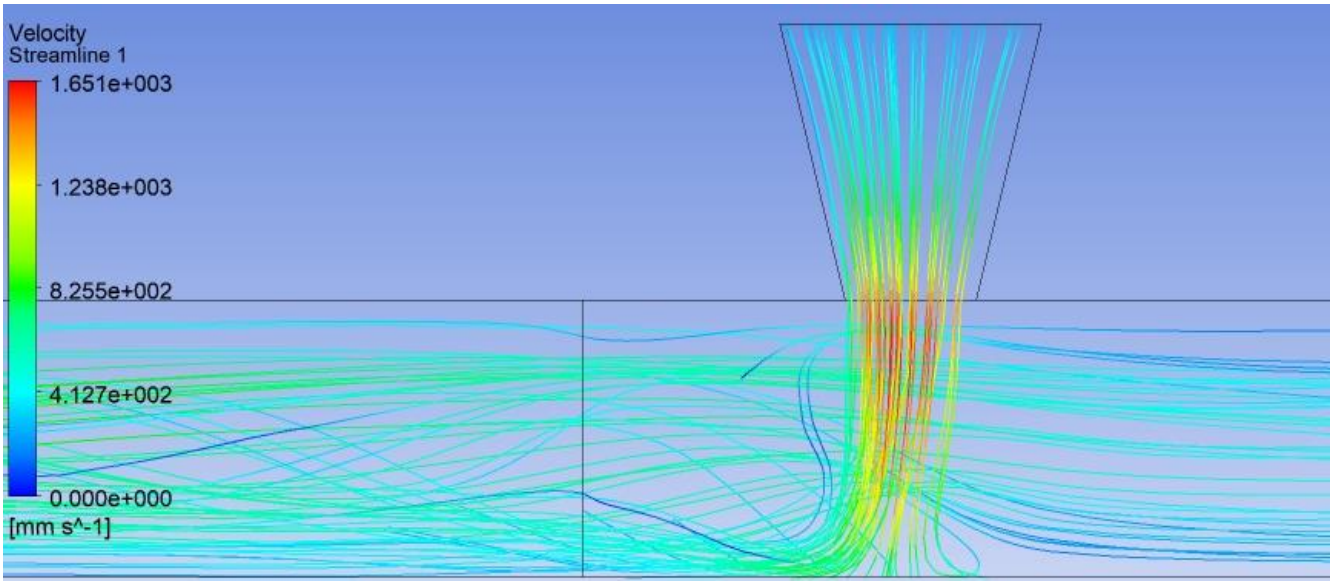

Figure 7.88: Streamlines at Height ratio $\left(\frac{H_{ch}}{D_j}\right) = 1$, Pitch ratio$\left(\frac{Ph}{D_j}\right)$ = 10 for Al_2O_3-water Nanofluid

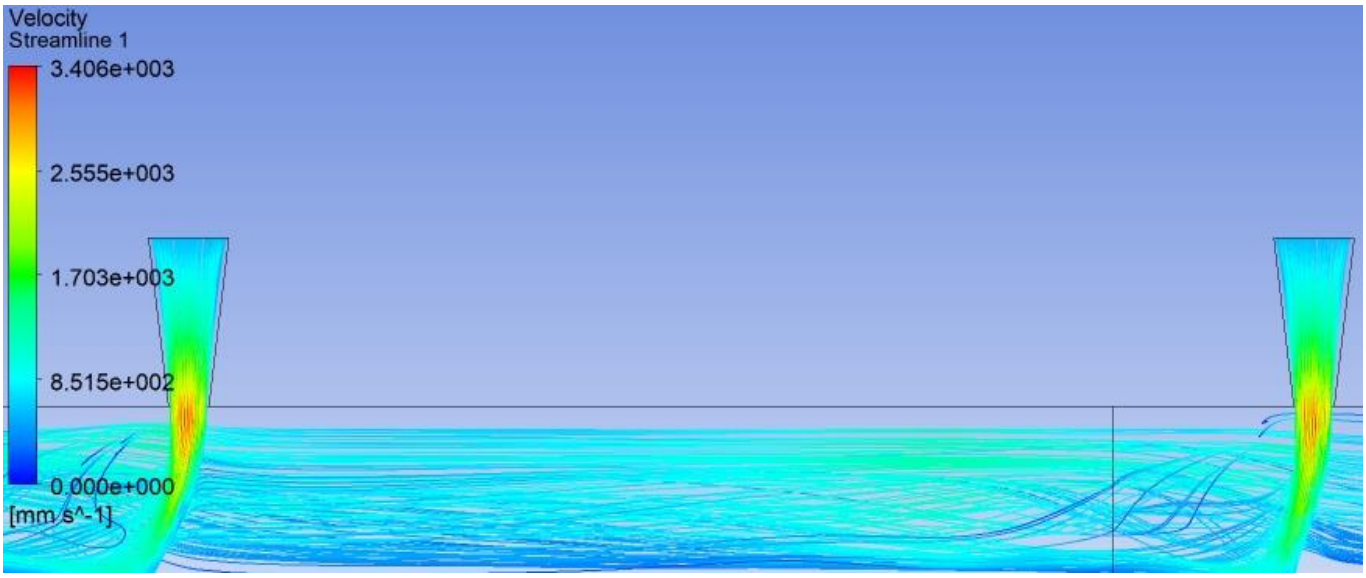

Figure 7.89: Streamlines at Height ratio $\left(\frac{H_{ch}}{D_j}\right) = 2$, Pitch ratio$\left(\frac{Ph}{D_j}\right)$ = 10 for Al_2O_3-water Nanofluid

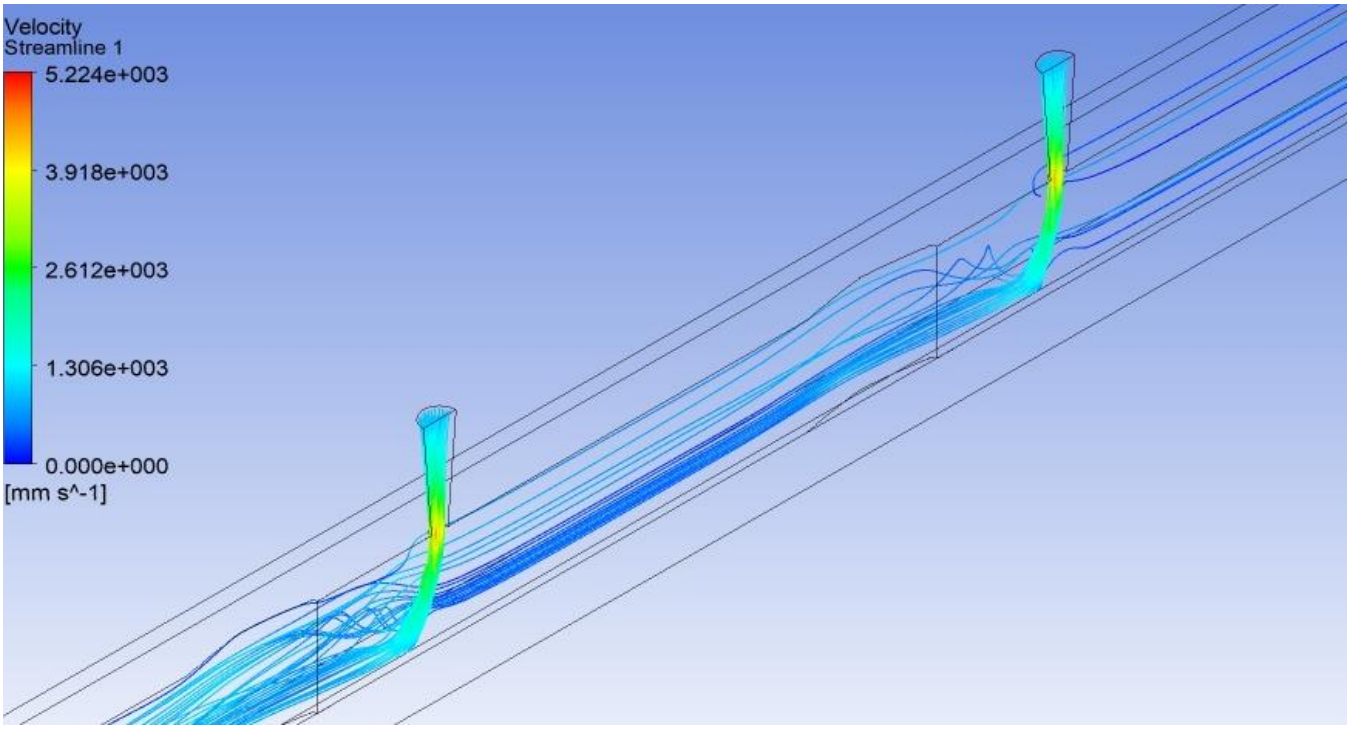

Figure 7.90: Streamlines at Height ratio $\left(\frac{H_{ch}}{D_j}\right) = 3$, Pitch ratio$\left(\frac{Ph}{D_j}\right)$ = 10 for Al_2O_3-water Nanofluid

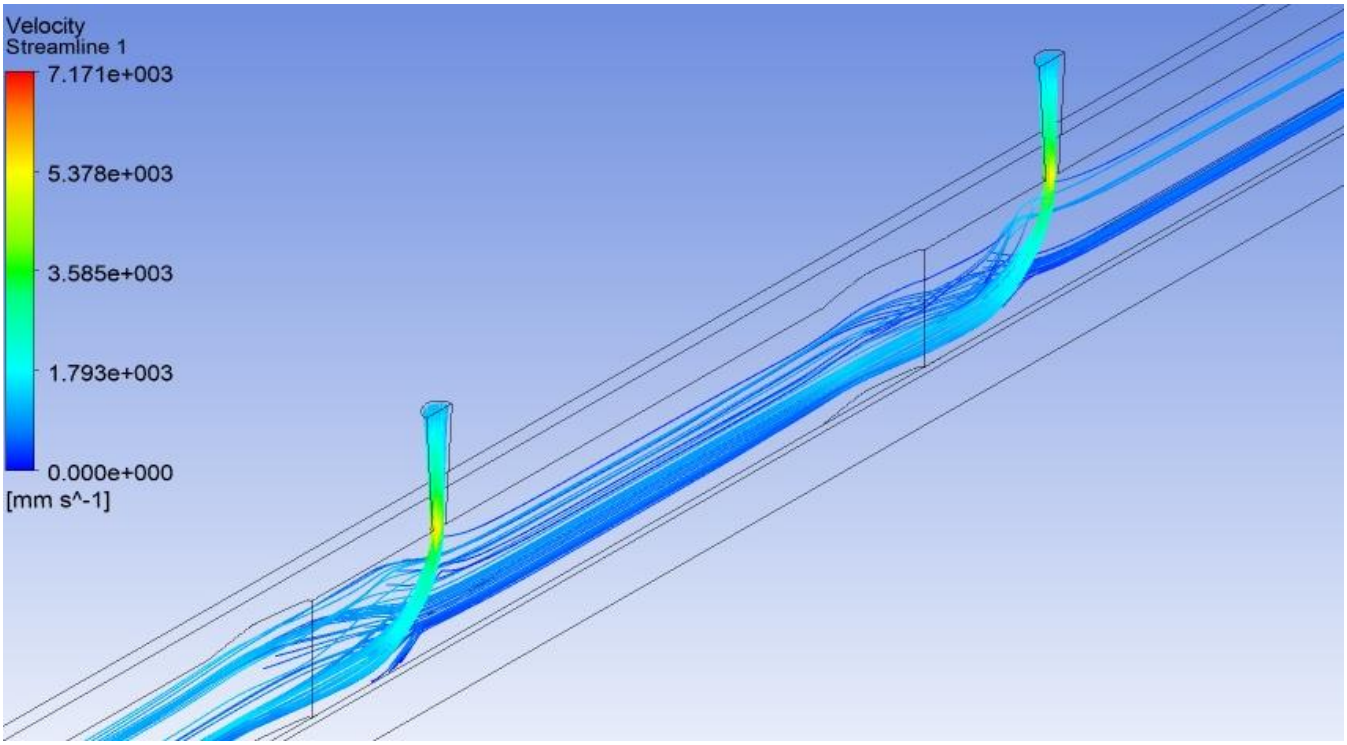

Figure 7.91: Streamlines at Height ratio $\left(\frac{H_{ch}}{D_j}\right) = 4$, Pitch ratio$(\frac{Ph}{D_j})$ = 10 for Al_2O_3-water Nanofluid

Figure 7.88 and 7.89 shows the streamlines using Al_2O_3 – water Nano fluid for $\frac{H_{ch}}{D_j} = 1, \frac{Ph}{D_j}$ = 10 and $\frac{H_{ch}}{D_j} = 2, \frac{Ph}{D_j}$ = 10 respectively. The minimum and maximum value of velocity vector is shown in the above figures. Figure 7.90 and 7.91 shows the flow pattern contours using Al_2O_3 – water Nano fluid for $\frac{H_{ch}}{D_j} = 3, \frac{Ph}{D_j}$ = 10 and $\frac{H_{ch}}{D_j} = 4, \frac{Ph}{D_j}$ = 10 respectively. The minimum and maximum value of velocity vector is shown in the above figures.

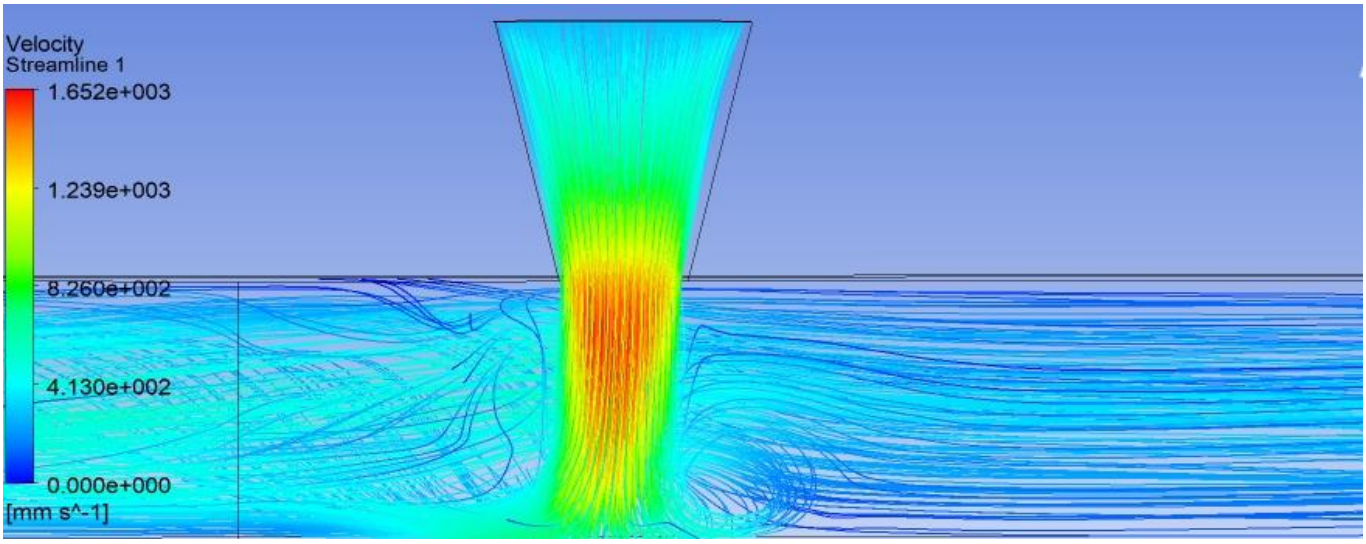

Figure 7.92: Streamlines at Height ratio $\left(\frac{H_{ch}}{D_j}\right) = 1$, Pitch ratio$(\frac{Ph}{D_j})$ = 12 for Al_2O_3-water Nanofluid

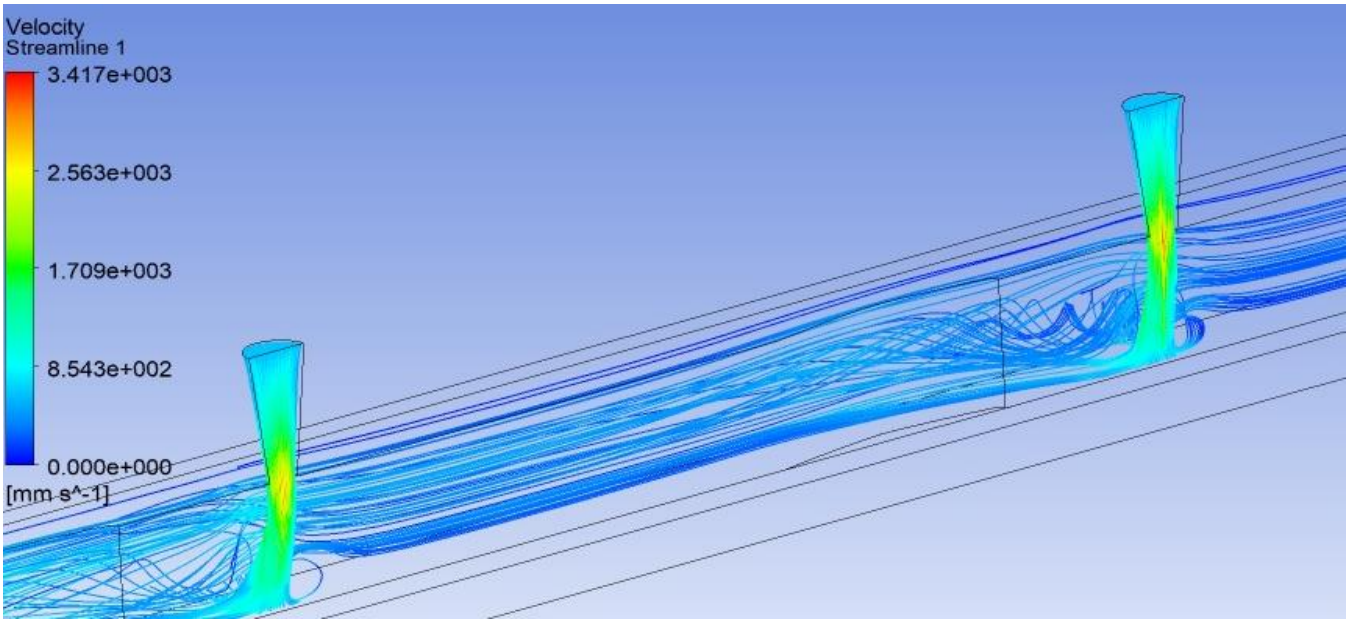

Figure 7.93: Streamlines at Height ratio $\left(\frac{H_{ch}}{D_j}\right) = 2$, Pitch ratio$(\frac{Ph}{D_j})$ = 12 for Al_2O_3-water Nanofluid

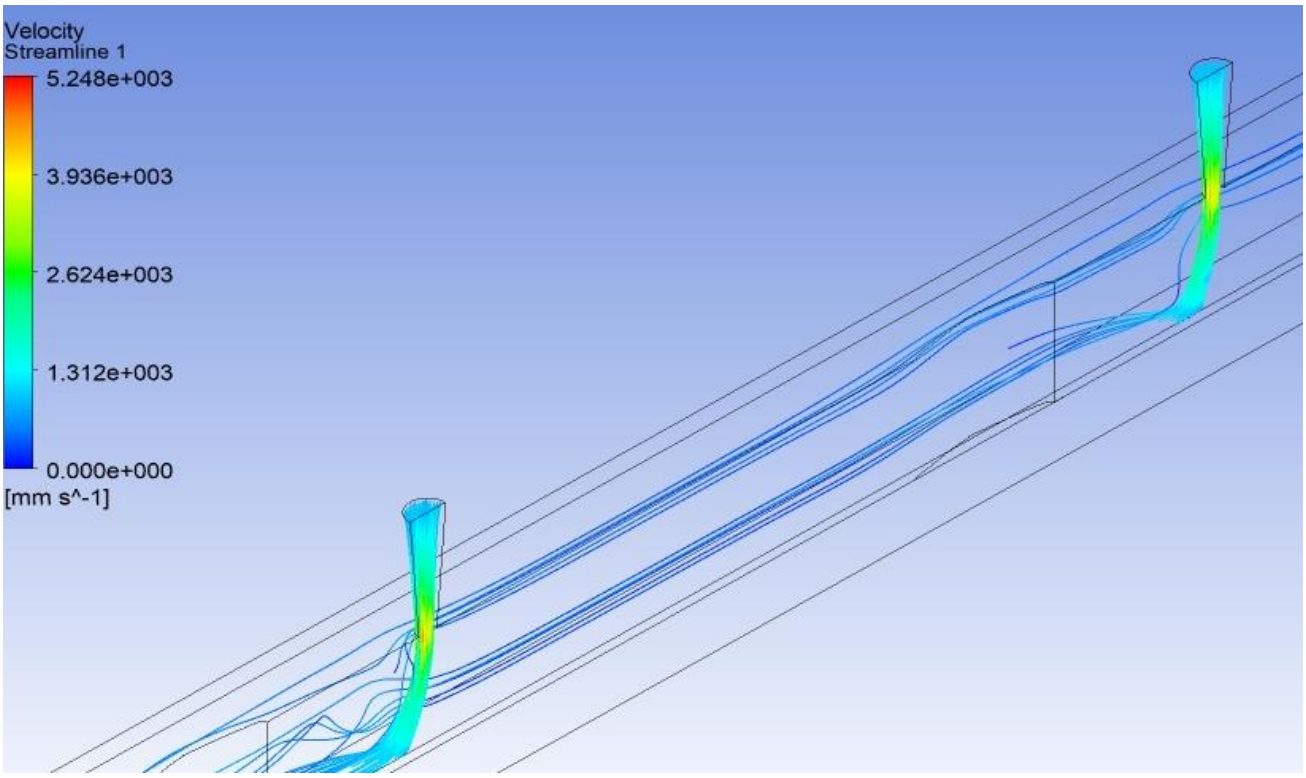

Figure 7.94: Streamlines at Height ratio $\left(\frac{H_{ch}}{D_j}\right) = 3$, Pitch ratio$(\frac{Ph}{D_j})$ = 12 for Al_2O_3-water Nanofluid

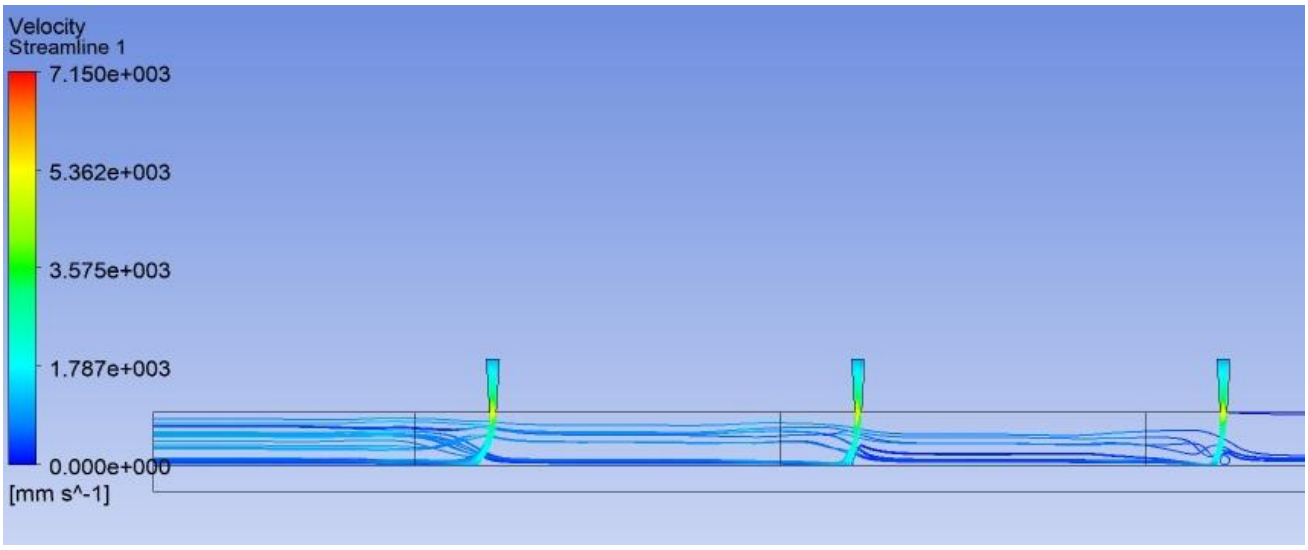

Figure 7.95: Streamlines at Height ratio $\left(\frac{H_{ch}}{D_j}\right) = 4$, Pitch ratio$(\frac{Ph}{D_j})$ = 12 for Al_2O_3-water Nanofluid

Figure 7.92 and 7.93 shows the streamlines using Al_2O_3 – water Nano fluid for $\frac{H_{ch}}{D_j} = 1, \frac{Ph}{D_j} = 12$ and $\frac{H_{ch}}{D_j} = 2, \frac{Ph}{D_j} = 12$ respectively. The minimum and maximum value of velocity vector is shown in the above figures. Figure 94 and 95 shows the flow pattern contours using Al_2O_3 – water Nano fluid for $\frac{H_{ch}}{D_j} = 3, \frac{Ph}{D_j} = 12$ and $\frac{H_{ch}}{D_j} = 4, \frac{Ph}{D_j} = 12$ respectively. The minimum and maximum value of velocity vector is shown in the above figures.

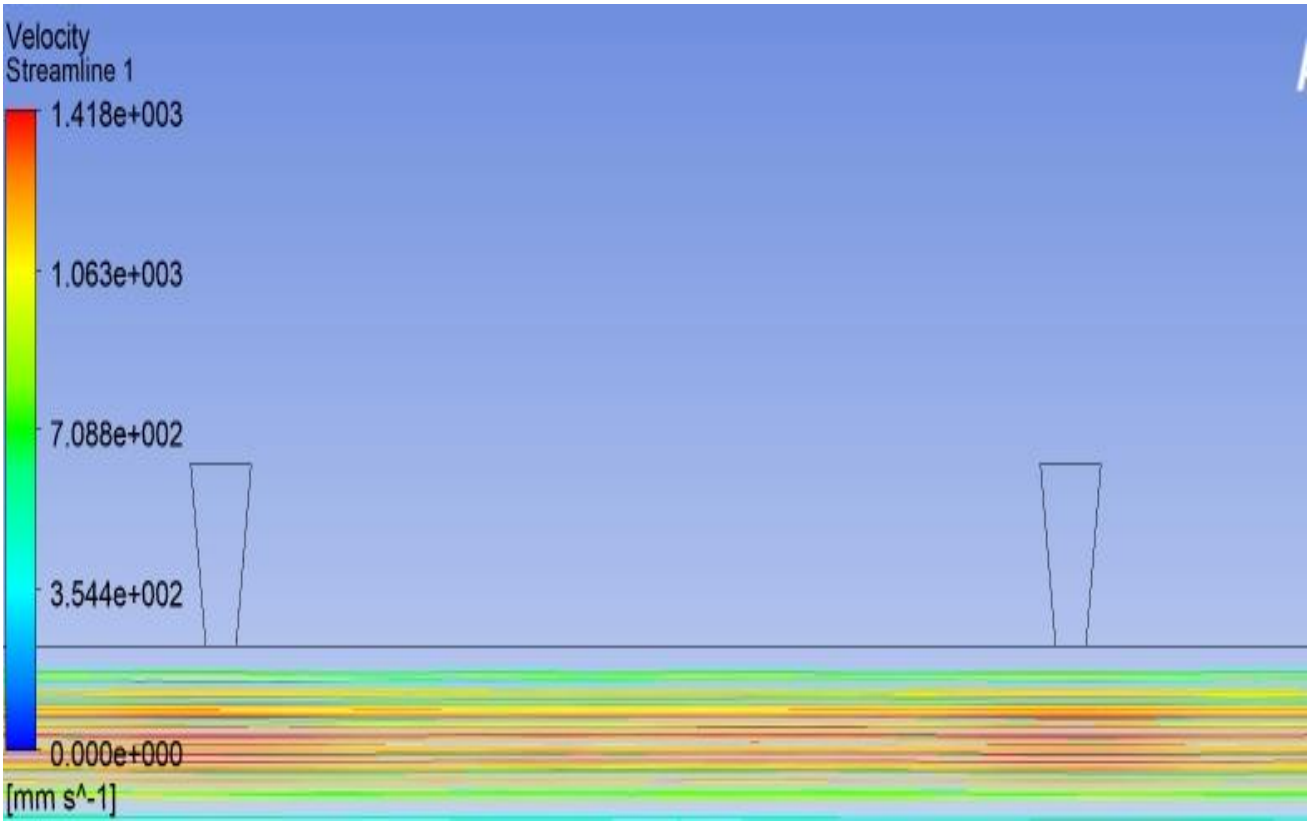

Figure 7.96: Streamlines for channel flow for Al_2O_3-water Nano Fluid

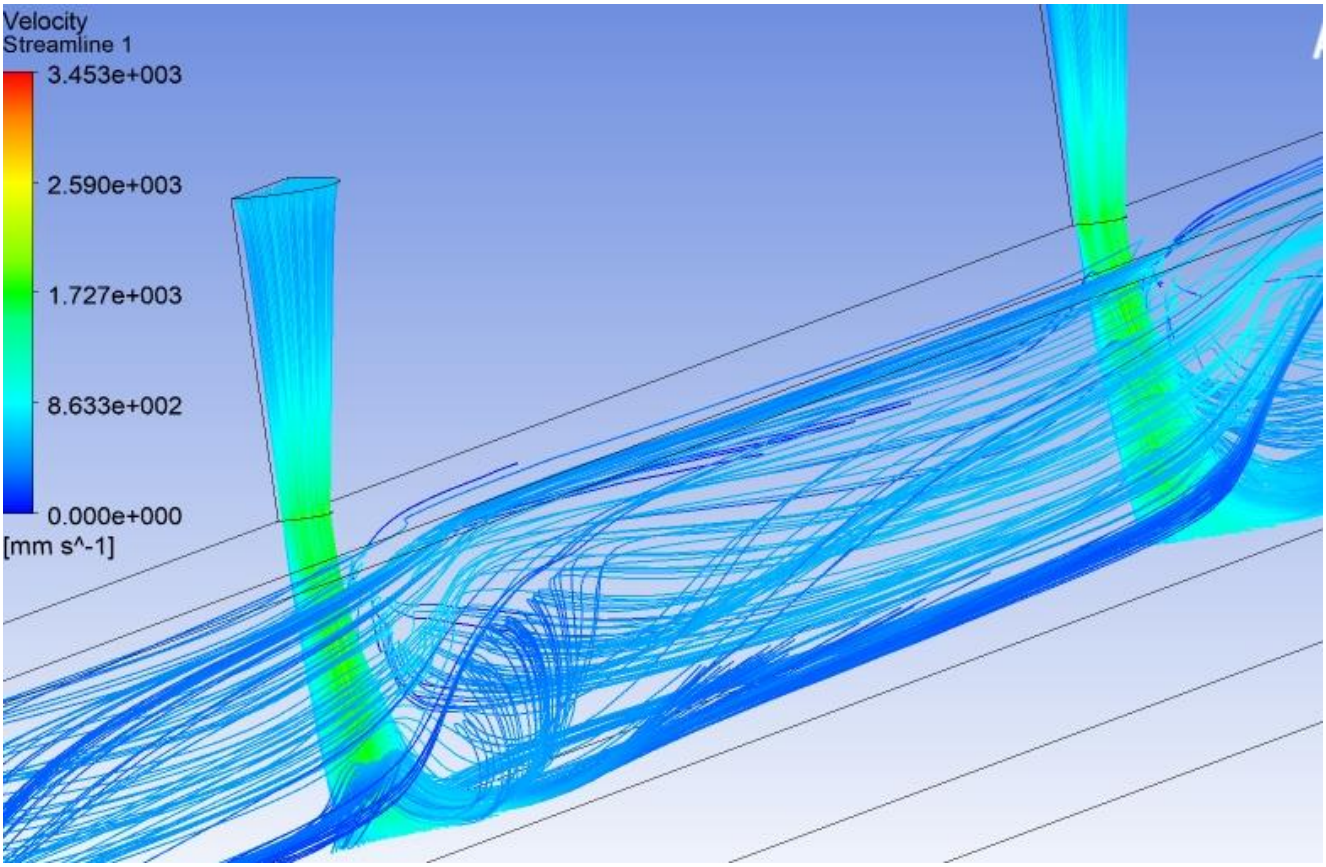

Figure 7.97: Streamlines for jet flow for Al_2O_3-water Nano Fluid

Figure 7.96 shows the streamlines contours in case of channel flow. Similarly figure 7.97 shows the streamlines in case of jet flow. The minimum and maximum value of velocity vector is shown in the above figures.

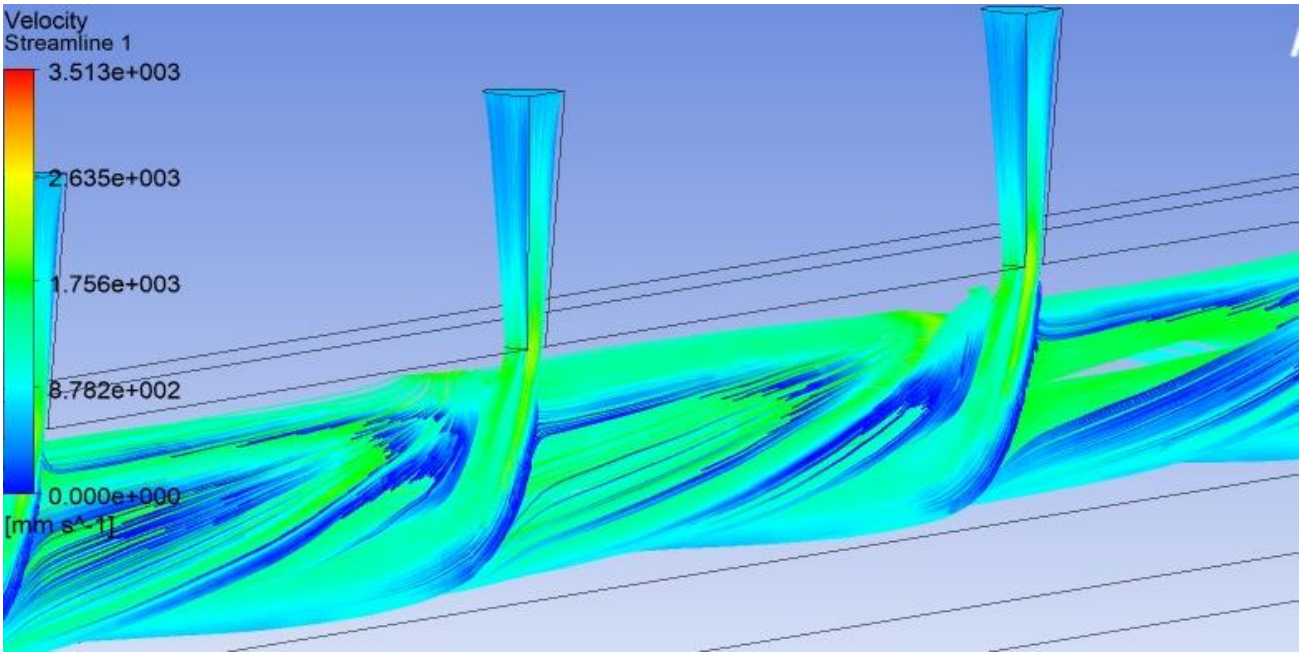

Figure 7.98: Streamlines for jet and channel flow for Al_2O_3-water Nano Fluid

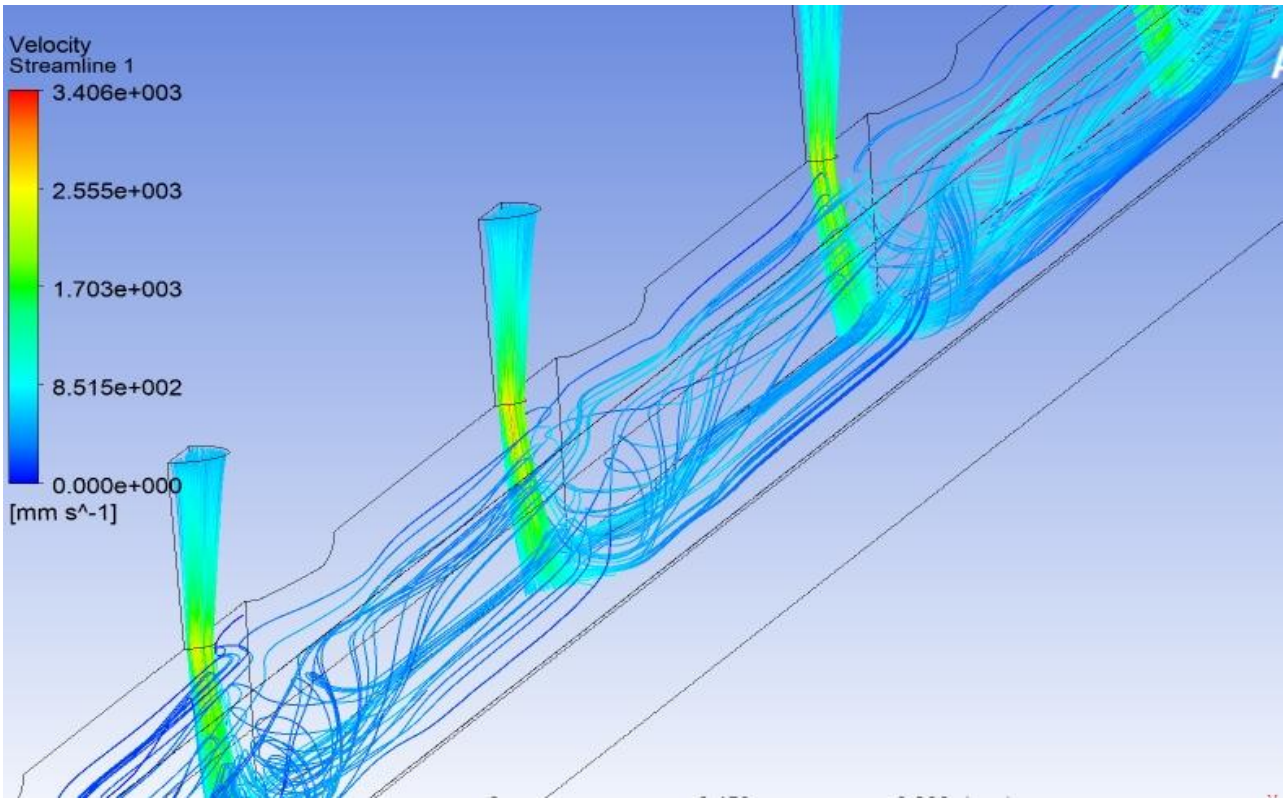

Figure 7.99: Streamlines for jet – pillar combination for Al_2O_3-water Nano Fluid

Figure 7.98 shows the streamlines contours in case of channel and jet flow combination. Similarly figure 7.99 shows the contours of streamlines in case of jet- pillar combination. The minimum and maximum value of velocity vector is shown in the above figures.

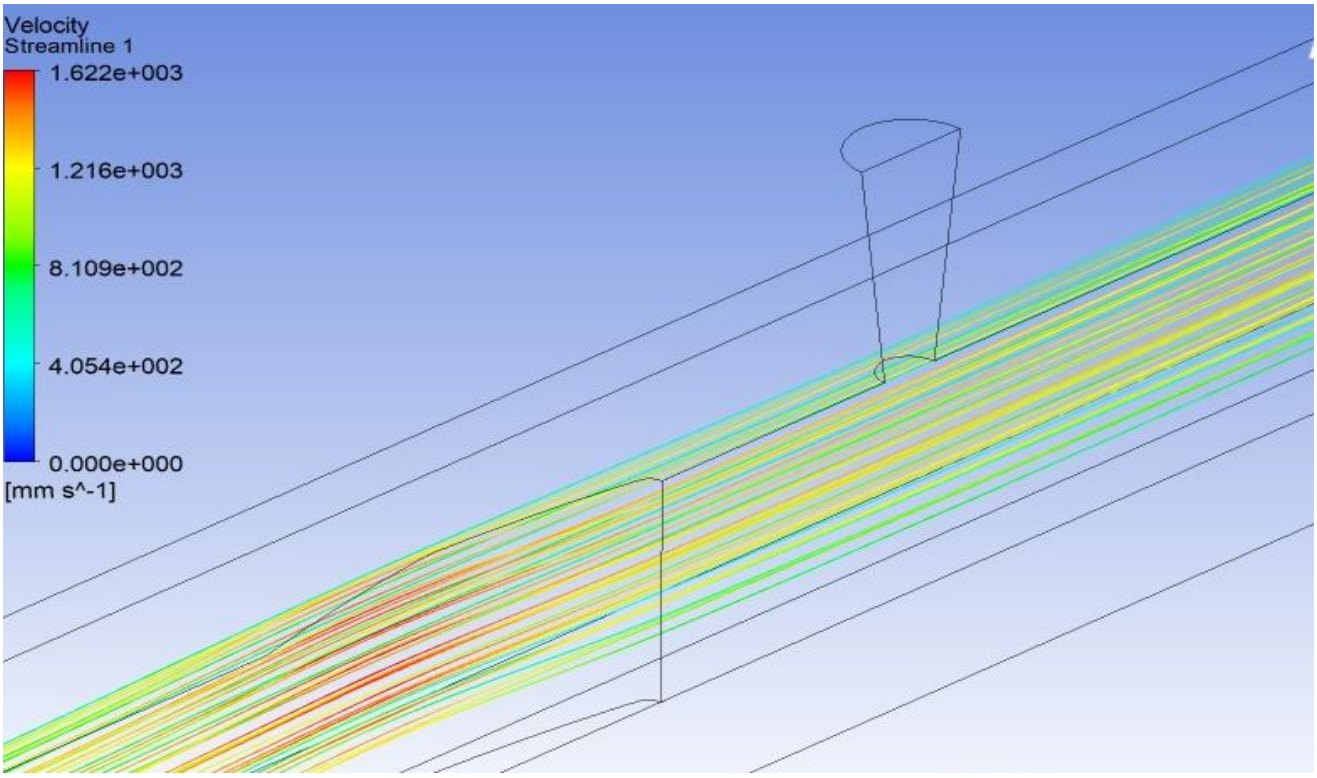

Figure 7.100: Streamlines for channel – pillar combination for Al_2O_3-water Nano Fluid

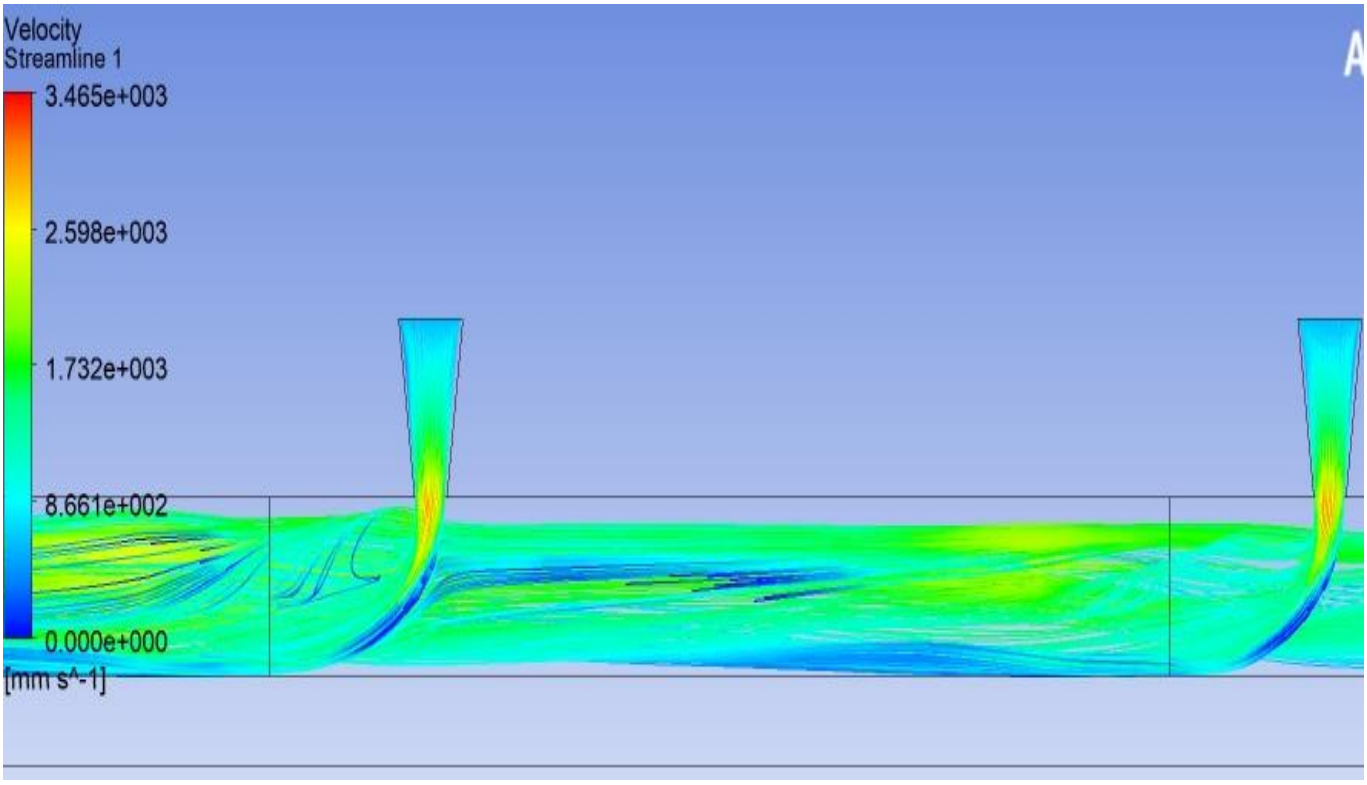

Figure 7.101: Streamlines for jet – channel – pillar combination for Al_2O_3-water Nano Fluid

Figure 7.100 shows the contours of streamlines in case of channel - pillar flow combination. Similarly figure 7.101 shows the streamlines contours in case of jet- channel -pillar combination. The minimum and maximum value of velocity vector is shown in the above figures.

CHAPTER - 8

CONCLUSIONS

A numerical model has been constructed to study and analyze the outcomes of air foil shaped pillars on the accomplishments of a heat based sink with jet impingement technique in micro channel and with Nano fluids.

From the results it has been found that rise in maximum temperature was obtained with height ratio 1 and pitch ratio 10. The drop in pressure was found lowest in case of ratio 1 and pitch ratio 12. Heat transfer coefficient is found highest in case of height ratio 4 and pitch ratio 6. Also the value of Nusselt number is highest with height ratio 1 and pitch ratio 6. Thermal resistance is predicted minimum in case of height ratio 4 and pitch ratio 6. Pumping power has been observed minimum with height ratio 2 and pitch ratio 6. So highest temperature rises and lowest pressure drop has been found with increasing pitch ratio. The channel flow results in the reduction of the jet end results. So a proper selection of parameters is required to augment the heat dissipation.

With the use of water – CuO Nano fluid with 0.5% concentration, the temperature of the substrate base is reduced in differentiation with the pure water case. Maximum reduction in temperature is deduced at Pitch ratio = 6 and Height ratio = 2. Coefficient of heat transfer is increased in case of 0.5% concentration of Nano fluid as compared to the pure water case. Highest surge is noticed at Height ratio = 2 and Pitch ratio =6 combination. Almost 28.2 % enhancement is detected. Nusselt number is also increased in case of water – CuO Nano fluid in differentiation to pure water. Also the highest value of Nu is deduced at Pitch ratio = 6 and Height ratio= 2. Thermal resistance is lower in case of water – CuO Nano fluid as compared to pure water. Maximum reduction in

thermal resistance is detected at Pitch ratio = 6 and Height ratio = 2. Pumping power and drop in pressure is surged in case of water – CuO Nano fluid.

The current investigation suggests a sincere idea for the optimum use of different combinations of jet-channel- pillars of air foil shape with the application of CuO –water base Nano fluids. Power required to drive the fluid flow and the thermal resistance are two important parameters for the optimum combinations for use. At the higher side of the former, lower values are found for the other one. So the combination having minimum value of both can be chosen for further study also. Coefficient of heat exchange and Nusselt number is more for jet-pillar and jet-channel- airfoil pillars arrangement. So jet- pillar arrangement with Nano fluid can be a better option for the heat dissipation.

Using water with increase in height ratio, rise in maximum temperature decreases. Maximum 44 % reduction in base temperature is noticed with the use of airfoil pillars. Same trend is observed in case of thermal resistance.14 % reduction in resistance is marked. Increasing trend is noticed in drop in pressure with increase in Height ratio. Same type of pattern is detected in case of pumping power. Coefficient of heat transfer has been increased with increase in Height ratio. 24% enhancement is noticed in heat transfer coefficient with the use of pillars. In case of Nusselt number, with advancement in Height ratio, it also shows increasing trend. Maximum 16 % improvement in Nusselt number is noticed.

From the comparative study of water and Nano fluid with 1% concentration Reverse trend is observed between Height ratio and Temperature of the base. With the augmentation in Height ratio the temperature rise reduces both in case of water as well as Nano fluid. However, Nano fluid case has been found to be more effective. Direct proportion has been noticed in between heat exchange coefficient and Height ratio for a particular value of pitch ratio. In the case of Nano fluid higher

augmentation has been found in the value of heat transfer coefficient in differentiation to pure water. Indirect proportion has been accounted in between Nusselt number and Height ratio for a particular value of Pitch ratio. However, when differentiated with water higher value of Nusselt number has been accounted.

This work also provides a suitable usage of jet – channel and pillar combination using Al_2O_3 – water Nano fluid with 5 % concentration. So the combination has been studied for different parameters like temperature, pressure, heat transfer coefficient etc. For the maximum value of pumping power, minimum value of thermal resistance has been found. The results are found in a similar fashion with the CuO- water Nano fluid.

The model can be designed for the optimum values of parameters to increase the performance. For the future research this type of arrangement with Nano fluids can be of more importance. Some important points are as follows.

1. With an increase in the pitch ratio, rise in temperature is detected. This is because of the decrease in the number of impingements which results due to increase in the pitch ratio.

2. Increase in pitch ratio from 6 to 12 also results in decrease in the overall pressure drop from jet inlet to the channel outlet. But due to the frictional losses overall pressure drop has a tendency to increase.

3. With an increase in the pitch ratio, convection heat transfer is reduced. The reason for the same is increase in the boundary layer thickness. Because with an increase in the pitch ratio, the counting of jets decreases. And hence the wall jet gets more space to spread in the radial direction. And finally the interaction with the other jets decreases and hence temperature of the substrate increases.

4. Another important aspect of the increase in the pitch ratio is that less space will be there and the counting of airfoil pillars for a particular space decreases. And the same thing happens with the number of nozzles. Due to the less number of pillars, loss of momentum will be less for the heat sink. This would finally result in lower pressure drop in case of channel flow.

5. Another important advantage of airfoil pillars is that it leads to boundary layer bifurcation. Due to this reason the two combinations (Jet- channel- airfoil pillars and Jet- airfoil pillars) results in less increase in the temperature. And this results in high convection heat transfer. For the jet – pillar combination heat transfer coefficient is found to be highest because of the more distractions.

6. Impingement of jet leads to the formation of vortices.

7. Airfoil pillars results in the separation of the vortices. However, channel flow decreases the vortices.

8. Nanofluid results in increase in the convection heat transfer because of the increase in the thermal conductivity.

9. Also the effect on the overall pressure drop in not found to be significant in case of Nanofluid. Due to this thermal uniformity is achieved.

10. The thermophysical properties of Nanofluid plays an important role in decreasing the temperature of the base and attainment of the uniformity.

11. Thermal dispersion of the Nanofluid is the main reason for the decrease in the thermal resistance of the channel.

SCOPE FOR FUTURE WORK

Here in the present analysis jet impingement heat sink with microchannel with air foil shape of pillars has been studied for water, water based CuO and Al_2O_3 Nano fluids. The recommendations for future work are as follows.

- The study can be performed other shape of pillars and can be optimized for best one.
- The analysis can be performed for other Nano fluids as well.
- The study can be utilized for different concentrations also.
- The study can be used for other dimensionless variables.

REFERENCES

[1] Tuckerman and Pease, (1981) High-performance Heat Sinking for VLSI, IEEE Electron Device Letters 2 (5) 126-129.

[2] R.J. Phillips, L. Glicksman, R. Larson. (1987), "Forced-convection, Liquid-cooled, Micro channel Heat Sinks for High power Density Microelectronics", Proc. Intl. Symp. Cooling Technology for Electronic Equipment, Honolulu, Hawaii, pp. 227-248

[3] J. Pfahler, J. Harley, H. Bau. (1990), "Liquid Transport in Micron and Submicron Channels, Sensors and Actuators", Vol. A21-A23, pp. 431-434

[4] Chapman, C. L., Lee, S., and Schmidt, B. L. (n.d.). (1994) Thermal performance of an elliptical pin fin heat sink. Proceedings of 1994 IEEE/CHMT 10th Semiconductor Thermal Measurement and Management Symposium (SEMI-THERM).

[5] M. Richter, P. Woias, D. Weiβ. (1997), "Micro channels for applications in liquid dosing and flow-rate measurement", Sensors and Actuators, Vol. A62, pp. 480-483

[6] Lee and Vafai (1999). Comparative analysis of jet impingement and microchannel cooling for high heat flux applications. International Journal of Heat and Mass Transfer, 42(9), 1555–1568.

[7] Brignoni and Garimella (1999). Experimental optimization of confined air jet impingement on a pin fin heat sink. IEEE Transactions on Components and Packaging Technologies, 22(3), 399–404.

[8] Seo Young Kim, Jae-Mo Koo, Andrey V. (2001). Effect of Anisotropy in Permeability and Effective Thermal Conductivity On Thermal Performance of an Aluminum Foam Heat Sink. Numerical Heat Transfer, Part A: Applications, 40(1), 21–36.

[9] Kim and Webb (2003) "Thermal Performance Analysis of Fan-Heat Sinks for CPU Cooling." Proceedings of the ASME 2003 International Mechanical Engineering Congress and Exposition. Heat Transfer, Volume 2. Washington, DC, USA. November 15–21, 2003. pp. 235-243. ASME.

[10] Kandlikar and Grande (2003), "Evolution of micro channel flow passages-thermo hydraulic performance and fabrication technology", Heat Transfer Eng., 24 (1), 2003, pp. 3-17

[11] E.N. Wang, L. Zhang, L. Jiang, J.M. Koo, J.G. Maveety, E.A. Sanchez, K.E. Goodson, T.W. Kenny, (2004) Micro machined Jets for Liquid Impingement Cooling of VLSI Chips, Journal of Microelectromechanical Systems 13 (5) 833–842.

[12] Chein and Huang (2005), Analysis of micro channel heat sink performance using Nano fluids, Applied thermal engineering, *25*(17-18), 3104-3114.

[13] E.N. Wang, L. Zhang, L. Jiang, J.M. Koo, J.G. Maveety, E.A. Sanchez, K.E. Goodson, T.W. Kenny, (2004) Micro machined Jets for Liquid Impingement Cooling of VLSI Chips, Journal of Microelectromechanical Systems 13 (5) (2004) 833–842.

[14] Shah, A., Sammakia, B. G., Srihari, H., and Ramakrishna, K. (2004). A Numerical Study of the Thermal Performance of an Impingement Heat Sink—Fin Shape Optimization. IEEE Transactions on Components and Packaging Technologies, 27(4), 710–717.

[15] Seo Young Kim, Myung Ho Lee, and Kwan-Soo Lee. (2005). Heat removal by aluminum-foam heat sinks in a multi-air jet impingement. IEEE Transactions on Components and Packaging Technologies, 28(1), 142–148.

[16] Li, H.-Y., Chao, S.-M., and Tsai, G.-L. (2005). Thermal performance measurement of heat sinks with confined impinging jet by infrared thermography. International Journal of Heat and Mass Transfer, 48(25-26), 5386–5394.

[17] Mahalingam and Glezer (2005). Design and Thermal Characteristics of a Synthetic Jet Ejector Heat Sink. Journal of Electronic Packaging, 127(2), 172.

[18] Chein and Huang (2005). Analysis of microchannel heat sink performance using Nano fluids. Applied Thermal Engineering, 25(17-18), 3104–3114.

[19] Li, H.-Y., Chiang, M.-H., and Chen, K.-Y. (2007). Performance Analysis of Pin-Fin Heat Sinks with Confined Impingement Cooling. IEEE Transactions on Components and Packaging Technologies, 30(3), 383–389.

[20] Li, H.-Y., Chiang, M.-H., & Chen, K.-Y. (2007). Performance Analysis of Pin-Fin Heat Sinks with Confined Impingement Cooling. IEEE Transactions on Components and Packaging Technologies, 30(3), 383–389.

[21] Kandlikar and Bapat (2007). Evaluation of Jet Impingement, Spray and Microchannel Chip Cooling Options for High Heat Flux Removal. Heat Transfer Engineering, 28(11), 911–923.

[22] Li and Chen (2007). Thermal performance of plate-fin heat sinks under confined impinging jet conditions. International Journal of Heat and Mass Transfer, 50(9-10), 1963–1970.

[23] Chiang, K.-T. (2007). Modeling and optimization of designing parameters for a parallel-plain fin heat sink with confined impinging jet using the response surface methodology. Applied Thermal Engineering, 27(14-15), 2473–2482.

[24] Chandratilleke, T. T., Jagannatha, D., and Narayanaswamy, R. (2009). Performance analysis of a synthetic jet-microchannel hybrid heat sink for electronic cooling. 2009 11th Electronics Packaging Technology Conference. Singapore, pp. 630-635.

[25] Naphon and Wongwises (2010). Investigation on the jet liquid impingement heat transfer for the central processing unit of personal computers. International Communications in Heat and Mass Transfer, 37(7), 822–826.

[26] Barrau, J., Chemisana, D., Rosell, J., Tadrist, L., and Ibañez, M. (2010). An experimental study of a new hybrid jet impingement/micro-channel cooling scheme. Applied Thermal Engineering, 30(14-15), 2058–2066.

[27] Escher, W., Michel, B., and Poulikakos, D. (2010). A novel high performance, ultra-thin heat sink for electronics. International Journal of Heat and Fluid Flow, 31(4), 586–598.

[28] Naphon and Klangchart (2011). Effects of outlet port positions on the jet impingement heat transfer characteristics in the mini-fin heat sink. International Communications in Heat and Mass Transfer, 38(10), 1400–1405.

[29] Shalchi and Seyf (2012). Analysis of entropy generation and convective heat transfer of Al_2O_3 Nano fluid flow in a tangential micro heat sink. International Journal of Heat and Mass Transfer, 55(15-16), 4366–4375.

[30] Naphon and Nakharintr (2012). Nano fluid jet impingement heat transfer characteristics in the rectangular mini-fin heat sink. Journal of Engineering Physics and Thermophysics, 85(6), 1432–1440.

[31] Selvakumar and Suresh (2012). Convective performance of CuO/water Nano fluid in an electronic heat sink. Experimental Thermal and Fluid Science, 40, 57–63.

[32] Mushtaq I. Hasan, Abdul Muhsin A. Rageb and Mahmmod Yaghoubi (2012). Investigation of a Counter Flow Microchannel Heat Exchanger Performance with Using Nanofluid as a Coolant. Journal of Electronics Cooling and Thermal Control, 2012, 2, 35-43.

[33] Husain, A., Kim, S.-M., and Kim, K.-Y. (2013). Performance analysis and design optimization of micro-jet impingement heat sink. Heat and Mass Transfer, 49(11), 1613–1624.

[34] Husain, A., Kim, S.-M., Kim, J.-H., and Kim, K.-Y. (2013). Thermal Performance Analysis and Optimization of Microjet Cooling of High-Power Light-Emitting Diodes. Journal of Thermophysics and Heat Transfer, 27(2), 235–245.

[35] Song, X., Zhang, J., Kang, S., Ma, M., Ji, B., Cao, W., and Pickert, V. (2014). Surrogate-Based Analysis and Optimization for the Design of Heat Sinks with Jet Impingement. IEEE Transactions on Components, Packaging and Manufacturing Technology, 4(3), 429–437.

[36] Karami and Rahimi (2014). Heat transfer enhancement in a hybrid microchannel-photovoltaic cell using Boehmite Nano fluid. International Communications in Heat and Mass Transfer, 55, 45–52.

[37] Selimefendigil, and Öztop (2014). Pulsating Nano fluids jet impingement cooling of a heated horizontal surface. International Journal of Heat and Mass Transfer, 69, 54–65.

[38] Lelea and Laza (2014). The water based Al2O3 Nano fluid flow and heat transfer in tangential micro tube heat sink with multiple inlets. International Journal of Heat and Mass Transfer, 69, 264–275.

[39] Lelea and Laza, (2014). The water based Al2O3 Nano fluid flow and heat transfer in tangential micro tube heat sink with multiple inlets. International Journal of Heat and Mass Transfer, 69, 264–275.

[40] Kumar, D. (2014). Study and Analysis of Flow of an In-compressible Fluid past an Obstruction. International Journal of Engineering Research and General Science Volume 2, Issue 4, June-July, 2014, 815-824.

[41] Ariz, M., Huda, N., and Husain, A. (2015). Thermal Performance Analysis of Jet Impingement with Effusion Scheme. Procedia Engineering, 127, 110–117.

[42] Miry, S. Z., Roshani, M., Hanafizadeh, P., Ashjaee, M., and Amini, F. (2015). Heat Transfer and Hydrodynamic Performance Analysis of a Miniature Tangential Heat Sink Using Al2O3–H2O and TiO2–H2O Nano fluids. Experimental Heat Transfer, 29(4), 536–560.

[43] Chingulpitak and Wongwises (2015). A review of the effect of flow directions and behaviors on the thermal performance of conventional heat sinks. International Journal of Heat and Mass Transfer, 81, 10–18.

[44] Gong, L., Zhao, J., and Huang, S. (2015). Numerical study on layout of micro-channel heat sink for thermal management of electronic devices. Applied Thermal Engineering, 88, 480–490.

[45] Azizi, Z., Alamdari, A., and Malayeri, M. R. (2015). Convective heat transfers of Cu–water Nano fluid in a cylindrical microchannel heat sink. Energy Conversion and Management, 101, 515–524.

[46] Husain, A., Ariz, M., Al-Rawahi, N. Z. H., and Ansari, M. Z. (2016). Thermal performance analysis of a hybrid micro-channel, -pillar and -jet impingement heat sink. Applied Thermal Engineering, 102, 989–1000.

[47] Husain, A., Al-Azri, N. A., Al-Rawahi, N. Z. H., and Samad, A. (2016). Comparative Performance Analysis of Microjet Impingement Cooling Models with Different Spent-Flow Schemes. Journal of Thermophysics and Heat Transfer, 30(2), 466–472.

[48] Lam and Prakash (2016). Thermodynamic investigation and multi-objective optimization for jet impingement cooling system with Al_2O_3 /water Nano fluid. Energy Conversion and Management, 111, 38–56.

[49] Radwan, A., Ahmed, M., and Ookawara, S. (2016). Performance enhancement of concentrated photovoltaic systems using a microchannel heat sink with Nano fluids. Energy Conversion and Management, 119, 289–303.

[50] Zheng, L., Zhang, D., Xie, Y., and Xie, G. (2016). Thermal performance of dimpled/protruded circular and annular microchannel tube heat sink. Journal of the Taiwan Institute of Chemical Engineers, 60, 342–351.

[51] Husain, A., Ariz, M., Al-Rawahi, N. Z. H., and Ansari, M. Z. (2016). Thermal performance analysis of a hybrid micro-channel, -pillar and -jet impingement heat sink. Applied Thermal Engineering, 102, 989–1000.

[52] Husain, A., Al-Azri, N. A., Al-Rawahi, N. Z. H., and Samad, A. (2016). Comparative Performance Analysis of Microjet Impingement Cooling Models with Different Spent-Flow Schemes. Journal of Thermophysics and Heat Transfer, 30(2), 466–472.

[53] Li, B., Baik, Y.-J., and Byon, C. (2016). Enhanced natural convection heat transfer of a chimney-based radial heat sink. Energy Conversion and Management, 108, 422–428.

[54] Zheng, L., Zhang, D., Xie, Y., and Xie, G. (2016). Thermal performance of dimpled/protruded circular and annular microchannel tube heat sink. Journal of the Taiwan Institute of Chemical Engineers, 60, 342–351.

[55] Bahaidarah, H. M. S. (2016). Experimental performance evaluation and modeling of jet impingement cooling for thermal management of photovoltaics. Solar Energy, 135, 605–617.

[56] Radwan, A., Ahmed, M., and Ookawara, S. (2016). Performance enhancement of concentrated photovoltaic systems using a microchannel heat sink with Nano fluids. Energy Conversion and Management, 119, 289–303.

[57] Sun, B., Qu, Y., and Yang, D. (2016). Heat transfer of Single Impinging Jet with Cu Nano fluids. Applied Thermal Engineering, 102, 701–707.

[58] Wang and Wang (2017). Intelligent dimensional and thermal performance analysis of Al_2O_3 Nano fluid. Energy Conversion and Management, 138, 686–697.

[59] Nakharintr and Naphon (2017). Magnetic field effect on the enhancement of Nano fluids heat transfer of a confined jet impingement in mini-channel heat sink. International Journal of Heat and Mass Transfer, 110, 753–759.

[60] Zunaıd, M., Jindal, A., Gakhar, D., Sinha, A., (2017). Numerical Study of Pressure Drop and Heat Transfer in A Straight Rectangular and Semi Cylindrical Projections Microchannel Heat Sink. Journal of Thermal Engineering, 3 (5), 1453-1465.

[61] Nakharintr and Naphon (2017). Magnetic field effect on the enhancement of nanofluids heat transfer of a confined jet impingement in mini-channel heat sink. International Journal of Heat and Mass Transfer, 110, 753–759.

[62] De Oliveira and Barbosa (2017). Novel two-phase jet impingement heat sink for active cooling of electronic devices. Applied Thermal Engineering, 112, 952–964

[63] Kim, T. H., Do, K. H., and Kim, S. J. (2017). Closed-form correlations of pressure drop and thermal resistance for a plate fin heat sink with uniform air jet impingement. Energy Conversion and Management, 136, 340–349.

[64] Zunaıd, M., Jindal, A., Gakhar, D., Sinha, A., (2017). Numerical Study of Pressure Drop and Heat Transfer in A Straight Rectangular and Semi Cylindrical Projections Microchannel Heat Sink. Journal of Thermal Engineering, 3 (5), 1453-1465.

[65] Rehman, M. M. U., Qu, Z. G., Fu, R. P., and Xu, H. T. (2017). Numerical study on free-surface jet impingement cooling with Nano encapsulated phase-change material slurry and Nano fluid. International Journal of Heat and Mass Transfer, 109, 312–325.

[66] Hasan, H. A., Sopian, K., Jaaz, A. H., and Al-Shamani, A. N. (2017). Experimental investigation of jet array Nanofluid impingement in photovoltaic/thermal collector. Solar Energy, 144, 321–334.

[67] Zahmatkesh and Naghedifar (2017). Oscillatory mixed convection in the jet impingement cooling of a horizontal surface immersed in a Nano fluid-saturated porous medium. Numerical Heat Transfer, Part A: Applications, 72(5), 401–416.

[68] Arshad and Ali (2017). Experimental investigation of heat transfers and pressure drop in a straight minichannel heat sink using TiO_2 Nano fluid. International Journal of Heat and Mass Transfer, 110, 248–256.

[69] Arshad and Ali (2017). Graphene Nano platelets Nano fluids thermal and hydrodynamic performance on integral fin heat sink. International Journal of Heat and Mass Transfer, 107, 995–1001.

[70] Tang, Z., Liu, Q., Li, H., and Min, X. (2017). Numerical simulation of heat transfer characteristics of jet impingement with a novel single cone heat sink. Applied Thermal Engineering, 127, 906–914.

[71] Chiu, H.-C., Hsieh, R.-H., Wang, K., Jang, J.-H., and Yu, C.-R. (2017). The heat transfer characteristics of liquid cooling heat sink with micro pin fins. International Communications in Heat and Mass Transfer, 86, 174–180.

[72] Ziaedin Miry, S., Lohrasbi, S., Irani, H., Ashjaee, M., and Domiri Ganji, D. (2017). Thermal energy absorption in a heat sink with elliptical cross section and tangential impinging inlet flow of Nano fluid. Experimental Thermal and Fluid Science, 89, 50–61.

[73] Wang, R., Wang, W., Wang, J., and Zhu, Z. (2017). Analysis and Optimization of Trapezoidal Grooved Microchannel Heat Sink Using Nano fluids in a Micro Solar Cell. Entropy, 20(1), 9.

[74] Selimefendigil and Öztop (2017). Jet impingement cooling and optimization study for a partly curved isothermal surface with CuO-water Nano fluid. International Communications in Heat and Mass Transfer, 89, 211–218.

[75] Ali and Arshad (2017). Effect of channel angle of pin-fin heat sink on heat transfer performance using water based graphene Nano platelets Nano fluids. International Journal of Heat and Mass Transfer, 106, 465–472.

[76] Zunaid, M., Cho, H. M., Husain, A., Jindal, A., Kumar, R., and Chauhan, B. S. (2018). Computational Analysis of Liquid Jet Impingement Micro-Channel Cooling. Materials Today: Proceedings, 5(14), 27877–27883.

[77] Naphon, P., Nakharintr, L., and Wiriyasart, S. (2018). Continuous Nano fluids jet impingement heat transfer and flow in a micro-channel heat sink. International Journal of Heat and Mass Transfer, 126, 924–932.

[78] Siavashi, M., Rasam, H., and Izadi, A. (2018). Similarity solution of air and Nano fluid impingement cooling of a cylindrical porous heat sink. Journal of Thermal Analysis and Calorimetry.

[79] Selimefendigil and Öztop (2018). Analysis and predictive modeling of Nano fluid-jet impingement cooling of an isothermal surface under the influence of a rotating cylinder. International Journal of Heat and Mass Transfer, 121, 233–245.

[80] Selimefendigil and Öztop (2018). Al_2O_3-water Nano fluid jet impingement cooling with magnetic field. Heat Transfer Engineering, 1–33.

[81] Alirezaie, A., Hajmohammad, M. H., Hassani Ahangar, M. R., and Hemmat Esfe, M. (2018). Price-performance evaluation of thermal conductivity enhancement of Nano fluids with different particle sizes. Applied Thermal Engineering, 128, 373–380.

[82] Ming, T., Cai, C., Yang, W., Shen, W., and Gan, T. (2018). Optimization of Dimples in Microchannel Heat Sink with Impinging Jets — Part A: Mathematical Model and the Influence of Dimple Radius. Journal of Thermal Science, 27(3), 195–202.

[83] Zunaid, M., Cho, H. M., Husain, A., Jindal, A., Kumar, R., and Chauhan, B. S. (2018). Computational Analysis of Liquid Jet Impingement Micro-Channel Cooling. Materials Today: Proceedings, 5(14), 27877–27883.

[84] Nakharintr, L., Naphon, P., and Wiriyasart, S. (2018). Effect of jet-plate spacing to jet diameter ratios on Nano fluids heat transfer in a mini-channel heat sink. International Journal of Heat and Mass Transfer, 116, 352–361.

[85] Naphon, P., Wiriyasart, S., Arisariyawong, T., and Nakharintr, L. (2019). ANN, numerical and experimental analysis on the jet impingement Nano fluids flow and heat transfer characteristics in the micro-channel heat sink. International Journal of Heat and Mass Transfer, 131, 329–340.

[86] Izadi, A., Siavashi, M., and Xiong, Q. (2019). Impingement jet hydrogen, air and Cu H2O Nano fluid cooling of a hot surface covered by porous media with non-uniform input jet velocity. International Journal of Hydrogen Energy.

[87] Wang, J., Kong, H., Xu, Y., and Wu, J. (2019). Experimental investigation of heat transfers and flow characteristics in finned copper foam heat sinks subjected to jet impingement cooling. Applied Energy, 241, 433–443.

[88] Abo-Zahhad, E. M., Ookawara, S., Radwan, A., El-Shazly, A. H., and Elkady, M. F. (2019). Numerical analyses of hybrid jet impingement/microchannel cooling device for thermal management of high concentrator triple-junction sol*ar* cell. Applied Energy, 253, 113538.

[89] Sarafraz, M. M., Yang, B., Pourmehran, O., Arjomandi, M., and Ghomashchi, R. (2019). Fluid and heat transfer characteristics of aqueous graphene Nano platelet (GNP) Nano fluid in a microchannel. International Communications in Heat and Mass Transfer, 107, 24–33.

[90] Bahiraei, M., Mazaheri, N., Sheykh Mohammadi, M., and Moayedi, H. (2019). Thermal performance of a new Nano fluid containing biologically functionalized graphene Nano platelets inside tubes equipped with rotating coaxial double-twisted tapes. International Communications in Heat and Mass Transfer, 108, 104305.

[91] Ambreen, T., Saleem, A., and Park, C. W. (2019). Numerical analysis of the heat transfers and fluid flow characteristics of a Nano fluid-cooled micro pin-fin heat sink using the Eulerian-Lagrangian approach. Powder Technology.

[92] Abo-Zahhad, E. M., Ookawara, S., Radwan, A., El-Shazly, A. H., and Elkady, M. F. (2019). Numerical analyses of hybrid jet impingement/microchannel cooling device for thermal management of high concentrator triple-junction solar cell. Applied Energy, 253, 113538.

[93] Sorour, M. M., El-Maghlany, W. M., Alnakeeb, M. A., and Abbass, A. M. (2019). Experimental Study of Free Single Jet Impingement Utilizing High Concentration SiO Nanoparticles Water Base Nano fluid. Applied Thermal Engineering, 114019.

[94] Hempijid and Kittichaikarn (2019). Effect of Heat Sink Inlet and Outlet Flow Direction on Heat Transfer Performance. Applied Thermal Engineering, 114375.

[95] Duan, Z., Lv, X., Ma, H., Su, L., and Zhang, M. (2019). Analysis of Flow Characteristics and Pressure Drop for an Impinging Plate Fin Heat Sink with Elliptic Bottom Profiles. Applied Sciences, 10(1), 225.

[96] Ghanbari and Javaherdeh (2019). Thermal Performance Enhancement in Perforated Baffled Annuli by Nano porous Graphene Non-Newtonian Nano fluid. Applied Thermal Engineering, 114719.

[97] Freegan, B., Hussain, A. A., Falih, A. H., and Towsyfyan, H. (2019). CFD analysis of heat transfer enhancement in plate-fin heat sinks with fillet profile: investigation of new designs. Thermal Science and Engineering Progress, 100458.

[98] Datta, A., Kumar, S., and Halder, P. (2019). Heat Transfer and Thermal Characteristics Effects on Moving Plate Impinging from Cu-Water Nano fluid Jet. Journal of Thermal Science.

[99] Wiriyasart and Naphon (2019). Liquid impingement cooling of cold plate heat sink with different fin configurations: High heat flux applications. International Journal of Heat and Mass Transfer, 140, 281–292.

[100] Ulises Gonzalez-Valle, C., Samir, S., and Ramos-Alvarado, B. (2019). Experimental Investigation of the Cooling Performance of 3-D Printed Hybrid Water-Cooled Heat Sinks. Applied Thermal Engineering, 114823.

[101] Yabo, W., Kai, Z., Zhuo, C., and Jie, W. (2019). Effects of the location of the inlet and outlet on heat transfer performance in pin fin CPU heat sink. Applied Thermal Engineering.

[102] Hussain, A. A., Freegah, B., Khalaf, B. S., and Towsyfyan, H. (2019). Numerical investigation of heat transfer enhancement in plate-fin heat sinks: Effect of flow direction and fillet profile. Case Studies in Thermal Engineering, 13, 100388.

[103] Neyestani, M., Nazari, M., Shahmardan, M. M., Sharifpur, M., Ashouri, M., and Meyer, J. P. (2019). Thermal characteristics of CPU cooling by using a novel porous heat sink and Nano fluids. Journal of Thermal Analysis and Calorimetry.

[104] Izadi, A., Siavashi, M., Rasam, H., and Xiong, Q. (2019). MHD enhanced Nano fluid mediated heat transfer in porous metal for CPU cooling. Applied Thermal Engineering, 114843.

[105] Ambreen, T., Saleem, A., and Park, C. W. (2019). Numerical analysis of the heat transfers and fluid flow characteristics of a Nano fluid-cooled micro pin-fin heat sink using the Eulerian-Lagrangian approach. Powder Technology.

[106] Hadad, Y., Rangararajan, S., Nemati, K., Ramakrishnann, B., Pejman, R., Chiarot, P. R., and Sammakia, B. (2020). Performance analysis and shape optimization of a water-cooled impingement micro-channel heat sink including manifolds. International Journal of Thermal Sciences, 148, 106145.

[107] Wiriyasart and Naphon (2020). Heat spreading of liquid jet impingement cooling of cold plate heat sink with different fin shapes. Case Studies in Thermal Engineering, 100638.

[108] Yang, L., Huang, J., Mao, M., and Ji, W. (2020). Numerical assessment of Ag-water Nano-fluid flow in two new microchannel heatsinks: Thermal performance and thermodynamic considerations. International Communications in Heat and Mass Transfer, 110, 104415.

[109] Anitha, S., Loganathan, K. and Pichumani, M. (2020). Approaches for modelling of industrial energy systems: correlation of heat transfer characteristics between magneto hydrodynamics hybrid Nano fluids and performance analysis of industrial length-scale heat exchanger. J Therm Anal Calorim.

[110] Mohammad and Lee, A (2020). Investigation of nanoparticle effects on jet impingement heat transfer: A review. Journal of Molecular Liquids, 113819.

[111] Ambreen, T., Saleem, A., and Woo Park, C. (2020). Analysis of hydro-thermal and entropy generation characteristics of Nano fluid in an aluminum foam heat sink by employing Darcy-Forchheimer-Brinkman model coupled with multiphase Eulerian model. Applied Thermal Engineering, 115231.

[112] Yang, L., Huang, J., Mao, M., and Ji, W. (2020). Numerical assessment of Ag-water Nano-fluid flow in two new microchannel heatsinks: Thermal performance and thermodynamic considerations. International Communications in Heat and Mass Transfer, 110, 104415.

[113] Bahiraei, M., Jamshidmofid, M., and Dahari, M. (2020). Second law analysis of hybrid Nano fluid flow in a microchannel heat sink integrated with ribs and secondary channels for utilization in miniature thermal devices. Chemical Engineering and Processing - Process Intensification, 107963.

[114] Mahdavi, M., Sharifpur, M., Meyer, J. P., and Chen, L. (2020). Thermal analysis of a Nano fluid free jet impingement on a rotating disk using volume of fluid in combination with discrete modelling. International Journal of Thermal Sciences, 158, 106532.

[115] Ramesh, K.N., Sharma, T.K. and Rao, G.A.P. (2020). Latest Advancements in Heat Transfer Enhancement in the Micro-Channel Heat Sinks: A Review. Arch Computed Methods Eng.

[116] Chen and Cheng (2020). A numerical analysis on the heat transfer of jet impingement with Nano fluid on a concave surface covered with metal porous block. Heat and Mass Transfer. Heat Mass Transfer **56,** 3071–3083 (2020).

[117] M and Venkatasubbaiah (2020). Numerical investigation of jet impingement flows with different Nano fluids in a mini channel using Eulerian-Eulerian two-phase method. Thermal Science and Engineering Progress, 100585.

[118] Pratap, A., Baghel, Y. K., and Patel, V. K. (2020). Effect of impingement height on the enhancement of heat transfer with circular confined jet impingement using Nano fluids. Materials Today: Proceedings.

[119] Li, Y., Gong, L., Xu, M., and Joshi, Y. (2020). Enhancing the performance of aluminum foam heat sinks through integrated pin fins. International Journal of Heat and Mass Transfer, 151, 119376.

[120] Izadi, A., Abdipour, M., and Rasam, H. (2020). MHD forced convection of Nano fluid flow in an open-cell metal foam heatsink under LTNE conditions. Journal of Thermal Analysis and Calorimetry.

[121] Ho, C. J., Hsieh, Y.-J., Rashidi, S., Orooji, Y., and Yan, W.-M. (2020). Thermal-hydraulic analysis for alumina/water Nano fluid inside a mini-channel heat sink with latent heat cooling ceiling-An experimental study. International Communications in Heat and Mass Transfer, 112, 104477.

LIST OF PUBLICATIONS BASED ON RESEARCH WORK

Paper Published in International Journals

1. Kumar, D., Zunaid, M. & Gautam, S. “Thermal Performance Exploration of Air Foil Shape of Pillars using Impinging Jet in Heat Sink” published in " Tobacco Regulatory Science, 7(5-1) ,2021, 2794-2807 . (SCIE).

2. Kumar, D., Zunaid, M. & Gautam, S. “Performance Evaluation of Thermal Attributes in Impinging Jet Heat Sink using Airfoil Pillars with and without Nano Fluid” published in " Tobacco Regulatory Science, 7(5-1)2021, 2808-2820 . (SCIE)

Paper Published in International/ National conference proceedings

1. Kumar, D., Zunaid, M. & Gautam, S. “Analysis of airfoil pillars with impinging jets in a heat sink” published in "Materials Today Proceedings, Volume 45, Part, February 2021, pp. 4498-4503. (Scopus)
2. Kumar, D., Zunaid, M. & Gautam, S. “Heat sink analysis in jet impingement with air foil pillars and nanoparticles” published in "Materials Today Proceedings Volume 6, Part 20, February 2021, pp.10752-10756. (Scopus)

BIOGRAPHICAL PROFILE OF RESEARCHER

Deepak Kumar is currently working as an Assistant Professor in the Department of Mechanical Engineering, Amity University Haryana, Gurgaon. He received his Bachelor's degree in Mechanical Engineering from M.D.U. Rohtak. He completed his Master's Degree in Thermal Engineering from National Institute of Technology (NIT), Kurukshetra, India. He has published more than twenty research papers in international/national journals and conferences. He qualified GATE examination four times and also Indian Engineering Services exam in 2009. Also he has more than ten years of teaching experience.